NASA CR 72126

260-IN.-DIA MOTOR FEASIBILITY DEMONSTRATION PROGRAM

Volume V: 260-SL Motor Chamber and Nozzle Shell Fabrication of 18%-Nickel Maraging Steel

Appendix B: Material and Process Evaluation Program

Prepared for

NATIONAL AERONAUTICS AND SPACE ADMINISTRATION

CONTRACT NO. NAS3-6284

FACILITY FORM 602

(ACCESSION NUMBER)	(THRU)
440 (PAGES)	1 (CODE)
CR. 72126 (NASA CR OR TMX OR AD NUMBER)	28 (CATEGORY)

AEROJET GENERAL

AEROJET-GENERAL CORPORATION

SACRAMENTO, CALIFORNIA

NASA CR 72126

FINAL PHASE REPORT

260-IN.-DIA MOTOR FEASIBILITY DEMONSTRATION PROGRAM

VOLUME V

260-SL MOTOR CHAMBER AND NOZZLE SHELL FABRICATION OF 18%-NICKEL MARAGING STEEL

APPENDIX B: MATERIAL AND PROCESS EVALUATION PROGRAM

Prepared for

NATIONAL AERONAUTICS AND SPACE ADMINISTRATION

8 April 1966

CONTRACT NAS3-6284

Technical Management
NASA Lewis Research Center
Cleveland, Ohio
James J. Kramer

AEROJET-GENERAL CORPORATION
A SUBSIDIARY OF THE GENERAL TIRE & RUBBER COMPANY

Report NASA CR 72126, Appendix B

TABLE OF CONTENTS

		Page
I.	Program Objectives	1
II.	Parent Plate Evaluation	1
	A. Evaluation of Parent Plates (Republic Heats 3960524 and 3920556)	2
	B. Evaluation of Lukens Plate R-599-1	15
III.	Forging Material Evaluation	27
	A. Entrance Flange	27
	B. Intermediate Section and Exit Flange	35
	C. Testing Conducted by Sun	44
	D. Conclusions	48
IV.	Parent Metal Bar Stock Evaluation	50
	A. Evaluation Program	50
	B. Results and Discussion	52
V.	Plate Welding Evaluation	54
	A. Weld Process Development and Filler-Wire Selection	55
	B. Evaluation of Selected Weld Filler Wire and Weld Process	79
VI.	Evaluation of the Effects of Cold Forming on the Tensile and Fracture-Toughness Properties of Plate	113
	A. Material Utilized	113
	B. Forming	113
	C. Specimen Preparation and Testing Procedure	114
	D. Results	116
VII.	Evaluation of Straightening Welded Joints	119
	A. Procedure	119
	B. Results	120
VIII.	Maraging System Demonstration	121
	A. Maraging System Design	121
	B. Furnace Demonstration Run	123
	C. Evaluation of Specimens Maraged with 280-in. dia Chamber	127
	D. Additional Testing to Evaluate the Strength Increase	128

TABLE OF CONTENTS (cont.)

		Page
IX.	Evaluation of Hydrostatic-Test Fluid	136
	A. Hydrostatic-Test Media	136
	B. Materials	137
	C. Experimental Procedures	137
	D. Results of Discussion	140
X.	Process Evaluation Test Vehicles (PETV)	144
	A. Process Evaluation Test Vehicle Design and Fabrication	144
	B. Maraging Heat Treatment	148
	C. Hydrostatic Burst Tests of 36-in. dia PETV's	150
	D. Conclusions	158

FIGURE LIST

	Figure
Tensile, Slow-Notch-Bend, and Precracked Charpy Impact Test Specimen Configuration	1
Test-Specimen Orientation	2
Composition of 18%-Nickel Steel	3
Typical Microstructure, Grain Size, and Inclusion Content of 0.6-in.-thick Plate; Republic Heat 3960524	4
Typical Microstructure, Grain Size, and Inclusion Content of 0.6-in.-thick Plate; Republic Heat 3920556	5
Effects of Specimen Orientation, Aging Temperature, and Aging Time on the Tensile Properties of 0.6-in.-thick 18%-Nickel Maraging Steel Plate, Mill Annealed at 1500°F for 1 hr; Republic Heat 3960524	6
Effects of Aging Time and Temperature on the Tensile Properties of 0.6-in.-thick 18%-Nickel Maraging Steel Plate, Mill Annealed at 1500°F for 1 hr Prior to Aging; Republic Heat 3960524	7
Effects of Specimen Orientation, Aging Temperature, and Aging Time on the Tensile Properties of 0.6-in.-thick 18%-Nickel Maraging Steel Plate, Mill Annealed at 1500°F for 1 hr; Republic Heat 3920556	8
Effects of Aging Time and Temperature on the Tensile Properties of 0.6-in.-thick 200 grade 18%-Nickel Maraging Steel Plate, Mill Annealed at 1500°F for 1 hr Prior to Aging; Republic Heat 3920556	9
Effects of Orientation, Aging Time, and Temperature on the Slow-Notch-Bend Fracture Toughness of Plate from Republic Heat 3960524	10
Summary of Plane-Strain Fracture Toughness of Plate from Republic Heat 3960524	11
Effects of Orientation, Aging Time, and Temperature on the Slow-Notch-Bend Fracture Toughness of Plate from Republic Heat 3920556	12

FIGURE LIST (cont.)

	Figure
Summary of Plane-Strain Fracture Toughness, Plate from Republic Heat 3920556	13
Effects of Specimens Orientation, Aging Temperature, and Test Temperature on the Precracked Impact Fracture Toughness (W/A) of Republic Heat 3960524	14
Precracked Impact Fracture Toughness (W/A) vs Test Temperature for Various Aging Cycles - Republic Heat 3960524	15
Effects of Specimen Orientation, Aging Temperature, and Test Temperature on the Precracked Impact Fracture Toughness (W/A) of Republic Heat 3920556	16
Mills Certified Analysis of Chemical Composition, Lukens Plate R-599-1	17
Location of Specimens, Lukens Heat R-599-1	18
Typical Load vs Strain Curve for Slow-Notch-Bend Specimens Tested by Sun Shipbuilding	19
Tensile Data Obtained from Lukens Plate R-599-1	20
Effect of Aging Temperature and Time on the Yield Strength of Lukens Plate, Heat R-599-1	21
Effect of Aging Temperature and Time on the Ultimate Tensile Strength of Lukens Plate, Heat R-599-1	22
Effect of Aging Time and Temperature on the Ductility of Lukens Plate, Heat R-599-1	23
Effect of Aging Temperature and Time on the Reduction of Area of Lukens Plate, Heat R-599-1	24
Plane-Strain Fracture Toughness vs Yield Strength for Lukens Plate Heat R-599-1	25
Effect of Aging Time and Temperature on the Plane-Strain Fracture Toughness of Lukens Plate, Heat R-599-1 Slow-Notch-Bend Specimens	26

FIGURE LIST (cont.)

	Figure
Plane-Strain Fracture Toughness and Yield Strength vs Maraging Time for Lukens Plate, Heat R-599-1 Longitudinal Test Specimens	27
Plane-Strain Fracture Toughness and Yield Strength vs Maraging Time for Lukens Plate, Heat R-599-1 Transverse Test Specimens	28
Plane-Strain Fracture Toughness and Yield Strength vs Maraging Time for Lukens Plate, Heat R-599-1 Transverse Test Specimens	29
Plane-Strain Fracture Toughness vs Maraging Time for Lukens Plate, Heat R-599-1 Short Transverse Test Specimens	30
Allegheny Ludlum Comparison of Tensile Properties on Solution Annealing at 1500°F and Resolution Annealing at 1650°F	31
Allegheny Ludlum Comparison of Tensile Properties on Solution Annealing at 1500°F	32
Resolution Annealing Evaluation, Tensile Property Data Taken from Four Allegheny Plates Initially Solution Treated at 1500°F	33
W/A Values from Impact Specimens from Crop Ends of Four Allegheny Ludlum Plates; Specimens Re-Annealed at 1600°F, and 1700°F	34
The Effects of Specimen Width on W/A Values, Allegheny Ludlum Plate 25000-1; All Specimens Re-Annealed at 1650°F	35
Comparison of Tensile Properties of Republic Plates Solution Annealed at 1500°F and Resolution Annealed at 1650°F	36
Preliminary Tensile Property Data Taken from Seven Republic Plates Before Solution Annealing	37
Effect of Solution-Annealing Temperature on Grain Size and Re-Crystallization on Seven Republic Plates; Performed Before Annealing	38
Solution Annealing Evaluation Tensile Property Data Taken from Three Cameron Plates Before Solution Annealing	39

FIGURE LIST (cont.)

	Figure
Acceptance Tensile Property Data on Cameron Plates	40
Chemical Analysis of Lukens Heat R-559	41
Tensile Test Results of Specimens Removed from Forged Test Bars	42
Test Ring Locations	43
Test Specimen Orientation	44
Gradient Bar Microstructures, Magnification 100X	45
Mechanical Property Data for Various Solution Annealing Temperatures	46
Aging Response Evaluation	47
Room Temperature Tensile Results	48
Precracked Charpy V-Notch Impact Test Results	49
Precracked Impact Notch Toughness; Orientation and Test Temperature Effects	50
Chemical Analysis of Allegheny Ludlum Heat 25005	51
Solution Heat-Treating Evaluation, Intermediate Section	52
Solution Heat-Treating Evaluation, Exit Flange	53
Axial Forging Test Ring CFA; Radial Forging Test Ring CFR	54
Product Test Evaluation, Intermediate Section Tensile Test Data	55
Product Test Evaluation, Intermediate Section, Room Temperature Precracked Charpy V-Notch Impact Test Data	56
Product Test Evaluation, Exit Flange Tensile Test Data	57
Product Test Evaluation, Exit Flange, Room Temperature Precracked Charpy V-Notch Impact Test Data	58

FIGURE LIST (cont.)

	Figure
Product Test Evaluation, Intermediate Section and Exit Flange, Precracked Charpy V-Notch Impact Test Data	59
Ladish Metallurgical Department Microcleanliness Grain Size Results	60
Results of Testing Conducted at Lehigh Test Laboratories	61
Weld Test Plate from 70-in.-dia Forging	62
Report of Tensile Properties (0.250-in.-round Tensile Specimens), Weld Metal Evaluation - 70.5-in. Flange Material Weld Wire; Armetco Heat 08436	63
Fracture Toughness (W/A) Values for Impact Specimens From Entrance Flange for 120-SS Nozzle Shell (Lukens Heat R-559) Welded with Armetco Heat 08436 Wire	64
Fracture Toughness (G_{nc}) Values for Slow-Notch-Bend Specimens From Entrance Flange for 120-SS Nozzle (Lukens Heat R-599) Welded with Armetco Heat 08436 Wire	65
Weld in Forged Test Ring	66
Weld in Forged Test Ring	67
Precracked Impact Specimens for Maraging with Nozzle Shell	68
Test Results of Tensile Specimens Maraged with the 120-SS Nozzle Shell	69
Test Results of Precracked Impact Specimens Maraged with the 120-SS Nozzle Shell	70
Composition of 18%-Nickel Maraging Steel Bar Stock	71
Typical Microstructure, Grain Size and Inclusion Content of 2.5-in.-thick Bar Stock from Republic Heat 3920556	72
Test Specimens	73
Orientation of Specimens Taken from 2-1/2 by 8-in. Bar Stock, Republic Heat 3920556, 18%-Nickel Maraging Steel	74

FIGURE LIST (cont.)

	Figure
Effects of Aging Time and Temperature and Specimen Orientation on the Tensile Properties of Republic Heat 3920556, Grade 200, 2-1/2-in.-thick 18%-Nickel Maraging Steel Bar Stock	75
Effects of Aging Time and Temperature and Orientation of the Precracked Charpy Impact Fracture Toughness of Republic Heat 3920556, Grade 200, 2-1/2-in.-thick, 18%-Nickel Maraging Steel Bar Stock	76
Effects of Orientation, Aging Time, and Temperature on the Slow-Notch Bend Fracture Toughness of Republic Heat 3920556, 2-1/2-in.-thick Bar Stock	77
Plane-Strain Fracture Toughness of Republic Heat 3920556, Grade 200, 2-1/2-in.-thick, 18%-Nickel Maraging Steel Bar Stock	78
Welding Fixture	79
Weld-Joint Design and Welding Conditions for Double-V Joint, 18%-Nickel Maraging Steel Plate Material	80
Weld-Joint Design and Welding Conditions for Single-U Joint, 18%-Nickel Maraging Steel Plate Material	81
Precracked Charpy Impact Specimen	82
Orientation of Weld-Joint Test Specimens	83
Filler Wire and Base Metal Compositions	84
Longitudinal Tensile Properties of Welded Joints in Republic Heat 3960524, 18%-Nickel Maraging Steel Plate after Aging at 900°F for 8 hr	85
Composition of Weld Metals Obtained in TIG-Welded F public Heat 3960524, Grade 200, 0.6-in.-thick 18%-Nickel Maraging Steel Plate with Five Filler Wires	86
Effects of Aging Temperature and Time on the Longitudinal Tensile Properties of Welded Joints in Republic Heat 3960524, 18%-Nickel Maraging Steel Plate Made with 07495 Filler and a Double-V Joint Design	87

FIGURE LIST (cont.)

	Figure
Effects of Aging Time and Temperature on the Longitudinal Tensile Properties of Weld Metals Deposited with Filler Wire 07495 in Republic Heat 3960524, 18%-Nickel Maraging Steel Plate Material (As Welded and Aged Conditions)	88
Effects of Aging Temperature and Time on the Longitudinal Tensile Properties of Welded Joints in Republic Heat 3960524, Grade 200, 0.6-in.-thick, 18%-Nickel Maraging Steel Plate Made with 34428-0.31 Ti Filler Wire and Double-V and Single-U Joint Designs	89
Ultimate Tensile Strength and Failure Locations of Transverse Weld Tensile Specimens from Weldments in Republic Heat 3960524, Grade 200, 0.6-in.-thick, 18%-Nickel Maraging Steel Plate Made with 07495 and 34428-.31 Ti Filler Wires and Double-V and Single-U Joint Design	90
Precracked Impact Fracture Toughness of Weld Metal and Heat Affected Zones of Weldments Made in Republic Heat 3960524, Grade 200, 0.6-in.-thick, 18%-Nickel Maraging Steel Plate with 07495 Filler Wire and Double-V Joint	91
Precracked Impact Fracture Toughness of TIG Weldments Made in Republic Heat 3960524, Grade 200, 0.6-in.-thick, 18%-Nickel Maraging Steel Plate with 34428-0.31 Ti Filler Wire and Double-V Joint	92
Precracked Charpy Impact Fracture Toughness of TIG Weldments Made in Republic Heat 3960524, Grade 200, 0.6-in.-thick, 18%-Nickel Maraging Steel Plate with Filler Wire 34428-.31 Ti and Single-U Joint	93
Precracked Charpy Impact Fracture Toughness of TIG Weld Metal Deposited in Republic Heat 3920556, Grade 200, 0.6-in.-thick, 18%-Nickel Maraging Steel Plate with Inco Filler Wire and Single-U Joint	94
Slow-Notch-Bend Fracture Toughness of Weldments Made in Republic Heat 3960524 with 07495 Filler Wire and Double-V Joints	95
Slow-Notch-Bend Fracture Toughness of Weldments Made in Republic Heat 3960524 with 34428-.31 Ti Filler Wire and Single-U Joints	96

FIGURE LIST (cont.)

	Figure
Slow-Notch-Bend Fracture Toughness of Weldments Made in Republic Heat 3960524 with 34428-.31 Ti Filler Wire and Double-V Joints	97
Slow-Notch-Bend Fracture Toughness of Weldments Made in Republic Heat 3960524 with Inco Filler Wire and Single-U Joints	98
Notch Locations for Weld and Heat Affected Zone Slow-Notch-Bend and Precracked Charpy Impact Test Specimens	99
Weld-Joint Design and Welding Condition for Single-U Joint Gap-Weld Test, 18%-Nickel Maraging Steel Plate Material	100
Tensile Properties of Weldments Made in Republic Heat 3920556 with 07495 Filler Wire, 0.070-in.-wide Root Gap, and Single-U Joints	101
Precracked Impact Fracture Toughness of Weldments Made in Republic Heat 3920556 with 07495 Filler Wire, 0.070-in.-wide Root Gap, and Single-U Joints	102
Slow-Notch-Bend Fracture Toughness of Weld Metal and Heat-Affected Zone, Republic Heat 3920556, Grade 200, Vacuum-Arc Remelted, 18%-Nickel Maraging Steel Plate, 07495 Filler Wire, and Single-U Joint with 0.070-in. Root Gap	103
Mill Certified Analysis on Chemical Composition of Weld Wire; Mill Certified Chemical Analyses	104
Joint Detail for Weld Test Plates	105
Locations of Notches for Weld Heat-Affected-Zone Slow-Notch-Bend Specimens, Calibration Bars, and Precracked Impact Specimens	106
Tensile Specimen, 0.250-in. Round	107
Slow-Notch-Bend Specimen	108
Charpy V-Notch Impact Specimen	109
Load Deflection Curve Showing Deviation from Linearity	110
Tensile Test Data Obtained from Lukens Plate R-599-1 and Special Metals Weld Wire 34428	111

FIGURE LIST (cont.)

	Figure
Tensile Test Data Obtained from Lukens Plate R-599-1 and Special Metals Weld Wire 34428	112
Effect of Aging Time and Temperature on the Plane-Strain Fracture Toughness of Welds Made with Lukens Plate R-599-1 and Special Metals Weld Wire 34428; Slow-Notch-Bend Specimens	113
Tensile Test Data Obtained from Lukens Plate R-600-1 and Special Metals Weld Wire 34481	114
Tensile Test Data Obtained from Lukens Plate R-600-1A and Armetco Weld Wire 08436	115
Effect of Aging Time and Temperature on the Plane-Strain Fracture Toughness of Welds and Weld Heat-Affected Zone of Lukens Plate R-600-1 and Special Metals Weld Wire 34481; Slow-Notch-Bend Specimens	116
Effect of Aging Time and Temperature on the Plane-Strain Fracture Toughness of Welds and Weld Heat-Affected Zone of Lukens Plate R-600-1A and Armetco Weld Wire 08436; Slow-Notch-Bend Specimens	117
Plane-Stress Fracture Toughness of Welds Made with Lukens Plate R-600-1 and Special Metals Weld Wire 34481	118
Plane-Stress Fracture Toughness of Welds Made with Lukens Plate R-600-1A and Armetco Weld Wire 08436	119
Tensile Test Data Obtained from Welds Made with 260-SL-1 Plate and Special Metals Weld Wire 63343	120
Effect of Aging Time and Temperature on the Plane-Strain Fracture Toughness of Welds Made with Allegheny Ludlum Plate 25000-1 and Special Metals Weld Wire 63343 Slow-Notch-Bend Specimens	121
Effect of Specimen Depth on the Plane-Strain Fracture Toughness of Welds Made with Special Metals Weld Wire Heat 63343; Slow-Notch-Bend Specimens	122

FIGURE LIST (cont.)

	Figure
Plane-Strain Fracture Toughness of the Weld Heat-Affected Zone, Allegheny Ludlum Plate 25000-1 and Special Metals Weld Wire 63343; Slow-Notch-Bend Specimens	123
Plane-Stress Fracture Toughness of Welds Made with 260-S1-1 Plate and Special Metals Weld Wire 63343	124
Flat Tensile Test Data Obtained from Repair Welds Made with Lukens R-600 and 604 Plate and Weld Wire Heats 34481 and 08436	125
Plane-Stress Fracture Toughness of Welds Made with Lukens Plate R-600-1 and Special Metals Weld Wire 34481	126
Microhardness Transverse Summary; Manual Repair in Automatic TIG Weld	127
Microphotographs of Weldments	128
Plane-Stress Fracture Toughness of Welds Made with Lukens Plate R-600-1A and Armetco Weld Wire 08436	129
Plane-Stress Fracture Toughness of Welds Made with Lukens Plate R-604-1 and Armetco Weld Wire, Heat 08436	130
Joint Configurations Used to Determine the Tensile Properties and Fracture Toughness of Original Welds in Grade 200, 18%-Nickel Maraging Steel	131
Typical Macrostructure of TIG Weldments Processed with a Conventional-U and Narrow-Gap Joint Designs	132
Joint Configurations and Locations Used to Determine the Tensile Properties and Fracture Toughness of Repair Welds in Grade 200, 18%-Nickel Maraging Steel (Heat 3920556) Made with Filler Wire from Heat 34482	133
Tensile, Slow-Notch-Bend, and Precracked Charpy Impact Test Specimens	134
Composition of Republic Heat 3920556, 18%-Nickel Maraging Steel Plate and Heat 34482 Filler Wire	135

FIGURE LIST (cont.)

	Figure
Effects of Double-Aging Treatment on the Tensile Properties of 0.6-in.-thick Republic Heat 3920556, Grade 200, 18%-Nickel Maraging Steel Plate	136
Precracked Charpy Impact Fracture Toughness of 0.6-in.-thick Republic Heat 3920556, Grade 200, 18%-Nickel Maraging Steel Plate after Two Aging Treatments at 900°F for 8 hr	137
Effects of Double-Aging Treatment and Specimen Orientation of Plane-Strain Fracture Toughness of Republic Heat 3920556 Grade 200, 18%-Nickel Maraging Steel Plate; Slow-Notch-Bend Test	138
Effects of Double-Aging Treatments on the Tensile Properties of TIG Weldments Deposited in 0.6-in.-thick Republic Heat 3920556, Grade 200, 18%-Nickel Maraging Steel Plate with Heat 34482 Filler Wire and Single-U Joint Configuration	139
Effects of Double-Aging Treatments on the Room Temperature Precracked Impact Fracture Toughness of Weld Metals Deposited with a Single-U Joint Configuration and Filler Wire 34482 in 0.6-in.-thick Republic Heat 3920556, Grade 200, 18%-Nickel Maraging Steel Plate	140
Effects of Double-Aging Treatments on the Slow-Notch-Bend Fracture Toughness of Weld Metals Deposited with a Single-U Joint Configuration and Filler Wire 34482 in 0.6-in.-thick Republic Heat 3920556, Grade 200, 18%-Nickel, Maraging Steel Plate	141
Effects of Double-Aging Treatments on the Room Temperature Precracked Impact Fracture Toughness of Heat-Affected Zones of Weldments Made with a Square-Butt Joint Design and Filler Wire 34482 in 0.6-in.-thick Republic Heat 3920556, Grade 200, 18%-Nickel Maraging Steel Plate	142
Effects of Double-Aging Treatments on the Slow-Notch-Bend Fracture Toughness of Heat Affected Zones of Weldments Made with a Square-Butt Joint Design and Filler Wire 34482 in 0.6-in.-thick Republic Heat 3920556, Grade 200, 18%-Nickel, Maraging Steel Plate	143
Effects of Double-Aging Treatments on the Critical Flaw Length of Weldments Prepared in 0.6-in.-thick Republic Heat 3920556, 18%-Nickel Maraging Steel Plate with Filler Wire 34482	144

FIGURE LIST (cont.)

	Figure
Transverse Tensile Properties of Weldments Made with Filler Wire 07495 and Single-U Joints in Previously Aged Plate from Republic Heat 3920556, Grade 200, 18%-Nickel Maraging Steel	145
Effects of Aging the Base Metal Prior to Welding on the Room Temperature Precracked Impact Fracture Toughness of Heat-Affected Zones of Weldments Made with a Square-Butt Joint Design and Filler Wire 34482 in 0.6-in.-thick Republic Heat 3920556, Grade 200, 18%-Nickel Maraging Steel Plate	146
Effects of Aging the Base Metal Prior to Welding on the Slow-Notch-Bend Fracture Toughness of Heat Affected Zone of Weldments Made with a Square-Butt Joint Design and Filler Wire 34482 in 0.6-in.-thick Republic Heat 3920556, Grade 200, Maraging Steel Plate	147
Transverse Tensile Properties of Repair Welds Made in 0.6-in. thick Republic Heat 3920556, Grade 200, 18%-Nickel Maraging Steel Plate with Filler Wire 34482 and a Single-U Joint Configuration	148
Precracked Charpy Impact Fracture Toughness of Repair-Weld Heat-Affected Zones in 0.6-in.-thick Republic Heat 3920556, Grade 200, 18%-Nickel Maraging Steel Plate with Filler Wire 34482	149
Slow-Notch-Bend Fracture of Repair-Weld Heat Affected Zones in 0.6-in.-thick Republic Heat 3920556, Grade 200, 18%-Nickel Maraging Joint Configuration Steel Plate with Filler Wire 34482	150
Longitudinal Tensile Properties of Repair Weld Metals Deposited in 0.6-in.-thick Republic Heat 3920556, Grade 200, 18%-Nickel Maraging Steel Plate with Filler Wire 34482	151
Precracked Charpy Impact Fracture Toughness of Repair Weld Metals Deposited in 0.6-in.-thick Republic Heat 3920556, Grade 200, 18%-Nickel Maraging Steel Plate with Filler Wire 34482	152
Slow-Notch-Bend Fracture Toughness of Repair Weld Metal Deposited in 0.6-in.-thick Republic Heat 3920556, Grade 200, 18%-Nickel Maraging Steel Plate with Filler Wire Heat 34482	153

FIGURE LIST (cont.)

	Figure
Summary of Slow-Notch-Bend Fracture Toughness Data of Grade 200, 18%-Nickel Maraging Steel Plate, Weldments, and Repair Weldments	154
Layout of Gore-1-2B on Plate R-600-1A	155
Mill Certified Chemical Analysis of Lukens Plate R-600-1A	156
Comparison of Strength and Toughness Data for Plate R-600-1A and Formed Material from Gore 1-2B	157
Layout of Gore 1-2B	158
Specimen Configurations and Dimensions	159
Photomicrograph of a Cross-Section of Gore Segment 1-2B Through Joggle	160
Microhardness Transverse Results	161
Photomicrography of Resolution Annealed Material from Plate R-600-1A	162
Vertical Flanging Press Being Used for Cold Weld Straightening	163
Tensile Test Data Obtained from Straightened Welds Made with Lukens Plate R-600-1A and Special Metals Weld Wire 34481	164
A Comparison of Plane-Strain and Plane-Stress Fracture Toughness Values, Lukens Plate R-600-1A and Special Metals Weld Wire 34481	165
Effect of Cold Straightening of the Plane-Strain Fracture Toughness of Welds Made with Lukens Plate R-600-1A and Special Metals Weld Wire 34481, Slow-Notch-Bend Specimens	166
Plane-Stress Fracture of Straightened Weldments Made with Lukens Plate R-600-1A and Special Metals Weld Wire 34481	167
Assembled Furnace for Maraging 260-in.-dia Chamber	168
Thermocouple Recording Points, 280-in.dia Case	169

FIGURE LIST (cont.)

	Figure
260 Chamber Maraging Demonstration	170
Maximum and Minimum Case Temperature During Maraging Cycle	171
Greatest Temperature Difference for Case	172
Temperature Extremes vs Time, Forward Y-Joint Location	173
Temperature Extremes vs Time, Aft Y-Joint Location	174
Greatest Temperature Difference for Line 3	175
Identification of Plates Selected for the Complete Profile Maraging Study for 260-SL-1 Material	176
2600-SL-1 Material Characterization Tensile Data for a Complete Profile Maraging Cycle	177
260-SL-1 Material Characterization G_{nc} Data for a Full Profile Maraging Cycle	178
Effect of Heat-Up and Cool-Down Rates on Tensile Properties of Plate M, Plate A, and 63343 Automatic Welds	179
Effect of Hold Temperature on Tensile Properties of Plate M and 63343 Automatic Welds	180
Change in Strength of Plate M During Heat-Up to the Maraging Temperature	181
Composition of Republic Heat 3920556, 18%-Nickel Maraging Steel Plate and Filler Wire 34482	182
Fatigue Cracked Stress-Corrosion Specimen	183
Stress-Corrosion Test Fixture	184
Center-Notched Tensile Properties of Republic Heat 3920556 Grade 200, 18%-Nickel Maraging Steel Plate and Weld Deposited with Filler Wire 34482	185
Effects of Sodium Dichromate Inhibitor on the Stress-Corrosion Susceptibility of Grade 200, 18%-Nickel Maraging Steel Plate and Weldments	186

FIGURE LIST (cont.)

	Figure
Intergranular Cracking Observed in Center-Notch Tensile Specimen Prepared from 0.6-in.-thick Republic Heat 3920556, Grade 200, 18%-Nickel Maraging Steel Plate and Subjected to a Sustained Tensile Load of 170 ksi While Immersed in 1% Sodium Dichromate Solution for 45 Days	187
Process Evaluation Test Vehicle (PETV)	188
Configuration of PETV 1	189
Configuration of PETV 2	190
Thermocouple Location and Material Test Specimens for PETV 1	191
Thermocouple Location and Material Test Specimens for PETV 2	192
Test Results of Tensile Specimens Maraged with PETV 1	193
Test Results of Precracked Impact Specimens Maraged with PETV 1	194
Test Results of Tensile Specimens Maraged with PETV 1	195
Test Results of Tensile Specimens Maraged with PETV 2	196
Test Results of Slow-Notch-Bend Specimens Maraged with PETV 2	197
Test Results of Precracked Impact Specimens Maraged with PETV 2	198
Test Results of Weldment Specimens Maraged with PETV 2	199
Out-of-Round Measurements, Weld Identification, and Chamber Sections for PETV 1	200
Out-of-Round Measurements, Weld Identification, and Chamber Sections for PETV 2	201
Contour Map of PETV 1	202
Contour Map of PETV 2	203
Strain Gage Locations on PETV 1	204
Strain Gage Locations on PETV 2	205

FIGURE LIST (cont.)

	Figure
Strain Gage Locations Summary for 36-in.-dia PETV's	206
Typical Bolt Strain Gage (Strainsert) Installation	207
Test Setup Showing Chamber and Protective Netting	208
Test Setup Showing Forward Portion of Chamber and Wooden Test Stand	209
Hydraulic Schematic for PETV	210
PETV 1 After Burst	211
PETV 1 After Burst	212
Fracture in Forward Head of PETV 1	213
Fracture in Chamber Section of PETV 1	214
Fracture in 14-in.-dia Closure of PETV 1	215
PETV 1 After Burst	216
Strain-vs-Pressure Plot of Strain Gage Locations 1 and 15 on PETV 1	217
Pressure-vs-Inside of Outside Stress Plot at Strain Gage Location 2 on PETV 1	218
Pressure-vs-Strain Plot at Location 2 on PETV 1	219
Pressure-vs-Strain Plot at Locations 1 and 4 on PETV 1	220
Pressure-vs-Strain Plot at Locations 3 and 5 on PETV 1	221
Pressure-vs-Strain Plot at Locations 8 and 13 on PETV 1	222
Pressure-vs-Strain Plot at Locations 9, 11, and 14 on PETV 1	223
Pressure-vs-Strain Plot at Locations 10, 12, and 15 on PETV 1	224
Bolt Load-vs-Pressure Plot for PETV 1	225

FIGURE LIST (cont.)

	Figure
Fracture Pattern for PETV 1	226
PETV 2 After Burst	227
Aft Head and Portion of Cylinder after Burst of PETV 2	228
Fracture in Forward Head of PETV 2	229
Pressure-vs-Inside and Outside Hoop Stress at Strain Gage Location 8 on PETV 2	230
Pressure-vs-Strain Plot at Strain Gage Locations 1 and 2 on PETV 2	231
Pressure-vs-Strain Plot at Strain Gage Locations 3, 9, and 10 on PETV 2	232
Pressure-vs-Strain Plot at Strain Gage Locations 4, 5, 6 and 7 on PETV 2	233
Pressure-vs-Strain Plot at Strain Gage Locations 8 and 11 on PETV 2	234
Pressure-vs-Strain Plot at Strain Gage Locations 12 and 13 on PETV 2	235
Pressure-vs-Strain Plot at Strain Gage Locations 14 and 15 on PETV 2	236
Bolt Load-vs-Pressure Plot for PETV 2	237
Posttest View of Bulged Area Along Weld No. 2W1 on PETV 2	238
Posttest View of Fracture Pattern on PETV 2	239
Fracture Pattern for PETV 2	240

Report NASA CR 72126, Appendix B

I. PROGRAM OBJECTIVES

The material and process evaluation program was initiated to evaluate the material properties and fabrication process characteristics of the 18%-nickel steel. The program was conducted in a logical sequence to investigate and define significant variables early in the program (i.e., weld-wire composition, weld processing sequence, etc.) and to permit the fabricator to qualify his processes and personnel before initiating fabrication.

This procedure avoided, insofar as possible, the requirement to provide solutions to fabrication-process development problems concurrent with the fabrication of the 260-SL motor components. All work in this program was performed using the procedures, specifications, equipment, material, and personnel applicable to fabrication of the 260-SL motor chamber and nozzle shell. The effort resulted in the solving of process development problems ranging in character from re-establishing the plate solution-annealing temperature to training personnel for repair welding and operation of the maraging furnace.

II. PARENT PLATE EVALUATION

The objective of this phase of the material and process evaluation program was to evaluate the aging response, tensile and fracture toughness properties, and metallurgical characteristics of the parent metal plate.

The parent plate evaluation determined the acceptability of the Aerojet plate procurement specification and also served as a baseline for selecting weld-filler-wire chemistry and welding procedures.

The parent-plate evaluation was conducted both by Aerojet, Sacramento, and the chamber fabricator, Sun Shipbuilding. Aerojet evaluated two heats of plate material (Republic heats 3960524 and 3920556) to clearly establish material properties for subsequent welding investigations. Sun concurrently

II, Parent Plate Evaluation (cont.)

evaluated plate-material (Lukens heat R-599-1) mechanical properties and uniformity and metallurgical characteristics as a function of the temperature-time maraging cycle variable.

A. EVALUATION OF PARENT PLATES (REPUBLIC HEATS 3960524 AND 3920556)

The grade 200, 18%-nickel maraging steel alloy was specified for use in fabricating chamber and nozzle shell assemblies and components in the program. Prior to the initiation of the program, only limited studies had been conducted to establish welding techniques, parameters, and filler-wire compositions for joining grade 200, 18%-nickel maraging steel plate. To adequately evaluate the effectiveness of the welding parameters established in the welding evaluation program and the tensile, fracture-toughness, and metallurgical properties of the weldments produced, it was necessary to compare these properties with the mechanical and metallurgical properties of the base metals used in the welding studies. Consequently, the investigations outlined in this section were conducted to determine the aging response, tensile properties, fracture toughness, and metallurgical properties of the parent plate materials (Republic heats 3960524 and 3920556) used in the TIG welding investigations.

1. Experimental Procedures

a. Specimen Preparation

Tensile, slow-notch bend, and precracked Charpy impact tests were used to evaluate the aging response, tensile properties, and fracture toughness of the plate materials. The dimensions of these test specimens are shown in Figure 1. Two sizes of precracked Charpy impact specimens were used; a standard sized (0.394 by 0.394 in.) specimen for both heats 3960524 and 3920556 and a plate thickness (0.600 by 0.394 in.) specimen for heat 3920556.

II, A, Evaluation of Parent Plates (cont.)

The test specimens were oriented both longitudinally and transverse to the final rolling direction of the plates (see Figure 2). In the longitudinal test specimens, maximum strain was parallel to the final plate rolling direction. All fracture toughness specimens were machined with the notch through the thickness of the plate as indicated in Figure 2. In the longitudinal specimens, fracture was parallel to the rolling direction.

The test specimens were cut from the as-received plate, which was in the solution annealed condition. After machining to the dimensions shown in Figure 1, the specimens were age-hardened (maraged). Subsequent to aging and prior to testing, surface scale that had formed on the tensile specimens was removed with abrasive paper and the fracture toughness specimens were subjected to cyclic stresses to form a fatigue crack at the root of the notch.

b. Specimen Testing

Tensile specimens were tested in triplicate for each variable investigated. These tests were conducted in accordance with Federal Test Method Standard 151, using a strain rate of 0.005 in./in. Load and strain were recorded during the tensile tests and the resulting load strain diagram was used to determine the 0.2% offset yield strength. Elongation was measured over a 1-in. gage length.

Five slow notch bend specimens were tested for each variable to determine qualitative plane-strain fracture toughness values and the effect of aging cycle and specimen orientation on this material property.

Eight precracked Charpy impact specimens were tested to determine qualitative plane-stress fracture toughness values for each heat of plate material. Duplicate specimens were tested at each of four temperatures

"REPRODUCIBILITY OF THE ORIGINAL PAGE IS POOR;
FOR BETTER COPY CONTACT THE DOCUMENT ORIGINATOR"

to establish the relationship between fracture toughness and test temperature. The precracked Charpy impact specimens were tested at ManLabs Inc., using a subsize impact testing machine that provides energy readings with an accuracy of ±0.010 ft-lb in the low energy range of 1 to 5 ft-lb.

Conventional metallographic procedures were followed during the program. Inclusion ratings were established by examining the specimens in the as-polished condition. Grain-size determinations were made with a 10% chromic-acid electrolytic etch to define the prior austenitic grain size which was rated according to ASTM E112-61. General microstructure evaluations were performed using Marble's etchant in order to emphasize the martensitic microstructure and, in conjunction with Knolls etchant, to determine the presence of banding and/or severe alloy segregation.

2. Materials

Grade 200, vacuum-arc remelted, 18%-nickel maraging steel plate from Republic heats 3960524 and 3920556 was evaluated. Both heats of material were received in the solution-treated (1500°F for 1 hr) condition. Each plate was inspected for defects at the mill and at Aerojet, using ultrasonic and magnetic particle inspection techniques in accordance with Aerojet specifications AGC 32115 (ultrasonic) and AGC 32116 (magnetic particle) and were found to be within the acceptable requirements of these specifications. Copies of these specifications are included in Appendix A.

The chemical composition of the two heats and the composition limits specified in the applicable Aerojet procurement specification are presented in Figure 3. Although the cobalt and molybdenum contents of heat 3960524 were not in accordance with the procurement specification, the material was purchased because it was expected that its yield strength would fall within

II, A, Evaluation of Parent Plates (cont.)

the upper limit (235 ksi) specified for the 260-in.-dia motor program. In addition, previous experience with 18%-nickel maraging steel at this strength level indicated that the fracture toughness of heat 3960524 would be acceptable. The use of this heat also provided immediately available material for the welding evaluations which could not be obtained at any other source. As indicated in Figure 3, the chemical composition of heat 3920556 was within specified limits.

Metallographic examinations were conducted on each plate to establish microstructure, grain size, and inclusion ratings. Photomicrographs showing typical microstructures, prior austenitic grain size, and the most severe areas of inclusions, are presented in Figures 4 and 5. As indicated in these figures, a typical martensitic microstructure was observed in both heats of plate material, and no areas of banding or severe alloy segregation were noted. The prior austenitic grain size for both heats was ASTM 7, when rated in accordance with ASTM E112-61. This grain size is considered typical for 0.6-in.-thick, vacuum-arc remelted, 18%-nickel maraging steel plate and is within the requirements of the applicable Aerojet specification (AGC 34315). Inclusion ratings for the plates are shown below and are also within the requirements of the applicable Aerojet specification.

	A (Sulphides)		B* (Aluminates)		C (Silicates)		D (Oxides)	
Heat No.	Thin	Heavy	Thin	Heavy	Thin	Heavy	Thin	Heavy
3960524	<1/2	<1/2	1	1	<1/2	<1/2	<1/2	<1/2
3920556	<1/2	<1/2	1/2	1/2	<1/2	<1/2	<1/2	<1/2

*Titanium nitrite stringers are rated as type B inclusions.

II, A, Evaluation of Parent Plates (cont.)

3. Results and Discussion

The desirable combination of properties attained in the 18%-nickel maraging steel alloys was achieved by age-hardening the low-carbon martensite that is formed in these materials when they are cooled from the solution annealing temperature in excess of 1500°F. The extent to which the low-carbon martensite is age-hardened varies primarily as a function of the cobalt, molybdenum, and titanium content of the steel and the aging temperature and time employed in heat treatment. Relationships between tensile properties, fracture toughness, and aging temperature and time define the aging response of the material.

a. Aging Response--Tensile Properties

Tensile specimens from each heat were processed in accordance with the following schedule of aging treatments to establish relationships between tensile properties and aging time and temperature.

Heat No.	Aging Temperature, °F	Aging Time, hr
3960524	850	4, 8, 16, 24
	900	2, 4, 8, 16, 24
	950	2, 4, 8, 16, 24
3920556	850	8, 16, 24
	900	4, 8, 16, 24
	950	4, 8, 16, 24

These aging cycles were selected on the basis of previous investigations of 18%-nickel maraging steel alloys to provide tensile property data for the material in the underaged, maximum aged, and overaged condition, and which would bracket the aging cycle anticipated for heat-treating the 260-in.-dia motor components.

II, A, Evaluation of Parent Plates (cont.)

(1) Heat 3960524

The tensile properties of Republic heat 3960524 after various aging times and temperatures are listed in Figure 6. The tensile properties of this heat in the longitudinal orientation are plotted in Figure 7 to illustrate the effects of aging time and temperature on the 0.2% offset yield strength, ultimate tensile strength, and elongation and reduction of area. The effects of aging time and temperature on the 0.2% offset yield strength of this heat in the longitudinal orientation are summarized in the following tabulation:

Aging Temperature, °F	0.2% Offset Yield Strength, ksi Aging Time, hr				
	2	4	8	16	24
850	-	230	238	242	249
900	229	234	239	232	228
950	233	231	219	-	206

On aging at 850°F, the 0.2% offset yield strength increased with increasing aging times up to the maximum time investigated and did not show evidence of overaging. With an aging temperature of 900°F, tensile strength increased with aging times up to 8 hr and slight overaging, as indicated by a reduction in both 0.2% offset yield and ultimate strength, occurred after 16 and 24 hr. At the 950°F aging temperature, maximum strength was observed after the 2-hr aging treatment, and overaging occurred when aging times of 8 hr or greater were used.

It was possible to vary the tensile properties of heat 3960524 over a wide range by varying the aging treatment. The 0.2% offset yield strength of this heat ranged from a maximum of 249 ksi after aging at

II, A, Evaluation of Parent Plates (cont.)

850°F for 24 hr to a minimum of 209 ksi after aging at at 950°F for 24 hr. Intermediate yield strengths of 220 to 239 ksi were obtained with aging times of 4 and 8 hr at 850°F, 2, 4, and 8 hr at 900°F, and 2 and 4 hr at 950°F.

The effects of specimen orientation on the tensile yield strength of plate from heat 3960524 are summarized in the following tabulation:

		0.2% Offset Yield Strength, ksi		
		Aging Time, hr		
Aging Temperatures, °F	Orientation	4	8	24
850	Longitudinal	230	238	249
	Transverse	-	248	250
900	Longitudinal	234	239	228
	Transverse	240	244	233
950	Longitudinal	231	219	206
	Transverse	226	-	210

After most aging cycles, the tensile yield strength of the plate in the transverse orientation was slightly higher than in the longitudinal orientation. The difference in yield strength ranged from a maximum of 10 ksi after aging at 850°F for 8 hr to a minimum of 1 ksi after aging at 850°F for 24 hr. The slight anisotropy observed in the yield strength of this heat is typical for the 18%-nickel maraging steels and varies with mill processing practice.

The ductility of plate from heat 3960524 varied with aging time and temperature, depending on the strength level attained after each aging cycle evaluated. The percent of elongation varied from a minimum of 9.7% in the transverse orientation after aging at 850°F for 24 hr to a maximum of 14.3% in the longitudinal orientation after aging at 950°F for 24 hr.

II, A, Evaluation of Parent Plates (cont.)

These minimum and maximum values in the percent of elongation accompanied the maximum and minimum values for 0.2% offset yield strength, respectively. Reduction of area varied from approximately 55 to 64%, but these minimum and maximum values were not directly related to the extreme values in the 0.2% offset yield strength.

All of the aging cycles investigated resulted in tensile yield strengths of plate from heat 3960524 above the minimum specified value (200 ksi) for the 260-in.-dia motor program. Also, after many of the aging cycles evaluated, the tensile yield strength of this heat exceeded the maximum value of 235 ksi specified. Consequently, this material may be considered to represent the higher strength heats that were accepted for use in fabrication of motor components.

(2) Heat No. 3920556

The effects of specimen orientation and aging time and temperature on the tensile properties of plate from heat 3920556 are shown in Figure 8. The tensile properties of this heat in the longitudinal orientation are plotted as a function of aging temperature and time in Figure 9. The 0.2% offset yield strength of this heat in the longitudinal orientation after various aging cycles is summarized below:

	0.2% Offset Yield Strength, ksi			
	Aging Time, hr			
Aging Temperature	4	8	16	24
850	198	211	220	239
900	214	218	223	231
950	215	219	222	225

II, A, Evaluation of Parent Plates (cont.)

As indicated by these data, the yield and ultimate strengths of this heat increased with increased aging time at each aging temperature, and evidence of overaging was not observed at any of the three aging temperatures for aging times up to 16 hr. However, the tensile strength was slightly lower after aging at 900 and 950°F for 24 hr than after aging at 850°F for 24 hr, which could evidence that slight overaging occurred during aging at 900 and 950°F for 24 hr.

The effect of specimen orientation on the tensile yield strength of heat 3920556 are summarized in the following tabulation:

		0.2% Offset Yield Strength, ksi			
		Aging Time, hr			
Aging Temperature, °F	Orientation	4	8	16	24
850	Longitudinal	-	211	-	239
	Transverse	-	214	-	233
900	Longitudinal	224	218	222	233
	Transverse	218	220	222	231
950	Longitudinal	215	-	-	225
	Transverse	219	-	-	220

With the exception of the 24-hr aging treatments, the yield strength in the transverse orientations was slightly higher than in the longitudinal orientation. However, the difference (6 ksi maximum) in yield strength as a function of specimen orientation is considered minimal and results primarily from variations in mill processing techniques. Variations in ductility (percent of elongation and reduction in area) with specimen orientation and aging cycle were similar to those observed with heat 3960524.

II, A, Evaluation of Parent Plates (cont.)

After aging at 850°F for 4 hr, the 0.2% offset yield strength (198 ksi) of this heat was slightly below the minimum specified (200 ksi) for the program. After aging at 850°F for 24 hr, the 0.2% offset yield strength (239 ksi) slightly exceeded the maximum (235 ksi) specified. Consequently, Republic heat 3920556 is considered a representative heat which would be obtained in accordance with the requirements of Aerojet Specification AGC 34315. Also, the ultimate strength of heat 3920556 was lower than that of heat 3960524, when both heats were aged to maximum strength. However, the ductilities of both heats were similar when heat-treated to the same level.

b. Fracture Toughness

The fracture toughness of each heat of 18%-nickel maraging steel plate was evaluated on the basis of slow-notch-bend (SNB) and precracked Charpy impact (PCI) tests with the notch oriented through the plate thickness. The plane-stress fracture toughness value (W/A) obtained from the PCI tests has been shown to approximate (within 10%) the plane-strain fracture toughness values (G_c) obtained with the center notch tensile test and also provides a measurement of the effect of test temperature on fracture toughness.

The aging cycles selected for fracture toughness evaluation using SNB and PCI specimens are shown below:

Specimen	Aging Temperature, °F	Aging Time, hr
Precracked Charpy Impact	850	8
	900	8
	950	8
	900	24
Slow-Notch-Bend	850	8, 16, 24
	900	4, 8, 16, 24
	950	4, 8, 16, 24

"REPRODUCIBILITY OF THE ORIGINAL PAGE IS POOR."

II, A, Evaluation of Parent Plates (cont.)

(1) Slow-Notch-Bend Test For Plane-Strain Fracture Toughness

(a) Heat 3960524

The plane-strain (SNB) fracture toughness of heat 3960524, as a function of specimen orientation, aging temperature and aging time, is shown in Figure 10. Fracture toughness was calculated by Bueckner's method and by the spring-constant method (using both Rawe's analysis and 5-point smoothing). The ranges and average values of fracture toughness based on the spring-constant (G_{Ic}) include two methods of analysis and two calibration runs.

As indicated by the data shown in Figure 11, at a given aging temperature, an increase in aging time (from 4 to 24 hr) had neither a significant nor a consistent effect on plane-strain fracture toughness in spite of a decrease in yield strength on overaging at 900 to 950°F. Likewise, aging temperature did not have a significant effect on fracture toughness. Conversely, test data for the two specimen orientations investigated appeared to be significantly different, with the transverse-specimen orientation exhibiting values of G_{Ic} between 40 and 211 in.-lb/sq in. lower than the longitudinal specimen orientation. The average difference in fracture toughness (G_{Ic}) between the transverse and longitudinal specimens was 106 in.-lb/sq in. The lower toughness in the transverse-specimen orientation was consistent with the higher 0.2% offset yield strength values in the transverse-specimen orientation.

II, A, Evaluation of Parent Plates (cont.)

(b) Heat 3920556

The plane-strain fracture-toughness data for heat 3920556 as a function of specimen orientation, aging temperature and aging time, are shown in Figure 12. Fracture toughness was calculated both by Bueckner's method and by the spring-constant method (5-point smoothing). As indicated by the data in Figure 13, aging temperature had no significant effect and, with one exception, aging time (from 4 to 24 hr) had no significant effect on the plane-strain fracture toughness irrespective of the significant increase in 0.2% offset yield strength with increased aging time. One exception was observed in the transverse-specimen orientation aged at 850°F where a decrease in toughness of more than 100 in.-lb/sq in. was encountered after aging at 24 hr in comparison to the data obtained after the 850°F for an 8-hr aging treatment. This decrease in toughness was accompanied by a significant increase (28 ksi) in yield strength. In contrast to heat 3960524, there was no significant difference between the fracture toughness of longitudinal and transverse specimen orientations. However, this effect was consistent with little or no difference in yield strength between the two specimen orientations.

(c) Critical Defect Size

A comparison of the fracture toughness data for heats 3920556 and 3960524 indicates that, when aged to the same 0.2% offset yield strength level, the two heats exhibited approximately the same slow-notch-bend fracture toughness, with average values ranging from approximately 450 to 600 in.-lb/sq in. at a 0.2% offset yield strength of 225 ksi. The G_{Ic} values correspond to K_{Ic} values of approximately 116 to 134 ksi $\sqrt{in.}$ and the following critical surface flaw lengths, assuming the indicated flaw shape and an operating stress of yield-strength (225 ksi) magnitude:

II, A, Evaluation of Parent Plates (cont.)

Flaw Configuration (Surface Depth/Length)	K_{Ic}, ksi $\sqrt{in.}$	Critcal Flaw Length, in.
0.1	116	0.62
0.1	134	0.84
0.3	116	0.33
0.5	116	0.31

In interpreting these data, a critical flaw shape, corresponding to a surface depth/length ratio 0.1, is the most severe condition from a performance consideration, while flaw depth/length ratios of 0.3 and 0.5 are the most critical in terms of nondestructive inspection capability. As indicated by these data, critical surface flaw lengths characteristic of both types of defects should be detected using available nondestructive inspection techniques (magnetic particle, X-ray, dye penetrant, and ultrasonic).

(2) Fatigue-Precrack Charpy Impact Testing for Plane-Stress Fracture Toughness

(a) Heat 3960524

The data presented in Figures 14 and 15 show the precrack Charpy impact fracture toughness (W/A) data for heat 3960524 after various aging treatments. These data show increasing toughness with increasing aging temperature, increasing toughness with increasing test temperature, and greater toughness in longitudinal test specimens. At a 900°F aging temperature, an increase in aging time from 8 to 24 hr produced a significant increase in toughness. Both the 950°F/8 hr and 900°F/24 hr aging treatments resulted in overaging as measured by tensile properties.

II, A, Evaluation of Parent Plates (cont.)

(b) Heat 3920556

The data presented in Figure 16 show the precrack Charpy impact fracture toughness (W/A) data for heat 3920556 after various aging treatments. These data show a trend toward decreasing toughness with increasing aging temperature, increasing toughness with test temperature, and little difference in fracture toughness between the longitudinal and transverse specimen orientation. A comparison between the precracked Charpy impact fracture toughness of heats 3960523 and 3920556 is complicated by a difference in specimen size. However, from the data shown in Figures 14 and 15, heat 3920556 was significantly tougher than heat 3960524, considering that a wider specimen was used in testing heat 3920556; the wider (0.575 in.) test piece would be expected to indicate lower fracture toughness values.

A comparison of the SNB and PCI test results for both heats indicates that, although specimen orientation had similar effect in the two tests, aging temperature produced different effects in the two tests. Aging temperature did not have a significant effect on SNB fracture-toughness in either plate material. However, PCI toughness increased with aging temperature in heat 3960524. The different trends in fracture toughness as a function of aging cycle are attributed to the fact that SNB fracture toughness is a function of the energy required to initiate crack growth while PCI fracture toughness is primarily a function of the energy to propagate fracture.

B. EVALUATION OF LUKENS PLATE R-599-1

This material evaluation task was conducted for the purpose of selecting optimum maraging cycles for production plate material characterizations that would give maximum values of toughness with satisfactory yield strength and to supplement the parent plate evaluation conducted by Aerojet-General. Lukens plate R-599-1 was selected for this study, since this material

II, B, Evaluation of Lukens Plate R-599-1 (cont.)

closely approximated the plates to be used in the actual fabrication of the motor chambers. This plate was rolled from a forged slab 119 by 61 by 6 in. thick which was cut from the bottom of a 30-in.-dia vacuum-arc remelted ingot. The plate was finished to a final size of 507 by 123 by 0.610 in. and solution-annealed at 1500°F for 1 hr. The mill-certified analysis on the chemical composition, averaged from four locations on the plate, is given in Figure 17. A complete report of this subtask of the materials and process evaluation program has been prepared by Sun Shipbuilding, Reference 5.

1. Specimen Preparation and Testing

A total of 168 tensile and slow-notch-bend tests were conducted to evaluate the tensile strength and plain strain fracture toughness of a 0.610-in.-thick, 200-ksi maraging steel plate in both the longitudinal and transverse directions. All specimens tested were taken from one plate area and compared the longitudinal and transverse directional properties of the plate. The data showed that the fracture toughness varies with the maraging cycle for plate material.

a. Tensile Specimens

Upon receipt of plate R-599-1, seventy-two 0.250-in.-dia specimens from the plate area (denoted as Top 5 in Figure 8), 36 in the longitudinal and 36 transverse to the rolling direction, were machined for tensile testing. All machining operations were performed with adequately cooled specimen material.

The samples were maraged in a calibrated convection furnace at the Sun Oil Metallurgical Laboratories at temperatures of 850, 900, and 950°F for periods ranging from 2 to 32 hr as shown below.

II, B, Evaluation of Lukens Plate R-599-1 (cont.)

Temperature, °F	Time, hr
850	4
	8
	16
	32
900	2
	4
	8
	16
950	2
	4
	8
	16

The specimens were testing on a 120,000-lbf Riehle universal hydraulic tensile tester with a certified calibration within ± 1.0%. The test area temperature ranged from 76 to 80°F, with the relative humidity between 24 and 48%. The strain rate during loading to yield was 0.010 in./in./min.

b. Slow-Notch-Bend Specimens

The fracture toughness testing was accomplished with 56 longitudinal, 20 transverse, and 20 short transverse specimens for the slow-notch-bend test and 10 calibration bars, all from the plate area denoted as Top 1 in Figure 18. The linear dimension from the root of the notch to one end of the specimen was held to within 0.002 in. during machining, thus enabling the specimen to be accurately positioned in the bending test fixture.

II, B, Evaluation of Lukens Plate R-599-1 (cont.)

All longitudinal and transverse bend specimens were notched through the plate thickness, and the short transverse specimens were notched along the plate surface. These specimens were maraged at the Sun Oil Metallurgical Laboratories at temperatures of 850, 900, and 950°F for periods, ranging from 4 to 32 hr as shown below:

Temperature, °F	Time, hr
850	4
	8
	16
	32
900	4
	8
950	4
	8
	16

After fatigue cracking, the bend specimens were tested in a Riehle universal hydraulic tensile tester with a Sun-designed and -fabricated, three-point bending fixture attached. A specimen rate of 0.020/0.025 in./min was used. Load and deflection were autographically recorded for each specimen; an example of such a record is shown in Figure 19. The deflection is picked up from a linear differential transformer located between the top and bottom plates of the fixture.

The point where the load deflection curve deviates from linearity is marked on the graph. This point is analyzed further to yield plane-strain fracture toughness values. On many of the load deflection curves, a jog (constant load with increasing deflection) was noted near the point of deviation from linearity. This jog probably corresponds with a rapid fracture.

II, B, Evaluation of Lukens Plate R-599-1 (cont.)

The calibration bars were loaded within their linear elastic limits, and the maximum loads for the various notch depths are given below:

Depth, in.	Maximum Load, lb
0	6000
0.100	6000
0.150	6000
0.175	6000
0.200	6000
0.225	6000
0.250	4800
0.275	4800
0.300	3600
0.325	3600

Each specimen was loaded three times and the average load deflection slope for the three runs was recorded.

Plane strain toughness values (G_{nc}) are calculated using the calibration curve for the material tested. Toughness values by the Bueckner analysis (G_{Ic}) were calculated, using half of each specimen positioned in a comparator, and notch depth was measured.

2. Analysis of Results

a. Tensile Specimens

The data from the tensile tests for all 72 specimens is tabulated in Figure 20 and is plotted in Figures 21 through 24. Upon examination of these plots, it can be seen that all of the maraging cycles, with the exception of the long-time 850°F cycle, produced yield strengths between 200

II, B, Evaluation of Lukens Plate R-599-1 (cont.)

and 235 ksi. The strength response to the various maraging cycles is considered typical for this material. Where strength losses were observed at times longer than those which showed maximum yield strengths, overaging of the material was indicated. The results of the aging cycles for each orientation are discussed separately.

(1) Longitudinal Orientation

At 850°F the yield strength for the longitudinal specimens increased with the longer aging times. At 900°F the maximum strength was achieved at about 4-hr aging time and remained constant to 16 hr. Maximum strength was achieved in 4 hr at 950°F; however, longer aging times resulted in a loss in strength, although no additional strength losses occurred between 8 and 16 hr, which indicates that the material had been overaged at 950°F.

With higher longitudinal strength levels, a characteristic decrease in reduction of area values was exhibited. This characteristic was independent of orientation as evidenced by comparing the transverse to the longitudinal direction values shown in Figure 21. However, at 850°F, the 8 to 16 hr cycles in which the significant strength increases occurred showed no losses in reduction of area values. All tensile-specimen reduction of area values fell between 48 and 61%.

(2) Transverse Orientation

Throughout all of the maraging cycles, the transverse strengths were consistently higher than the longitudinal strengths. At 950°F, where a loss in strength had been exhibited at longer times in the longitudinal direction, no strength change occurred in the transverse direction, but a decrease of 2 to 3% in reduction of area values did occur. Although the reduction of area measurement (Figure 20) is considered to be a more sensitive measurement of ductility, elongation measurements made for all aging cycles

II, B, Evaluation of Lukens Plate R-599-1 (cont.)

within one orientation showed no significant variation as a function of aging cycle. All values were between 10 and 11%. The minimum anistropy in yield strength (3 to 4 ksi) occurred at 950°F for the 4-hr cycle and at 900°F for the 8-hr cycle.

b. Slow Notch Bend Specimens

The characteristic trend of increasing toughness values with decreasing strength values is shown in Figure 25. This figure is an overall presentation of the tensile and bend specimen data for the R-599-1 plate. The slope of the data band is indicative of the material toughness sensitivity to changes in yield strength. The slow-notch-bend data for plate R-599-1 is tabulated in Figure 26.

In Figures 27, 28, and 29, the influence of maraging time and terperature on strength and toughness is readily apparent. Figure 30 compares Bueckner's analysis to the spring constant method of analysis. The plane strain fracture toughness values (longitudinal) tend to peak around the 8-hr heat treatment. Underaging this plate material at 850°F and 900°F for 2 to 4 hr would not result in high toughness, although the yield strength values are low. Overaging at 950°F and the attempt to overage to 850°F did not result in low toughness in relation to yield strength. The specimens aged at 950°F possessed the highest toughness values and the lowest strength values.

Although the notches in the slow-notch-bend specimens are not geometrically similar to surface flaws, values of G_{nc} obtained from these specimens define a material property and may be used to calculate critical flaw sizes. For typical G_{nc} values, calculated critical surface flaw sizes with a depth to length ratio of 0.1 are as follows:

II, B, Evaluation of Lukens Plate R-599-1 (cont.)

Orientation	G_{nc}, in.-lb/in.^{2}	Critical Flaw Depth, in.
Longitudinal	350	0.070
Transverse	250	0.050

C. EVALUATION OF PLATE-ANNEALING TEMPERATURE

During the early phases of steel plate procurement, the plate suppliers recommended changes in the solution-annealing temperature for plate material specified in the Aerojet procurement specification; the specification requirement was 1500°F ± 25°F. The need for a change in the solution-annealing temperature became evident when the plates produced exceeded the maximum yield strength level (235 ksi). An evaluation of the effect of solution-annealing temperature was then conducted and a report was prepared by Sun Shipbuilding, (Ref 6).

By February 1964, 13 Allegheny Ludlum plates and five Republic plates had been solution-annealed. Allegheny Ludlum informed Sun that tensile tests and photomicrographs taken from crop ends on four plates would not meet the Aerojet plate material procurement specification. At this time, four other Allegheny Ludlum plates annealed at 1500°F had been completely processed and shipped. It was not possible to reanneal these plates since they had been ground to gage and sufficient material was not present to remove the scale which would result from reannealing.

To determine the minimum annealing temperature for the remaining plates produced, as well as for reannealing plates not yet delivered, a test plan that combined metallographic and mechanical testing was prepared. Sun obtained crop ends from four Allegheny Ludlum plates for use in this evaluation. Republic Steel ran pilot tests to reanneal four plates and to qualify the annealing of ten additional plates. Cameron also ran qualifying tests on three 1-1/2-in. gage plates before annealing.

II, B, Evaluation of Lukens Plate R-599-1 (cont.)

1. Allegheny Ludlum Plate Material

The first indication that Allegheny Ludlum plates would not meet the Aerojet plate specification was received in February 1964. Allegheny Ludlum had conducted pilot tensile tests on plates from four heats of material listed in Figure 31. These specimens were taken from crop ends after the plates were annealed at 1500°F. Transverse yield strengths from 235 ksi to 243 ksi resulted from an aging cycle of 890°F for 4 hr. Directionality in strength between longitudinal and transverse orientations was between 7 ksi and 27 ksi, and the microstructures were not recrystallized.

For comparison purposes, the tensile results obtained from the same plate material after a 1650°F reannealing heat treatment are also shown in Figure 31. An average decrease in transverse strength of 15 ksi is shown, while the longitudinal strength decreased only 5 ksi after the reannealing. Comparing all of the reannealed plates in both plate orientations, the maximum strength difference was 14 ksi. A general increase in ductility was also shown in the reannealed plate specimens.

The tensile results for plates annealed at 1500°F by Allegheny Ludlum are tabulated in Figure 32. The yield strength values are not appreciably higher than those for the reannealed plates, and the strength directionality was less than 10 ksi. However, these plates did not show fully recrystallized microstructures. Additional testing to further evaluate strength and toughness was performed as part of the material characterization program.

After the Allegheny Ludlum test results were received, Sun obtained unannealed crop ends of the four plates annealed at 1500°F. The results of metallographic analysis conducted at Sun Oil indicate the recrystallization of the microstructure occurred between 1600 and 1700°F. To assure recrystallization of different gage plates annealed with a 50°F temperature tolerance, a solution-annealing temperature range of 1650 to 1700°F was selected

II, B, Evaluation of Lukens Plate R-599-1 (cont.)

for evaluation. To assure that strength properties would be satisfactory in this temperature range, tensile specimens were taken from each plate. The specimens were laboratory annealed at 1600, 1650, and 1700°F before aging. The test results are tabulated in Figure 33. The test data show an excellent grouping of strength results, which was generally around 220 ksi yield strength in the longitudinal direction and 225 ksi yield strength in the transverse direction. These data agree with the mill test results (Figure 31), and indicate that recrystallization had occurred in this temperature range and that changes in microstructure had not taken place before changes in strength.

PCI specimens were also taken from the four plates listed in Figures 31 and 33, and the test results are tabulated in Figure 34. In general, the W/A values for the two plates that were 0.610-in. gage were about 825-in.-lb/sq-in., while the 0.410-in. gage plate values were around 575 in.-lb/sq in. No difference in W/A values resulted from specimens annealed at 1650 and 1700°F. The 1600°F annealed specimens were incorrectly tested at -40°F. This latter data grouped more closely together, but this is a characteristic of the impact test at the lower test temperature.

It was difficult to evaluate the reason for a 50% difference in W/A values for the different gage plates, which had essentially the same plate chemistries, strengths, grain sizes, and inclusion ratings. Because of the difference in plate gage, the impact specimens were 0.394 and 0.600 in. wide. To determine whether part of the difference in W/A values arose from specimens of different width, a comparison was made using Allegheny Ludlum plate 25000-1.

The impact data shown in Figure 35 compares W/A values for Allegheny plate 25000-1 of impact specimens which were 0.394 and 0.600 in. wide. All specimens were taken along the longitudinal plate orientation, and the specimens of different width were aligned to eliminate variations in plate location.

II, B, Evaluation of Lukens Plate R-599-1 (cont.)

It was concluded that from these data the influence of the precracked impact specimen width (0.394 and 0.600 in.) on W/A values is not appreciable and is generally within a 10% band of experimental accuracy. This comparison is valid over a range of W/A values from 700 to 1000 in.-lb/sq in. The 50% difference in W/A values exhibited by the four-plate comparison must then be a true difference which is not obscured by specimen size or scatter of data.

2. Republic Plate Material

Four Republic plates were ordered to be reannealed at 1650 and 1700°F. Comparison data for the 1500°F and the 1650 to 1700°F reannealing temperature are shown in Figure 36. A decrease of about 15 ksi in transverse yield strength and about 5 ksi in longitudinal yield strength was evidenced by the higher reannealing temperature. All plate yield strength ranged between 204 and 219 ksi for both orientations, with less than 10 ksi directionality after reannealing.

On subsequent plates, Republic was requested to perform a combined tensile and metallographic study before annealing. The results of these studies are shown in Figures 37 and 38. In the annealing temperature range of 1650 to 1700°F, no significant changes in strength were noted. For all seven plates, yield strength ranged between 205 ksi and 211 ksi with directionality less than 10 ksi. The metallographic analysis showed recrystallized microstructures with fine grain structures at annealing temperatures between 1650 and 1700°F.

3. Cameron Plate Material

Cameron conducted a solution-annealing evaluation on the three 1-1/2-in. gage plates that was scheduled for the 260-SL-1 nozzle shell

"REPRODUCIBILITY OF THE ORIGINAL PAGE IS POOR"

II, B, Evaluation of Lukens Plate R-599-1 (cont.)

cone sections. The tensile results from this study are shown in Figure 39. The photomicrographs for these plates showed an equiaxed grain structure at the lower annealing temperatures with a tendency toward further refinement at the 1650 and 1700°F annealing temperature.

Based on the plate acceptance data shown in Figure 40, all strength values ranged between 210 and 216 ksi with very minor directionality.

Based on the findings of this evaluation, all subsequent orders for plate material for both motors were placed with a 1650 to 1700°F solution-annealing temperature range. In addition, the Aerojet plate procurement specification AGC-34315 was revised to require solution-annealing in the range between 1650 and 1700°F.

III. FORGING MATERIAL EVALUATION

The design of the 260-in.-dia motor chamber and nozzle shell components required the use of large-diameter, thin-walled, ring-rolled forgings, which were used in the chamber forward and aft Y-ring skirt attachments and the chamber-to-nozzle attachment flange. Forgings were also used in the nozzle shell for the entrance flange, throat section, and exit section. Each component represented custom-forged shapes; very little experience existed in forging 18%-nickel steel, particularly to the size and configuration required.

A program was developed for forging evaluation consistent with the overall program objective of thorough understanding of material and process characteristics. The three forged components of the 120-in.-dia motor nozzle shell were tested and evaluated as subscale components for 260-in.-dia motor application. The complete results of this forging evaluation program are presented in a report prepared by Sun Shipbuilding (Ref 7).

Because of the differences in material, forging configuration, and the type of test material available, the test program for the entrance flange differed from that for the intermediate section and exit flange; hence, the two test programs are discussed separately. Additional testing performed on the forgings by Sun Shipbuilding, including acceptance tests and experimental weldments, was also presented in the evaluation.

A. ENTRANCE FLANGE

1. History of Material and Forging Practice

Vacuum-arc remelted, 200-ksi maraging steel from Lukens heat R-559 was supplied to Ladish in the form of a 10-in.-thick slab, measuring 50 in. long by 28 in. wide. A 2-in.-thick coupon was removed from one end of the slab section, and stock acceptance tests were conducted for comparison to Aerojet Specification AGC-34316. This testing included the analyses presented below.

III, A, Entrance Flange (cont.)

a. Chemical Analysis

The chemical analysis of the slab section conformed to specification requirements, as shown in Figure 41.

b. Microcleanliness

The Ladish microcleanliness rating for the slab section is recorded below.

	AGC-34316 Limits		Slab Section	
Inclusion Type	Thin	Heavy	Thin	Heavy
A	2	1.5	0	0
B	2.5	1.5	0	0
C	2	1.5	0	0
D	2.5	2	0.5	0

Ladish did not rate titanium nitrides in the microcleanliness check. If rated by the D type, the values would be 1.5 for thin series and 1.0 for heavy series.

c. Mechanical Properties

Room-temperature tensile tests were conducted on specimens machined from the test bars forged at 1900°F. These forged test bars were subsequently solution-annealed at 1500°F for 1 hr, air cooled, aged at 890°F for 4 hr, and again air cooled (in accordance with Aerojet specification AGC-34316). The resultant properties of the specimens in the forging directions indicated are listed in Figure 42.

III, A, Entrance Flange (cont.)

2. Forging Procedures

The following forging practice was used to shape the entrance flange from the slab section:

a. Reforge to approximately 20-in. octagon from original 10-in.-thick by 28-in.-wide stock size. Metal temperature during working was 2060 to 1510°F.

b. Upset to 9 in. thick by 41 in. diameter. Metal temperature range was 2030 to 1715°F.

c. Plug and punch hole. Metal temperature range was 1960 to 1660°F.

d. Three-pass saddle roll to 19-in. ID by 44-in. OD by 12 in. high. Metal temperature range was 1980 to 1490°F.

e. Flatten and ring roll in four passes to final forging configuration. Metal temperature range was 1900°F to color (approximately 1400°F).

After forging, the flange was rough-machined to a rectangular cross section and tested ultrasonically using Ladish in-process quality control inspection routines; no defects were noted.

After ultrasonic inspection, an ID test ring was parted from the as-rolled flange and metallurgically evaluated to determine the optimum solution annealing temperature. An optimum annealing temperature of 1625°F was established, after which the test ring was laid into its original position in the flange, and both were solution annealed.

III, A, Entrance Flange (cont.)

Subsequent to solution annealing, an OD test ring was parted from the flange, and the balance of the process evaluation testing was performed on both test rings. Figure 43 shows the approximate dimensions and locations of the test rings in the final rough machined configuration.

After completion of the heat treatment and machining to final rough machined configuration, the flange was again ultrasonically inspected. Magnetic particle inspection in accordance with the provisions of Aerojet specification AGC-32116 was also performed; no defects were noted.

3. Testing Procedures and Results

The testing conducted by Ladish fell into three general categories:

a. Solution annealing response.
b. Maraging response.
c. Uniformity and directionality.

Procedures for these tests and results obtained are outlined below; locations of test material are shown in Figure 43.

a. Solution Annealing Response

A preliminary investigation to determine the optimum solution-annealing temperature for the flange was conducted by removing a tangential gradient bar from the ID test ring B (Figure 44) and solution-annealing over a temperature range from 1100 to 2100°F. Photomicrographs were taken at 100°F intervals along the bar, as shown in Figure 45. It can be seen that recrystallization (evidenced by the equiaxed, refined microstructure) is complete at 1600°F, and grain coarsening begins at approximately 1800°F.

III, A, Entrance Flange (cont.)

Based on the metallographic examination of the tangential gradient bar, five solution-annealing temperatures (1500, 1600, 1700, 1800, and 1900°F) were selected for study. Two tensile specimens (four at 1800 and 1900°F), two V-notch Charpy impact specimens, and three precracked impact specimens from the ID test ring B, shown in Figure 43, were solution-annealed at each of these temperatures, maraged at 890°F for 4 hr, and tested at room temperature. The orientation of the specimens is shown in Figure 44; test results are tabulated in Figure 46.

Upon review of these test results, Sun selected a temperature of 1625°F for solution-annealing the flange and the balance of the test material.

b. Maraging Response

To evaluate the response of the forged material to maraging, 15 tangential tensile specimens were machined from the solution-annealed ID test ring B. Groups of three specimens each were maraged at five different cycles, and tested at room temperature; the results are recorded in Figure 47.

c. Uniformity and Directionality

The overall quality of the flange was evaluated with respect to uniformity and directional characteristics by testing tensile specimens which represented three directions and two locations, and PCI specimens which represented four orientations. Macroetches and ASTM grain size determinations were also included in these evaluations.

III, A, Entrance Flange (cont.)

The tensile specimens were selected for a comparison of the three principal directions in the forging (tangential, radial, and axial) from two locations around the circumference, and the OD and ID of the flange. Tangential specimens were taken from two locations 180-degrees apart on the OD test ring A-2 and two locations 180-degrees apart on the ID test ring B. Radial specimens were taken from two locations 180-degrees apart on the OD test ring A-2, and axial specimens were taken from two locations 180-degrees apart on the ID test ring B. The machined specimens were maraged at 890°F for 4 hr and tested at room temperature. All tests were made in duplicate. Specimen location diagrams and tensile results are shown in Figure 48.

To evaluate the notch toughness of the flange in various directions, PCI specimens were machined from the test rings at four different orientations. Tangential specimens were taken from the OD test ring A-2 and notched so that the fracture would propagate in an axial direction, and the plane fracture would be perpendicular to the flow line direction of the forging. Presumably, this orientation would show the maximum toughness values of the flange. Radial specimens were also taken from the OD test ring A-2 and notched so that the fracture would propagate axially with the plane of fracture parallel to the flow line direction. Axial specimens were removed from the ID test ring B and notched in two different directions so that toughness could be evaluated with the direction of fracture propagation perpendicular to the flow line direction and parallel to the flow line direction; plane of fracture in both cases would be parallel to the flow line direction. It was presumed that the axial orientation with the direction of fracture propagation parallel to the flow lines would show the minimum toughness values. Specimen orientations are shown in Figure 49.

III, A, Entrance Flange (cont.)

All of the impact specimens were maraged at 890°F for 4 hr, fatigue cracked, and tested at -40°F, room temperature, and 200°F; three specimens were tested per orientation and test temperature. These test results are shown in Figures 49 and 50.

4. Discussion of Results

a. Solution Annealing Response

While the yield strength of the material solution-annealed at 1500°F was approximately the same as that for similarly treated 5/8-in.-thick plate, a decrease of approximately 12 ksi occurred when the solution-annealing temperature was increased to 1600°F. This decrease in yield strength was accompanied by a corresponding increase in toughness values. These trends, along with the photomicrograph study (Figure 45), indicate that a large amount of recrystallization occurred between these two temperatures.

At the 1800°F solution annealing temperature, the Charpy values were maximized, and the W/A values were correspondingly high, but the yield strength was below the 200-ksi minimum strength. Conversely, the 1900°F samples showed a slight restoration of tensile properties, but showed a loss of toughness indicative of grain coarsening. This correlates closely with the gradient bar photomicrographs shown in Figure 45. It was apparent that neither of these temperatures would be satisfactory for solution-annealing this material.

The best combination of acceptable yield strength and maximum Charpy and W/A values was obtained in the temperature range of 1600 to 1700°F. The yield strengths were on the lower side of the 200 to 235 ksi

III, A, Entrance Flange (cont.)

range, but it was felt that these would increase with additional time at the maraging temperature. Since slightly better W/A values were developed with the 1600°F solution-annealing treatment than with the 1700°F treatment, a temperature of 1625°F was selected for solution-annealing of the flange.

b. Maraging Response

The five maraging cycles chosen for evaluation all produced yield strengths within the 200 to 235 ksi range, elongations of 11 to 14%, and reduction of areas of 55 to 60%. While all yield strengths were acceptable and differences in ductility were minor, two noteworthy observations were made:

(1) The 850 and 890°F cycles produced generally higher yield strengths with greater ductility than did the 950°F cycle and should be more suitable for maraging this material.

(2) The anticipated increase in yield strength was gained when the aging time at 890°F was increased from 4 to 8 hr.

c. Uniformity and Directionality

A comparison of three directions, two locations on the circumference and the OD and ID sections of the entrance flange forging, showed yield strength to be uniform within a range of 8 ksi. Specifically, the maximum data point spread for a single orientation was 7 ksi on the radial specimens, and the maximum difference among all specimens at all orientations was 8 ksi. These data are shown in Figure 48.

III, A, Entrance Flange (cont.)

A greater degree of anisotropy was observed in ductility. Maximum elongation and reduction of area were associated with the tangential orientation and the minimum with the axial orientation.

Although the W/A values obtained from the PCI specimens were different with different orientations, the observed differences were not considered large for a wrought shape with a preferred orientation. As expected, the tangential specimens showed the highest W/A values at all three test temperatures, and the axial specimens notched parallel to the radius showed the lowest values. The axial specimens notched parallel to the ID and the radial specimens showed W/A values similar to those of the other orientations. The results are shown in Figures 49 and 50. In all cases, the W/A values increased with increasing test temperature and directional difference decreased with decreasing test temperature.

The tangential grain-flow pattern observed on the macroetched coupons was substantiated by the impact data. The tangential specimen orientation showed the highest W/A values indicating the largest resistance to crack propagation. From a structural viewpoint, the grain-flow pattern was ideally located to support the hoop stresses encountered in service.

B. INTERMEDIATE SECTION AND EXIT FLANGE

1. History of Material and Forging Practice

Vacuum-arc remelted, 200-ksi grade maraging steel from Allegheny Ludlum heat 25005 was obtained by Ladish in the form of a 19-in. billet. Tests were conducted for comparison to Aerojet specification AGC-34316 stock acceptance requirements from half of a 2-in.-thick slice representing the top of the billet. This testing included the following:

III, B, Intermediate Section and Exit Flange (cont.)

a. Chemical Analysis

The Ladish check analysis of the billet is tabulated in Figure 51.

b. Microcleanliness

The Ladish microcleanliness rating for the billet is recorded below.

Inclusion Type	AGC-34316 Limits		Center		Mid-radius		Surface	
	Thin	Heavy	Thin	Heavy	Thin	Heavy	Thin	Heavy
A	2	1.5	-	-	-	-	-	-
B	2.5	1.5	-	-	-	-	-	-
C	2	1.5	-	-	-	-	-	-
D	2.5	2	0.5	-	1.0	0.5	0.5	-
E*	2.5	1.5	2.5	1.0	2.0	1.5	1.5	0.5

c. Mechanical Properties

Two longitudinal 0.252-in.-dia tensile test specimens were taken from a 3 by 6 by 2 in. (longitudinal direction) test block reforged to 3 by 3 in. by length-of-stock (longitudinal direction). Maximum forging temperature was 1950°F. Specimens were solution-annealed at 1500°F for 1 hr and air cooled, then aged at 890°F for 4 hr and air cooled prior to testing. The results are shown in the following tabulation:

*Type "E" for rating titanium nitrides only.

III, B, Intermediate Section and Exit Flange (cont.)

0.2% Offset Yield Strength, ksi	Ultimate Tensile Strength, ksi	Elongation in 1 in. %	Reduction in Area, %
218.0	229.5	10	42
215.3	225.6	10	52

The tensile results conformed to the Aerojet specification of 200 to 235 ksi yield strength.

2. Forging Procedures

a. Intermediate Section

The following forging practice was used to shape the intermediate section from the billet stock:

(1) Break corners and upset to 27-5/8 in. diameter. Metal temperature was 1940 to 1470°F during working.

(2) Extrude and punch hole. Metal temperature was 1945 to 1710°F.

(3) Saddle roll to 18-1/2-in. ID in three heats. Metal temperature was 1870 to 1400°F.

(4) Flatten to 34-1/4 by 19-in. ID. Metal temperature was 1655 to 1480°F.

(5) Ring roll to 28-1/2-in. ID in two heats Metal temperature was 1910 to 1415°F.

III, B, Intermediate Section and Exit Flange (cont.)

(6) Conically saddle to 32-1/2 by 40-1/2-in. ID in four passes. Metal temperature was 1630 to 1400°F.

(7) Swage to forging print in two passes. Metal temperature was 1630 to 1440°F.

b. Exit Flange

To shape the exit flange from the billet stock, the following forging practice was used:

(1) Break corners, upset, plug, and punch. Metal temperature during working was 2060 to 1610°F.

(2) Saddle roll from 7-1/4 to 15-in. ID in two heats. Metal temperature was 2015 to 1400°F.

(3) Flatten to 17 in. thick in two heats. Metal temperature was 1965 to 1550°F.

(4) Ring roll to 49-3/16-in. OD. Metal temperature was 1970 to 1540°F.

(5) Swage to forging print. Metal temperature was 1595 to 1450°F.

A 3-1/4-in. wall by 5/8-in. high test ring (CFR) was parted from each forging in the as-forged condition for use in determining the optimum solution annealing temperature. The forgings were solution annealed with the test rings in their original positions. After solution

III, B, Intermediate Section and Exit Flange (cont.)

annealing, a 1-in. wall by 3-1/4-in.-high test ring (CFA) was parted from each of the forgings for use in product evaluation.

3. Procedures and Results

Ladish testing on the intermediate section and exit flange is classified in two categories and described below.

a Solution-Annealing Response (CFR Rings)

The effect of solution annealing temperature upon the mechanical properties of the forgings was evaluated by solution-annealing three tangential tensile specimens and three tangential PCI specimens from each of the two forgings at each of the following temperatures: 1500, 1600, 1650, 1700, and 1800°F. Following solution annealing, all specimens were maraged at 890°F for 4 hr and tested. All tests were conducted at room temperature. The results are presented in Figures 52 and 53.

Solution-annealing temperatures of 1625°F for the intermediate section and 1650°F for the exit flange were specified after evaluating the mechanical property testing and metallographic study. The criteria for selection of the solution-annealing temperatures were a fine grained, recrystallized microstructure, and maximum fracture toughness (W/A) with acceptable yield strength (200 to 235 ksi). The forgings were solution-annealed for 3 hr at these temperatures.

b. Product Evaluation (CFA and CFR Rings)

The mechanical properties were evaluated at two locations 180 degrees apart on each forging with tensile and PCI tests. Specimens were maraged at two cycles, 890°F for 4 hr and 890°F for 8 hr.

III, B, Intermediate Section and Exit Flange (cont.)

The groups of three tangential specimens were removed from the CFR ring so that one specimen from each group represented the ID of the forging, one specimen represented the midwall, and one specimen represented the OD.

The PCI specimens were notched so that the direction of fracture propagation was axial on the tangential specimens, tangential on the radial specimens, and radial from OD to ID on the axial specimens. These orientations are shown in Figure 54. Results of product-evaluation mechanical tests are tabulated in Figures 55 through 59.

In addition to the mechanical property testing, metallographic specimens were prepared from 0- and 180-degree locations on each of the forgings and were rated for microcleanliness and apparent (ASTM) grain size; the ratings are tabulated in Figure 60. Both forgings showed satisfactory cleanliness and fine grain size.

4. Discussion of Results

a. Solution-Annealing Response

In contrast to the solution annealing response of the entrance flange, the intermediate section and exit flange showed smaller changes in strength, and in ductility or notch toughness (W/A) with change of annealing temperature. In progressing from 1500 to 1650°F, a decrease of 5 ksi to 10 ksi yield strength was noted which is indicative that recrystallization occurred. Yield strengths were acceptable (200 to 235 ksi) at all of the annealing temperatures, and elongations and reductions of area remained fairly constant.

III, B, Intermediate Section and Exit Flange (cont.)

The fracture toughness of both forgings responded in an expected manner to changes in yield strength (i.e., the toughness increased with decreases in strength). High toughness was developed in both parts by solution annealing at 1650°F, the temperature at which yield strength was minimum. At all of the solution annealing temperatures surveyed, the fracture toughness values of the intermediate section were highest, while the values for the exit flange were similar to the values for the entrance flange.

Examination of the solution-annealing data for the intermediate section and exit flange showed that any temperature in the 1600 to 1700°F range would produce acceptable yield strength and high fracture toughness. To avoid any possibility of grain coarsening at the high end of the solution-annealing temperature tolerance range (± 25°F), the annealing temperature chosen for the intermediate section was 1625°F. For the exit flange, 1650°F was chosen to avoid the lower fracture toughness condition observed in the 1600°F tests.

b. Product Evaluation

The product evaluation tensile test results showed that on both the intermediate section and the exit flange acceptable yield strength was developed with both maraging cycles of 900°F for 4 hr and 900°F for 8 hr. Ductility associated with these tensile results was as expected for material of this grade with two exceptions:

(1) Elongations and reductions of area of all specimens from the intermediate section maraged at 8 hr were lower than expected.

(2) Elongations and reductions of area for all radial specimens from the exit flange were lower than expected.

"REPRODUCIBILITY OF THE ORIGINAL PAGE IS POOR."

III, B, Intermediate Section and Exit Flange (cont.)

For the intermediate section, low ductility was independent of orientation. For the exit flange, low ductility was associated with the short transverse (radial) orientation.

Although it is generally accepted that ductility as measured by elongation and reduction of area of tensile specimens is an indication of fracture toughness, it appears that this is not always the case. In contrast to the good ductility with average W/A values on the entrance flange, the radially oriented impact specimens from the exit flange showed rather high W/A values in comparison to the low ductility measured in this direction.

As anticipated when the selection of orientations for the PCI specimens was made, the average radial or short transverse W/A values for both forgings were lower than the average tangential and axial values. One data group from the intermediate section showed about 20% higher short transverse W/A values and was comparable to the other orientations. The strength data from the same location on the test ring showed a yield strength decrease of about 10 ksi. These data illustrate the variations in product uniformity. However, it was not anticipated that the tangential and axial W/A values would be equivalent. The explanation for this result is that the axial elongation resulting from forming the high walls on these forgings must have been roughly equivalent to the tangential deformation resulting from rolling the diameters of the rings. The general level and anisotropy of W/A values at all test temperatures were approximately the same as those for maraging steel plate of this strength grade. Only minor variations in W/A values resulted at the three test temperatures, indicating that the material toughness is not highly temperature dependent.

III, B, Intermediate Section and Exit Flange (cont.)

Examination of the PCI test results revealed that the intermediate section showed consistently higher W/A values than did the exit flange. Since the tensile properties of the two forgings were similar and the chemical analyses were almost identical, this difference is apparently attributed to differences in forging procedure necessitated by differences in part configuration. One of the major factors determining the forging procedure for ring forgings of similar diameter processed from similar size billets is the height-to-wall thickness ratio. This ratio for all three of the 120-in.-dia nozzle forgings is shown below.

Part	Height-to-Wall Thickness Ratio
Exit Flange	3.6
Intermediate Section	7.5
Entrance Flange	0.62

A comparison of these figures shows that the intermediate section with the highest ratio received a greater amount of reduction in forging than did the exit flange, since the two were forged from similar size billets. This greater reduction may account for the higher W/A values exhibited by this forging, particularly in the short transverse orientation, as compared with those exhibited by the exit flange. The finer grain size rating of the intermediate section is probably a result of the greater reduction also. A comparison of the entrance flange properties to those of the other parts on this basis is not necessarily valid because of the differences in chemistry and original stock size; however, while the entrance flange with its low height-to-wall ratio showed greater ductility than did the other parts, the W/A values were approximately the same as the exit flange.

III, Forging Material Evaluation (cont.)

C. TESTING CONDUCTED BY SUN

1. Procedures and Results

a. Chemical Analysis

The chemical analysis of the 120-SS-1 nozzle parts was performed by Lehigh Testing Laboratories. The results are tabulated in Figure 61. No significant differences in chemistry were noted, and all of the analyses conformed to Aerojet specification AGC-34316.

b. Microcleanliness

Microcleanliness ratings were performed at Sun Oil according to the specifications of ASTM E-45 on specimens from the 120-SS-1 nozzle components. The results are recorded below:

	Inclusion Type							
	A		B		C		D	
	Thin	Heavy	Thin	Heavy	Thin	Heavy	Thin	Heavy
ASTM E-45 (limits	2	1.5	2.5	1.5	2	1.5	2.5	2
Entrance Flange (Ring A-2)	0	0	0	0	0	0	4.0	1.0
Intermediate Section (Ring CFR)	0	0	0	0	0	0	4.0	1.5
Intermediate Section (Ring CFA)	0	0	5.0	0	0	0	4.0	1.5
Exit Flange (Ring CFR)	0	0	0	0	0	0	5.0	1.0
Exit Flange (Ring CFA)	0	0	0	0	0	0	5.0	1.5

All inclusions observed on these samples were titanium nitrides or carbo-nitrides; these were rated as either type B or D according to their appearance. All of these ratings exceeded the specified limits and differed markedly from the ratings supplied by Ladish. These differences were

III, C, Testing Conducted by Sun (cont.)

traced to the techniques used in measuring and reporting the inclusion ratings. Since the depth of field on the microscope is very limited (less than 0.005 in.), the larger inclusions can be focused and photographed, while the smaller inclusions just below this plane are missed. However, a careful technique does show the smaller and more numerous inclusions and, since the ASTM does not specify a minimum particle size, these inclusions should be reported. Even though these ratings were beyond the specification limits, the nature and distribution of these inclusions did not cause structural impairment of the components.

c. Grain Size

Apparent (ASTM) grain size measurements were performed on specimens from the 120-SS-1 nozzle parts at Sun Oil according to Federal Test Method Standard 151A. The results are recorded below.

Part	Apparent (ASTM) Grain Size
Entrance Flange (Ring A-2)	4
Intermediate Section (Ring CFR)	7
Intermediate Section (Ring CFA)	7-1/2
Exit Flange (Ring CFR)	6
Exit Flange (Ring CFA)	5

These grain size measurements are approximately the same as those supplied Ladish.

d. Test Weldment

A test weldment designed to simulate an automatic circumferential weld on the nozzle shell was prepared from a section of test

III, C, Testing Conducted by Sun (cont.)

ring B from the entrance flange, using Armetco heat 08436 weld wire. Edge preparation was a single U; all welding was performed using the TIG technique in the downhand position. A sketch of the weld test specimen is shown in Figure 62. From the test weldment, nine transverse (to weld) tensile specimens, 12 weld zone PCI specimens, 12 heat-affected-zone PCI specimens, six weld-zone slow-notch-bend specimens, and five weld-zone calibration bars were prepared. Specimen locations and orientations are shown in Figure 62, details A, B, and C. Half of the machined test specimens were maraged at 900°F for 4 hr, and half for 8 hr at Sun Oil. All calibration bars were maraged at 900°F for 8 hr. Test results are tabulated in Figures 63 through 65. Sun Oil also conducted a metallographic examination of the weldment including microhardness transverses. The microhardness results are tabulated in Figures 66 and 67.

e. Maraging of the 120-SS-1 Nozzle Shell

When the fabricated nozzle shell was maraged at the J. W. Rex Company, a total of 36 test specimens, (18 tensile and 18 precracked impact specimens with tangential and axial orientations) were maraged along with the part. These specimens were machined from the test rings from the nozzle forgings and were attached to the forging they represented during maraging. PCI specimen orientations are shown in Figure 68. The maraging treatment to which the nozzle shell and the specimens were subjected was nominally 900°F ± 15°F for 4 hr. Test results and identifications of specimens with the forging test rings from which they were machined are recorded in Figures 69 and 70.

III, C, Testing Conducted by Sun (cont.)

2. Discussion of Results

a. Test Weldment

After the maraging treatment at 900°F for 4 hr, the yield strength of the weldment was below the specified minimum of 200 ksi and was 5 to 25 ksi lower than the forgings. After 8 hr at 900°F, a yield strength of 200 ksi was developed. In keeping with the low strength level, ductility was good and the PCI fracture toughness (W/A) values for the weld zone specimens were high. Heat-affected zone specimens showed W/A values higher than similarly oriented specimens from the parent material, but lower than those from the weld zone.

The unusually high weld-zone (W/A) values can be explained only in part by the low strength of the weldment. An additional factor which may have influenced the toughness is that the weld-zone specimens were oriented so that the notch was centered on the root pass of the weld. This portion of the weld was subjected to the largest amount of repetitious thermal cycling during welding, and hence may have been overaged. This assumption was not substantiated, however, by the microhardness traverses performed on the as-welded and the maraged joint. Soft areas near the root pass were not apparent; in fact, the range of average hardness values for all areas tested corresponded to only five Rc points (Rc44 to 48).

b. Maraging of the 120-SS-1 Nozzle Shell

The test results on the specimens maraged with the 120-SS-1 nozzle shell compared with the test data from the component evaluation showed that the yield strengths obtained during maraging were much higher and the W/A values were correspondingly lower. These higher strengths were

III, C, Testing Conducted by Sun (cont.)

attributed to the contributions in maraging of the long heat-up, stabilization, and cool-down times to which the part and specimens were subjected.

D. CONCLUSIONS

General conclusions were made from the results of the testing program conducted on each of the three forged components: the entrance flange, intermediate section, and exit flange of the 120-SS-1 nozzle shell. These conclusions were as follows:

1. Forging with grade 200, 18%-nickel steel in accordance with the procedures used produced acceptable motor components.

2. The best combination of acceptable yield strength and maximum notch toughness on forged material of this grade should be obtained by solution-annealing in the temperature range of 1600 to 1700°F. This was found to be dependent upon forging methods and forging temperatures.

3. Acceptable yield strength after solution-annealing in the 1600 to 1700°F range was developed in this material with a wide range of maraging treatments; however, the 850 and 900°F temperatures were more desirable than the 950°F temperature.

4. There was an inverse relationship between yield strength and fracture toughness; as strength increases, W/A values decrease.

5. In general, the lower ductility developed on ring-rolled maraging-steel forgings, as measured by elongation and reduction of area, was associated with the smallest forged dimension on the component.

III, D, Conclusions (cont.)

6. Minimum fracture toughness on the ring-rolled maraging-steel forgings was measured on specimens oriented so that the fracture propagated in a direction parallel to the direction of preferred orientation. Maximum fracture toughness was usually measured on specimens with the axis parallel to the direction of preferred orientation.

7. Mechanical properties of the three forgings evaluated compared favorably with 5/8-in.-thick, grade 200, 18%-nickel steel.

8. Welds could be made which were at least as tough as the parent material and had acceptable joint efficiency.

IV. PARENT METAL BAR STOCK EVALUATION

The Y-ring skirt attachment used in the 260-in.-dia motor chamber was ring-roll forged. However, this program was initiated to evaluate the tensile and fracture toughness properties of bar stock as a back-up for the forged components. The parent metal evaluation was also necessary in order to obtain comparative data that could be used to evaluate welding procedures and filler wires in the event bar stock was required to be used in the fabrication program.

A. EVALUATION PROGRAM

1. Material Evaluated

Two-and-one-half in.-thick, 8-in.-wide, grade 200, 18%-nickel maraging steel bar stock from Republic heat 3960556 was evaluated. Plate (0.6 in. thick) material from this same heat was evaluated in the parent metal plate evaluation program discussed in a previous section of this report. The chemical composition of this heat is listed in Figure 71, and conforms to the requirements of the applicable Aerojet procurement specification (AGC-34315).

The microstructure, grain size, and area representing the most severe inclusion content observed are shown in Figure 72. A general martensitic structure was observed in which the outline of the prior austenitic grains could be noted. The grain size of the bar stock was approximately 3 to 4 when rated in accordance with ASTM E112-61. This grain size is coarse in comparison to the grain size of 7 obtained in the 0.6-in.-thick, 18%-nickel maraging steel plate material from the same heat. This apparently results from the difference in working imparted to the two products during mill processing. The inclusion rating of this material was within the requirements of the applicable Aerojet Specification (AGC-34316).

IV, A, Evaluation Program (cont.)

2. Specimens Tested

Tensile, SNB, and PCI specimens were tested to determine the tensile properties and fracture toughness of the bar stock. The dimensions of the specimens are shown in Figure 73. The tensile specimens were oriented both transverse and longitudinal to the final rolling direction of the bar stock. The fracture-toughness specimens were prepared in the transverse, longitudinal, and short transverse orientations as shown in Figure 74.

The test specimens were machined from the as-received bar stock which was mill-annealed at 1500°F for 3 hr. After machining, the specimens were age-hardened in accordance with selected aging cycles (900°F for 8 and 16 hr). Prior to testing, the tensile specimens were abraded to remove surface scale and the fracture-toughness specimens were subjected to cycle stresses to form a fatigue crack at the root of the notch.

Tensile specimens were tested in triplicate for each variable investigated. These tests were conducted in accordance with Federal Test Method Standard 151 with a strain rate of 0.005 in./in. to the yield point. The stress-strain diagram was used to determine the 0.2% offset yield strength. Elongation measured over a 1-in. gage length.

Five SNB specimens were tested for each variable to determine the effect of specimen orientation and aging cycle on the plane-strain fracture toughness (G_{Ic} and K_{Ic}) of the bar stock. Six PCI specimens were tested for each condition to determine qualitatively their effects on the plane-stress fracture toughness, (G_c and K_c) of the bar stock. Duplicate specimens were tested at each of the three test temperatures to establish relationships between fracture toughness and test temperature. The impact specimens were tested at ManLab Inc.

IV, Parent Metal Bar Stock Evaluation (cont.)

B. RESULTS AND DISCUSSION

1. Tensile Properties

The tensile properties of 2-1/2-in.-thick bar stock after aging at 900°F for 8 and 16 hr are listed in Figure 75. Both aging cycles resulted in tensile properties which were very similar to those exhibited by the 0.6-in.-thick plate material from the same heat after the same aging treatments. Also, the tensile properties of the bar stock in both the longitudinal and transverse orientations were comparable.

2. Fracture Toughness

The PCI fracture toughness (W/A) of the bar stock after aging treatments of 900°F for 8 and 16 hr is listed in Figure 76. As indicated by these data, the fracture toughness of the bar stock was comparable after both aging treatments. Also, the fracture toughness was higher in the longitudinal orientation than in the transverse, surface-notched transverse, or short transverse orientations, with the latter two orientations exhibiting comparable toughness values. Compared with the fracture toughness of 0.6-in.-thick plate for Republic heat 3920556 after aging at 900°F for 8 hr, the PCI fracture toughness of the bar stock in the longitudinal orientation was comparable to that of the plate in the transverse orientation. However, the toughness of all specimen orientations in the bar stock were lower than longitudinally oriented specimens from the plate material.

The results of SNB fracture-toughness tests on bar stock are shown in Figure 77 and summarized in Figure 78. For comparison purposes, fracture toughness data for the 0.6-in.-thick plate material from the same heat of material are also shown in Figure 78.

IV, B, Results and Discussion (cont.)

3. Conclusions

A comparison between the characteristics of bar stock and plate indicated no significant difference in toughness in the longitudinal specimen orientation after aging at 900°F for 8 hr; whereas, in the transverse-specimen orientations, the bar stock was significantly less tough than the plate. These differences in toughness may be related to variations in working during primary processing of the plate and bar products.

On the basis of the limited evaluation conducted on the bar-stock parent material, there were no problems or limitations apparent in fabricating thick sections of the motor pressure vessel with bar stock.

V. PLATE WELDING EVALUATION

Motor component weldments with high strength-to-weight ratios, in combination with sufficient fracture toughness to withstand service stresses in the presence of small defects, were required to obtain reliable performance from large-diameter, rocket-motor pressure vessel components. To achieve this combination of properties in the program, Grade 200, 18%-nickel maraging steel plate and forgings with a yield strength range of 200 to 235 ksi had been specified for fabricating chamber components and assemblies. However, when the material selection was made for the program, data were limited regarding the tensile and fracture toughness properties of weldments in this material and the effects of varying filler wire composition and joint designs on these properties. Consequently, the welding process evaluation program was undertaken jointly by Aerojet and Sun to evaluate welding procedures and filler wires for processing large-diameter motor chambers, using Grade 200, 18%-nickel maraging steel material.

The gas-shielding TIG welding process was evaluated in the welding program. This welding process was selected because previous studies had indicated that sound weldments with higher fracture toughness could be prepared with greater reliability using the TIG process than with the other welding techniques that had been adapted to the processing of the 18%-nickel maraging steels. In evaluating the TIG welding process, filler wire composition, weld-joint geometry, and welding procedures were varied to evaluate their effects on the aging response, tensile properties, and fracture toughness of the weldments. The information that was obtained from these evaluations was subsequently used in selecting filler wire compositons, joint designs and welding procedures.

The welding evaluation program was based on comparisons between the aging response, tensile properties, and fracture toughness of the parent metal plate and weldments.

V, Plate Welding Evaluation (cont.)

A. WELD PROCESS DEVELOPMENT AND FILLER-WIRE SELECTION

1. Experimental Procedures

a. Welding Procedures

Weldments in 18%-nickel maraging steel plate were made using the TIG welding process. The weldments were 12 in. long and were produced by joining two 4-in.-wide by 0.6-in.-thick test plates. This test-weldment size was selected to provide sufficient material for preparation of the various test specimens that were used in the program. Individual weld test plates were machine-cut, and all plate edges were machined for welding. This technique was used so that the plate edges would not be subjected to thermal cycles, such as those that are encountered in flame or power cutting, which might affect the mechanical properties and metallurgical characteristics of welded joints. After machining, the plates were degreased and the plate surfaces were ground to remove oxide scale. Immediately before welding, the joint edges were wiped with acetone to remove oil film and other foreign materials.

The weld test plates were clamped to a rigid, water-cooled, copper backup bar that also aligned the plates during welding. The backup bar was water-cooled to increase the weld cooling rates. The backup bar was grooved to control weld penetration and to provide a means of introducing inert gas to shield the root of the weld. A sketch of this component, with the groove dimensions and the method for supplying shielding gas to the root of the weld, is shown in Figure 79.

Precautions were taken during welding operations to obtain fast weld-cooling rates and to minimize the size of weld heat-affected zones. Preheating and postheating of the welds were not used. Also, the

V, A, Weld Process Development and Filler-Wire Selection (cont.)

weldments were allowed to cool between passes so that the interpass temperature did not exceed 200°F. These were standard precautions taken in welding 18%-nickel maraging steel plate to minimize austenite reversion in the weld heat-affected and fusion zones during welding.

A HWM-2 automatic welding head, equipped with a HW-13 welding torch, EG103 governor-controlled, cold-wire feeder, and a 400-amp dc welding-power source, was used to accomplish the TIG welds. The weld-joint configurations and welding schedules were developed as shown in Figures 80 and 81. The root-land dimension of the joints was adjusted to assure complete penetration of the root pass without a root gap. The welding and shielding conditions were adjusted to provide sound welds in accordance with applicable X-ray (AGC 13860, Class 1), ultrasonic (AGC 32115), and magnetic particle (AGC 32116) nondestructive inspection specifications. Copies of the specifications are presented in Appendix A.

b. Specimen Preparation

Tensile, SNB, and PCI tests were used to evaluate the aging response, tensile properties, and fracture toughness of the weldments. The dimensions of the specimens are shown in Figure 82. The orientation of specimens is shown in Figure 83. The gage length of longitudinal tensile specimens was oriented to consist almost entirely of weld metal. The gage length of the transverse tensile specimen extended across the welded joint and included the weld fusion zone, the two weld heat-affected zones, and unaffected base metal.

All fracture-toughness specimens were machined transverse to the weld with the notch oriented through the thickness of the weld as indicated in Figure 83. Full-weld-thickness (0.6-in.) PCI and SNB specimens were used. Notches in the fracture-toughness specimens were located in the weld

V, A, Weld Process Development and Filler-Wire Selection (cont.)

metal or heat-affected zones. To locate the notches, specimen blanks were etched (Marbles etchant) and scribe lines were drawn to represent the center line of the notch. The notches then were machined to coincide with the scribed lines.

The test specimens were machined from as-welded plate. After machining, the specimens were age-hardened in accordance with the selected aging cycle. Subsequent to testing, the surface scale formed on the tensile specimens was removed with abrasive paper, and the fracture-toughness specimens were subjected to cyclic stresses to form a fatigue crack at the root of the notch.

c. Testing Procedures

Tensile specimens were tested in triplicate for each variable investigated. These tests were conducted in accordance with Federal Test Method Standard 151, using a strain rate of 0.005 in./in. to the yield point. Stress-strain diagrams were used to determine the 0.2% offset yield strength. Elongation was measured over a 1-in. gage length.

The transverse tensile specimens were used to determine the ultimate tensile strength and location of tensile failures in weld-joint specimens. Yield strength (0.2% offset), percent elongation, and percent reduction-of-area measurements were made on the transverse tensile specimens. However, these data must be interpreted cautiously, since transverse-weld tensile specimens vary in thermal history and composition along the specimen gage length from the presence of the welded joint. The longitudinal-weld tensile specimens were prepared to determine the yield strength and ductility of the weld metals. The combined data from transverse and longitudinal tensile specimens were used to evaluate the tensile properties of the weldments.

V, A, Weld Process Development and Filler-Wire Selection (cont.)

Five SNB specimens were tested for each variable to determine qualitative plane-strain fracture toughness, G_{Ic} and K_{Ic}, and the effects of aging cycle, filler wire composition, and welding procedures on this property. Six PCI specimens were tested for each welding variable to determine qualitatively their effects on the plane-stress fracture toughness, G_c and K_c, of weldments. Duplicate impact specimens were tested at each of three test temperatures (-40°F, room temperature, and +200°F) to establish relationships between fracture toughness and test temperature. The impact specimens were tested at ManLabs, Inc.

2. Materials

All welding tests were conducted using 0.6-in.-thick, Grade 200, 18%-nickel maraging steel plate from Republic Heats 3960524 and 3920556. Plate from heat 3960524 is considered to represent high-strength heats that may be used in the program, while heat 3920556 is considered to represent heats at the lower end of the specified 200 to 235 ksi yield-strength range. The results of detailed mechanical and metallurgical properties evaluations of both heats of plate material are presented in the parent metal plate evaluation section of this report.

The following target values were established for the 0.2% offset yield strength of the weld metals to be evaluated:

Minimum Yield Strength: 200 ksi
Maximum Yield Strength: 220 ksi

The minimum target value was selected to correspond to the minimum design value required for welded joints, and the maximum limit was selected to obtain acceptable fracture toughness in the weld deposit and provide for anticipated chemical composition variations in weld filler wires and deposited weld metals.

V, A, Weld Process Development and Filler-Wire Selection (cont.)

Five filler wires were screened in the program. The compositions of the five filler wires are listed in Figure 84 with the compositions of the base metal plates. All filler wires were selected on the basis of chemical composition to obtain weld-metal yield strengths in the 200 to 220 ksi range. Although these filler wires were ordered to provide a considerable variation in cobalt (7 to 8.5%), molybdenum (3.5 to 4.5%) and titanium (0.2 to 0.4%) contents, the actual heats produced by the material vendor did not meet this requirement. Except for the Inco filler wire, there were only minor variations between the compositions of the various filler wires. However, the wires were accepted for evaluation, since the slight variations in composition were expected to result in a range of weld metal tensile yield strengths within the desired range of 200 to 220 ksi.

Except for the cobalt content of the Inco filler wire and the titanium content of all filler wires, the composition of the welding filler wires also was comparable to that of the parent metal plate. The cobalt content of the Inco filler wire was only about half as high as that of the base metal, while the titanium contents of the filler wires ranged from approximately 1-1/2 to 3 times higher than those of the base metals.

3. Results and Discussion

a. Preliminary Screening Tests

Preliminary screening tests were conducted, using Republic heat 3960524 base plate to evaluate the five weld filler wires and two joint designs on the basis of longitudinal weld-metal tensile properties. The weld-metal tensile data (as welded and aged at 900°F for 8 hr) obtained from the screening tests are presented in Figure 85. The tensile yield strengths of the weld metals ranged from a low of 207 ksi for the Inco wire to a high of 231 ksi

V, A, Weld Process Development and Filler-Wire Selection (cont.)

for the 06887 filler wire. All values exceeded the 200 ksi minimum yield strength requirement. The elongation and reduction of area values were generally high and comparable to the parent metal properties. Also, the weld tensile properties obtained with filler wires 06887 and 07495 were, in most instances, higher for the single-U design than for the double-V joint. Selected single-U and double-V joint tensile specimens were sectioned and subjected to metallographic examination to determine if the differences in tensile properties were caused by the presence of overaged heat-affected base metal in the specimens machined from the double-V joints. Specimens machined from welds made with both joint designs contained approximately the same amount of base metal in the cross section of the tensile specimens. Consequently, it was not possible to state conclusively whether the presence of base metal in the cross sections of the tensile specimens contributed to the difference in properties. However, the lower tensile properties obtained in evaluating specimens from the double-V weldments may result from the presence of a more overaged condition in the center of the weld thickness where the tensile specimen was located when compared to the single-U weldments.

The cobalt, molybdenum, and titanium contents of the weld metals that were deposited with the five weld filler wires are listed in Figure 86. Similar data for the filler wires and base metal are also included for comparison. As indicated by these data, weldments processed with the single-U joint design had slightly higher titanium contents than those obtained with the double-V joints. This variation in titanium content indicated that base metal dilution was less in the single-U than in the double-V joint. Such a difference in dilution would be expected in comparing the two joint desig The slightly higher titanium content of the single-U weld deposits was consistent with the slightly higher strengths of these weld metals and may partially explain the difference in tensile properties observed in comparing the single-U and double-V joint designs. Also, the variations in tensile properties of the weld

V, A, Weld Process Development and Filler-Wire Selection (cont.)

deposits obtained with the various weld filler wires were consistent with the cobalt, molybdenum, and titanium contents of the weld metals.

On the basis of the results shown in Figures 85 and 86, three filler wires, (07495, 34428-.31 Ti, and Inco) were selected for further evaluation. These filler wires were selected to represent weldment yield strength levels within the desired range of 200 to 220 ksi (and slightly above) in order to determine the effect of variations in filler-wire chemical composition on weldment aging response and fracture toughness.

Also, both the double-V and single-U joints were considered acceptable for use in the fabrication program, and both joint designs were used to prepare specimens for aging response tests and tensile and fracture toughness determinations.

b. Aging Response

(1) Longitudinal Tensile Properties

The aging response of the weld metals was evaluated on the basis of relationships between longitudinal weld-metal tensile properties and aging time and temperature.

(a) Filler Wire 07495

To evaluate the aging response of the weld metal obtained in welding with the 07495 filler wire, three longitudinal tensile specimens were aged in accordance with each of ten selected aging cycles. The aging response data obtained from filler wire 07495 deposited in a double-V joint in Republic heat 3960524, Grade 200, 18%-nickel maraging steel plate (0.6 in. thick) are listed in Figure 87 and plotted as a function of aging

V, A, Weld Process Development and Filler-Wire Selection (cont.)

cycle in Figure 88. The 0.2% offset yield strengths of the weld metal are summarized below on the basis of aging cycle and compared with similar data from parent metal plate from Republic heats 3960524 and 3920556.

Temperature, °F		0.2% Offset Yield Strength, ksi Aging Time, hr 2	4	8	16
850	07495 Weld Metal	-	205	217	221
	Base Metal (3960524)	-	230	238	242
	Base Metal (3920556)	-	198	211	220
900	07495 Weld Metal	208	216	216	219
	Base Metal (3960524)	229	234	239	232
	Base Metal (3920556)	-	214	218	223
950	07495 Weld Metal	208	216	207	-
	Base Metal (3960524)	233	231	219	216
	Base Metal (3920556)	-	215	219	222

As indicated by these data, the aging response of the 07495 weld metal was comparable to that of the parent metal plate. At the 850°F temperature, the tensile yield strength of the weld metal and wrought plate increased with aging time. At the 900°F temperature, the yield strength of the weld metal and parent metal plate from heat 3920556 also increased with aging time, whereas slight overaging, as evidenced by reduced strength, was observed after aging parent metal plate from heat 3960524 for 16 hr. At 950°F, overaging was observed in the weld metal and parent metal plate from heat 3960524, but was not observed in parent metal plate from heat 3920556. The yield strength of the weld metal was approximately 10 to 20 ksi lower than that of plate from heat 3920524, but was comparable to that of plate from heat 3920556 after similar aging treatments at 850 and 900°F.

The tensile elongation of the 07495 weld metal is summarized and compared with that of the base metals in the tabulation below.

V, A, Weld Process Development and Filler-Wire Selection (cont.)

Aging Temperature, °F	Material	Elongation in./in., % Aging Time, hr 2	4	8	16
850	07495 Weld Metal	-	16	14	14
	Base Metal (3960524)	-	12	12	11
	Base Metal (3920556)	-	12	12	10
900	07495 Weld Metal	15	14	16	16
	Base Metal (3960524)	12	12	12	12
	Base Metal (3920556)	12	11	11	12
950	07495 Weld Metal	17	18	23	-
	Base Metal (3960524)	12	12	12	12
	Base Metal (3920556)	12	12	12	12

The tensile elongation of the weld metal exceeded that of the base metals after all aging cycles and was approximately twice that of the base metal after aging at 950°F for 8 hr.

The reduction of area values of the 07495 weld metal are summarized and compared below with those of the base metals in the longitudinal orientation.

Aging Temperature, °F	Material	Reduction of Area, % Aging Time, hr 2	4	8	16
850	07495 Weld Metal	-	57	55	52
	Base Metal (3960524)	-	64	63	60
	Base Metal (3920556)	-	66	62	60
900	07495 Weld Metal	56	55	56	54
	Base Metal (3960524)	64	64	60	59
	Base Metal (3920556)	66	62	61	60
950	07495 Weld Metal	55	54	56	-
	Base Metal (3960524)	54	55	63	64
	Base Metal (3920556)	62	60	60	61

V, A, Weld Process Development and Filler-Wire Selection (cont.)

As indicated by these data, tensile reduction of area values for the weld metal were slightly lower than those of both base metals in the longitudinal orientation.

(b) Filler Wire 34428-.31 Ti

On the basis of the aging response of weld metal deposited with the 07495 filler wire, three aging cycles were selected to evaluate the aging response and tensile properties of weld metal deposited with 34428-.31 Ti filler wire in double-V and single-U joints in Republic heat 3960524 maraging steel plate. The tensile properties obtained in evaluating these weldments are listed in Figure 89. The average 0.2% offset yield strength values are compared below with the values obtained with the 07495 filler wire and the parent metal plate.

		0.2% Offset Yield Strength, ksi Material				
		34428-.31 Ti Weld Metal		07495 Weld Metal	Base Metal Heat 3960524	Base Metal Heat 3920556
Aging Cycle, °F	hr	Double-V	Single-U	Double-V		
850	8	212	207	217	238	211
900	8	215	212	216	239	218
950	8	207	203	207	219	219

As indicated by these data, the yield strength of weld metals deposited with filler wire 34428-.31 Ti was slightly lower in the single-U joint than in the double-V joint. This observation was opposite to that observed in the screening tests, but the differences in yield strength were only slight for this filler wire in both series of tests. Also, the 0.2% offset yield strength of 34428-.31 Ti filler wire weld deposits was in accordance with the program design requirements (200 to 220 ksi) for both joint designs and after each aging cycle investigated. In addition, the yield strengths of weld metals

V, A, Weld Process Development and Filler-Wire Selection (cont.)

obtained with both filler wires using a double-V joint design were comparable for the three aging cycles investigated and were comparable to those obtained in the Republic heat 3920556 plate material after the 900 and 950°F aging cycles. However, the yield strengths of the weld metals deposited with both filler wires were lower than those of Republic heat 3960524 parent metal plate after all aging cycles and were lower than that of Republic heat 3920556 parent metal plate after the 950°F aging cycle. The percent elongation values of weld metals deposited with the 34428-.31 Ti and 07495 filler wires and of the parent metal plate are tabulated below:

		Elongation in 1 in., % Material				
		34428-.31 Ti Weld Metal		07495 Weld Metal	Base Metal	Base Metal
Aging Cycle, °F	hr	Double-V	Single-U	Double-V	Heat 3960524	Heat 3920556
850	8	13.7	12.1	14	12	12
900	8	13.1	12.3	16	12	11
950	8	15.3	13.6	23	12	12

As shown above, the elongation values observed in weld metals deposited with 34428-.31 Ti filler wire in single-U joints were comparable to or slightly lower than those observed in weld metals deposited in double-V joints subjected to similar aging cycles. Also, except after the 950°F aging cycle where exceptionally high elongation was observed in the 07495 weld metal deposit, the elongation of 34428-.31 Ti weld deposits were slightly lower or comparable to that of weld metals deposited with 07495 filler wire. In addition, the elongation of all weld metals was slightly higher than that of both parent metal plates.

The reduction of area values of 34428-.31 Ti weld deposit were comparable to those of 07495 weld deposits which, in turn,

were slightly lower than those of the parent metal plate in the longitudinal orientation, as shown previously in the aging response of 07495 weld deposits.

On the basis of weld metal tensile properties, the 34428-.31 Ti filler wire also would be considered acceptable for welding Grade 200, 18%-nickel maraging steel plate. A desirable combination of tensile strength, elongation, and reduction of area was achieved in the weld metal after all aging cycles.

(2) Transverse Tensile Properties

The results from transverse tensile tests which were conducted on double-V and single-U weldments made with 07495 and 34428-.31 Ti filler wires and Republic heat 3960524 base plate are listed in Figure 90. As indicated by these data, the ultimate strengths of the joints were comparable to those of the weld metals shown in Figures 87 and 89 and were satisfactory for the 260-in.-dia motor program. Failures occurred in the weld metal or in the heat-affected zones. However, weld-metal failures were expected, since the filler wire compositions evaluated were selected to obtain slightly lower yield strength (200 to 220 ksi) weld metals in comparison to the actual yield strength (212 to 239 ksi) of the parent-metal plate material used.

c. Fracture Toughness

The fracture toughness of weld-fusion and heat-affected zones were determined to evaluate TIG welding procedures and filler wires, and to study the aging response of the weldments. Both SNB and PCI tests were used in these evaluations.

V, A, Weld Process Development and Filler-Wire Selection (cont.)

(1) Weld-Metal Fracture Toughness

(a) Precracked Charpy Impact Tests

The results of PCI tests of TIG weld metals deposited with selected filler wires and double-V and single-U joints in 0.6-in.-thick plate from Republic heats 3960524 and 3920556 are shown in Figures 91 to 94. For comparison purposes, the room-temperature fracture toughness (W/A) of the weld metals are summarized below.

Aging Cycle[a]		Fracture Toughness (W/A), in.-lb/in.^{2} Weld Metals			
		07495[b]	34428-.31 Ti[b]		Inco[c]
°F	hr	Double-V	Double-V	Single-U	Single-U
850	8	545	759	821	970
900	8	632	707	832	1027
950	8	958	837	840	1215

(a) As-welded and aged
(b) Deposited in plate from Republic heat 3960524
(c) Deposited in plate from Republic heat 3920556

As indicated by these data, Inco filler wire deposited with a single-U joint design in Republic heat 3920556 plate resulted in the highest weld-metal fracture toughness. The lowest fracture toughness was observed in weld metal deposited with filler wire 07495 in the double-V joint in Republic heat 3960524 plate, while weld metals deposited with 34428-.31 Ti filler wire in single-U and double-V joint designs in Republic heat 3960524 plate exhibited intermediate toughness values. Also, higher fracture-toughness values are noted for test specimens (34428-.31 Ti filler wire) representing the single-U joint design in comparison to specimens from the double-V joint.

V, A, Weld Process Development and Filler Wire Selection (cont.)

In general, the differences in weld metal fracture toughness are attributed to variations in yield strength and/or weld deposit composition that occurred when the various filler wires, joint designs, and aging cycles were employed. A tabulation of the weld metals in ascending order of fracture toughness is shown below.

Filler Wire	Aging Cycle °F	hr	0.2% Offset Yield Strength, ksi	W/A, in.-lb/in.^{2} Range	Average
07495	850	8	217	507-583	545
07495	900	8	216	560-704	632
34428-.31 Ti	900	8	215	677-737	707
07495	950	8	207	750-766	758
34428-.31 Ti	850	8	212	710-808	759
34428-.31 Ti	850	8	207	766-876	821
34428-.31 Ti	900	8	212	803-862	832
34428-.31 Ti	950	8	207	795-897	837
34428-.31 Ti	950	8	203	832-849	840
Inco	850	8	-	913-1028	970
Inco	900	8	-	1007-1047	1027
Inco	950	8	-	1178-1252	1215

In the above tabulation, the tendency for grouping of filler metals indicates that composition effects are important; however, compositional differences between the 07495 and 34428-.31 Ti filler wires were not great. Also, the tendency for decreasing yield strength with increased fracture toughness indicates that yield strength is important; in general, the relationship between weld deposit yield strength and fracture toughness followed the same trends previously established for the parent metal plate material (Republic heats 3960524 and 3920556). Although there was not a sufficient amount of this filler wire to determine the weld deposit tensile properties using a single-U joint design, weldments processed with the Inco filler wire and a double-V joint design in Republic heat 3960524 plate material exhibited the

V, A, Weld Process Development and Filler-Wire Selection (cont.)

lowest strength weld deposits in the screening studies. Consequently, the fracture-toughness data shown above for the Inco filler wire appears to follow the general trend of increased fracture toughness with decreasing yield strength. The same effect is noted when comparing test specimens representing the single-U and double-V joints welded with 34428-.31 Ti filler wire; the higher yield strength of the double-V joint design was accompanied by lower fracture toughness in comparison to specimens representing the single-U joint design.

Comparisons between fracture toughness of the weld metals and base metals are shown in the following tabulation.

		Fracture Toughness, (W/A) in.-lb/in.^{2}							
		Base Metals (a)				Weld Metals (b)			
		3960524		3920556		07495	34428-.31 Ti		Inco
Aging °F	Cycle hr	L(c)	T(c)	L(c)	T(c)	Double V	Double V	Single U	Single U
850	8	958	547	1548	1597	545	759	821	970
900	8	1006	728	1509	1340	632	707	832	1027
950	8	1356	1126	1326	1270	758	837	840	1215

(a) Mill annealed at 1500°F for 1 hr and aged
(b) As-welded and aged
(c) Specimen orientation: L, longitudinal and T, transverse

Precautions were necessary in comparing weld metal fracture toughness with that of the base metals because of the size of PCI specimens that were used. The specimens used to determine the fracture toughness of the Republic heat 3960524 base metal were 0.394 by 0.394 in. in cross section; whereas, 0.600- by 0.394-in. specimens were used to determine the fracture toughness of Republic heat 3920556 base metal and all weld metals. The larger of the two specimens generally results in lower fracture toughness values

"REPRODUCIBILITY OF THE ORIGINAL PAGE IS POOR."

than the smaller specimen, so that quantitative comparisons cannot be made between the fracture toughness properties of the weld metal and 3960524 base metal. However, a number of toughness trends can be observed in comparing these data.

As shown in the above tabulation, the fracture toughness of all weld metals were comparable to or exceeded that of Republic heat 3960524 plate material in the transverse orientation after the 850 and 900°F aging cycles, and the fracture toughness of the Inco weld metal was comparable to the values exhibited by test specimens from heat 3960524 plate in the longitudinal orientation. After these aging cycles, the yield strength of this heat was 238 and 239 ksi, which was slightly higher than specified for the plate material. However, after the 950°F aging cycle, which reduced the yield strength of heat 3960524 to 219 ksi, only the fracture toughness of the Inco weld metal was comparable to that of the heat 3960524 base metal plate. Therefore, with weld-deposit yield strengths in the range of 200 to 220 ksi, it appears that weld-metal fracture toughness can be achieved which is comparable to, or higher than, that of the high strength (230 to 240 ksi yield strength) heats of Grade 200, 18%-nickel maraging steel plate. However, it appears that the fracture toughness of the weld deposit may be lower than that of base-metal plate from heats such as Republic heat 3920556, which represents the middle or low strength heats that are purchased for the fabrication program.

(b) Slow-Notch Bend Tests

SNB fracture toughness (G_{Ic}) data for TIG weld metals deposited with the selected filler wires in 0.6-in.-thick base plate from Republic heats 3960524 and 3920556 are presented in Figures 95 to 98. The average weld-metal fracture toughness (G_{Ic}) data are tabulated below for comparison purposes.

V, A, Weld Process Development and Filler-Wire Selection (cont.)

Aging Cycle °F	hr	Fracture Toughness (G_{Ic}), in.-lb/in.^{2} (a) 07495 (b) Double-V	34428-.31 Ti (b) Double-V	34428-.31 Ti (b) Single-U	Inco (c) Single-U
850	8	333-492 Avg (5) 408	314-373 Avg (3) 352	308-368 Avg (5) 333	490-614 Avg (5) 553
900	8	222-322 Avg (5) 263	325-350 Avg (3) 339	353-625 Avg (4) 439	392-588 Avg (5) 459
950	8	238-314 Avg (5) 273	342-369 Avg (3) 358	341-441 Avg (4) 394	318-492 Avg (5) 430

(a) These data were calculated by Bueckner's method
(b) Deposited in plate from Republic heat 3960524
(c) Deposited in plate from Republic heat 3920556

As indicated by these data, the SNB fracture toughness of the weld deposits processed with heat 07495 filler wire was lower than weld deposits representing the other two heats of weld wire investigated. Also, weld deposits produced using the Inco filler wire exhibited the highest slow-notch-bend fracture toughness values. However, the Inco weld metal dropped in toughness as the aging temperature was increased until, at 950°F, the toughness was comparable to that of 34428-.31 Ti weld metal. This later effect may be associated with accompanying weld-metal yield strength variations as the result of the different aging treatments, although insufficient weld wire was available to evaluate these properties for the Inco wire. The SNB fracture toughness of weld metal heat 34428-.31 Ti was intermediate between heat 07495 and the Inco wire. Except for weld deposits representing the Inco filler wire, the SNB fracture toughness of the weld metals was not significantly affected by the various aging treatments investigated. Also, there appears to be no significant difference in fracture toughness between test specimens (filler wire heat 34428-.31 Ti) representing the single-U and double-V joint configurations.

V, A, Weld Process Development and Filler-Wire Selection (cont.)

The SNB fracture toughness of Republic heats 3960524 and 3920556 base metals are tabulated below for comparison with the weld metal data.

Aging Cycle °F	hr	Fracture Toughness (G_{Ic}), in.-lb/in.^{2} * Heat 3960524 Longitudinal	Heat 3960524 Transverse	Heat 3920556 Longitudinal	Heat 3920556 Transverse
850	8	442-568 Avg (4) 477	366-443 Avg (4) 372	526-667 Avg (5) 581	532-615 Avg (5) 569
900	8	413-501 Avg (10) 438	345-410 Avg (4) 376	459-639 Avg (5) 526	496-579 Avg (5) 538
950	8	432-582 Avg (3) 546	437-479 Avg (5) 456	496-601 Avg (5) 534	525-616 Avg (5) 589

* These data were calculated by Bueckner's method.

Comparisons between the weld-metal and base-metal SNB fracture-toughness data also show the same trends that were indicated previously for the PCI fracture toughness data, in that the fracture toughness values for the tougher weld metals were comparable to or exceeded the values obtained in evaluation base metal heats which exhibited strengths on the high side of the values specified (200 to 235 ksi yield strength) for the program. However, the weldment fracture toughness may be lower than that of base-metal heats which are in the intermediate or low yield strength range of the specified limits.

Weld-metal deposit with 34428-.31 Ti filler wire, which is considered representative of the filler wire composition recommended for the fabrication program, exhibited SNB fracture toughness (G_{Ic}) values of 340 to 360 in.-lb/in.,^{2} after aging at 850, 900, and 950°F for 8 hr at a 0.2% offset yield strength of 207 to 215 ksi. These G_{Ic} values correspond to K_{Ic} values of 101 to 104 ksi $\sqrt{in.}$ and the following critical surface flaw lengths, assuming the indicated flaw shape and an operating stress of yield strength (210 ksi) magnitude.

V, A, Weld Process Development and Filler-Wire Selection (cont.)

Defect Type	Flaw Configuration Depth/Length	Q	K_{Ic}, ksi $\sqrt{in.}$	Critical Flaw Size, in. Length	Depth
Semicircular Surface Crack	0.5	2.2	102	0.26	0.132
Long Shallow Surface Crack	0.1	0.88	102	0.53	0.053
Embedded Porosity	0.5	2.2	102	0.33*	---

Weld metal deposited with heat 07495 filler wire, which exhibited the lowest fracture toughness (G_{Ic}) values obtained in the program, had plane-strain fracture toughness (G_{Ic}) values of approximately 260 in.-lb/in.^{2} at a yield strength level of 207 to 216 ksi. This G_{Ic} value corresponds to a K_{Ic} of approximately 90 ksi $\sqrt{in.}$ and the following critical surface flaw lengths, assuming an operating stress of yield strength (210 ksi) magnitude.

Defect Type	Flaw Configuration Depth/Length	Q	K_{Ic}, ksi $\sqrt{in.}$	Critical Flaw Size, in. Length	Depth
Semicircular Surface Crack	0.5	2.2	90	0.22	0.11
Long Shallow Surface Crack	0.1	0.88	90	0.42	0.042
Embedded Porosity	0.5	2.2	90	0.26*	

* Diameter

In interpreting the above fracture toughness data, a critical flaw shape corresponding to a surface flaw depth/length ratio of 0.1 is the most severe condition from a performance consideration, while a flaw depth/length ratio of 0.5 is the most critical in terms of nondestructive inspection capability. As indicated by these data, critical surface-flaw lengths characteristic of both filler wire compositions and both defect configurations should be detected by available nondestructive inspection techniques (magnetic particle, X-ray, dye penetrant, and ultrasonic). Also, the porosity size indicated above can be detected by X-ray inspection and is

V, A, Weld Process Development and Filler-Wire Selection (cont.)

in excess of the maximum size (0.060 in.) permitted by current X-ray accept-reject criteria (specification AGC-13860 Class 1) used in the fabrication program.

(c) Part-Through-Crack Tensile Tests

It is significant to note that the SNB fracture-toughness data presented above is considered qualitative and conservative in that the fracture toughness (G_{Ic}, K_{Ic}) values and critical flaw sizes are less than those which could be obtained using valid, quantitative plane-strain fracture toughness, part-through-crack, tensile test specimens. Although weld deposit part-through-crack tensile tests were not conducted at Aerojet, Boeing performed these tests using filler wire (heat 06887) supplied by Aerojet and 0.75-in.-thick base plate from Republic heat 3920556. The test results obtained at Boeing are shown below:

Ultimate Strength, ksi	0.2% Offset Yield Strength, ksi	Elongation (2 in.), %	Reduction in Area, %	K_{Ic}, ksi $\sqrt{in.}$
213	210	13	38	131

As indicated by these data, weld deposit yield strength and fracture toughness (K_{Ic}) values of 210 ksi and 131 ksi $\sqrt{in.}$, respectively, were obtained. Assuming an operating stress of yield strength magnitude and flaw shapes of 0.1 and 0.5, critical surface flaw lengths of 0.9 in. and 0.46 in., respectively, are obtained.

(d) Heat-Affected-Zone Fracture Toughness

Weld heat-affected-zone fracture-toughness data must be interpreted with caution because of the considerable variations

in microstructure that occur in the plane of the test specimen notch from the irregular geometry of the weld heat-affected zones. The notches were located by etching the fracture-toughness specimens after rough machining and by scribing a line on the specimens to show the notch location. In evaluating each weldment, the notch was located to extend from the edge of the weld fusion zone at the surface of the plate through the thickness of the plate. In double-V welds the notch extended from the edge of the weld fusion zones on both plate surfaces through high- and low-temperature areas of the heat-affected-zones near both surfaces and through low-temperature heat-affected zones and partially unaffected base-metal plate in the center of the plates. In the single-U welds, the notches extended from the edge of the fusion zone on the face of the weld through high- and low-temperature areas of the heat-affected zones near the face of the weld and through low-temperature areas of the heat-affected zone and partially unaffected base metal of the root of the weld. These effects are illustrated in Figure 99. Also, because the heat-affected zones were narrow and had steep temperature gradients during welding, it was not possible to locate notches in metal that had undergone identical thermal cycles from one specimen to the next. As a result, the heat-affected zone fracture-toughness data can be used to provide a qualitative comparison with the base metal, but cannot be analyzed to obtain quantitative comparisons between the effects of varying welding procedures and joint designs on the heat-affected zone fracture toughness.

1 Precracked Charpy Impact Tests

The PCI fracture toughness (W/A) of weld heat-affected zones in Republic heat 3960524 0.6-in.-thick plate material obtained with the various joint designs and filler wires are listed in Figures 91 through 94. The average room temperature values are summarized below.

V, A, Weld Process Development and Filler-Wire Selection (cont.)

		Fracture Toughness (W/A), in.-lb/in.^{2*}				
		Base Metal		Heat Affected Zones		
				Double-V Joint		Single-U Joint
Aging °F	Cycle hr	Long.	Trans.	Filler Wire 07495	Filler Wire 34428-.31 Ti	Filler Wire 34428-.31 Ti
850	8	958	547	844	952	1200
900	8	1006	728	845	1025	1284
950	8	1356	1126	961	1106	1495

* All base metal toughness data was obtained with a 0.394- by 0.394-in. specimen, and the weld heat-affected zone toughness data was obtained with a 0.600 by 0.394 in. or 0.575- by 0.394-in. specimen.

As indicated by these data, the room temperature fracture toughness of the weld heat-affected zones was comparable to, or exceeded, that of the base metal in the transverse orientation after all aging cycles. Also, with the exception of the welds made with 07495 filler wire (all aging cycles) and the double-V weldments processed with 34428-.31 Ti filler wire aged at 950°F for 8 hr, the fracture toughness of the weld heat-affected zones was comparable to that of the base metal in the longitudinal orientation. Consequently, the differences between the base metal and the weld heat-affected-zone fracture-toughness values were caused primarily by specimen orientation in respect to the plate rolling direction, and the data shown above indicate weld heat-affected-zone fracture-toughness properties which are comparable to the base metal.

2 Slow-Notch-Bend Tests

The SNB fracture toughness (G_{Ic}) of weld heat-affected zones in 0.6-in.-thick plate from Republic heat 3960524 is listed in Figures 95 through 98. The average values are summarized below.

V, A, Weld Process Development and Filler-Wire Selection (cont.)

Aging °F	Cycle hr	Fracture Toughness (G_{Ic}) in.-lb/in.^{2*} 3960524 Plate Longitudinal	Transverse	Heat-Affected Zone Double-V	Single-U
850	8	442-568 Avg (4) 477	336-443 Avg (4) 372	485-564 Avg (3) 515	470-666 Avg (5) 531
900	8	413-501 Avg (10) 438	345-410 Avg (4) 376	448-632 Avg (3) 530 280-439 Avg (5) 347	452-581 Avg (5) 513
950	8	432-582 Avg (3) 546	437-479 Avg (5) 456	337-574 Avg (3) 490 352-499 Avg (5) 400	425-597 Avg (5) 517

* These data were calculated by Buechner's Method.

These data show the fracture toughness of heat-affected-zone specimens representing both double-V and single-U joint configurations and indicate that no significant difference in fracture toughness properties between the two joint designs exists. Also, with the exception of one double-V weldment, the fracture toughness (G_{Ic}) of the heat-affected zones was comparable to that of the base metal in the longitudinal orientation. However, the fracture toughness values obtained on testing specimens from the heat-affected zone of the weldment that was the exception were comparable to the fracture toughness of the base metal in the transverse orientation. It is believed that the lower fracture-toughness values obtained on testing specimens from the latter weldment was due to the orientation of the weld heat-affected zone test specimens in relating to the rolling direction of the plate. Metallographic examinations were conducted to verify this belief, but the results were not conclusive.

V, A, Weld Process Development and Filler-Wire Selection (cont.)

d. Root Gap Opening

Studies were also conducted to determine the effects of variable root gap on welding procedures and the tensile and fracture toughness properties of the weldments. Initially, weld test plates machined from 0.6-in.-thick, 18%-nickel maraging plate (Republic heat 3920556) with a single-U weld groove preparation were welded to determine the maximum gap that could be tolerated before burnthrough occurred. Figure 100 shows the joint configuration and indicates the various weld schedules employed in these investigations and the root gap at which burnthrough occurred. Successful welds were made with root-gaps ranging from 0.000 to 0.070 in. However, when the gap was increased to 0.100 in., severe burnthrough was encountered. Consequently, the maximum root gap that can be tolerated without encountering burnthrough is approximately 0.070 in.

Subsequently, three plates were welded with a root gap of 0.070 in. extending the full length of each 12-in. joint. Filler wire 07495 and plate material from heat 3920556 were used to make the welds. All test specimens were tested in the as-welded and aged (900°F for 8 hr) condition. The results of the tensile, precracked charpy impact and SNB fracture-toughness tests are listed in Figures 101 to 103. As indicated by these data, the tensile strength and weld-metal fracture toughness of the weldments processed with 0.070-in. root gap were comparable to, or exceeded, the values obtained previously in evaluating double-V welds made with the same filler wire (heat 07495) in Republic heat 3960524 plate. Also, the fracture toughness of the weld heat-affected zone was comparable to that of the base metal in both the longitudinal and transverse orientations. Consequently, a root gap of 0.070 in. had no apparent effect on the weldment tensile and fracture toughness properties in comparison to weldments processed with zero root gap.

V, A, Weld Process Development and Filler-Wire Selection (cont.)

e. Recommended Welding Procedures for the 260-in.-dia Motor Program

On the basis of the results obtained in this program, the following recommendations were made for joining Grade 200, 18%-nickel, maraging steel plate material in the 260-in.-dia motor fabrication program.

Filler Wire Composition, wt%

C	Ni	Co	Mo	Ti	Al	Mn	P	S	Si
0.03	17.5/18.5	7.5/8.0	3.6/3.8	0.26/0.30	0.10 Added	0.10 Max	0.01 Max	0.01 Max	0.01 Max

Filler Wire Melting Practice

Vacuum arc remelt or vacuum induction melting process

Welding Process - Tungsten Inert Gas (TIG)

Joint Design - Single-U or Double-V

Maximum Root Gap - 0.070 in.

B. EVALUATION OF SELECTED WELD FILLER WIRE AND WELD PROCESS

After preliminary determination of the filler-wire chemistry, welding parameters, and weld-joint design previously discussed, the next step in the material and process evaluation program was to assure that the welding procedures used in the actual fabrication resulted in weldments with high toughness and adequate strength that consistently met the quality requirements for actual fabrication. This phase of the program was accomplished using the fabrication shop TIG welding equipment operated by the shop personnel to be used in fabrication. All test specimens were prepared in the shop environment. Particular interest in this phase of the evaluation was to develop a complete understanding of the welding process characteristics and necessary controls when welding 18%-nickel steel and to carefully evaluate the process for inherent defects or process characteristics which could jeopardize the reliability of the motor pressure vessel components.

V, B, Evaluation of Selected Weld Filler Wire and Weld Process (cont.)

This analysis was accomplished with four filler wire and plate combinations for evaluation of the automatic welding process and also included the development and evaluation of repair welding techniques. The chemical analyses of the 18%-nickel filler wire and plate material used in the evaluation is shown in Figure 104.

Weld-deposit strength and toughness were evaluated with four or more maraging cycles. The primary heat-affected zone was also evaluated using various plate and weld wire combinations. For the toughness evaluations, SNB and PCI specimens were used. Various weld-repair techniques were extensively evaluated and indicated satisfactory strength and toughness after severe repairs. The latter evaluation was borne out in the hydrostatic tests of the first and second 36-in.-dia Process Evaluation Test Vehicles (PETV) where the automatic and repair welds were extremely successful. A report, Reference 8, was prepared on this phase of the material and process evaluation program.

1. Welding Procedures and Equipment

The weld joint detail for single-U butt-joint preparation is shown in Figure 105. This joint detail was used for plate thicknesses from 0.410- to 0.710-in. gage. The major welding parameters and equipment used are listed below.

Welding Condition	Parameter
Current	370 amp
Arc voltage	11 v
Weld travel speed	8 in./min (5 in./min root pass)
Heat input	30,000 joules/in.
Cold wire feed	60 in./min
Gas shielding	Argon gas: torch, 30 cu ft/hr; backing shield, 20 cu ft/hr

V, B, Evaluation of Selected Weld Filler Wire and Weld Process (cont.)

Welding Condition	Parameter
Wire diameter	0.060 in.
Electrode diameter	0.150 in. (2% thoriated)
Welding torch	Linde HW-27 (gas lens type)
Automatic arc voltage control	Linde HWM-2
Power source	Miller 600 amps at 60% duty cycle, rectifier type (constant amperage)

The automatic-welded test plates were 8 in. wide by 18 in. long, while the manual-weld test plates were 8 in. wide by 6 in. long. After completion of welding, the top and bottom weld surfaces were ground, and the weldment was X-rayed in accordance with production requirements. All welding conditions on each bead were recorded, and comments, such as nonwetting, rounded bead, etc., were recorded. After quality inspection requirements, the weld plates were machined to produce the test specimens.

2. Specimen Preparation

All tensile, SNB and PCI specimens were machined at the Wetherill plant of Sun Shipbuilding Co. and by Lehigh Testing Laboratories. All specimen blanks were sawed; powder-burning or any other hot-cutting methods were not allowed. Machining operations were performed in a manner that precluded significant heating of the material. Each specimen was inspected for conformance to drawing tolerances. An optical comparator was used to inspect notch radii and other critical dimensions.

The heat-affected zones on the PCI and SNB specimens were determined by an acid etch. The heat-affected-zone notch was positioned on each etched specimen at the edge of the fusion line at the top of the weld, as shown in Figure 106. Many of the weld deposit PCI and SNB specimens were also acid-etched to ensure that the machined notch would be centered in the weld deposit. All impact and bend specimens were notched in the thickness direction.

V, B, Evaluation of Selected Weld Filler Wire and Weld Process (cont.)

Tensile specimens were machined transverse and longitudinal (weld metal only) to the weld joint. Sketches of the specimen dimensions are shown in Figures 107, 108, and 109.

3. Testing Procedures

All of the specimens were maraged at Sun Oil in a calibrated convection-type furnace. Temperatures of 850, 900, and 950°F and times from 4 to 16 hr were used for maraging cycles. The furnace accuracy was within ± 5°F. Furnace charts were maintained for each series of specimens.

After heat treatment, the tensile specimens were tested at Sun Oil with a 120,000 lbf Riehle universal hydraulic tensile machine. The test temperature varied from 70 to 80°F and the relative humidity from 35 to 55%. The strain rate during loading to yield was 0.010 in./in.

The impact specimens were shipped to Manlabs, Inc., for fatigue cracking and testing after maraging was completed. A Manlabs fatigue precracking machine, Model FCM-300, was used for cracking. This equipment produced a nominal fiber stress of 70 ksi during cracking. Impact testing was conducted on a 128 ft-lb impact machine, Model CIM-128.

The SNB specimens were sent to the Vertol Division of the Boeing Company for fatigue cracking after maraging. A Sonntag SF-1U universal fatigue-testing machine with an attached bend fixture was used for fatigue cracking. Fatigue cracking time was set at around 6 min, which required about 7000 to 12,000 cycles. During this procedure, the nominal fiber stress was estimated to be 75% of the material yield strength. After fatigue cracking, the specimens were tested to destruction in a Riehle universal hydraulic tensile tester with a three-point bending fixture attached. A loading rate

of 0.020/0.025 in./min was used during testing. Specimen load and deflection were autographically recorded for each test. The deflection was measured by a linear differential transformer located between the top and bottom plates of the bending fixture.

The point where the load deflection record deviated from linearity was marked on the graph. This point was further analyzed to calculate the strain energy release rate (G_{nc}) at the onset of rapid crack growth. A considerable amount of trouble was encountered in this measurement from weldment bend bars. In many cases, the gradual deviation from linearity was evident, as shown in Figure 110, and the proportional load was as much as 35% lower than the maximum load. The condition, which may be indicative of slow crack growth and yielding, results in low G_{nc} values. Where a jog in the load deflection curve occurs (constant load with increasing deflection) near the proportional load value, a "pop-in" or rapid fracture is believed to be present. The latter was not apparent on many of the weld bend bars.

Calibration bars were tested with relatively blunt notch radii (approximately 0.010 in. radius). Notch depths were varied in these bars to supply a calibration curve for the material tested and to calculate the first derivative of the reciprocal of the spring constant with respect to notch depth. Ten bars were used to calibrate weldments, and five bars were used for the heat-affected-zone analysis.

The calibration bars were loaded within their elastic limits and the maximum loads for the various notch depths are given below.

V, B, Evaluation of Selected Weld Filler Wire and Weld Process (cont.)

Depth, in.	Maximum load, lbf
0	6000
0.100	6000
0.150	6000
0.175	6000
0.200	6000
0.225	6000
0.250	4800
0.275	4800
0.300	3600
0.325	3600

Each specimen was loaded and unloaded three times and the average load deflection slope for the three runs were recorded.

For each set of SNB bars, the total notch depth was measured. A convention of measuring the notch depth at the middle of the specimen was adopted since this is where the greatest stress concentration occurs. However, the weld and heat-affected-zone bars showed considerable variation in fatigue notch depth due to the nonhomogeneity and nature of the structure being tested. The measured notch depth was used to calculate G_{Ic} values by the Bueckner analysis. The notch measurements were made on an optical comparator where the fracture surfaces were greatly magnified.

4. Discussion and Results

a. Heat 34428 Weld Wire and Plate R-599-1

(1) Tensile Data

The strength of weld wire of this chemistry was expected to range from 200 to 220 ksi. The maximum weldment yield strength

with an 8-hr aging time, 220 ksi, was developed at 900°F. The minimum weldment yield strength was 207 ksi when the material was maraged at 850°F for 8 hr. With the four aging cycles used, all transverse yield strengths ranged between 210 and 220 ksi, as shown in Figure 111. The weld tensile-ductility values were comparable to that of the parent plate material.

In comparing the weld metal only (longitudinal) and transverse yield strengths, a decrease of 3 to 6 ksi was noted. This difference was attributed to anisotropy of stringer bead weldments.

Tensile specimens from three manually welded test plates had a much lower (24 ksi average) average yield strength than the automatically welded specimens, and they fractured in the heat-affected zone rather than the weld zone (Figure 112). Subsequent heats of weld wire were investigated to determine the causes for this loss of strength.

(2) Slow-Notch-Bend Data

The G_{nc} values presented in Figure 113 show high values, around 400 in.-lb/in.^{2}, for the 900°F aging cycles. That these values are above the parent-plate longitudinal values (350 to 400 in.-lb/in.^{2}) indicates a satisfactory choice of weld-wire chemistry and welding procedure. The latter requirements are very desirable since residual stresses are higher and defects are more likely in the weld metal than in the parent metal.

b. Heat 34481 and Heat 08436 Weld Wire with Plate R-600-1 and Plate R-600-1A

These two weld-wire and plate evaluations are discussed together since they represent the welding materials used in the first PETV cylindrical section and hemispherical head. Also, as shown in Figure 104,

V, B, Evaluation of Selected Weld Filler Wire and Weld Process (cont.)

the weld-wire chemistries were very similar; the plate chemistries were alike since the two plates were rolled from the same slab.

(1) Tensile Data

All strength data for these two heats of weld wire fell between the limits of 205 and 218 ksi, as shown in Figures 114 and 115. The 34481 heat of wire was about 5 to 10 ksi stronger than the 08436 heat. These strength values represent joint efficiencies of 95 and 91%, respectively, based on the yield strength of the parent plate material. The tensile ductility of the welds was comparable to that of the plate.

In comparing the weld metal only (longitudinal) data with the transverse data; a decrease of 4 to 6 ksi was noted. This minor difference was attributed to anisotropy of stringer bead weldments.

(2) Slow-Notch-Bend Data

Both heats of weld wire gave intermediate toughness values in the range of 250 to 300 in.-lb/sq in. These G_{nc} values for the weldments equalled the range of values exhibited by the parent plates. The toughness in the heat-affected zone was around 250-in.lb/sq in. in the R-600-1 plate but higher, around 350 in.-lb/sq in., in the R-600-1A plate.

However, the G_{Ic} values for these weldments and heat-affected zones fell in the range of 300 to 350 in.-lb/sq in. Why they were higher than the G_{nc} values was not completely evident. For the 34481 weldments and heat-affected zone, many "a" measured values are higher than the corresponding "a" effective values; this difference tends to make G_{Ic} higher than G_{nc} values. Another comparison of the 08436 weldments and heat-affected zone shows that the effective "a' values were higher than "a"

V, B, Evaluation of Selected Weld Filler Wire and Weld Process (cont.)

measured values, yet the weldment K_{Ic} values were again higher than the G_{nc} values. These data are listed in Figures 116 and 117.

(3) Precracked Impact Data

The plane stress W/A values are presented in Figures 118 and 119. At room temperature, W/A was between 1000 and 1500 in.-lb/sq in. for these weldments, which should correspond to a G_{nc} of 300-in.-lb/sq in. and above. Values in the R-600-1A heat-affected zone were above those in the parent plate, whereas in R-600-1, the heat-affected-zone values were nearly equal to parent-plate values.

c. Special Metals Weld-Wire Heat 63343 with Plate Heat 25000-1

The Special Metals wire heat 63343 was intended for the longitudinal and girth seams of the second PETV and in the 260-SL-1 motor chamber. The evaluation of welding with this heat of wire was extended to a complete characterization for fully understanding the properties to be expected in the second PETV and for the subsequent characterization requirements of production materials. The chemistry shown in Figure 104 was comparable to that of the earlier heats of weld wire evaluated.

(1) Tensile Data

The yield strengths (Figure 120) at the 900°F aging cycles lie between 205 and 211 ksi. These strength values represent joint efficiencies of 90 to 95% based on yield strengths with various plates. At the 950°F maraging temperature, overaging of the weld was apparent, and all strength values ranged between 200 and 190 ksi for the automatic welds. To further examine the maraging temperature range between 900 and 950°F,

V, B, Evaluation of Selected Weld Filler Wire and Weld Process (cont.)

tensile specimens were tested at 925°F. At 925°F, the yield strength values were the same as at 900°F, indicating that the overaging temperature was between 925 and 950°F.

A comparison of the data for the weld metal only (longitudinal) and the transverse tensile data showed the maximum difference was 7 ksi; this was again attributed to anisotropy of stringer bead weldments.

(2) Slow-Notch-Bend Data

The SNB tests of this heat of weld wire yielded low G_{nc} values (200 to 225 in.-lb/sq in.). At 950°F, the G_{nc} value rose to 291 in.-lb/sq in., but this corresponds to a yield strength of only 196 ksi (Figure 121). The parent plate G_{nc} values were about 250 in.-lb/sq in.

To examine the influence of specimen size on G_{Ic} values, larger specimens were machined, of the same width but deeper than the standard specimen. The effects of specimen size on G_{Ic} values are shown in Figure 122. The most important trend was one of increasing G_{Ic} with specimen depth. A realistic G_{Ic} value for these welds was 425 in.-lb/sq in., which was considered to be a valid test value. Another trend was one of decreasing nominal stress at the notch. On the basis of results obtained by other experimenters with other types of specimens, this trend was expected.

The G_{Ic} values for the 0.6- by 0.6-in. heat-affected-zone specimens were between 375 and 400 in.-lb/sq in. These values were above the parent-plate values and almost equal to the weld values (Figure 123).

V, B, Evaluation of Selected Weld Filler Wire and Weld Process (cont.)

(3) Precracked Impact Data

The room temperature W/A values for these welds were between 1000 and 1400 in.-lb/sq in. The heat-affected-zone values ranged around 1000 in.-lb/sq in., which was above the parent-plate range of 800 to 900 in.-lb/sq in. and below the weld values. No significant variations of W/A values with test temperature were noted. The weld specimens aged with the second PETV showed 10 to 20% lower W/A values than the laboratory-aged specimens, but the heat-affected zone specimens agreed well with their counterparts (Figure 124).

d. Conclusions

On the basis of the larger specimens taken from weldments made with the 63343 heat of weld wire, G_{nc} values of 425 in.-lb/sq in. were estimated. The W/A values and strength values were in excellent agreement for all the weldments.

Critical flaw sizes were calculated for these weldments as follows:

(1) The critical dimensions of a long, shallow surface flaw are 0.075 in. deep by 0.75 in. long.

(2) The critical diameter of an internal flaw (a round porosity with sharp edges) diameter is about 0.4 in., which is two-thirds of the plate thickness.

The size of the critical surface flaw was above the 3% thickness notch criterion used in ultrasonic testing of parent plate and well above the 50% response from a 1/8-in. hole half-thickness depth used for weldment inspection. With careful inspection techniques, flaws smaller than critical size should be found.

V, B, Evaluation of Selected Weld Filler Wire and Weld Process (cont.)

5. Repair-Welding Evaluation

It became apparent early in the fabrication program that manual repair welding could result in lower strengths than in automatic weldments, depending upon the repair-welding techniques used. Examples of these strength values are shown in Figure 112, where Special Metals weld wire 34428 was used. The yield strength of manual welds performed by three different operators was 24 ksi lower than in the comparable automatic welds.

The first concern with repair welding was that there may be a loss in critical chemical elements in transfer across the welding arc. To investigate this possibility, two test plates were prepared with 34481 weld wire. Tensile specimens were also taken from both test plates. The chemical analysis of the weld deposit from both of the plates is shown below.

Element, wt%	Test Plate WT-2	Test Plate WT-4	Weld-Wire Analysis (Heat 34481
Nickel	18.22	18.28	18.4
Cobalt	7.63	7.64	7.73
Molybdenum	3.75	3.72	3.6
Titanium	0.25	0.25	0.26
Aluminum	0.01	0.01	0.08

If the minor chemical differences are taken into account, no strength difference between wire and weld chemistries is estimated by the Aerojet regression formula. Yield strengths from an average of three tensile specimens from each of the two manually welded plates were 189 and 203 ksi, respectively. Automatic-weld yield strengths ranged between 213 and 218 ksi with this heat of weld wire. The data showed that the yield strength of manual welds depended on the skill and technique of the operator.

V, B, Evaluation of Selected Weld Filler Wire and Weld Process (cont.)

a. Equipment and Parameters for Manual Welds

The welding conditions evaluated for manual welds are shown below. It must be recognized that considerable variations exist in such variables as welding speed, wire feed, etc., since they depend greatly on operator technique.

Welding Condition	Parameter
150-200 amp	Current
11.5-11 vdc	Arc voltage
About 1 in./min	Weld travel speed
110,000 joules/in.	Heat input
18 in.	Cold wire feed
Argon gas-torch; 30 cu ft/hr	Gas shielding
0.060 in.	Wire diameter
0.125 in. (2% thoriated)	Electrode diameter
Linde HW-19	Welding torch
Miller 600 amp at 60% duty cycle, rectifier type (constant amperage)	Power source

A comparison of the manual and the automatic welding conditions showed that in manual welding the heat input (joules/in.) could be four times higher. Maraging steel that was exposed to temperatures in the 1100 to 1200°F range for extended periods would have a tendency to form austenite which does not transform to martensite. This retained austenite in localized large amounts would tend to lower the strength of the joint.

V, B, Evaluation of Selected Weld Filler Wire and Weld Process (cont.)

b. Evaluation of Repair Procedures

To investigate the effects of various manual weld-repair procedures, repair areas were ground out to various depths in a number of weld test plates, using a high-speed rotary file with a tungsten-carbide tool bit. These repair areas were generally less than 2 in. long and were similar in size to the areas expected to be encountered during production.

Flat tensile specimens were used for evaluating the strength of the repair-weld joints. Gage length and width were 2 in. by 1/2 in. by material thickness. Top and bottom weld reinforcements were machined flush. PCI specimens were used for toughness evaluations since the repair areas were small. Also, the PCI averages toughness through changes in structure, a service that the larger SNB specimens cannot perform.

(1) Repair Procedure 1

The initial repair-welding evaluations were similar to the repairs being performed on a longitudinal seam in the cylindrical section of the first PETV. This procedure is outlined below:

(a) R-600-1 test plate automatically welded to half thickness (0.300 in.).

(b) Weld deposit machined to 0.100-in. depth at the root.

(c) Plate automatically welded again to half thickness.

V, B, Evaluation of Selected Weld Filler Wire and Weld Process (cont.)

(d) Weld deposit machined again to 0.100-in. depth at the root.

(e) Plate automatically welded again to half thickness.

(f) Weld deposit ground out in specified areas to 0.020-in. depth and manually repaired.

(g) Remainder of joint then automatically welded.

In some areas of the test plates, repair welding was performed five times (four automatic, one manual). The resulting joint yield strength of flat tensile specimens (Figure 125) shows values of 200 to 210 ksi (900°F for 4 hr) and 215 to 220 ksi (900°F for 8 hr). The impact data listed in Figure 126 showed W/A values for welds and heat-affected zones between 1500 and 2000 in.-lb/in.^{2}. These values are higher than the values given by automatic welds and heat-affected zone specimens (Figure 118).

This repair weld was also examined with microhardness traverses, and no softened maraged areas were found; the data are shown in Figure 127. For comparative purposes, a similar set of microhardness traverses are listed for a sample from a manual weldment. Photomicrographs of these welds are shown in Figure 128. The weld hardness was generally below that of base metal and local variations of 5 points (Rockwell C) were noted. The manual-weld hardness was lowest near the root area, a condition which was not true in the repair weld. Based on the specimen data compiled, this repair procedure was considered to yield good joint strength and adequate fracture toughness.

V, B, Evaluation of Selected Weld Filler Wire and Weld Process (cont.)

(2) Repair Procedure 2

Another repair procedure was investigated that paralleled the repairs performed on the hemispherical heads of the first PETV. The procedure is outlined below.

(a) R-600-1A heat test plate automatically welded to full thickness.

(b) Root side of joint ground out with a rotary file and rewelded manually.

(c) Weld deposit machined to half depth (0.350 in.).

(d) Joint manually rewelded.

(e) Weld deposit machined again to half depth.

(f) Joint manually rewelded again.

In some areas of these test plates, manual repair welding was performed three times. This procedure was believed to be a more severe test than the first repair procedure. However, as shown in Figure 125, the joint strength was still 200 ksi. The strength data were also correlated with smaller 1/4-in.-round tensile specimens.

As with other repair welds, the PCI data shown in Figure 129 exhibited weld toughness values equal to or higher than those of automatic welds. The W/A values for the welds fall between 1100 and 1800 in.-lb/in.^{2}. The heat-affected zone data from the repair welds showed

values which were lower than the corresponding zone for the automatic welds. This is explained by two facts: first, because of the large weld nugget at the top of the weld, the machined notch runs mainly through base-plate metal; and secondly, the specimen orientation compares with the transverse base-plate orientation. The average base-metal values for the same aging cycle were 814 and 610 in.-lb/in.^{2} (dependent on specimen location), which correspond very well with the heat-affected zone W/A of 823 in.-lb/in.^{2}.

(3) Repair Procedure 3

A third repair procedure was evaluated which simulated the root-side repair of welds that exhibited incomplete penetration. This procedure is outlined below.

(a) R-604-1A test plate automatically welded full thickness with incomplete penetration of the root side.

(b) Incomplete penetration was ground out and manually repaired.

(c) X-ray showed unsatisfactory repair and root ground to about quarter depth and manually repaired again.

The flat tensile data showed 210 ksi yield strength for this repair procedure, as shown in Figure 125. This value correlated with 205 ksi from the 1/4-in.-round tensile data from welds with Armetco 08436 weld wire.

V, B, Evaluation of Selected Weld Filler Wire and Weld Process (cont.)

Again, the impact values for this weld procedure were high (Figure 130). These values are equivalent to the test data from the automatic welds (Figure 119).

6. Repair Welding After Maraging

The objective of this investigation was to evaluate the tensile and fracture-toughness properties and metallurgical characteristics of maraged plate and welded joints that have been repair welded and reaged in the event this type of repair effort might be required in the 260-in.-dia-motor fabrication program.

Repair-welding operations on age-hardened large-diameter rocket-motor cases result in thermal cycles not encountered in processing the original welds or repair-welding chambers before they are age-hardened. For example, it would be necessary to reage the repair weld by locally heating the chamber. During this local aging operation, welded joints and base metal adjacent to the repair weld would be subjected to a second aging cycle, and the maximum temperature reached in these zones would range from ambient temperature to the aging temperature, depending on their location with respect to the repair weldments. The fusion zone and high-temperature portion of the repair-weld heat-affected zones would correspond to welds made before aging, because they would be heated above solution-annealing temperatures and effects of previous aging treatments would be eliminated. However, the low-temperature portions of the heat-affected zones would undergo thermal cycles in which additional aging or austenite reversion could occur. These low-temperature heat-affected zones could be located in previously aged base metal, weld metals, and heat-affected zones of the original welds.

V, B, Evaluation of Selected Weld Filler Wire and Weld Process (cont.)

The repair welding evaluation program was conducted to evaluate the tensile and fracture toughness properties of: (1) base metal, weld metals, and weld heat-affected zones that were subjected to a second aging cycle to simulate the thermal cycles encountered when repair welds are locally aged, and (2) the low-temperature portion of repair-weld heat-affected zones, which may be located in previously aged base metal, weld-metal, or the original weld heat-affected zones, where additional aging could occur. Except for limited evaluations to provide baseline information, the properties of the repair-weld fusion zones and high-temperature portions of the repair-weld heat-affected zones were not determined, since these areas would exhibit properties which are comparable to the original weldments produced before aging and chamber assembly.

a. Welding Equipment and Procedures

The weldments were prepared in Grade 200, 18%-nickel maraging-steel plate (Republic heat 3920556) with the TIG welding process to evaluate repair-welding procedures. The weldments were 12-in. long, and were produced by joining two 4-in.-wide by 0.6-in.-thick test plates. This test weldment size was selected to provide sufficient material for preparation of the various test specimens that were used in the program. Individual weld test plates were machine-cut and all plate edges were machined for welding. After machining, the plates were degreased and the plate surfaces were ground to remove oxide scale. Immediately before welding, the joint edges were cleaned with acetone to remove oil film and other foreign materials.

A HWM-2 automatic welding head, equipped with a MW-13 welding torch; a EG103 governor-controlled cold-wire feeder; and a 400-amp dc welding-power-source was used to prepare the TIG weldments. The weld-test plates were clamped to a rigid, water-cooled, copper backup bar that also aligned the plates during welding.

V, B, Evaluation of Selected Weld Filler Wire and Weld Process (cont.)

Weld joint configurations and welding and shielding conditions duplicated those previously used in the plate welding studies conducted at Aerojet in support of the 260-in.-dia motor program and were adjusted to provide sound welds in accordance with applicable radiographic (AGC 13860, Class 1), ultrasonic (AGC 32115), and magnetic particle (AGC 32116) nondestructive inspection specifications.

Precautions were taken during the welding operations to obtain fast weld-cooling rates and to minimize the size of weld heat-affected zones. Pre- and post-heating were not used. Also, the weldments were allowed to cool between passes so that the interpass temperature did not exceed 200°F. These are standard precautions taken in welding 18%-nickel maraging steel plate to minimize austenite reversion in the weld heat-affected and weld-fusion-zones during welding.

Weldments were prepared with several variations in joint configuration and thermal history to develop information on the tensile and fracture toughness properties of repair welds in aged plate and weldments. Figure 131 shows schematic diagrams of the single-U and square-butt-joint configurations that were used. The single-U configuration corresponds to that used in fabricating large diameter chamber components for the program and was used to prepare specimens for evaluating the tensile properties of the weld metal and weldments and the fracture toughness of the weld metal. The square-butt joint configuration was used to prepare precracked Charpy impact and slow notched bend specimens to evaluate the fracture toughness of the weld heat-affected zones. The square-butt joint configuration was selected so that notches could be located entirely in the weld heat-affected zones, thereby eliminating previous difficulties encountered when evaluating the fracture toughness of the heat affected zone in weldments processed with a single-U joint design. The notch in specimens processed with a U-joint was located

V, B, Evaluation of Selected Weld Filler Wire and Weld Process (cont.)

in widely different microstructures, which varied from that representing the high-temperature heat-affected zone at the face of the weld to unaffected base metal at the root side of the weld. However, as indicated in Figure 132, the heat-affected zone of the square butt joint was more uniform through the plate thickness, and the test results more accurately define the fracture toughness of the heat-affected zone.

The joint configurations illustrated in Figure 131 were welded with the plate material in the solution-annealed (1500°F for 1 hr) and aged conditions. Welds made in solution-annealed plate were subjected to single- and double-aging treatments at 900°F for 8 hr. Weldments made in aged plate were subjected to single-aging treatments at 900°F for 8 hr. This time and temperature were selected on the basis of the plate welding evaluation to obtain a desirable combination of weldment tensile properties and fracture toughness, and are considered representative of the aging cycle which could be used on the motor chamber.

The weld-joint configurations shown in Figure 133 were used to simulate the repair of weldments. Typical repair-welding schedules for the U and square-butt joint configurations are shown below:

Pass	Amp	Volt	Welding Speed, in./min	Wire Feed, in./min	Argon Gas, cu ft/hr
			Square Butt Joint Design		
1	130	11	6	15	50
2	150	11			
3	175	11			
4	180	10			
5-12	200	10			
			Single-U Joint Design		
1	165	9	12	8	25
2-6	200	9.5	10		
7-13	200	10	25		
14-19	240	10	36		

V, B, Evaluation of Selected Weld Filler Wire and Weld Process (cont.)

The original welds were made in solution-annealed base plate. Part of the original welds were age-hardened at 900°F for 8 hr, while the remaining welds were left in the as-welded condition. The original welds were machined as shown in Figure 133 and rewelded to simulate repair welding operations. The simulated repair welds were then aged at 900°F for 8 hr. The joint A configuration was welded to determine if the tensile properties of the repair welds were affected by locating the heat-affected zones to coincide with the heat-affected zones of the original weld and if the tensile properties and fracture toughness of the repair weld fusion-zone diluted with weld metal from the original weld were different from those of the original weld fusion zone. The joint B configuration was welded to determine if the tensile properties of the repair weld were affected by locating one of the repair weld heat-affected zones in the weld metal of the original weld. The square butt repair welds made with Joints C and D were used to prepare specimens for evaluating the fracture toughness of repair weld heat-affected zones that were located to coincide with those of the original weld or were located in the fusion zone of the original weld.

b. Specimen Preparation

Tensile, slow-notch-bend, and precracked Charpy impact tests were used to evaluate the tensile properties and fracture toughness of the weldments. The dimensions of the specimens are shown in Figure 134. The gage length of longitudinal tensile specimens were oriented to consist almost entirely of weld metal. The gage length of the transverse tensile specimen extended across the welded joint and included the weld fusion zone, both weld heat-affected zones, and unaffected base metal.

V, B, Evaluation of Selected Weld Filler Wire and Weld Process (cont.)

All fracture toughness specimens were machined transverse to the weld with the notch oriented through the thickness of the plate. Full weld thickness (0.6-in.) precracked Charpy impact and slow-notch-bend specimens were used. Most notches for heat-affected-zone fracture-toughness specimens were located in the low-temperature portion of weld heat-affected zones. To locate the notches, specimen blanks were etched (Marbles etchant) and scribe lines were drawn to represent the center line of the notch. The notches then were machined to coincide with the scribed lines.

The test specimens were machined and then age-hardened. After aging, the surface scale formed on the tensile specimens was removed with abrasive paper, and the fracture-toughness specimens were subjected to cyclic stresses to form a fatigue crack at the root of the notch.

c. Testing Procedures

Tensile specimens were tested in triplicate for each variable investigated. These tests were conducted in accordance with Federal Test Method Standard 151, using a strain rate of 0.005 in./in. to the yield point. Stress-strain diagrams were used to determine the 0.2%-offset yield strength. Elongation was measured over a 1-in. gage length.

The transverse tensile specimens were used to determine the ultimate tensile strength and location of tensile failures in weldments. Yield strength (0.2% offset), elongation, and reduction of area were measured on the transverse tensile specimens, but these data must be interpreted cautiously since transverse weld tensile specimens vary in thermal history and composition along the specimen gage length because of the presence of the welded joint. The longitudinal tensile specimens were prepared to determine the yield strength and ductility of the weld metal. Data were required for both transverse and longitudinal tensile specimens to fully evaluate the tensile properties of weldments.

V, B, Evaluation of Selected Weld Filler Wire and Weld Process (cont.)

Five SNB specimens were tested for each variable to determine qualitative plane-strain fracture toughness (G_{Ic} and K_{Ic}) and the effects of aging and welding sequence on this property. Six PCI specimens were tested for each welding and heat-treatment variable to determine qualitatively their effects on the plane-stress fracture toughness (G_c and K_c) of weldments. Duplicate PCI specimens were tested at each of three test temperatures (-40°F, room temperature, and +200°F) to establish relationships between fracture toughness and test temperature. The PCI specimens were tested on a subsize impact-testing machine, which provides energy readings with an accuracy of $\pm$ 0.010 ft-lb in the low energy range of 1 to 5 ft-lb.

d. Materials

All welding tests were conducted using 0.6-in.-thick, Grade 200, 18%-nickel maraging steel plate from Republic heat 3920556. The composition of this plate is within the range specified (AGC 34315) for the program and the tensile properties and fracture toughness of the plate are discussed in other sections of this report. On the basis of these properties, heat 3920556 is considered to represent heats at the lower end of the 200- to 235-ksi yield-strength range, which generally exhibit higher fracture toughness properties in comparison to heats representing strength levels at the higher end of that yield-strength range.

Special Metals heat 34482 filler wire was selected for the repair-welding program. This filler wire was purchased by Sun for fabricating chambers for the 260-in.-dia motor program. The composition of this filler wire fell within the range of composition specified (AGC 34326) for the program, as shown in Figure 135.

V, B, Evaluation of Selected Weld Filler Wire and Weld Process (cont.)

e. Discussion of Results

(1) Effects of Double-Aging Treatments

Base metal and weldments adjacent to repair welds made in age-hardened chambers would be subjected to a second aging cycle if the repair welds were locally aged. The second aging cycle that these zones would undergo would depend on their location with respect to the repair welds. Areas immediately adjacent to the repair weld ld be subjected to a second aging cycle at 900°F for 8 hr, whereas areas at greater distance would be subjected to similar temperatures for shorter times or to lower temperatures for similar times.

A series of tests were performed to evaluate the effects of the second aging cycle on the tensile properties and fracture toughness of the base metal, weld metal, and weld heat-affected zones. An aging cycle of 900°F for 8 hr was selected for this second aging cycle on the basis of the aging-response data for parent-metal plate and weldments. At the 900°F aging temperature, age-hardening increased in both the base metal and weld metals with aging times up to 16 hr. Consequently, double-aging at 900°F for 8 hr would result in maximum strengthening of the base metal and weld metal. Since this strengthening was expected to be accompanied by a maximum reduction in fracture toughness in the base metal and weldments, any detrimental effects of double-aging treatment or improper repair welding procedures would be more easily observed than in specimens processed by other representative chamber-aging treatments.

V, B, Evaluation of Selected Weld Filler Wire and Weld Process (cont.)

(a) Base Metal

Base-metal tensile specimens, oriented longitudinally and transversely to the rolling direction, were subjected to two aging cycles at 900°F for 8 hr to determine the effects of double-aging treatments on base-metal tensile properties. As expected, additional age-hardening occurred during the second aging cycle. This additional hardening was reflected by an increase in the 0.2%-offset yield strength and ultimate tensile strength of the base metal. As indicated in Figure 136, the increase ranged from 4 ksi in the longitudinal orientation to 7 ksi in the transverse orientation. Also, the yield strength after two separate aging cycles at 900°F for 8 hr was comparable to, or slightly exceeded, that observed when a single-aging cycle at 900°F for 16 hr was used. Further, the elongation and reduction of area values observed after two aging cycles at 900°F for 8 hr were lower than those observed after single-aging treatments at 900°F for 8 or 16 hr. Although the losses in elongation and reduction of area are not considered significant to chamber performance, they indicate the possibility of a change in age-hardening kinetics as a result of the additional heating and cooling cycles involved in the double-aging treatment.

The higher tensile strength that occurred as a result of double-aging treatments also was accompanied by lower PCI and SNB fracture toughness. As indicated in Figures 137 and 138, the reduction in fracture toughness was most pronounced in the transverse orientation, in which yield strength increased most after double-aging. The reduction in fracture toughness in the longitudinal specimens was not considered significant, since the changes were less than the scatter observed in individual test results. The reduction of fracture toughness in the transverse orientation after the second aging cycle was comparable to that in the original weld metal after a single-aging treatment. Also, the critical defect sizes

V, B, Evaluation of Selected Weld Filler Wire and Weld Process (cont.)

associated with both the parent metal (double-aging) and the weldment (single-aging) areas should be well within the detective capability of present non-destructive testing techniques used in the fabrication program.

(b) Weld Metal

Longitudinal-weldment tensile specimens, which consisted primarily of weld metal deposited with 34482, filler wire, were tested to determine the effects of double-aging treatments on the tensile properties of the weld metal. The results of these tests shown in Figure 139, indicate that no significant difference in properties was observed between specimens subjected to single aging and those subjected to double aging at 900°F for 8 hr. The PCI and SNB fracture toughness of the weld metals are listed in Figures 140 and 141. The fracture toughness of the weld metals also was not significantly different after single- and double-aging cycles. On the basis of these data, neither age-hardening nor overaging occurred in the weld metal during the second aging cycle.

(c) Heat-Affected Zones

PCI fracture-toughness data indicated that overaging occurred in the weld heat-affected zones during the second aging cycle, but such an effect was not confirmed by the tensile and SNB fracture-toughness results. As shown by the data in Figure 142, evidence of possible overaging during the second aging cycle was indicated by the increase in the PCI fracture toughness of the heat-affected zone that was observed in specimens subjected to two aging cycles. After one aging cycle, the average room temperature W/A value was 1675 in.-lb/in.^{2} as compared to a value of 2013 in.-lb/in.^{2} after the second aging treatment. Normally such a change in fracture toughness also is accompanied by reduced tensile strength, which may be evidence of overaging.

V, B, Evaluation of Selected Weld Filler Wire and Weld Process (cont.)

Weld-joint transverse tensile specimens were tested to evaluate the effects of the second aging cycle on the tensile properties of the weld heat-affected zone. These properties were not affected significantly by the second aging cycle, as shown in Figure 139. However, all transverse tensile specimens failed in the weld metal, so that the tensile strength of the weld heat-affected zones were not overaged sufficiently to cause failures in these zones in preference to the weld deposit. Also, changes in PCI fracture toughness normally are accompanied by similar, but less pronounced, changes in SNB fracture toughness. As shown in Figure 143, significant changes were not observed in the SNB fracture toughness of the heat-affected zones as a result of the second aging cycle: therefore, it cannot be stated conclusively that the properties of the heat-affected zones were not altered by the second aging cycle. However, all test data indicated that the properties of these zones were not impaired by the second aging cycle and that double-aging treatments at 900°F for 8 hr should not produce a detrimental effect on chamber performance.

In view of these test data, double-aging treatments at 900°F for 8 hr did not seriously impair the properties of the weldments that were evaluated in this program. Increased base-metal tensile strength and reduced base-metal fracture toughness in the transverse orientation were the major effects that were observed. Because of these changes, the critical flaw size of the base metal in the transverse orientation was reduced to a value below that of the weld metal after a single aging treatment. These effects are illustrated by the data in Figure 144, which also show that the difference between the critical flaw size of the weld metal and double-aged base metal is not large enough to cause concern, since both should be detected with the nondestructive testing techniques used in the program.

V, B, Evaluation of Selected Weld Filler Wire and Weld Process (cont.)

However, the maraging-steel base plate (heat 3920556) evaluated in this study is considered representative of the relatively low-strength (200 to 220 ksi yield strength) heats purchased under Aerojet specification AGC 34315 for use in fabricating large-diameter rocket-motor case components. If a high-strength heat (220 to 235 ksi yield strength) had been evaluated with comparable results, the increased tensile strength and reduced fracture toughness that resulted from the double-aging treatment would reduce the critical defect size.

(2) Repair Welds in Aged Plate

Simulated repair welds following heat treatment were prepared by aging test plates from heat 3920556 at 900°F for 8 hr prior to welding. These test plates were welded with heat 07495 filler wire and the single-U joint configuration; and 34482 filler wire and the square butt-joint configuration (Figure 131). Transverse tensile specimens were machined from the single-U weldments and heat-affected-zone fracture-toughness specimens were machined from the square butt weldments. These specimens were reaged at 900°F for 8 hr prior to testing to simulate aging the repair weld.

The weldment transverse tensile properties and the fracture toughness of the heat-affected zone were evaluated to determine if aging treatments prior to welding affected the properties of the weld heat-affected zones. As indicated in Figure 145, the tensile specimens failed in the weld metal so that the tensile strength of the weld heat-affected zones was not determined. However, these tests showed that the ultimate tensile strength of the weld heat-affected zones exceeded that of the weld metal and was comparable to that obtained for the base metal after double-aging treatments at 900°F for 8 hr.

V, B, Evaluation of Selected Weld Filler Wire and Weld Process (cont.)

The PCI and SNB fracture toughness of the repair-weld heat-affected zones produced in aged plate did not show significant changes from the properties of weldments produced in solution-annealed plate. As shown by the data presented in Figure 146, the average PCI fracture toughness of the repair-weld heat-affected zone in aged plate was about 60 in.-lb/sq in. lower than that of similar heat-affected zones in solution-annealed plate, but this difference is less than the scatter observed in individual test results. Likewise, slightly lower fracture toughness, which also was less than the scatter of individual test results, was observed in SNB fracture-toughness tests of the heat-affected zones in aged plates, as shown in Figure 147. On the basis of these tensile and fracture-toughness data, repair welds in aged plate exhibit tensile and fracture-toughness properties equivalent to those of welds made in solution-annealed plate, provided that both welds are subjected to similar aging treatments after welding. However, the base metal adjacent to the repair weld is subjected to double-aging treatments, and the increased tensile strength that may result from this double-aging treatment of the base metal may prove to be of greater significance than the effects of aging the plate before welding, particularly if the plate material exhibits tensile properties in the higher range of the specified yield strength (200 to 235 ksi).

(3) Repair Welds in Aged Weldments

Simulated repair welds in aged weldments were prepared with the joint configurations shown in Figure 133. The original welds were made with the plate in the solution-annealed condition. Subsequently, some of the original welds were machined and repair welded in the as-welded condition, while the remaining weldments were aged (900°F for 8 hr) before machining and welding to provide comparative data for evaluating the effects of aging the weldments prior to repair welding. All of the simulated repair welds were aged at 900°F for 8 hr.

V, B, Evaluation of Selected Weld Filler Wire and Weld Process (cont.)

As indicated by the data shown in Figure 148, the simulated repair welds exhibited comparable transverse ultimate tensile strengths regardless of whether the repair was made before or after the original weld was aged, or whether the repair-weld heat-affected zones coincided with those of the original weld (Joint A in Figure 133) or were located in the weld metal of the original weld (Joint B in Figure 133). Also, these tensile properties were similar to those observed in original welds that were deposited in solution-annealed plate and aged at 900°F for 8 hr after welding. These data do not indicate if the tensile properties of repair-weld heat-affected zones that coincided with the original heat-affected zones were affected by the aging sequence, but do show that the ultimate tensile strength of heat-affected zones that are located in the weld metal was equal to or greater than that of the weld metal.

The specimens that had the repair-weld heat-affected zones located in the original weld metal exhibited slightly lower yield strengths and slightly higher elongation in comparison to specimens with the repair-weld heat-affected zones located in the original-weld heat-affected zone. This slight difference is attributed to (1) the wide weld-fusion zone (Joint B in Figure 133) in these specimens, and (2) the localization of plastic strain in the fusion zone, as evidenced by the location of weld tensile failures. Therefore, the combination of a wider fusion zone with localized plastic strain would be expected to cause reduced yield strengths and increased elongation.

The fracture toughness of the heat-affected zones of the simulated repair welds showed an effect due to aging the weldment before repair. However, the effects were not consistent in all tests. Consider first the test results for specimens representing the weld heat-affected zones that were located to coincide with the heat-affected zones of the original

weld (Joint C in Figures 149 and 150). The PCI fracture toughness of heat-affected zones in these welds was higher when the original weldments were aged before repair than when they were repaired in the as-welded condition. This change correlates with that observed in studying the effects of double-aging treatments (Figure 142). However, the SNB fracture toughness of similar weld heat-affected zones showed the opposite effect; namely, reduced fracture toughness when the original weld was aged before it was repaired. This latter effect corresponds to the change observed in double-aging the base metal in the transverse orientation (Figure 138). The reason for the two different trends observed in fracture toughness data cannot be explained on the basis of metallographic examinations and hardness surveys that were conducted on the welded joints. However, the change in SNB fracture toughness is considered to be of greater significance than the changes in PCI fracture toughness because of the thickness of the materials that are used in the large-diameter rocket-motor cases.

When the repair-weld heat-affected zones were located in the weld metal of the original weld, aging before repair resulted in lower PCI fracture toughness than when the repair weld was made with the original weld in the as-welded condition (Joint D in Figure 149). Also, lower SNB fracture toughness was observed under these same conditions (Figure 150), although the change was not large enough to be significant.

(4) Effects of Weld-Metal Dilution

As shown in Figure 135, the compositions of the filler wires used to weld the maraging steel are similar to those of the base metals, except for titanium content, which may be considerably higher in the filler wire than in the base metal. Because of these differences in alloy content, variations in alloy content may occur in making repair welds, depending on their location in base metal or weld-metal areas of the weldment.

V, B, Evaluation of Selected Weld Filler Wire and Weld Process (cont.)

The composition of the weld fusion zone of original welds in maraging steel plate was a function of the amount of base metal that was melted and the filler metal that was added, less any loss in alloy content that occurs from vaporization in the arc or gas metal reactions that occur during welding. The composition of repair-weld fusion zones, which are deposited in the fusion zone of the original weld, is a function of the composition and amount of original weld metal that is melted and of filler metal that is added.

Although composition variations were expected to be minor with the combination of base metal and filler metal evaluated in this program, tests were conducted to determine if the tensile properties and fracture toughness of the repair-weld fusion zones deposited in the original weld differed from those of the original-weld fusion zone. For these tests, simulated repair welds deposited in the joint A configuration (Figure 133) were evaluated after one aging cycle at 900°F for 8 hr. The tensile properties and fracture toughness of the repair-weld metals are listed in Figures 151 to 153. As expected, the properties of the repair-weld metals do not vary significantly from those of the original welds after similar aging treatments. The properties of original weld metals are listed in Figures 139 to 141.

With the attainment of yield strengths within the specified range, SNB fracture toughness is the most important criterion for evaluating repair-weld procedures because of its relationship to the critical flaw length that must be nondestructively detected. Figure 154 summarizes the plane-strain fracture toughness data and corresponding critical flaw lengths representing the various conditions encountered in repair-welding age-hardened chambers. Two conditions reduced plane-strain fracture toughness: (1) double-aging treatments (900°F for 8 hr) for the base metal in the transverse orientation, and (2) repair welding age-hardened weldments so that the heat-affected zone of the repair weld coincided with that of the original weld or was located in the weld fusion zone.

V, B, Evaluation of Selected Weld Filler Wire and Weld Process (cont.)

However, the reduction in plane-strain fracture toughness observed with the base metal-filler metal combination used in the program was not considered serious because the resulting critical flaw lengths should be detectable by available nondestructive inspection techniques (magnetic particle, X-ray, dye penetrant, and ultrasonic). Also, it was significant to note that these SNB fracture toughness data were considered to be qualitative and conservative, in that the fracture-toughness (G_{Ic}, K_{Ic}) values and critical flaw sizes were less than those which would be indicated using valid, quantitative, plane-strain, fracture-toughness, part-through-crack tensile-test specimens.

However, if similar effects had been encountered with higher-strength base metals, weld metals at the high end or in excess of the yield strength range specified, the decrease in critical flaw size could become a concern.

VI. EVALUATION OF THE EFFECTS OF COLD FORMING ON THE TENSILE AND FRACTURE-TOUGHNESS PROPERTIES OF PLATE

This phase of the material and process evaluation program was initiated to determine the effects of cold forming on the tensile and fracture-toughness properties of grade 200, 18%-nickel steel. This program ensured an understanding, before the start of fabrication, of the behavior of the 18%-nickel steel when subjected to severe, cold press-forming. This evaluation was originated particularly to evaluate alloy-segregated or banded material. However, the grade 200, 18%-nickel steel produced with the vacuum-arc remelting process did not produce banded material on this program. This task is reported in Reference (9).

A. MATERIAL UTILIZED

Lukens plate R-600-1A, a section of which is shown in Figure 155, was formed into an aft-head gore section for the first PETV. The gore was rejected for use on the PETV because of a forming defect.

The plate was rolled from a 41.5- by 60- by 6-in. slab, which was cut from the middle of a 118- by 41.5- by 6-in. slab that was forged from a 30-in.-dia vacuum-arc remelted ingot. The plate was finished to a size of 254 by 61 by 0.610 in. and was annealed at the mill at 1500°F for 1 hr. The mill-certified chemical analysis for this plate is listed in Figure 156. Plate mechanical properties are tabulated in Figure 157.

B. FORMING

The gore segment was cold-formed by holding it on female dies and pressing it with male dies 568 times with forces up to 2000 tons. Two different hydraulic presses, one rated at 2000 tons and the other at 200 tons, were used. Break, preform, and finishing dies in eight different operations,

VI, B, Forming (cont.)

some using wooden shims, were used. The straight flange portion of the gore was formed in four operations using 88 presses. The configuration of the gore is shown in Figure 158. A joggle defect was created when, during the straightening of the flange, the gore was struck by the edge of the die about 8 in. from its bottom and 10-3/4 in. from the right side, as shown in Figure 158. The maximum reduction in thickness resulting from cold-forming was 13.7%, and the nominal plastic strain formed by the spherical radius was about 2%.

C. SPECIMEN PREPARATION AND TESTING PROCEDURE

1. Tensile Specimens

After sectioning the gore, as shown in Figure 158, 12 tensile specimens were machined by Lehigh Testing Laboratory. Six tensile specimens were cut from each section, three in the longitudinal orientation and three in the transverse orientation.

To meet the specimen tolerances, moderate straightening of the specimen blanks was required. All machining operations were performed in such a way as to ensure that the material was not excessively heated. The samples, machined to the configuration shown in Figure 159, were then sent to Sun Oil where the samples from Section A were maraged for 4 hr at 900°F in a calibrated convection furnace (±5°F). The samples from Section B were re-solution-annealed for 1 hr at 1675°F and then maraged for 4 hr at 900°F. After completion of maraging, the tensile specimens were tested on a 120,000-lb Riehle universal hydraulic tensile machine at a strain rate of 0.010 in./in./min to the yield point.

The test area temperature range was 74 to 78°F with a relative humidity of 50 to 54%.

VI, C, Specimen Preparation and Testing Procedure (cont.)

2. Slow Notch Bend Specimens

Ten SNB specimens (five longitudinal and five transverse) and three longitudinal calibration bars were machined from both Sections A and B at Sun's Wetherill Plant to the configuration shown in Figure 159.

The samples were then sent to Sun Oil where samples from Section A and the calibration bars were maraged for 4 hr at 900°F; samples from Section B were re-solution-annealed for 1 hr at 1675°F and maraged for 4 hr at 900°F. The test specimens were fatigue-cracked at the Vertol Division of The Boeing Company using a Sonntag SF-1U universal fatigue-testing machine with a bend fixture attached. After fatigue cracking, the specimens were tested at a rate of deflection of 0.020 to 0.025 in./in./min on a Riehle testing machine, with a three-point bending fixture. Load and deflection were autographically recorded for each specimen. The test temperature was 77°F and the relative humidity was 56%.

3. Precracked Impact Specimens

From both Sections A and B, 18 specimens (six longitudinal, six transverse, and six short transverse) were machined by Sun in accordance with the dimensions shown in Figure 159. The specimens from A were maraged by Sun Oil for 4 hr at 900°F. The specimens from B were re-solution-annealed for 1 hr at 1675°F prior to maraging for 4 hr at 900°F and were then fatigue-cracked to a nominal crack depth of 0.020 in. and tested on an impact machine at Manlabs, Inc.

VI, C, Specimen Preparation and Testing Procedure (cont.)

4. Macrosection of Joggle

a. Macroetch

A section of the gore, 2-5/8 by 3-5/8 in. by plate thickness, which contained the joggle, was macroetched using the procedures of ASTM-A317-54 with a solution consisting of 50% hydrochloric acid and 50% water at a temperature of 160 to 180°F. The plate section is shown in Figure 160.

b. Microhardness Traverses

Five microhardness traverses were made as shown in Figure 161. On each traverse, 10 microhardness readings were made using a Knoop hardness tester (500-gm load). The sample was then maraged at 900°F for 4 hr, and hardness readings were retaken.

D. RESULTS

1. Specimens from Cold-Formed and Maraged Material

The specimen results of the cold-formed and maraged material are shown in Figure 157. The tensile strength of the formed material was 9 ksi lower than that of the parent plate for the longitudinal direction and 6 ksi lower than that of the parent plate for the transverse direction. Although the specimens from the gore were taken from the top one-fifth of the plate and the specimens of unformed material were removed from the bottom end, the difference in strength could not be attributed to the difference due to location in the plate. Tensile data from the top end of the plate showed a maximum difference of only 2 ksi (Figure 156) compared to specimens from the

VI, D, Results (cont.)

bottom end of the plate. The difference in strength from transverse to longitudinal orientation was 7 ksi for the plate material and 10 ksi for the formed material.

The plane-strain fracture-toughness values for the formed material were not appreciably different from the values obtained for the parent plate. The longitudinal orientation had values of G_{nc} that were about 15% lower for the formed plate than for the as-received material. The value for the transverse direction was about 10% higher for the formed plate than for the as-received material.

The plane-stress fracture-toughness values (W/A) at room temperature were comparable for the parent plate and the formed material. At the lower test temperature, the formed material W/A values were well below those of the parent plate. In general, the formed material did exhibit lower toughness at a lower strength level, but this difference was not considered significant.

2. Specimens from Cold-Formed Material Annealed Prior to Maraging

As shown in Figure 157, the tensile strength of the annealed and maraged specimens was 6 ksi lower for the longitudinal orientation and 13 ksi lower for the transverse orientation than in those specimens which were directly maraged. Strength directionality was reduced to 3 ksi as compared to 7 ksi for the plate. The microstructure of the formed material which was annealed prior to maraging was fully recrystallized (Figure 162).

VI, D, Results (cont.)

The values for plane-strain fracture toughness were the same as those for the samples which were maraged directly. From these data, it was concluded that solution-annealing prior to aging was not required to restore toughness to cold-formed plate material.

The plane-stress fracture-toughness values (W/A) were comparable to parent-plate values. The formed material did not show as large a difference between longitudinal and transverse values as compared to parent plate or aged specimens. Although the W/A level of the annealed and aged specimens was above that of the aged specimens, this was attributed mainly to the difference in strength.

3. Joggle

An examination of Figure 160 shows that the flow lines alter their path in the region of the joggle for the entire thickness of the plate. Work-hardening would be most pronounced in the region of these disturbed flow lines. The results of the hardness traverses do not give any indication that work hardening had taken place in this localized area. It can be seen in Figure 161 that traverses were from regions of undisturbed grain flow.

4. Conclusions

The cold-formed segments of the 260-SL cases would be worked about one-seventh as much as the material studied in this evaluation. Therefore, it was concluded that cold-forming would have a very minor influence on the strength and toughness of the formed material, and annealing was not required following forming.

VII. EVALUATION OF STRAIGHTENING WELDED JOINTS

Cold-straightening of welded joints was used as a means of ensuring that the cylinder and skirt longitudinal welds of the chamber met the specified diameter and contour requirements. This method was preferred to the alternative approach of building massive fixtures in an effort to prevent distortion during welding.

Equipment was available at Sun in the form of a vertical flanging press to be used with a 130-in.-radius die where welded seams could be pressed to contour (Figure 163). This facility was used for both of the PETV cylinder sections and for all 260-SL shell and skirt sections.

This evaluation was undertaken prior to initiating fabrication to examine how cold-straightening of welded joints affected the strength and notch toughness of the final maraged weldment. This evaluation is reported in Reference (10).

A. PROCEDURE

Three 8- by 13-in. weld test plates were prepared, using Lukens plate R-600-1A and Special Metals 34481 weld wire. The 13-in.-long welds were ground flush and inspected for defects in accordance with production program requirements. The plates were then cold-formed to an 18-in. cylindrical radius, using dies from the 36-in. PETV fabrication. This forming produced about a 2% permanent strain in the plates in the direction of the welds. This radius was then flattened in steps to cold-straighten the weld seam. This latter process was more severe than any straightening required in production.

Tensile, SNB, and PCI specimens were machined from the flattened plates at Sun Shipbuilding and maraged together at the Sun Oil laboratory. No annealing steps were included since these were not used in production.

VII, A, Procedure (cont.)

The tensile specimens were then tested in a 120,000-lbf Riehle universal testing machine at Sun Oil, while the impact specimens were sent to Manlabs, Inc., for fatigue cracking and testing. The bend specimens were fatigue cracked at the Boeing Vertol Division and tested at Sun Oil. Five calibration bars, representing the weld deposit and the heat-affected zone, were also tested. The fatigue cracks in the SNB specimens were very irregular because of poor cracking technique. However, the results shown in Figure 164 indicate that the data are valid.

B. RESULTS

As shown in Figure 164, the weld-joint yield-strength values compared very closely with those of flat weld plates. An increase of only 1 ksi from 209 to 210 ksi was noted, and this was not considered significant.

The longitudinal, weld-metal-only tensile specimens did show an increase of about 20 ksi, increasing from 205 to 225 ksi (Figure 164). This was expected, since the 2% strain was formed along this axis. If the plate were formed across the joint, an equal amount of cold work could be expected.

The fracture-toughness values, both SNB and PCI, correlated very closely with those of flat weld plates, as shown in Figure 165. Again, these data were not unexpected, since the major strain was not in the direction of the joint. The SNB and the PCI specimen data are shown in Figures 166 and 167, respectively, and the comparison data were taken from the referenced reports. It was concluded that straightening a weld along the weld axis had no significant effect on the strength or notch toughness of the weldment.

VIII. MARAGING SYSTEM DEMONSTRATION

The 30-ft-dia, 95-ft-high, maraging heat-treatment furnace used in the 260-in.-dia motor program was fabricated specifically for use on this program. The design concept also provided the versatility for maraging small parts, such as the motor nozzle shell, and the flexibility of expansion to marage full-length motor chambers. As shown in Figure 168, all components of the furnace shell and ducts are segmented for flexibility of shortening or lengthening the furnace. In addition, all aspects of the furnace were designed to be compatible with the 280-in.-dia mild-steel chamber fabricated by Sun Shipbuilding.

The demonstration was undertaken to show that the maraging system had the capacity, controllability, and working-zone temperature distribution to successfully marage the fabricated motor components. In addition to system design evaluation, the demonstration permitted an investigation of operational procedures and characteristics of the furnace and thorough training of operations and data-collection personnel. The complete results of this maraging demonstration program are presented in a report prepared by the Sun Shipbuilding and Dry Dock Co., Reference (11).

A. MARAGING SYSTEM DESIGN

1. Air Flow Distribution

The maraging system was designed to circulate the heated air over only the exterior surface of the chamber. The motor chamber was installed on the maraging-stand support ring forward-end down. A deflector covered the nozzle opening to streamline the air flow entering the top of the furnace and to prevent the heating air from circulating inside the chamber.

The maraging-furnace wall (chamber enclosure) was fabricated from corrugated steel plate and consisted of a base section, four center sections,

and a dome. Heating air was delivered at the top of the furnace through a 6-ft-square duct. The motor components were heated with recirculated clean air that was free of combustion products.

Turning vanes and air deflectors were installed to deflect approximately 50% of the heating air into the stagnation areas between the skirt interior and head exterior in the area of the forward and aft Y-rings. An air deflector was also installed under the forward head to ensure even heating along the full length of the forward head.

The heating air entering the top of the furnace passes in the annulus between the chamber and furnace enclosure to the forward head through slotted openings in the chamber support rings. The air was then ducted out of the bottom of the furnace for recirculation.

2. Fan System

The heating air was circulated through the system with three Garden City Fan and Blower fans. Each fan was capable of operating at 1000°F and delivering 75,000 cfm at 885 rpm, providing a total system capacity of 225,000 cfm. Each fan was driven by a 150-hp electric motor.

3. Heat Exchanger

The heat exchanger is the single-shell-pass, single-tube-pass concept with 655 sq ft of heat exchange area. The combustion gas made one pass through the fire tube and was discharged to the atmosphere. The heating air made one pass over the fire tubes. The primary heat-transfer mode was gas radiation. The heat exchanger operated at approximately 45% efficiency, which resulted in a maximum-capacity output of approximately 10.8 million Btu/hr.

VIII, A, Maraging System Design (cont.)

The heater is a natural-gas-fired tube boiler with 24 fire tubes. Each tube, 10 in. in dia and approximately 10.5 ft long, was rated at 1 million Btu/hr; hence, the boiler design was rated at 24 million Btu/hr.

B. FURNACE DEMONSTRATION RUN

The 280-in.-dia mild-steel chamber, fabricated by Sun prior to the start of the 260-in.-dia motor program, was positioned on the maraging support ring. The chamber enclosure, ducts, and air deflectors were installed in accordance with the design requirements for maraging 260-in.-dia motor components.

1. Test Instrumentation

Seventy-eight thermocouples were attached to the inside and outside of the chamber along four rows, as shown in Figure 169. These thermocouples were used to determine, in detail, the temperature distribution within the furnace and along the chamber.

Readings from the thermocouples were taken on three direct-print-out recorders. All of the recorders and thermocouples were calibrated at 900°F; the recorders showed less than 2°F deviation, and the thermocouples less than 5°F deviation. The recording-chart accuracy was around 5°F, so that corrected readings were not required.

2. Operational Procedure

a. The furnace inlet temperature entering the top of the furnace enclosure was increased to 750°F. The furnace damper system and gas-valve control were automatically adjusted by the furnace control system to maintain a 45°F temperature differential between furnace inlet and outlet

VIII, B, Furnace Demonstration Run (cont.)

temperatures. Thermocouples were monitored to ensure that the temperature spread in the steel parts of the chamber did not exceed 200°F.

b. When the furnace inlet temperature reached 750°F, the furnace controller was switched to maintain an inlet temperature of 750°F and was held at this temperature until the temperature of the steel parts reached 750 ± 30°F. The purpose of this step was to reduce the temperature spread in the steel parts before heating the furnace to the maraging temperature.

c. After steel parts had reached a temperature of 750 ± 30°F, the furnace controller was again switched to ΔT control, set at 60°F. All 24 burners were fired for the maximum output increase to the maraging temperature of 900°F.

d. When the furnace inlet temperature reached 900°F, the furnace controller was switched to maintain that inlet temperature. The number of burners in operation was reduced so that the remaining burners would operate at optimum performance to maintain the 900°F inlet temperature.

e. The furnace was operated in this stabilized condition to maintain the 900°F for the 8-hr maraging cycle. The 8-hr hold period began when all thermocouples attached to the chamber recorded temperatures above 850°F.

f. At the end of the 8-hr period, the furnace controller was placed in the normal cool position with the furnace ΔT set at 75°F. All main burners and 18 of the 24 pilots were shut off. The manual damper in the fan inlet duct was opened and the controller was switched to automatic.

g. The system was held stabilized at 600 ± 50°F for 1 hr to reduce the temperature gradient within the furnace.

VIII, B, Furnace Demonstration Run (cont.)

h. The remaining six pilots were shut off. The three fans were operated at 85% of available horsepower to cool the furnace to 200°F, at which point the furnace was shut down.

The maraging demonstration was uneventful with respect to the established procedure. To evaluate the controllability of the furnace-inlet air temperature, the inlet air temperature was increased 5° during the stabilized portion of the cycle at 900°F by a simple adjustment of the temperature controller and a subsequent slight readjustment. The increase to 905°F can be seen in the furnace temperature-time profile. The maraging system was very stable and controllable throughout the entire cycle.

Inasmuch as effective maraging of the 18%-nickel steel occurs above 900°F, the time required to heat from 750 to 900°F and to cool from 900 to 750°F was reduced to the minimum possible. All 24 burners were operated at maximum capacity to raise the furnace temperature to 900°F. The furnace inlet air was stabilized at 900°F after approximately 2 hr, demonstrating an acceptable response. The total elapsed time to reach the stabilized maraging temperature of 900°F was approximately 10 hr.

As the inlet air temperature approached 900°F, the number of burners operating was gradually reduced to avoid passing the 900°F range and to yield a smooth transition into stabilized operation. This operation was performed with a great degree of controllability and can be seen in the inlet air and steel-part temperature response plotted in Figure 170. The furnace was operating with 20 burners at 75% capacity just prior to stabilization and was further reduced to 14 burners at 75% capacity after approximately 2.5 hr. Furnace operation was reduced to 13 burners operating at 75% capacity after 4 hr of stabilization. After completion of the stabilized portion of the cycle, the chamber was cooled to 700°F in approximately 1.5 hr.

VIII, B, Furnace Demonstration Run (cont.)

3. Furnace Performance

The maraging system maintained a working-zone temperature spread of less than 30°F (inlet temperature minus outlet temperature) throughout the stabilized position of the cycle.

Figure 171 shows the maximum and minimum case temperatures recorded during the maraging portion of the cycle. The maximum recorded temperature was 915°F, and the minimum temperature recorded was 850°F. However, the case temperature range over most of the maraging cycle was around 40°F (870 to 910°F). During maraging, the highest temperatures were recorded in the interior of the aft skirt and the lowest temperatures in the interior of the forward skirt at the Y-ring. Sample material from three plates intended for use on the 260-SL-1 chamber were placed in the furnace to evaluate 18%-nickel steel plate maraged in the furnace.

Figure 172 shows the greatest case temperature differences over the entire chamber for the complete heating, maraging, and cooling cycle time of 19 hr. During heat-up to 750°F, differentials as large as 175°F were observed. In rising from 750 to 900°F, differentials as high as 125°F were recorded.

Figures 173, 174, and 175 show, for inside and outside chamber positions, temperature distributions in circumferential and longitudinal chamber orientations. The Y-joint areas showed the largest circumferential temperature differences. Figure 173 shows the forward Y-joint temperatures

VIII, B, Furnace Demonstration Run (cont.)

(bottom of furnace). These values were between 870 and 880°F during the maraging period. Figure 174 shows the temperature differences for the aft Y-joint (top of furnace) and values during maraging ranged between 880°F and 900°F.

The maximum temperature differences observed were longitudinal along the case, as shown in Figure 175. These values range between 870 and 900°F for the maraging period and are due mainly to a generally decreasing air temperature proceeding down the chamber resulting from heat losses through the insulation. Thermocouples in both the forward and aft skirt areas read close to the upper temperature range, and temperatures of approximately 910°F were recorded in the aft skirt area (top of furnace).

It was concluded from the maraging demonstration that the maraging system had the degree of controllability and the performance characteristics required for maraging the production motor components. Also, the temperature distribution within the furnace was within the requirements expected for maraging the components.

C. EVALUATION OF SPECIMENS MARAGED WITH 280-IN.-DIA CHAMBER

Three small test plates were placed near the bottom of the furnace inside the chamber forward skirt to provide information on the actual aging response of Grade 200 18%-nickel steel during the maraging demonstration. Laboratory testing of the specimens machined from the test plates resulted in yield-strength levels in excess of values obtained with laboratory maraging of the same heats of material. Maraging cycles were nominally 900°F for 8 hr in each case.

VIII, C, Evaluation of Specimens Maraged with 280-in.-dia Chamber (cont.)

The test data from the three heats of material are compared below. These three plate heats were used in the fabrication of the 260-SL-1 motor chamber.

Plate	Laboratory Maraging		280-in.-dia Motor Demonstration	Difference
25000-6A (M)	221	Yield Strength, ksi	238	17
25000-6A Weld	211		224	13
24997-1A (B)	234		245	11
3960819-B (EE)	216		228	12
25000-6A	655	Toughness (W/A), in. lb/sq in.	623	32
24997-1A	583		502	81
3960819-B	1124		838	286

The strength increase observed was of some concern since the increase would likely result in many of the plates used in fabrication exceeding the specified 235-ksi maximum yield strength. In addition, any strength increase was undesirable because of the tendency to reduce fracture toughness.

It was felt that the strength increase in the maraging demonstration was associated with the time required to reach maraging temperature (approximately 10 hr) and the time to cool from maraging temperature (approximately 2 hr). The specimens maraged in the laboratory were in a 900°F preheated oven and were air-cooled after maraging.

D. ADDITIONAL TESTING TO EVALUATE THE STRENGTH INCREASE

Two test programs were initiated to more clearly understand the material properties that could be expected after maraging the motor components (additional material characterization) and to understand to a limited degree

VIII, D, Additional Testing to Evaluate the Strength Increase (cont.)

the characteristic behavior of the material to certain variances in the maraging cycle (supplemental investigation).

1. Additional Material Characterization

a. Material

The material selected for additional characterization of material properties to be expected with the actual maraging cycle included the high-strength, lower-toughness material and the lower-strength, high-toughness material. The material selected for evaluation is shown in Figure 176.

b. Results

(1) Strength Properties

The maraging cycle used in the laboratory for this study was a 100°F/hr heat-up, 900°F for an 8-hr hold, and a 250°F/hr cool-down, for a total elapsed cycle time of approximately 19 hr. This laboratory cycle was chosen on the basis of the maraging cycle expected to be used for the 260-SL-1 chamber.

The results of the strength data evaluation is tabulated in Figure 177. Yield strengths for the original 900°F for 8-hr material characterization laboratory maraging cycle are also tabulated in Figure 177 for purposes of comparison.

A comparison of the yield strengths for the two maraging cycles showed that the complete profile cycle increased yield strengths from 6 to 17 ksi. The yield strengths for plates A, B, and C were above the 235-ksi maximum limit.

VIII, D, Additional Testing to Evaluate the Strength Increase (cont.)

The ductility measured on these plates was satisfactory with elongation of 10% or higher and reductions in area of 49% or higher.

Because of the notch location, the long-time maraged impact specimens failed in the weld metal. Thus the average W/A value of 912 in.-lb/sq in. does not correspond to the low measured yield strength, which was based on weld heat-affected zone failures. However, the similarity of the W/A values for the seven-time-repaired specimens and the one-time-repaired specimens indicate that the manual-weld-deposit toughness was not affected by multiple repairs.

(2) Slow Notch Bend Data

The plane-strain fracture-toughness (G_{nc}) values for the 260-SL-1 material maraged at the complete time profile cycle are tabulated in Figure 178 along with comparative original material characterization data. As anticipated from the strength data, the fracture toughness for the full profile cycle generally was lower than that for the material characterization heat treatment. However, the largest reductions in toughness were observed on the material which had the higher toughness initially and could best afford the loss. The largest reductions in G_{nc}, amounting to 30%, were observed on plate C. This plate increased to 14 ksi in yield strength for the full profile cycle. The four plates showing the lowest initial toughness, i.e., plates A, B, M, and P, suffered no measurable loss in toughness.

The 63343 automatic welds also decreased 30% in toughness. This reduction was coupled with a 13-ksi increase in strength.

VIII, D, Additional Testing to Evaluate the Strength Increase (cont.)

(3) Discussion and Conclusions

The additional characterization covering the extremes between high-strength, lower-toughness material and low-strength, high-toughness material used in fabrication, resulted in a maximum strength increase of 17 ksi and a maximum yield strength of 244 ski (9 ksi above the maximum specification limit). Plate of this strength level resulted in a plane strain fracture toughness value (G_{nc}) of 188 in.-lb/sq in. This combination of maximum-strength and lowest-toughness characteristics, resulting from the complete profile maraging cycle, was considered acceptable for the fabricated motor component. It was recognized, however, that any reduction in fracture toughness properties of the material was not desirable.

2. Supplemental Investigations

The supplemental testing was initiated to evaluate, to a limited degree, the behavior of the Grade 200, 18%-nickel steel to variances in the maraging cycle temperature-time profile that could occur as a result of either planned or unplanned deviations to the maraging cycle. It was expected that this investigation would reveal if either the heat-up or cool-down portions of the maraging cycle were the most significant contributor to the strength increase.

a. Effect of Heat-Up and Cool-Down Rates on Strength Increases

This phase of the evaluation was accomplished to determine if either the heat-up or cool-down portions of the maraging cycle was the major contributor to the strength increase. The results of this investigation are tabulated in Figure 179. The yield strengths developed by

"REPRODUCIBILITY OF THE ORIGINAL PAGE IS POOR."

maraging with a heat-up rate of 400°F/hr and ambient air cool-down were close to the strengths from the original material characterization baseline data. The yield strength for plate M was 4 ksi higher than the baseline strength; the strength for plate A was 1 ksi lower; and the strength for the 63343 weldment was the same (211 ksi). Increasing the heat-up rate from 400 to 800°F/hr decreased the yield strength of plate M to 221 ksi and increased the yield strength of the 63343 weldment to 214 ksi. Again, the results were very close to the baseline data.

The third maraging cycle used in the investigation, heat-up at 400°F/hr and cool-down at 250°F/hr (200°F/hr for plate M), developed yield strengths 7 ksi higher than the baseline strengths for both plate M and the 63343 weldment.

The results of this investigation indicated that a heat-up rate of 400°F/hr was rapid enough to avoid a significant increase in strength. However, cooling rates of 200 to 250°F/hr in conjunction with the 400°F/hr heating rate indicated a moderate strength increase.

b. Effect of Varying Stabilized Temperature

This segment of the investigation was accomplished to investigate the effects of varying the temperature in the stabilized portion of the cycle in conjunction with the slow heat-up and cool-down rates.

The strength data for plate M and the 63343 automatic weldment specimens for the four hold temperatures investigated (800, 850, 900, and 950°F) is recorded in Figure 180. Comparative baseline material characterization data are included where available.

VIII, D, Additional Testing to Evaluate the Strength Increase (cont.)

As expected, the slow heat-up and cool-down rates caused increases in strength above the baseline data at all hold temperatures for which comparative data was available. For plate M, the largest increase in strength (12 ksi) was observed for the 900°F hold and the smallest (7 ksi) for the 950°F hold. The weld specimens showed similar increases; however, with these specimens, the largest increase (11 ksi) was observed for the 950°F hold and the smallest (3 ksi) for the 850°F hold.

c. Investigation of the Rate of Strength Increase During Heatup

The rate of strength increase during heat-up was investigated to determine, if possible, the temperature at which the additional strengthening occurs. Specimens from plate heat 25000-6A (M) were heated at 100°F/hr in 100°F increments from 700 to 900°F, with 950°F the highest temperature evaluated. After heating to the desired temperature, the specimens were air-cooled. Solution-annealed strength was tested as a baseline understanding of the strength increase.

The tensile data from plate M are recorded in Figure 181. Comparison of this data to the baseline yield strength for this plate of 221 ksi (900°F/8 hr material characterization data) shows that, while the maraging reaction is detectable after slow heating to temperatures as low as 700°F, a large increase in strength occurs during heating between 850 and 900°F. During the slow heat-up to 900°F, 84% of the 900°F/8 hr baseline strength (185 ksi) was developed.

d. Effect of Double Heat-Up on Strength

The possibility of maraging furnace shutdown because of malfunction of furnace components would require a double (or repeated) heat-up

of the motor chamber. To understand the effect of double heating of the strength properties of Grade 200, 18%-nickel maraging steel, tensile specimens from plate M were maraged, simulating an interrupted cycle. The cycle used was to heat-up to 900°F at 100°F/hr, immediately air cool, reheat to 900°F at 100°F/hr, hold at 900°F for 8 hr, and air cool.

The average values of the test results from three tensile specimens from plate M are shown below:

0.2% Offset Yield Strength	226 ksi
Ultimate Tensile Strength	236 ksi
Elongation in 1 in.	10%
Reduction in Area	51%

The slow heat-up rate and interrupted hold increased the yield strength of the specimens 5 ksi above the baseline strength of 221 ksi. This change in strength is small compared to changes resulting from the initial heatup.

e. Discussion of Results

The investigations discussed were not intended to determine the cause of the strength increase resulting from metallurgical changes in the material, but did serve to increase the level of knowledge of the heat-up and cool-down parameters affecting this phenomenon and to localize the areas of interest in the maraging cycle for possible additional study.

Since the observed strength increases for 260-SL-1 chamber material subjected to complete profile maraging were much larger than the increases because of longer hold times at the maraging temperature,

VIII, D, Additional Testing to Evaluate the Strength Increase (cont.)

it is apparent that the higher strengths are caused by the heating and cooling rates used in the cycle. As an example, the yield strength of plate M increased 11 ksi from 221 to 232 ksi for a 900°F/8 hr maraging cycle as a result of heat-up at 100°F/hr and cool-down at 250°F/hr. The effect of increasing the time at 900°F from 8 to 16 hr was to decrease the yield strength slightly (221 to 219 ksi). While the overall maraging time for the slow heat-up, 8-hr hold, slow cool-down and the rapid heat-up, 16-hr hold, rapid cool-down cycles was similar, the effects of the two cycles on strength were quite different.

The strength increase was present for hold temperatures of 850, 900, and 950°F in conjunction with the slow heat-up and cool-down rates, but the specimens which were heated slowly and air cooled with no high temperature hold indicated that the temperature range from 850 to 900°F was probably the most critical for the development of high strength, at least during the heat-up period. Over the range of heating from 850 to 900°F, the strength of the plate M specimens increased an average of 21 ksi.

The outcome of the supplemental investigations of the effects of variations in the maraging cycle did indicate that the response of maraging material to the aging treatment was affected by both the heat-up and cool-down rates. Based on the limited data available, the critical heat-up rate to avoid the significant amount of strength increase was approximately 400°F/hr. No critical cool-down rate was determined; however, it was determined that a rate of 250°F/hr resulted in only a moderate increase in strength above that for ambient air cooling.

IX. EVALUATION OF HYDROSTATIC-TEST FLUID

This phase of the material and process evaluation program was undertaken to evaluate the effect of two hydrostatic-test fluids on the short-time stress-corrosion susceptibility of grade 200, 18%-nickel steel.

Short-time stress-corrosion susceptibility tests, using the fatigue-cracked center-notch tensile specimen, were selected to evaluate hydrostatic fluid for the large-diameter rocket motor chambers. This method of evaluation was selected because stress-corrosion susceptibility was the most important criteria to be considered in specifying pressurizing media for the hydrostatic testing of solid rocket motor chambers, and the test specimen selected contained a fatigue crack which simulates natural cracks or flaws that might be present in the chamber to initiate stress-corrosion attack. Also, this test technique has been successfully employed in determining the stress-corrosion susceptibility of chamber materials and hydrostatic-test media for use in the processing of Polaris and Minuteman motor chamber assemblies.

A. HYDROSTATIC-TEST MEDIA

Two hydrostatic-test fluids were evaluated (i.e., 1 and 2% solutions of sodium dichromate in water--the sodium dichromate is an anodic inhibitor. Such inhibitors are efficient when adequately and uniformly mixed with the water and, when added in sufficient quantity, will prevent corrosion. If added in insufficient quality, they often will reduce the area affected by corrosion more rapidly than they diminish total corrosion and thus increase the intensity of attack on the affected areas. Also, anodic inhibitors may be dangerous if the sodium dichromate is not adequately mixed with the water.

The solutions were prepared with tap water. Because the composition of tap water is variable, the pH of the as-mixed solutions was 4.1 and 3.85 for the 1% and 2% solutions, respectively. The pH level of the test fluid was maintained at 7.3 by adding sodium hydroxide.

IX, Evaluation of Hydrostatic-Test Fluid (cont.)

B. MATERIALS

The stress-corrosion tests were conducted using 0.6-in.-thick, maraging steel plate from Republic heat 3920556. The composition of this plate fell within the ranges specified for the program as shown in Figure 182. On the basis of tensile properties and fracture toughness, heat 3920556 were considered to represent heats at the lower range (200 to 220 ksi) of the 200 to 235-ksi yield strength range.

Special Metals heat 34482 maraging steel filler wire was used to prepare weldments for the investigations. The composition of this filler wire fell within the range of composition specified for production welding (Figure 182) and is considered to be representative of the filler wire which will be used in the fabrication of motor components.

C. EXPERIMENTAL PROCEDURES

The procedures that were used to prepare and evaluate parent and weld metal test specimens are described below:

1. Specimen Preparation

Center-notched tensile test specimens were prepared from 0.6-in.-thick, grade 200, 18%-nickel maraging steel plate and weldments for this evaluation. The dimensions of the center-notched specimens are shown in Figure 183. The specimens were prepared as follows:

a. The parent metal plate and weldments were parted to form longitudinal and transverse parent and transverse weld specimen blanks, measuring 8 by 2 by 0.6 in.

TX, C, Experimental Procedures (cont.)

b. Each specimen blank was parted in the short transverse orientation to form two 8 by 2 in. specimen blanks, which were machined to a thickness of 0.07 in.

c. The specimen blanks were aged at 900°F for 8 hr.

d. Each specimen blank was machined to form a reduced section, 1.75 in. wide and 0.060 in. thick.

e. Each specimen was electro-discharge-machined to provide pinholes in each end of the specimen and to form a small 0.06-in.-long notch in the center of the reduced section.

f. The notched specimens were cyclic loaded in tension to propagate a fatigue crack, approximately 0.06 in. long, from each end of the elox notch in the center of the reduced section. After fatigue cracking, the total center-notch (elox + fatigue cracked) length approximated 0.75 in.

The parent-metal plate specimens were oriented both transversely and longitudinally with respect to the final rolling direction of the plate. For longitudinal tests, the specimens were oriented with their major dimension parallel to the final rolling direction of the plate. For the transverse tests, the specimens were oriented with their major dimension normal to the rolling direction. The weld-metal test specimens were oriented transverse to the weld with the weld-metal zone in the center of the reduced section. In the welded specimens, the notch was located in weld metal.

2. <u>Welding Procedures</u>

The 18-in.-long weldments were produced by joining two 4-in.-wide, 0.6-in.-thick, grade 200, 18%-nickel maraging steel (heat 3920556) test

IX, C, Experimental Procedures (cont.)

plates. Individual weld test plates were machine cut and all plate edges were machined for welding. This technique was used so that the plate edges would not be subjected to thermal cycles such as those that are encountered in flames or powder cutting which might affect the mechanical properties and metallurgical characteristics of welded joints. After machining, the plates were degreased and the plate surfaces were ground to remove oxide scale. Immediately before welding, the joint edges were wiped with acetone to remove oil film and other foreign materials. The weldments were prepared with a single-U joint configuration to simulate weldments in the 260-in.-dia motor chamber components. The single-U joints were prepared with a 0.060-in. root land, 0.093-in. root radius, zero root gap, and 45-degree included angle.

3. Testing Procedures

Three series of tests were conducted during the program to evaluate the hydrostatic test fluid. In one series, base-metal and weld-metal center-notched tensile specimens were tested in air and loaded to failure. The maximum tensile loads recorded during these tests and the uncracked portion of the specimen gage width were used to calculate the ultimate tensile strength of the test specimen. These data were obtained for comparative purposes to evaluate the severity of the stresses imposed on specimens while they were immersed in the hydrostatic test fluid. In the second series of tests, base metal and weld metal center-notched tensile specimens were loaded to a sustained tensile stress of 170 ksi and immersed in the hydrostatic test fluid for an extended period of time. These specimens were examined periodically for failure. In the third series, base-metal and weld-metal center-notched tensile specimens were loaded to a sustained stress of 170 ksi and immersed in distilled water, which did not contain inhibitors, for an extended period of time. These specimens also were examined periodically for failure.

IX, C, Experimental Procedures (cont.)

Most of the center-notched tensile specimens that were subjected to sustained tensile loads, while immersed in hydrostatic test media or distilled water, were tested in the fixture shown in Figure 184. These specimens, with a strain gage attached, were mounted in the fixture and stressed in a standard tensile machine. When the desired stress level of 170 ksi (calculated on the basis of uncracked area) was reached, the end nuts on the fixture were tightened until the tensile load was transferred to the test fixture. The tensile machine load was then released and the stress level in the specimen verified by the strain gage attached to the specimen. If a relaxation of stress occurred when the tensile machine load was removed, the fixture nuts were tightened until the desired strain gage reading was re-established. The test fixtures and center-notched tensile specimens were then fully immersed in the hydrostatic test media or distilled water and were examined periodically for failure. As a control for specimens tested in the fixtures, several specimens also were tested in creep-testing machines with the hydrostatic test media continually circulated around the center-notch specimen.

D. RESULTS AND DISCUSSION

The ultimate tensile strength of center-notched tensile specimens prepared from 0.6-in.-thick, maraging steel plate (Republic heat 3920556) and weld metals (filler wire heat 34482) and tested in air is listed in Figure 185. The ultimate strength of these specimens ranged from 197 ksi for the weld metal to 210 ksi for the base metal in the longitudinal orientation. In all instances, these ultimate strength values were lower than the 0.2% yield strength values obtained in testing unnotched tensile specimens. For unnotched tensile specimens, the 0.02% yield strength was 218, 221, and 207 ksi for the base-metal longitudinal, base-metal transverse, and weld-metal specimens, respectively.

IX, D, Results and Discussion (cont.)

The center-notched tensile specimens were tested to failure to obtain comparative data for evaluating the sustained tensile loads applied to the specimens while they were immersed in hydrostatic test media. The 170-ksi sustained stress level corresponded to 81, 84, and 86% of the ultimate tensile strength of the center-notched base-metal longitudinal, base-metal transverse, and weld-metal specimens, respectively. On this basis, the sustained stress level was high and should cause stress corrosion cracking if the materials were susceptible to this phenomenon.

Although high sustained stress levels were imposed, failures were not observed in either base-metal or weld-metal center-notched tensile specimens that were stressed at 170 ksi while immersed in 1 and 2% sodium dichromate solutions during a 45-day (1080-hr) exposure period. The results of these tests are shown in Figure 186. After the 45-day exposure period, the tests were discontinued because this exposure time greatly exceeded that which would be encountered during hydrostatic test and was considered long enough to ensure that the rocket motor chambers would not be susceptible to stress corrosion attack during the hydrostatic testing operation. On the basis of these data, both proposed hydrostatic test media were considered to be satisfactory for hydrostatic testing of the rocket motor components.

Failures were not observed in base-metal, center-notched tensile specimens that were stressed and immersed in uninhibited distilled water for 45 days. However, weld-metal specimens that were immersed in distilled water failed after 15-, 16- and 20-day exposure. On the basis of these data, the weld metal was determined to be more susceptible to failure than the base metal, and the inhibitors are considered necessary to prevent stress-corrosion failure in welded chambers.

IX, D, Results and Discussion (cont.)

The specimens that were immersed in hydrostatic test fluid and distilled water were also examined for evidence of general surface pitting corrosion during exposure. No evidence of this condition was visible on the surface of specimens immersed in either the 1 or 2% sodium dichromate solutions; but general corrosion was observed on the specimens that were immersed in distilled water.

Although failure of the specimens tested in either of the sodium dichromate solutions was not encountered, several of the specimens tested in the 1% sodium dichromate solution were examined for evidence of crack growth and stress-corrosion cracking. For these examinations, the specimens were parted down the center line of the reduced section so that the fatigue-cracked area on each end of the electro-discharge machined notch could be examined. Half of each specimen was heated to 900°F to oxidize the surface of any existing crack and fractured to expose the surface of the fatigue crack. Any crack extension from the original fatigue crack was then measured from the end of the fatigue crack to the freshly fractured surface.

A small amount of crack growth was observed in each of the specimens that were examined. A total crack extension of 0.020 in. (0.010 in at each end of the fatigue crack) was observed in longitudinal base-metal specimens compared with about 0.010 to 0.014 in. of crack growth for the base-metal transverse and weld-metal specimens.

To obtain additional information regarding the small amount of crack growth that was observed, the crack in one base-metal longitudinal specimen was examined by metallographic techniques. For this examination, the specimen was ground from one surface to approximately the center of the thickness of the specimen. This surface was then polished and prepared for examination by electrolytic etching in a 10% chromic acid solution to reveal

IX, D, Results and Discussion (cont.)

the prior austenitic grain boundaries. The results of subsequent metallographic examinations are shown in Figure 187 and show the intergranular cracking or corrosion which was observed at the end of the fatigue crack.

It was not determined whether crack growth occurred in the testing period or if the condition noted in Figure 187 represents the termination of the original fatigue crack. It was concluded, however, that the exposure of the specimens tested in this program far exceeded time under stress in the hydrostatic test operation, and that 1 and 2% water solutions of sodium dichromate controlled to a pH of not less than 7.1 are acceptable solutions for hydrostatic test of the motor components.

X. PROCESS EVALUATION TEST VEHICLES (PETV)

Two 36-in.-dia Process Evaluation Test Vehicles (Figure 188) were designed and built for hydrostatic burst tests to determine that the design concepts, material selection, and fabrication techniques used were satisfactory for use in the 260-in.-dia motor program. This program determined that the total approach to design and fabrication yielded end product results consistent with the structural requirements of the motor components.

The materials (grade 200, maraging steel plate and forgings) used in fabrication of these test vehicles were extensively evaluated in order to determine that the material was representative of material to be used for motor component fabrication. The complete results of the plate and forging material evaluation are presented in a report prepared by Sun Shipbuilding, Reference (12). Weld wire heats 34481 and 08436 used in the welding of the first PETV were evaluated in complete detail in the plate welding phase of the material and process evaluation program and are reported in a previous section of this Appendix. Weld wire heat 63343 used in fabrication of the second PETV is reported in the material characterization section of this report.

A. PROCESS EVALUATION TEST VEHICLE DESIGN AND FABRICATION

The PETV designs, shown in Figures 189 and 190, were intended to duplicate design features and fabrication procedures, i.e., forming, welding, machining, nondestructive testing techniques, etc., to be used in fabrication of 260-in.-dia pressure vessel components.

The primary design requirement of the PETV's was to ensure that initial burst failure occurred in the cylindrical section of the vehicle. This permitted evaluation of the vehicle performance in an area effectively free of discontinuity stresses and in a biaxial stress field. The cylindrical-section thickness was selected to be equal to the thickness in the cylindrical

section of the 260-in.-dia motor chamber (0.600 in. minimum). The forward and aft heads and flange closures were designed to ensure greater safety factors (or less stress) than the cylindrical section at failure.

1. Forward and Aft Heads

The forward and aft heads of the PETV's were designed with a hemispherical contour representing that of the 260-in.-dia motor chamber and were fabricated with a 0.670-in. minimum thickness. As shown in Figures 189 and 190, a short transition area from head thickness to cylindrical-section thickness was provided in the cylindrical section, starting at the forward and aft equators. Openings in the forward and aft heads, 14 and 3 in. in diameter, respectively, provided access to the inside of the PETV's during fabrication. These openings were also used for routing instrumentation wires and pressurization lines during hydrostatic burst test.

The basic membranes of the forward and aft heads of the first and second PETV's were identical in structural design; however, the method of fabrication was different between the first and second PETV's. The heads of the first PETV were fabricated from four cold press-formed gore segments, which were longitudinally welded together to form the gore subassembly (Figure 189). The attachment flanges were girth welded to the subassembly, and the subassembly was then girth welded to the cylindrical section. This method of fabrication represented, in concept, the method of fabricating the heads of the 260-in.-dia motor chamber. The forward and aft heads of the second PETV were fabricated as one-piece forged-and-machined sections. The attachment flanges were integrally forged and machined with the basic membrane (Figure 190).

X, A, Process Evaluation Test Vehicle Design and Fabrication (cont.)

2. Cylindrical Sections

The cylindrical sections of the two PETV's were identical in design and fabrication approach, and were fabricated with cold roll-formed-and-welded plate with a minimum thickness of 0.600 in. This represented the method of construction and thickness of material to be used in the cylindrical section of the 260-in.-dia motor chamber. Although two longitudinal welds were made in each cylindrical course of the 260-in.-dia chamber, the two PETV's were fabricated with four longitudinal welds in the cylindrical courses, in order to more thoroughly evaluate the critical, high-stressed longitudinal welds.

The length of the PETV cylindrical section was established to assure a length-to-diameter ratio in excess of the theoretical 1.5 minimum ratio required to develop the biaxial strength gain. The actual length-to-diameter ratio of the PETV's was 1.78.

3. Welding

Welding of the 36-in.-dia PETV's was accomplished using the automatic TIG welding process with the downhand welding technique. Repair welding was accomplished with the manual TIG welding process.

The welding parameters used for both automatic and manual welding, i.e., amperage, voltage, welding speed, wire feed speed, etc., were developed in the weld process development phase of the material and process evaluation program for use in actual fabrication of motor components.

X, A, Process Evaluation Test Vehicle Design and Fabrication (cont.)

During fabrication of the PETV's, the maximum mismatch permitted by the 260-in.-dia motor component design and fabrication control drawing was recorded. The maximum mismatch was specified as 5% mismatch (95% minimum continuous membrane) for cylindrical-section longitudinal welds and 10% mismatch (90% minimum continuous membrane) for all other welds. In addition, a maximum of seven weld repairs was made in an overlapping area exceeding the specification limit of three repairs.

4. Nondestructive Test Methods

The nondestructive test methods used in the fabrication of the 36-in.-dia PETV's were identical to those used in fabrication of the 260-in.-dia motor components. The PETV's afforded the first evaluation, in pressure vessel form, of the adequacy of the nondestructive test requirements imposed on the 200 grade, 18%-nickel steel material and the welding process.

The nondestructive test methods used in the fabrication program are listed below. Detailed requirements and controls of each method are given in the applicable Aerojet-General specifications shown in Appendix A.

a. The plate and forging material were procured from the vendor subject to magnetic-particle and ultrasonic inspection requirements.

b. The chamber welds were inspected as follows:

(1) Magnetic-particle inspection of all welds after grinding (before aging) and after aging.

(2) Radiographic inspection of all welds before aging.

(3) Ultrasonic inspection of all welds before aging.

X, A, Process Evaluation Test Vehicle Design and Fabrication (cont.)

c. All final-machined surfaces were magnetic-particle-inspected before hydrostatic test.

B. MARAGING HEAT TREATMENT

Both PETV's were maraged at the J.W. Rex Co., Lansdale, Pa. The maraging cycles of 900°F for 4 hr and 900°F for 8 hr for the first and second PETV's, respectively, were selected to produce the best compromise between adequate yield strength and the best possible fracture toughness.

1. Maraging Procedure

The same maraging procedure was used for both PETV's for the different stabilized-temperature hold periods. The maraging procedure is presented below:

a. Preheat furnace to 300°F (permissible, but not necessary).

b. Raise furnace temperature to 700°F at a maximum rate of 200°F/hr. Permit all thermocouple readings to stabilize at 700°F $^{+0°F}_{-50°F}$.

c. Raise furnace temperature from 700 to 900°F rapidly, noting thermocouple readings. Start counting time at 900°F when all of the thermocouples read above 850°F. Hold at 900°F for specified time.

d. After specified time at 900°F, cut power and remove furnace lid. Do not turn the fan off. Record temperature until 800°F or lower is read on all thermocouples.

X, B, Maraging Heat Treatment (cont.)

Thermocouples and material test specimens were similarly placed on the PETV components during the maraging cycles, as shown in Figures 191 and 192.

2. Test Results of Specimens Maraged with the PETV's

a. PETV No. 1

Test results of the parent-metal specimens maraged with the case are recorded in Figures 193 and 194. Comparison of these test results with the results of specimens tested in the laboratory showed that, with the exception of the transverse tensile specimens from plate R-600-1, the specimens maraged with the case developed properties within ± 3 ksi of those specimens maraged at 900°F for 4 hr in the laboratory. The results for weld metal specimens maraged with the PETV are shown in Figure 195.

b. PETV No. 2

The parent-metal tensile, slow-notch-bend, and precracked-impact test results are recorded in Figures 196 through 198.

With the exception one transverse plate specimen with a yield strength of 236 ksi, all tensile results were within the specified 200 to 235 ksi yield strength limits. Compared to the laboratory specimens, those maraged with the case showed consistently higher yield strengths and consequently lower W/A values. Plane strain (G_{nc}) values were approximately the same within normal data scatter associated with the test. Specifically, the yield strengths of the specimens maraged with the case were 2 to 5 ksi higher than those maraged in the laboratory, and the W/A values were approximately 100 to 250 in.-lb/sq in. lower. The differences in properties are attributed to the longer heat-up and cooldown times associated with the maraging of the case.

X, B, Maraging Heat Treatment - VC (cont.)

The weld-metal tensile and precracked-impact test results are shown in Figure 199.

C. HYDROSTATIC BURST TESTS OF 36-IN. DIA PETV's

The tests of PETV's 1 and 2 were performed to determine the ultimate strength of the material and to determine if the design concepts, material selection, and fabrication techniques were satisfactory for use in fabrication of large-diameter, rocket-motor pressure-vessel components. The complete results of the hydrostatic burst tests of two chambers are presented in References (13) and (14).

Proof-pressure and hydrostatic-burst tests of PETV 1 and 2 were conducted at Aerojet, Sacramento, on 15 April 1964 and 22 June 1964, respectively.

1. Dimensional Analysis

A dimensional inspection was performed on each chamber before it was tested to determine the locations of the strain gages and the thicknesses at those locations.

a. Out-of-Roundness Check

The chambers were installed on a lathe and centered to within ± 0.002 in., based on the machined surfaces of each head boss. An arbitrary fixed point was chosen as the reference point. Out-of-roundness varied from +0.122 to -0.230 in. on PETV 1 and +0.038 to -0.033 in. on PETV 2; the negative sign indicates a smaller radius than reference. Out-of-round measurements and identification of welds and chamber sections are presented in Figures 200 and 201. A contour map of the chambers based on these data appears in Figures 202 and 203.

X, C, Hydrostatic Burst Tests of 36-in. Dia PETV's (cont.)

b. Vidigage Thickness Measurements

Thickness measurements were made in the cylinder sections of each PETV. Cylinder thickness varied from 0.635 to 0.675 in. for PETV 1 and 0.620 to 0.650 in. for PETV 2. These values are compared to the drawing tolerance of 0.600 to 0.656 in.

c. Pi Tape Measurements

Outside diameters of cylinder sections measured an average of 37.26 and 37.28 in. for PETV's 1 and 2, respectively.

2. Instrumentation

A total of 19 biaxial post-yield strain gages were mounted to the chamber exterior and interior surfaces in accordance with Figures 204 and 205.

Strain gage terminology used in this report is as follows:

		Strain gage location
15	MI	Grid oriented in hoop (H) or meridional (M) direction
		Inside (I) or outside (O) of chamber

The bases for selecting strain gage locations and the corresponding thicknesses are outlined in Figure 206.

Two 1-1/4-in.-dia bolts were instrumented with monofilament strain gages as shown in Figure 207. Prior to this test, the bolts were

X, C, Hydrostatic Burst Tests of 36-in. Dia PETV's (cont.)

calibrated to establish a relationship of tensile load to strain. In actual installation, the bolts were 90 degrees apart on the bolt pattern on the 14-in.-dia closure.

Pressures were monitored remotely during the test with a 10,000-psi pressure gage monitored with a television camera and receiver, and a Mosely X-Y plotter which plotted pressure versus time. Two 10,000-psig pressure transducers were employed for recording pressure. Acquisition of the strain and pressure data was accomplished on two CEC Model 5-123 recording oscillographs.

3. Test Setup

The 5/8-, 1- and 1-1/4-in.-dia bolts used to assemble the aft and forward closures to the chamber were torqued to 170, 525, and 1150 ft-lb, respectively. During installation of the forward closure, the two instrumented bolts were monitored at each torque increment.

The chamber was erected in the vertical position and supported on the 14-in.-dia closure on a wooden test stand (Figures 208 and 209).

Figure 210 is a schematic of the hydraulic system used in pressurizing the chambers. MIL-L-17672 specification oil was the pressurization medium.

4. Test Procedure

Prior to proof test, the system was checked for leakage at 50 psig and then cycled to 900 psig twice to test the instrumentation.

X, C, Hydrostatic Burst Tests of 36-in. Dia PETV's (cont.)

a. Proof Test

The chamber was pressurized at a rate of 220 psig/min to 5570 ± 20 psig and held at that pressure for 2 min before reducing to zero pressure.

b. Burst Test

The chamber was pressurized at 210 psig/min to burst.

5. Test Results

a. Proof Pressure Test of PETV's 1 and 2

Both chambers successfully withstood the proof pressure of 5570 psig with no evidence of yield. The control hoop stresses calculated at proof were as follows:

Unit	Calculated Stress, ksi	Theoretical Stress, ksi
PETV 1	156	157
PETV 2	160	156

b. Burst Test of PETV No. 1

The chamber burst at 8370 ± 20 psig because the strength of the material was exceeded. The chamber remained in one piece after burst, characterized by a ductile failure. Figures 211 through 216 show the test unit after failure.

X, C, Hydrostatic Burst Tests of 36-in. Dia PETV's (cont.)

Material at two locations, (Strain Gages 1 and 15) indicated a yield condition (0.2% offset) at time of failure as shown in Figure 217; however, both areas were intact after failure. Strain Gage 15 was located on the center line of weld W1, whereas Gage 1 was located on the parent material.

On the basis of the curve presented in Figure 217, the yield stress at Strain Gage 1 was determined to be 242 ksi. At the origin of failure, the 8370-psig burst pressure represented a calculated ultimate stress of 240 ksi. Strain Gage 1 was located on parent material having a thickness of 0.635 in., whereas the failure origin occurred at weld W1C, which had a thickness of 0.650 in.

Cylinder hoop and meridional stresses for control Strain Gage 2 and the theoretical hoop stress are plotted in Figures 218 and 219. These graphs show excellent correlation between theoretical and measured hoop stress throughout the elastic range. Stress calculations were based on a uniform modulus of elasticity. The modulus of elasticity of 27,300,000 psi and Poisson's ratio of 0.29, as determined from strain data at location 2, are also in good agreement with the 27,500,000 psi modulus and 0.31 Poisson's ratio derived from uniaxial test specimens.

Bending was evident at the one location (Gage 8, maximum mismatch area) on the aft head where inside and outside strains were recorded; bending stresses of 27,400 and 34,750 psi were calculated for the hoop and meridional directions, respectively. Maximum stress at this location was 150,900 psi (membrane plus bending); however, while bending stresses in this area were significant, the magnitude of the membrane stresses were such that the total stress (membrane plus bending) was insignificant when compared with the stress level in the cylinder.

X, C, Hydrostatic Burst Tests of 36-in. Dia PETV's (cont.)

Strain-vs-pressure curves are presented in Figures 220 through 224 for all strain gage locations except Gages 6 and 7, located on the closure where strains were insignificant.

Bolt loading in the two instrumented bolts due to chamber pressure loads is shown in Figure 225. After initial chamber pressures, the bolt loading appears to be linear until failure. The average bolt load due solely to pressure was approximately 17,000 lbf at failure. Accuracy of bolt load measurement was ± 1200 lbf. Bolt preload prior to test for Bolts 9 and 10 were 178,000 and 145,000 lbf, respectively. Based on instrumented bolt calibration of three bolts, the range of bolt preload for the 1150 ft-lb torque varied from 145,000 to 183,000 lbf.

The shear lip on the large hydrostatic-test cover snapped off at one location (Figure 215). The time of this shear-lip failure is undetermined but it is presumed to have occurred after the initial chamber failure. The pattern of the crack propagation into the forward head and around the flange indicates that, during chamber failure, the cover may have been subjected to excessive strains, thus initiating shear-lip failure. Removal of the cover revealed that both the 1- and 1-1/4-in.-dia bolts had experienced shear loading.

Similar results (shear-lip failure and shear loading of bolts) were observed in the small hydrostatic-test cover and bolts. The time of this shear lip failure is undetermined but it is also presumed to have occurred after initial chamber failure.

The design of these two covers has been reviewed and the following correction action has been initiated:

(1) The tolerances of the covers and flanges were revised to ensure that the bolts could not be loaded in shear.

X, C, Hydrostatic Burst Tests of 36-in. Dia PETV's (cont.)

(2) The shear lips were strengthened.

Post-failure inspection of the support stand on which the chamber was vertically mounted substantiates the conclusion that the chamber failed along aft weld W1C near the aft circumferential weld, as shown in Figure 226. Impressions of the bolt heads from the chamber closure were apparent in the support stand in the area 180 degrees opposite from weld line W1C, while no impressions occurred under the W1C weld line. These impressions indicate a reaction (from oil expulsion) along weld W1C and near the aft circumferential weld. Had the origin of failure occurred in either the aft head or the forward portion of the cylinder, a complete bolt-head pattern impression or no bolt-head impressions at all would have resulted.

c. Burst Pressure Test of PETV 2

The chamber burst at 8250 ± 20 psig, representing a theoretical hoop stress of 241 ksi (based on minimum wall thickness). After failure, the chamber consisted of three principal parts as evidenced in Figures 227 to 229.

No evidence of yield (0.2% offset) was detected at any gage location at the time of burst. Maximum strain recorded was 9070 micro-in./in. at Strain Gage 7.

Cylinder inside and outside hoop stresses for control Gage 8 and theoretical hoop stresses are plotted in Figure 230. These curves show good correlation between theoretical and measured hoop stress throughout the elastic range. Stress calculations were based on a uniform modulus of elasticity.

X, C, Hydrostatic Burst Tests of 36-in. Dia PETV's (cont.)

Bending stresses in the loop direction for Strain Gages 8, 9, 11 and 13 were calculated on the basis: $\sigma_{bending} = \frac{\sigma \text{ inside} - \sigma \text{ outside}}{2}$. Bending stresses were found to be less than 10 ksi at these locations throughout the elastic range.

Strain-vs-pressure curves are presented in Figures 231 through 236.

Loading of Bolt 3 due to internal chamber pressure is shown in Figure 237. Bolt loading increased approximately 14,000 lbf over preload for the 8250 psig pressure. Bolt 4 instrumentation malfunctioned, and no data were obtained.

Visual observations of the failed chamber indicate that the origin of failure occurred along longitudinal weld 2W1 approximately 19 in. from the forward circumferential weld. Visual observations are based on the following evidence:

(1) A bulged area occurred near midcylinder along the crack pattern (Figure 238).

(2) The stored energy in the chamber at burst inflicted the most damage to the cylindrical section, as shown in Figures 239 and 240. The deformation of the origin area is significantly greater than that of the other two sections.

(3) The condition of the test support stand indicates failure near midcylinder. The reaction at burst sheared off a portion of the wooden support stand and was the result of a horizontal side force applied near the chamber center of gravity.

X, Process Evaluation Test Vehicles (PETV) (cont.)

D. CONCLUSIONS

PETV's 1 and 2 demonstrated excellent structural capabilities in attaining burst pressures of 8370 and 8250 psig, respectively. The burst pressures represented basic membrane hoop stresses of 240 and 241 ksi, respectively. The performance of both PETV's exceeded the predicted burst pressures of 8020 and 8060 psig, respectively. It was concluded from these burst tests that the 18%-nickel steel selected for fabrication and the fabrication approach were capable of producing reliable motor components consistent with the structural requirements for use in the 260-in.-dia motor fabrication program.

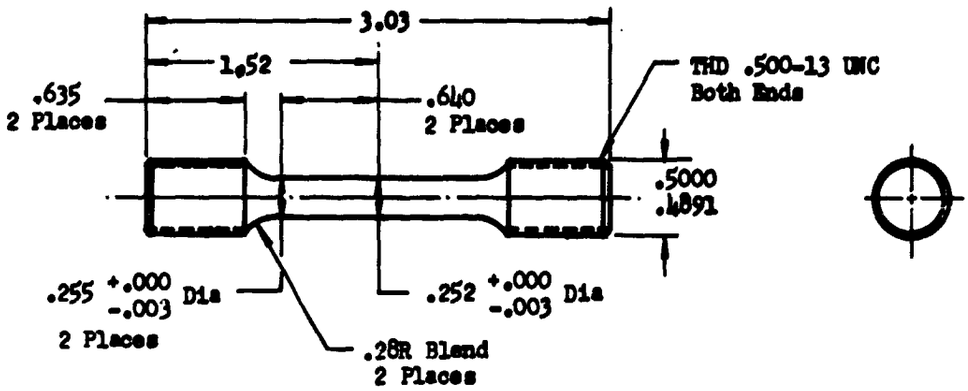

Tensile Specimen

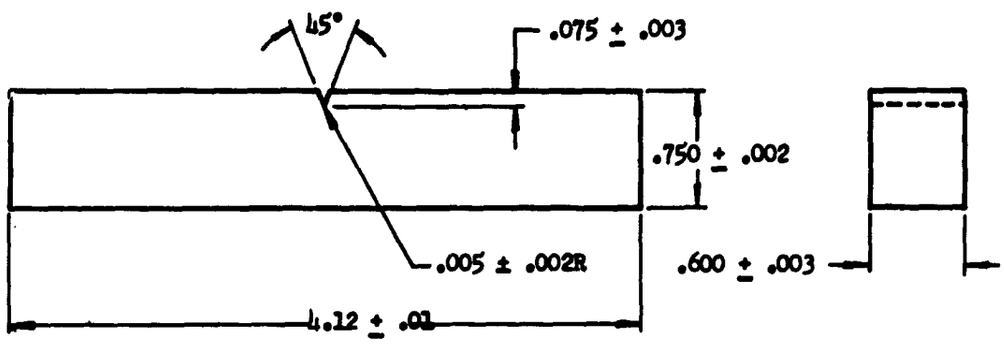

Slow-Notch-Bend Specimen

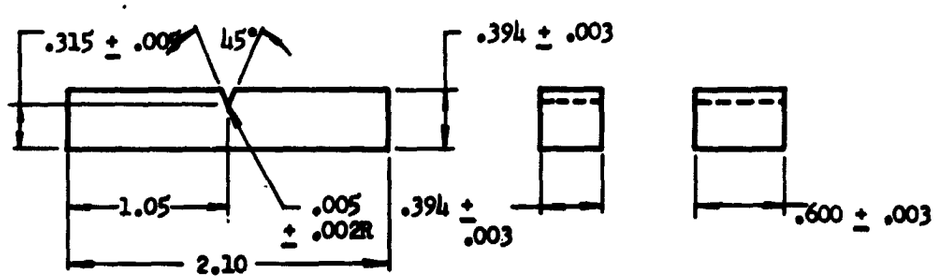

Precracked Charpy Impact Specimen

Tensile, Slow-Notch-Bend, and Precracked Charpy Impact Test Specimen Configuration

Figure 1

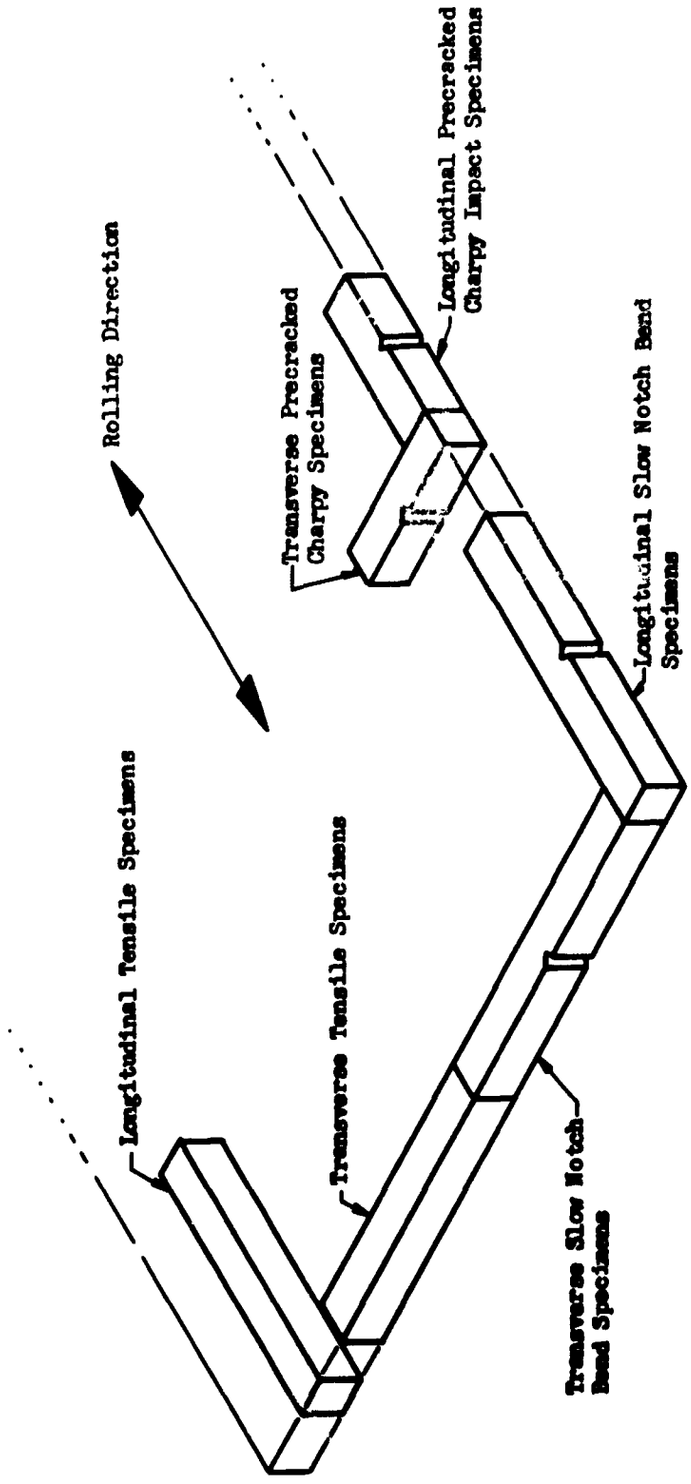

Test-Specimen Orientation

Figure 2

Heat No.[b]	Composition, Weight Percent[a]									
	C	Mn	Si	Ni	Co	Mo	Ti	Al	P	S
3960524	0.026	0.06	0.05	19.0	9.0	3.5	0.22	0.07	0.005	0.008
3920556	0.02	0.05	0.08	17.68	7.9	4.2	0.16	0.16	0.008	0.006
Specified Limits, Max.	0.03	0.10	0.10	17.5 19.0	7.0 8.0	4.0 4.5	0.05 0.25	0.05 0.15	0.025	0.01

(a) Mill certified analyses.
(b) Both heats are vacuum arc remelted material supplied by Republic Steel Corporation

Composition of 18%-Nickel Steel

Figure 3

Etchant: Marbles Mag: 100X

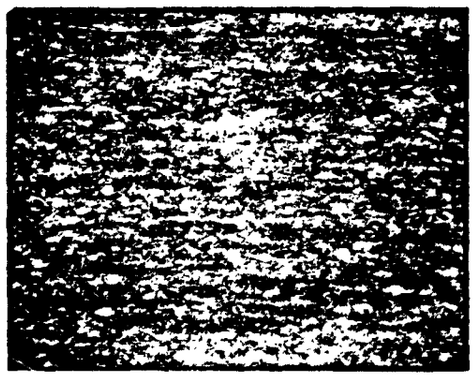

Etchant: 10% Chromic Mag: 100X

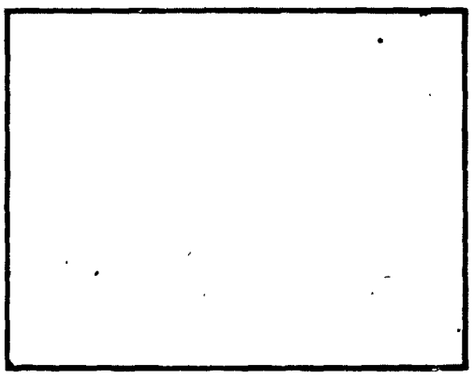

Unetched Mag: 100X

Typical Microstructure, Grain Size, and Inclusion Content of 0.6-in.-thick Plate; Republic Heat 3960524

Figure 4

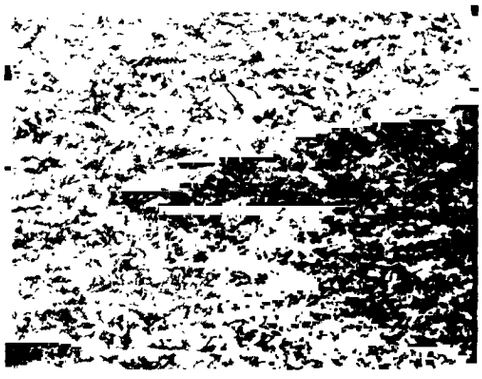

Etchant: Marbles Mag: 100X

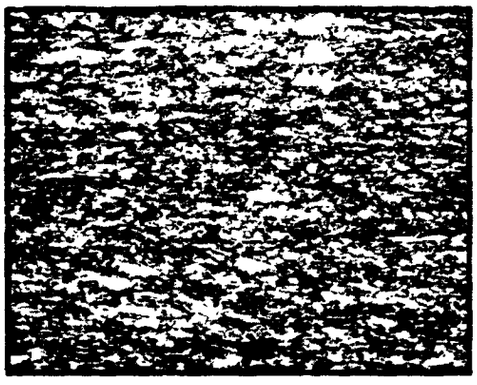

Etchant: 10% Chromic Mag: 100X

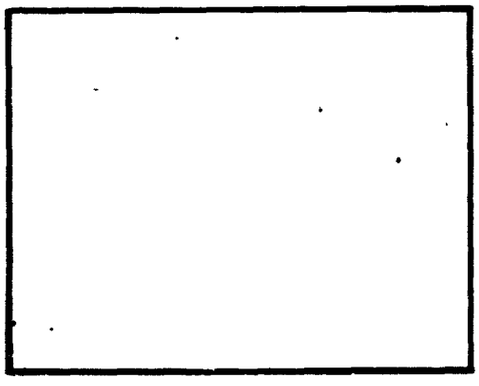

Unetched Mag: 100X

Typical Microstructure, Grain Size, and Inclusion Content of 0.6-in.-thick Plate; Republic Heat 3920556

Figure 5

Aging Cycle °F	Aging Cycle Hr.	Orientation	Yield Strength at 0.2% Offset, ksi	Ultimate Tensile Strength	Elongation in 1 in. %	Reduction in Area, %
850	4	Longitudinal	230	234	12.9	64.0
			230	233	13.5	62.5
			230	232	11.0	63.5
		Avg.	230	233	12.4	63.5
850	8	Longitudinal	238	242	11.8	63.6
			239	244	11.4	62.2
			237	244	11.6	62.9
		Avg.	238	243	11.6	62.9
		Transverse	244	248	11.7	55.0
			252	253	11.0	56.0
			247	251	10.8	55.0
		Avg.	248	[illegible]	11.2	55.3
850	16	Longitudinal	242	248	11.6	61.7
			242	248	11.1	60.3
			243	248	11.0	58.0
		Avg.	242	248	11.2	60.0
850	24	Longitudinal	248	252	11.1	54.1
			249	252	10.3	56.0
		Avg.	248	252	10.7	55.5
		Transverse	250	253	9.6	56.4
			251	253	9.9	54.7
		Avg.	250	253	9.7	55.7
900	2	Longitudinal	229	233	12.1	63.4
			229	232	12.4	64.0
			230	231	12.2	65.5
		Avg.	229	232	12.2	64.2
900	4	Longitudinal	230	234	12.6	64.8
			235	237	11.9	63.8
			235	236	12.4	63.0
		Avg.	234	236	12.3	64.0

Effects of Specimen Orientation, Aging Temperature, and Aging Time on the Tensile Properties of 0.6-in.-thick 18%-Nickel Maraging Steel Plate, Mill Annealed at 1500°F for 1 hr; Republic Heat 3960524

Figure 6, Sheet 1 of 3

Aging Cycle °F	Hr.	Orientation	Yield Strength at 0.2% Offset, ksi	Ultimate Tensile Strength	Elongation in 1 in. %	Reduction in Area, %
		Transverse	241	242	10.8	56.0
			240	243	11.0	57.6
			239	243	11.0	56.2
		Avg.	240	243	11.0	56.8
900	8	Longitudinal	237	241	12.1	63.6
			238	240	11.3	61.0
			241	242	11.5	54.4
		Avg.	239	241	11.6	59.5
		Transverse	245	248	10.2	54.6
			243	246	10.4	56.0
			243	245	10.6	53.7
		Avg.	244	246	10.4	54.8
900	16	Longitudinal	231	236	12.0	62.2
			232	236	11.5	60.0
			232	237	12.3	61.5
		Avg.	232	236	11.9	61.4
900	24	Longitudinal	227	231	11.3	59.4
			228	231	10.9	60.1
		Avg.	227	231	11.1	59.7
		Transverse	232	235	10.2	54.7
			233	237	11.7	56.0
		Avg.	232	236	10.9	55.3
950	2	Longitudinal	231	236	11.7	54.5
			236	238	9.8	53.0
			233	238	11.2	55.8
		Avg.	233	237	10.9	54.4
		Transverse	228	231	13.5	60.7
			229	232	12.6	58.0
			229	233	13.1	59.8
		Avg.	228	232	13.1	95.5
950	4	Longitudinal	231	236	12.3	56.8
			232	236	12.0	51.9
			230	235	12.1	56.4
		Avg.	231	236	12.1	55.0

Effects of Specimen Orientation, Aging Temperature, and Aging Time on the Tensile Properties of 0.6-in-thick 18%-Nickel Maraging Steel Plate, Mill Annealed at 1500°F for 1 hr; Republic Heat 3960524

Figure 6, Sheet 2 of 3

Aging Cycle °F	Hr.	Orientation	Yield Strength at 0.2% Offset, ksi	Ultimate Tensile Strength	Elongation in 1 in. %	Reduction in Area, %
950	4	Longitudinal	231	236	12.3	56.8
			232	236	12.0	51.9
			230	235	12.1	56.4
		Avg.	231	236	12.1	55.0
		Transverse	227	231	13.2	58.1
			226	230	13.3	62.8
			225	230	12.8	58.5
		Avg.	226	230	13.1	59.8
950	8	Longitudinal	220	228	13.1	64.0
			220	226	13.1	63.0
			216	222	12.9	62.5
		Avg.	219	225	13.0	63.3
950	16	Longitudinal	214	221	13.3	65.0
			218	224	13.0	63.4
		Avg.	216	222	13.2	64.2
950	24	Longitudinal	209	215	14.5	61.8
			202	209	14.2	61.1
		Avg.	205	212	14.3	61.4
		Transverse	210	214	10.9	58.0
			211	216	11.1	54.8
		Avg.	210	215	11.0	56.4

Effects of Specimen Orientation, Aging Temperature, and Aging Time on the Tensile Properties of 0.6-in-thick 18%-Nickel Maraging Steel Plate, Mill Annealed at 1500°F for 1 hr; Republic Heat 3960524

Figure 6, Sheet 3 of 3

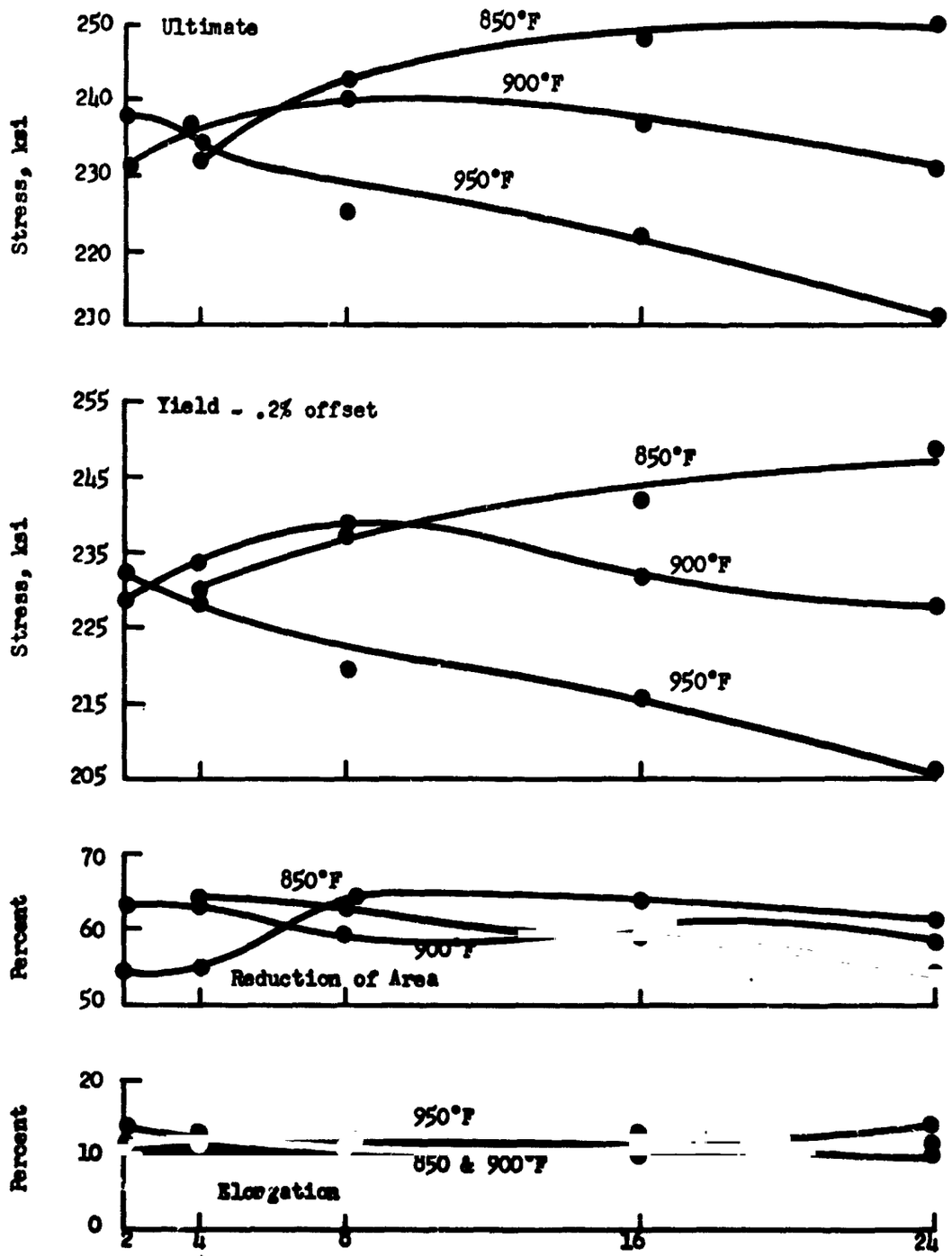

Effects of Aging Time and Temperature on the Tensile Properties of 0.6-in.-thick 18%-Nickel Maraging Steel Plate, Mill Annealed at 1500°F for 1 hr Prior to Aging; Republic Heat 3960524

Figure 7

Aging Cycle °F	Aging Cycle Hr.	Orientation	Yield Strength at 0.2% Offset, ksi	Ultimate Tensile Strength, ksi	Elongation in 1 in. %	Reduction of Area, %
850	4	Longitudinal	194.1	206.0	11.9	63.3
			199.8	210.1	12.6	68.7
			200.0	211.8	12.0	64.6
		Avg.	197.5	209.0	12.3	65.5
850	8	Longitudinal	212.0	222.8	11.9	63.0
			208.9	221.2	11.4	58.7
			212.7	223.1	12.3	63.5
		Avg.	211.2	222.4	11.9	61.7
		Transverse	213.6	226.1	10.7	61.1
			214.6	226.7	10.9	60.7
			213.8	225.8	10.6	59.5
		Avg.	214.0	226.2	10.7	60.4
850	16	Longitudinal	219.3	230.8	10.7	60.2
			219.8	231.3	10.0	58.2
			220.2	231.2	10.5	57.4
		Avg.	219.8	231.1	10.4	58.6
850	24	Longitudinal	239	244	10.9	56.4
			240	243	10.9	57.4
			236	241	10.0	57.8
		Avg.	239	243	10.6	57.2
		Transverse	232	238	11.4	59.1
			235	239	11.5	60.8
			232	238	11.0	61.5
		Avg.	233	238	11.3	60.5
900	2	Longitudinal	195.3	205.5	12.4	64.2
			198.2	207.0	12.2	65.8
			196.9	206.2	12.1	67.8
		Avg.	196.8	206.2	12.2	65.9

Effects of Specimen Orientation, Aging Temperature, and Aging Time on the Tensile Properties of 0.6-in.-thick 18%-Nickel Maraging Steel Plate, Mill Annealed at 1500°F for 1 hr; Republic Heat 3920556

Figure 8, Sheet 1 of 3

Aging Cycle °F	Hr.	Orientation	Yield Strength, at 0.2% Offset, ksi	Ultimate Tensile Strength, ksi	Elongation in 1 in. %	Reduction of Area, %
900	4	Longitudinal	217.0	227.0	11.9	62.6
			212.2	222.6	11.0	61.9
			213.2	222.8	10.9	62.5
		Avg.	214.1	224.1	11.3	62.3
		Transverse	216.6	226.5	11.5	62.2
			217.9	228.1	11.0	60.4
			218.5	227.1	11.3	60.0
		Avg.	217.7	227.2	11.3	60.9
900	8	Longitudinal	217.9	227.9	11.5	60.8
			217.0	227.5	11.5	62.5
			218.7	226.7	11.1	60.7
		Avg.	217.9	227.4	11.3	61.3
		Transverse	219.9	231.7	11.4	59.0
			220.9	233.6	11.4	59.1
			220.7	233.7	12.0	59.1
		Avg.	220.5	233.0	11.6	59.1
900	16	Longitudinal	222.6	234.5	11.9	60.8
			222.6	234.5	11.9	60.8
			222.6	234.6	11.2	57.5
		Avg.	222.6	234.5	11.7	59.7
		Transverse	222.0	234.2	12.6	60.1
			223.6	235.0	11.7	62.5
			221.6	235.6	12.9	61.0
		Avg.	222.4	234.9	12.4	61.2
900	24	Longitudinal	235	242	11.4	58.0
			231	242	12.1	58.0
			234	240	11.5	59.1
		Avg.	233	241	11.6	58.4
		Transverse	231	237	13.0	63.1
			231	237	12.2	61.1
			230	237	13.2	62.5
		Avg.	231	237	12.8	61.7

Effects of Specimen Orientation, Aging Temperature, and Aging Time on the Tensile Properties of 0.6-in-thick 18%-Nickel Maraging Steel Plate, Mill Annealed at 1500°F for 1 hr; Republic Heat 3920556

Figure 8, Sheet 2 of 3

Aging Cycle °F	Hr.	Orientation	Yield Strength at 0.2% Offset, ksi	Ultimate Tensile Strength ksi	Elongation in 1 in. %	Reduction of Area, %
950	2	Longitudinal	212.2	223.6	12.3	60.8
			209.3	220.1	11.9	61.6
			208.2	219.1	11.5	62.0
		Avg.	209.9	220.9	11.9	61.5
950	4	Longitudinal	214.1	226.9	12.6	62.2
			216.2	228.7	12.4	59.2
			213.9	225.3	12.0	59.5
		Avg.	214.7	227.0	12.3	60.3
		Transverse	219.2	230.7	12.0	58.0
			218.6	229.8	13.7	58.5
			219.7	231.2	11.4	58.7
		Avg.	219.2	230.6	12.4	58.4
950	8	Longitudinal	219.5	230.3	11.7	59.4
			219.1	229.9	12.5	59.5
			218.7	230.5	12.9	59.7
		Avg.	219.1	230.2	12.4	59.5
950	16	Longitudinal	—	—	—	—
			—	—	—	—
			—	—	—	—
		Avg.	222	235	12.4	61.2
950	24	Longitudinal	227	234	12.0	55.4
			226	233	11.2	55.0
			223	232	13.0	56.4
		Avg.	225	233	12.1	55.6
		Transverse	220	228	13.9	61.5
			221	229	13.5	58.5
			219	229	14.0	6.21
		Avg.	220	226	13.8	60.7

Effects of Specimen Orientation, Aging Temperature, and Aging Time on the Tensile Properties of 0.6-in-thick 18%-Nickel Maraging Steel Plate, Mill Annealed at 1500°F for 1 hr; Republic Heat 3920556

Figure 8, Sheet 3 of 3

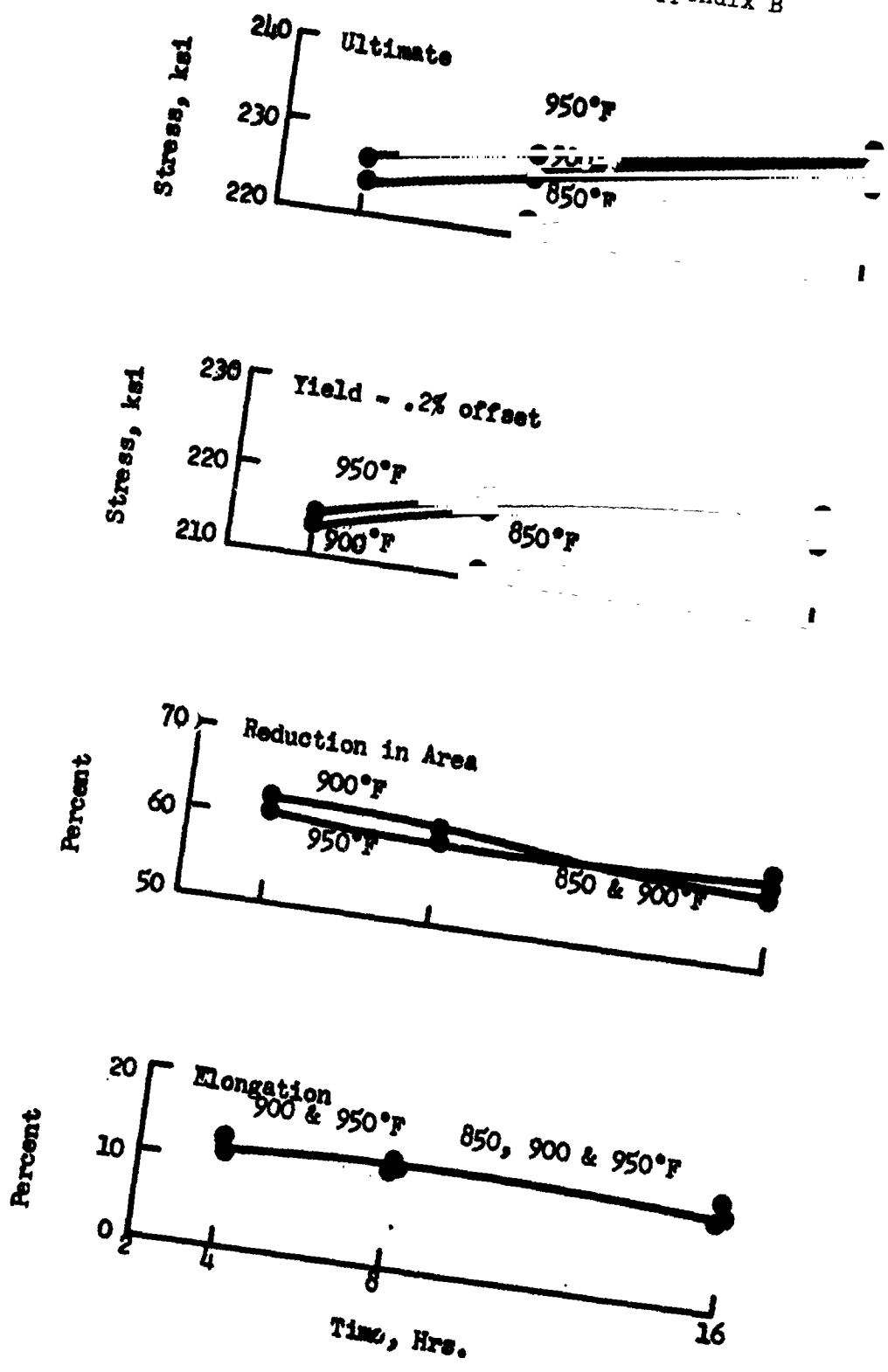

Effects of Aging Time and Temperature on the Tensile Properties of 0.6-in.-thick 200 Grade 18%-Nickel Maraging Steel Plate, Mill Annealed at 1500°F for 1 hr Prior to Aging; Republic Heat 3920556

Figure 9

Specimen Number	Aging Cycle °F - hr	Specimen Orientation	.2% Offset Yield (ksi)	Width b (in.)	Depth d (in.)	Proportional Limit Load (L) (lb)	Proportional Limit Deflec. (e) (in.)	Maximum Load (L) (lb)	eb/L (in.²/lb)x10⁻⁸	Notch + Cra Effective a_1(in.)(1)	a_2(in.)(2)	a_3(in.)(3)
R 360	850-8	Longitudinal	238	.601	.751	10200	.0222	10760	133	.200	.196	.186
R 362				.602	.750	9900	.0189	10260	115	.226	-	.226
R 363				.595	.751	9700	.0193	10150	118	.236	-	.242
R 364				.600	.751	8550	.0178	9130	125	.252	-	.261
R 380	850-8	Transverse	248	.600	.754	8425	.0143	9550	102	.170	-	.159
R 381				.602	.754	7050	.0161	7600	138	.276	-	.279
R 383				.600	.753	7700	.0151	8200	118	.232	-	.239
R 384				.604	.752	9100	.0169	9240	111	.212	-	.213
R 540	850-16	Longitudinal	242	.600	.750	9250	.0203	9975	132	.198	.190	.190
R 541				.600	.750	9500	.0207	9650	130.5	.192	.184	.186
R 542				.600	.750	9450	.0202	9660	128	.183	.172	.176
R 543				.600	.750	8300	.0193	8800	138	.217	.214	.216
R 556	850-24	Longitudinal	249	.601	.751	5625	.0191	5900	205	.327	.328	-
R 557				.601	.750	7550	.0200	7800	159	.262	.262	.262
R 558				.601	.750	8950	.0190	9700	127.5	.180	.170	.173
R 559				.601	.750	8000	.0182	8980	136.7	.212	.210	.207
R 574	850-24	Transverse	250	.602	.751	8250	.0182	8720	133	.202	.196	.193
R 575				.602	.751	9300	.0240	9480	155	.254	.254	.255
R 576				.602	.751	9800	.0192	10180	118	.132	.106	.130
R 577				.602	.751	8300	.0193	8470	140	.222	.221	.218
R 370	900-4	Longitudinal	234	.600	.751	9750	.0222	10700	136.6	.212	.208	.207
R 371				.600	.751	8450	.0208	9375	147.8	.240	.240	.238
R 372				.599	.750	7550	.0199	8585	158	.260	.261	.260
R 373				.599	.746	8950	.0218	9470	146	.236	.236	.234
R 390	900-4	Transverse	240	.601	.750	6750	.0181	7200	161	.266	.266	.266
R 391				.602	.751	8400	.0187	8980	134	.204	.200	.198
R 392				.599	.750	6675	.0179	7000	161	.266	.266	.265
R 393				.599	.750	7350	.0178	6075	145	.234	.234	.232
R 394				.602	.749	7100	.0167	7995	142	.226	.266	.222
R 355	900-8	Longitudinal	239	.601	.752	5500	.0217	5630	237	.354	.364	-
R 356				.602	.744	10200	.0243	10375	146	.236	.236	.228
R 357				.602	.751	5950	.0217	6140	220	.340	.346	-
R 359				.599	.753	9100	0222	9350	146	.236	.236	.234
R 375	900-8	Transverse	244	.600	.750	9000	.0162	9040	108	.200	-	.190
R 376				.599	.749	7000	.0135	7550	114	.223	-	.229
R 377				.600	.750	8300	.0153	8645	109.5	.206	-	.196
R 379				.602	.746	11000	.0211	11600	115	.114	.08	.117

(1) Rowe's Analysis, First Run Calibration Data; Calibration Curve Constants: $Q = 1.86 \times 10^{-5}$ $R = -9.83 \times 10^{-5}$ $S = 21.94 \times 10^{-5}$

(2) Rowe's Analysis, Second Run Calibration Data, Calibration Curve Constants: $Q = 1.03 \times 10^{-5}$ $R = -3.00 \times 10^{-5}$, $S = 7.50 \times 10^{-5}$

(3) 5-Point Smoothing Technique, First Calibration Data;

( ) 5-Point Smoothing Technique, Second Calibration Data;

Buechner's Analysis

ck Depth		Plane-Strain Fracture Toughness in. lb/in.^{2}					Stress Intensity Factor 1000 psi in.				
a_4(in.)(4)	Measured a_o(in.)(5)	G_{nc_1}(1)	G_{nc_2}(2)	G_{nc_3}(3)	G_{nc_4}(4)	G_{Ic}(5)	K_{nc_1}(1)	K_{nc_2}(2)	K_{nc_3}(3)	K_{nc_4}(4)	K_{Ic}(5)
.187	.195	385	406	419	418	442					
	.205	427	-	416	-	456					
	.205	473	-	505	-	443					
	.270	440	-	482	-	568					
		Avg 431	Avg 406	Avg 456	Avg 418	Avg 477	Avg 114	Avg 101	Avg 118	Avg 113	Avg 120
	.210	-	-	-	-	336					
	.260	399	-	399	-	348					
	.240	279	-	301	-	360					
	.225	302	-	290	-	443					
		Avg 327		Avg 330		Avg 372	100		Avg 100		Avg 106
.191	.195	312	321	356	357	367					
.186	.195	313	325	363	363	387					
.176	.195	288	296	332	323	383					
.214	.230	303	307	353	344	394					
		Avg 304	Avg 312	Avg 351	Avg 347	Avg 383	Avg 96	Avg 97	Avg 103	Avg 103	Avg 108
-	.320	496	334	-	-	358					
.260	.280	418	362	453	410	479					
.173	.215	252	261	289	279*	404					
.206	.230	266	276	305	301	365					
		Avg 358	Avg 308	Avg [illegible]	Avg 330	Avg 402	Avg 104	Avg 97	Avg 103	Avg 100	Avg 111
.194	.220	256	264	290	291	354					
.252	.195	578	535	601	565	366					
-	.170	238	201	-	-	326					
.215	.235	318	320	355	345	405					
		Avg 348	Avg 330	Avg 415	Avg 400	Avg 362	Avg 103	Avg 100	Avg 102	Avg 110	Avg 105
.206	.195	397	405	454	448	405					
.235	.245	406	385	423	411	457					
.257	.260	411	362	436	399	483					
.231	.230	436	421	463	450	472					
		Avg 412	Avg 393	Avg 444	Avg 427	Avg 454	Avg 112	Avg 109	Avg 116	Avg 114	Avg 107
.264	.280	350	298	386	344	383					
.198	.225	271	282	312	311	383					
.263	.285	345	294	374	334	392					
.229	.245	287	280	309	300	349					
.220	.235	243	329	269	260	300					
		Avg 299	Avg 297	Avg 330	Avg 310	Avg 361	Avg 95	Avg 95	Avg 100	Avg 97	Avg 105
-	.350	635 *	419	-	-	426					
.224	.205	560	541	574	556	501					
-	.325*	638	427	-	-	414					
.231	.215	428	435	481	467	413					
		Avg 565	Avg 456	Avg 528	Avg 512	Avg 438	Avg 131	Avg 118	Avg 126	Avg 124	Avg 114
	.200	262	-	213	-	362					
	.255*	207	-	218	-	345					
	.235	238	-	195	-	410					
	.160	286	-	247	-	386					
		Avg 248		Avg 218		Avg 376	Avg 87		Avg 82		Avg 107

Effects of Orientation, Aging Time, and Temperature on the Slow-Notch-Bend Fracture Toughness of Plate from Republic Heat 3960524

Figure 10, Sheet 1 of 2

Specimen Number	Aging Cycle °F - hr	Specimen Orientation	.2% Offset Yield (ksi)	Width b (in.)	Depth d (in.)	Proportional Limit Load (L) (lb)	Proportional Limit Deflec. (e) (in.)	Maximum Load (L) (lb)	eb/L (in.^{2}/lb)x10^{-8}	a_1(in.)(1)	a_2(in.)(
R 544	900-16	Longitudinal	232	.600	.750	9500	.0203	9775	128.5	.184	
R 545				.600	.750	8100	.0192	8635	142	.226	
R 546				.600	.751	7500	.0191	8100	153	.250	
R 547				.600	.751	6450	.0203	6920	190	.310	
R 536	900-24	Longitudinal	228	.600	.750	11500	.0247	12200	126	.174	
R 537				.600	.750	10000	.0230	11200	138	.217	
R 538				.600	.750	10000	.0222	11250	136	.211	
R 539				.600	.750	11050	.0232	12500	121	.150	
R 566	900-24	Transverse	233	.601	.750	8250	.0197	8950	143.2	.230	
R 567				.600	.751	9750	.0211	9875	129.8	.189	
R 568				.602	.750	7900	.0188	8880	143.2	.230	
R 569				.602	.750	8600	.0190	9240	132.5	.200	
R 548	950-4	Longitudinal	229	.600	.750	13000	.0247	14150	114	.106	
R 549				.600	.750	9500	.0218	11225	138	.217	
R 550				.600	.751	9250	.0236	9850	153	.249	
R 551				.600	.751	9700	.0247	10480	153	.250	
R 570	950-4	Transverse	232	.602	.750	6500	.0173	7770	160.5	.265	
R 571				.602	.751	9500	.0210	10180	132.8	.200	
R 572				.602	.750	10450	.0202	11565	116.0	.120	
R 573				.602	.750	8900	.0220	9140	148.0	.240	
R 366	950-8	Longitudinal	219	.600	.751	7300	.0224	8035	184	.302	
R 367				.598	.750	10000	.0231	11065	138	.216	
R 385	950-8	Transverse	-	.600	.753	8300	.0169	8800	121	.243	
R 386				.602	.752	7700	.0168	8350	132	.266	
R 387				.602	.753	9400	.0217	9820	139	.208	
R 388				.602	.753	9650	.0182	9950	114	.222	
R 389				.602	.752	9400	.0168	9960	108	.200	
R 552	950-16	Longitudinal	-	.600	.750	13400	.0238	15800	106.5	.044	
R 553				.600	.751	9750	.0213	11375	131	.194	
R 554				.600	.751	10000	.0223	11600	134	.205	
R 555				.600	.750	8400	.0205	10550	143.8	.232	
R 560	950-24	Longitudinal	206	.600	.750	8000	.0238	9155	179	.296	
R 561				.600	.750	7900	.0218	9425	166	.274	
R 562				.600	.750	6300	.0202	7860	191.8	.312	
R 563				.600	.750	13500	.0241	15600	107	.050	
R 578	950-24	Transverse	210	.601	.750	10300	.0220	11600	128.6	.184	
R 579				.602	.750	9100	.0212	10120	140	.222	
R 580				.602	.750	9850	.0236	10580	143.8	.231	
R 581				.602	.750	8100	.0207	9225	154	.252	

(1) Rawe's Analysis, First Run Calibration Data; Calibration Curve Constants: Q = 1.86 x10^{-5} R = - 9.83 x10^{-5} S = 21.94 x10^{-5}

(2) Rawe's Analysis, Second Run Calibration Data, Calibration Curve Constants: Q = 1.03 x10^{-5} R = - 3.00 x10^{-5} , S = 7.50 x10^{-}

(3) 5-Point Smoothing Technique, First Calibration Data;

(4) 5-Point Smoothing Technique, Second Calibration Data;

(5) Buckner's Analysis

Notch + Crack Depth: Effective a_2 (in.)(2)	Effective a_3 (in.)(3)	Effective a_4 (in.)(4)	Measured a_o (in.)(5)	Plane-Strain Fracture Toughness: in. lb/in.^{2} G_{nc_1}(1)	G_{nc_2}(2)	G_{nc_3}(3)	G_{nc_4}(4)	G_{Ic}(5)	Stress Intensity Factor: 1000 psi $\sqrt{in.}$ K_{nc_1}(1)	K_{nc_2}(2)	K_{nc_3}(3)	K_{nc_4}(4)	K_{Ic}(5)
.174	.176	.176	.200	293	304	334	326	404					
.226	.224	.221	.235	318	318	357	346	390					
.251	.249	.246	.270	359	330	367	352	437					
.320	-	.307	.315	541	414	-	464	454	—	—	—	—	—
				Avg 378	Avg 342	Avg 353	Avg 372	Avg 421	Avg 107	Avg 102	Avg 104	Avg 106	Avg 113
.162	.178	.178	.190	400	410	501	492	543					
.214	.211	.210	.225	440	445	494	485	549					
.208	.195	.195	.212	414	426	434	435	494					
.129	.166	.165	.180	325	304	417	387	460	—	—	—	—	—
				Avg 395	Avg 396	Avg 462	Avg 450	Avg 512	Avg 109	Avg 109	Avg 118	Avg 117	Avg 124
.230	.228	.225	.240	344	340	377	366	420					
.180	.182	.183	.215	321	333	372	369	478					
.280	.227	.224	.240	314	454	344	333	384					
.193	.194	.194	.230	273	282	317	318	420	—	—	—	—	—
				Avg 313	Avg 352	Avg 352	Avg 346	Avg 425	Avg 98	Avg 104	Avg 104	Avg 102	Avg 113
.070	.110	-	.150	-	-	-	-	482					
.214	.210	.209	.225	397	402	442	435	496					
.250	.250	.247	.300	540	498	562	538	835					
.250	.249	.246	.275	601	547	613	588	759	—	—	—	—	—
				Avg 513	Avg 482	Avg 539	Avg 520	Avg 643	Avg 124	Avg 121	Avg 128	Avg 126	Avg 139
.265	.264	.262	.275	320	274	346	311	341					
.196	.194	.195	.230	333	351	388	388	509					
.090	.122	-	.150	-	-	-	-	310					
.240	.241	.238	.260	447	424	474	460	569	—	—	—	—	—
				Avg 367	Avg 350	Avg 403	Avg 386	Avg 432	Avg 106	Avg 103	Avg 111	Avg 108	Avg 114
.302	-	.300	.315	631	462	-	571	582					
.216	.215	.210	.215	438	455	499	489	510	—	—	—	—	—
				Avg 534	Avg 458	Avg 499	Avg 530	Avg 546	Avg 127	Avg 118	Avg 123	Avg 127	Avg 128
-	.254	-	.250	371	-	422	-	452					
-	.271	-	.265	421	-	436	-	437					
.208	.214	.213	.225	352	374	444	434	473					
-	.220	-	.220	386	-	360	-	479					
-	.188	-	.215	284	-	227	-	439	—	—	—	—	—
				Avg 363	Avg 374	Avg 378	Avg 434	Avg 456	Avg 105	Avg 106	Avg 107	Avg 102	Avg 118
-	-		.150	-	-	-	-	512					
.187	.186	.187	.250	335	349	387	387	632					
.200	.197	.197	.235	390	402	442	442	591					
.231	.235	.232	.265	366	356	410	398	531	—	—	—	—	—
				Avg 363	Avg 369	Avg 413	Avg 409	Avg 566	Avg 105	Avg 106	Avg 102	Avg 111	Avg 131
.294		.293	.311	707	522	-	648	683					
.274	.273	.273	.302	531	436	598	523	622					
.312		.311	.345	528	372	-	456	548					
-	.073	-	.150	-	-	-	-	520	—	—	—	—	—
				Avg 589	Avg 443	Avg 598	Avg 542	Avg 593	Avg 133	Avg 116	Avg 134	Avg 128	Avg 134
.174	.176	-	.220	344	356	394	-	558					
.221	.218	.219	.235	382	385	429	363	490					
.230	.230	.225	.225	494	482	542	609	529					
.253	.252	.249	.290	426	388	436	419	593	—	—	—	—	—
				Avg 412	Avg 403	Avg 450	Avg 464	Avg 542	Avg 102	Avg 111	Avg 117	Avg 120	Avg 128

Effects of Orientation, Aging Time, and Temperature on the Slow-Notch-Bend Fracture Toughness of Plate from Republic Heat 3960524

Figure 10, Sheet 2 of 2

Specimen Orientation/ Aged (°F)	Method of Calculation	Fracture Toughness in-lb/in^2* Aging Time (Hr.) 4 Hrs.	8 Hrs.	16 Hrs.	24 Hrs.
Longitudinal 850	Spring Const.	-	385-505 Avg(10)437	303-363 Avg(12)335	266-453 Avg(8)349
	Bueckner	-	422-568 Avg(4)477	307-394 Avg(4)383	358-479 Avg(4)402
Transverse 850	Spring Const.	-	279-399 Avg(6)328	-	256-601 Avg(12)393
	Bueckner	-	336-443 Avg(4)372	-	326-405 Avg(4)362
Longitudinal	Spring Const.	362-463 Avg(16)420	427-638 Avg(10)511	318-367 Avg(8)343	414-494 Avg(8)447
	Bueckner	405-483 Avg(4)454	413-501 Avg(4)438	390-454 Avg(4)421	460-549 Avg(4)512
Transverse	Spring Const.	243-386 Avg(16)309	-	-	273-454 Avg(16)342
	Bueckner	300-383 Avg(5)361	345-410 Avg(4)376	-	384-478 Avg(4)425
Longitudinal 950	Spring Const.	397-613 Avg(12)514	438-499 Avg(4)470	335-442 Avg(12)389	436-707 Avg(7)568
	Bueckner	482-835 Avg(4)643	432-582 Avg(3)546	512-632 Avg(4)566	520-683 Avg(4)593
Transverse 950	Spring Const.	274-474 Avg(12)377	227-444 Avg(12)377	-	363-609 Avg(12)447
	Bueckner	310-569 Avg(4)432	437-479 Avg(5)456	-	490-593 Avg(4)542

*Values in parenthesis indicate number of tests in computing the average.

Summary of Plane-Strain Fracture Toughness of Plate from Republic Heat 3960524

Figure 11

Specimen Number	Aging Cycle °F - hr	Specimen Orientation	.2% Offset Yield (ksi)	Width b (in.)	Depth d (in.)	Proportional Limit Load (L) (lb)	Proportional Limit Deflec. (e) (in.)	Maximum Load (L) (lb)
R 39	850 - 16	Longitudinal	220	.600	.750	9000	.02490	9905
R 40				.599	.750	10220	.02431	11650
R 41				.600	.749	9700	.02431	11080
R 42				.600	.750	10250	.02490	11465
R 43	850 - 24	Longitudinal	239	.599	.750	10050	.02356	11980
R 44				.599	.750	11600	.02470	13725
R 45				.600	.750	9500	.02358	10710
R 46				.599	.750	9600	.02358	11000
R 19	850 - 24	Transverse	233	.600	.750	11000	.02413	11500
R 20				.599	.750	8950	.02095	9770
R 21				.600	.750	8800	.02195	9260
R 22				.599	.750	8000	.0205[illegible]	8810
R 47	900 - 4	Longitudinal	214	.600	.750	10200	.02509	12500
R 48				.600	.750	9000	.02539	10420
R 49				.599	.751	8700	.02415	10570
R 50				.600	.750	8200	.02585	9535
R 23	900 - 4	Transverse	218	.600	.751	11500	.02413	14500
R 24				.600	.750	9450	.02241	10545
R 25				.600	.750	10400	.02412	11800
R 26				.600	.752	10600	.02392	12950
R 51	900 - 16	Longitudinal	223	.599	.751	10100	.02470	11850
R 52				.599	.750	8700	.02394	9745
R 53				.600	.751	10700	.02530	12180
R 54				.601	.751	10500	.02450	12350
R 55	900 - 24	Longitudinal	233	.600	.750	8900	.02280	11070
R 56				.600	.750	9300	.02361	11870
R 57				.599	.751	10450	.02442	12550
R 58				.600	.750	10450	.02320	13130
R 27	900 - 24	Transverse	231	.600	.750	9200	.02260	10450
R 28				.600	.750	10450	.02319	11735
R 29				.599	.750	10800	.02358	11800
R 30				.600	.750	9900	.02186	11210
R 59	950 - 4	Longitudinal	215	.599	.750	8800	.02430	11000
R 60				.600	.749	9750	.02507	11810
R 61				.600	.750	10050	.02469	12960
R 62				.600	.750	5800	.02241	7365
R 31	950 - 4	Transverse	219	.600	.750	9700	.02346	10990
R 32				.600	.750	9850	.02240	11470
R 33				.599	.750	10500	.02400	12475
R 34				.600	.750	9800	.02280	11660
R 63	950 - 16	Longitudinal	222	.600	.750	11400	.02545	14450
R 64				.600	.750	9800	.02507	11935
R 65				.599	.751	9900	.02450	12150
R 66				.600	.750	6950	.02528	8225
R 67	950 - 24	Longitudinal	225	.599	.748	9300	.02482	11390
R 68				.600	.749	9600	.02394	12060
R 69				.599	.750	7950	.02621	9000
R 70				.599	.749	10100	.02508	12740
R 35	950 - 24	Transverse	220	.599	.749	10200	.02328	11880
R 36				.599	.749	10000	.02318	11620
R 37				.599	.750	9900	.02375	11550
R 38				.599	.750	10350	.02585	13275

* (1) Five-Point Curve Fitting
(2) Four-Point Curve Fitting
(3) Buschmer's Analysis

eb/L	Notch Plus Crack Depth: Effective	Notch Plus Crack Depth: Measured	Plane-Strain Fracture Toughness, in. lb/in.^{2}		Stress Intensity Factor, 1000 psi in.	
$(in.^2/lb)x10^{-8}$	a_1(in.)	a_o(in.)	G_{nc_1}*(1)	G_{nc_1}*(3)	K_{nc_1}	K_{Ic}
166	.256	.269	501	628		
142	.193	.232	499	609		
150	.214	.238	476	577		
146	.201	.228	511	591		
			Avg 497	Avg 601	123	136
140	.187	.214	478	509		
128		.183		522		
149	.210	.243	450	572		
147	.205	.239	454	568		
			Avg 461	Avg 543	118	128
132		.181		460		
140	.166	.223	378	434		
149	.211	.248	388	511		
153	.222	.253	336	440		
			Avg 367	Avg 461	105	118
148	.206	.232	513	605		
169	.264	.271	523	638		
166	.257	.270	471	590		
189		.301		666		
			Avg 502	Avg 625	123	137
125		.171		457		
142	.192	.228	425	502		
139	.184	.207	507	513		
135		.207	534 *(2)	526		
			Avg 489	Avg 589	122	133
146	.203	.228	500	572		
165	.253	.275	463	617		
142	.191	.222	543	610		
140	.187	.216	517	558		
			Avg 506	Avg 589	124	133
154	.223	.246	415	514		
145	.198	.236	463	576		
140	.187	.213	517	543		
133	.167	.206	507 *(2)	514		
			Avg 476	Avg 537	120	127
147	.206	.240	417	524		
133	.167	.215	507 *(2)	553		
131	.161	.199	529 *(2)	519		
132	.165	.211	452 *(2)	480		
			Avg 476	Avg 519	120	125
165	.254	.260	477	562		
154	.224	.242	502	602		
147	.206	.223	497	546		
232		.355	-	502		
			Avg 492	Avg 553	122	130
145	.200	.233	456	551		
136	.176	.213	466 *(2)	483		
133	.167	.201	543 *(2)	528		
140	.184	.220	451	507		
			Avg 479	Avg 517	120	125
134	.169	.184	609 *(2)	507		
153	.222	.237	502	580		
148	.208	.212	487	483		
218		.304		486		
			Avg 533	Avg 514	127	125
160	.244	.248	540 *(2)	585		
150	.212	.229	463	526		
197		.315		698		
149	.209	.226	510	570		
			Avg 504	Avg 595	123	134
137	.177	.221	502 *(2)	559		
139	.183	.218	470	584		
144	.196	.233	472	576		
150	.212	.194	539	457		
			Avg 496	Avg 589	123	126

Effects of Orientation, Aging Time, and Temperature on the Slow-Notch-Bend Fracture Toughness of Plate from Republic Heat 3920556

Figure 12, Sheet 1 of 2

Specimen Number	Aging Cycle °F - hr	Notch Location	.2% Offset Yield (ksi)	Width b (in.)	Depth d (in.)	Proportional Limit Load (L) (lb)	Proportional Limit Deflec. (e) (in.)	Maximum Load (L) (lb)	eb/L (in.^{2}/lb) x 10^{-8}	Effective a_1(in.)(1)	Effective a_2(in.)(2)	Effective a_3(in.)(3)	Effective a_4
660	850-8	Longitudinal	211	.575	.749	9000	.0230	10230	147	.218	.212	.211	[illegible]
661				.576	.749	9000	.0240	10340	153	.234	.227	.230	[illegible]
662				.576	.749	9800	.0238	10800	140	.198	.193	.189	[illegible]
663				.576	.749	10800	.0243	11400	130	.162	.162	.149	[illegible]
664				.576	.749	12200	.0277	13350	131	.168	.166	.154	[illegible]
680	850-8	Transverse	214	.577	.751	10300	.0272	11300	152	.231	.224	.227	[illegible]
681				.577	.751	9750	.0255	10800	151	.229	.222	.223	[illegible]
682				.578	.751	10750	.0258	11800	139	.195	.190	.184	[illegible]
683				.577	.751	9750	.0260	10600	154	.236	.230	.230	[illegible]
684				.577	.751	9250	.0253	10000	158	.245	.240	.240	[illegible]
655	900-8	Longitudinal	218	.575	.749	10300	.0266	11000	148	.220	.214	.216	[illegible]
656				.576	.749	9500	.0228	11400	138	.191	.188	.183	[illegible]
657				.576	.749	9300	.0224	11240	139	.195	.190	.184	[illegible]
658				.576	.749	6500	.0228	7740	205	.314	.320	.306	[illegible]
659				.576	.749	8600	.0236	9760	158	.245	.240	.240	[illegible]
675	900-8	Transverse	220	.578	.751	8750	.0243	9500	160	.248	.244	.246	[illegible]
676				.578	.751	9200	.0254	9490	160	.248	.244	.244	[illegible]
677				.577	.751	9750	.0251	10250	149	.222	.218	.216	[illegible]
678				.578	.751	8000	.0235	8325	172	.270	.270	.268	[illegible]
679				.577	.751	8600	.0247	8950	166	.260	.257	.258	[illegible]
665	950-8	Longitudinal	219	.576	.750	15750	.0315	17700	116	.092	.109	.082	[illegible]
666				.576	.750	10250	.0256	11225	144	.210	.204	.202	[illegible]
667				.576	.749	8600	.0241	9000	162	.253	.246	.248	[illegible]
668				.576	.749	10000	.0243	10720	140	.198	.193	.188	[illegible]
669				.577	.750	10800	.0256	11990	137	.188	.184	.177	[illegible]
685	950-8	Transverse		.578	.751	11300	.0260	11950	133	.176	.172	.163	[illegible]
686				.578	.751	8250	.0228	8850	160	.249	.244	.244	[illegible]
687				.578	.751	8750	.0217	9700	143	.207	.202	.200	[illegible]
688				.578	.751	10250	.0232	10825	131	.168	.166	.154	[illegible]
689				.578	.751	10500	.0240	10925	132	.172	.169	.159	[illegible]

(1) First Calibration Curve Run; Rowe's Analysis. Calibration Curve Constants: $Q = 22.00 \times 10^{-6}$; $R = -115.00 \times 10^{-6}$; $S = 250.00 \times 10^{-6}$

(2) Second Calibration Curve Run; Rowe's Analysis. Calibration Curve Constants: $Q = 19.86 \times 10^{-6}$; $R = -71.67 \times 10^{-6}$; $S = 130.56 \times 10^{-6}$

(3) 5-Point Curve Fitting; First Calibration Curve Run

(4) 5-Point Curve Fitting; Second Calibration Curve Run

(5) Least-Squares Statistical Analysis, First Calibration Curve Run. Curve Equation $\vartheta = 8.82 \times 10^{-7} + 5.14a \times 10^{-6} - 2.68a^2 \times 10^{-5} + 7.11a^3 \times 10^{-5}$

(6) Least-Squares Statistical Analysis, Second Calibration Curve Run. Curve Equation $\vartheta = 1.48 \times 10^{-6} - 1.86a \times 10^{-5} + 1.30a^2 \times 10^{-4} - 4.38a^3 \times 10^{-4} + 5.98a^4 \times$

(7) Boeshaar's Analysis

Notch + Crack Depth			Measured	Plane-Strain Fracture Toughness in-lb/in.^{2}							Stress Intensity Factor 1000 psi $\sqrt{\text{in.}}$						
(in.)(4)	a_5(in.)(5)	a_6(in.)(6)	a_e(in.)(7)	G_{nc_1}(1)	G_{nc_2}(2)	G_{nc_3}(3)	G_{nc_4}(4)	G_{nc_5}(5)	G_{nc_6}(6)	G_{I_c}(7)	K_{nc_1}	K_{nc_2}	K_{nc_3}	K_{nc_4}	K_{nc_5}	K_{nc_6}	K_{I_c}
.204	.215	.205	.235	434	457	464	433	444	437	525							
.222	.232	.223	.250	515	493	502	460	528	438	592							
.186	.193	.184	.225	427	493	453	490	414	526	576							
.159	.150	.156	.195	409	529	308	589	348	635	546							
.162	.155	.159	.190	538	685	435	750	460	814	667							
				Avg 465	Avg 531	Avg 432	Avg 524	Avg 439	Avg 570	Avg 581	Avg 119	Avg 127	Avg 115	Avg 126	Avg 115	Avg 131	Avg 132
.219	.229	.219	.205	650	634	649	592	668	570	532							
.215	.226	.215	.225	570	562	575	522	576	510	561							
.183	.189	.181	.205	479	582	519	583	474	629	577							
.223	.233	.223	.225	616	588	588	540	621	513	561							
.234	.241	.234	.250	614	561	553	512	613	472	615							
				Avg 506	Avg 585	Avg 577	Avg 549	Avg 590	Avg 539	Avg 569	Avg 124	Avg 133	Avg 132	Avg 129	Avg 134	Avg 128	Avg 131
.209	.219	.208	.225	582	605	627	[illegible]	606	573	639							
.181	.187	.180	.210	379	454	401	[illegible]	366	495	479							
.183	.189	.181	.210	375	439	391	[illegible]	358	474	459							
.317	.307	.319	.310	685	497	589	[illegible]	572	523	489							
.235	.242	.234	.255	533	487	482	446	534	410	562							
				Avg 511	Avg 496	Avg 498	Avg 494	Avg 487	Avg 495	Avg 526	Avg 124	Avg 123	Avg 123	Avg 123	Avg 121	Avg 123	Avg 126
.242	.247	.241	.245	567	513	522	475	578	431	528							
.239	.245	.239	.242	627	567	564	518	627	472	570							
.209	.220	.208	.210	529	550	558	511	540	510	496							
.265	.264	.264	.265	614	511	601	449	573	415	515							
.255	.257	.254	.260	632	541	607	493	620	448	579							
				Avg 594	Avg 536	Avg 590	Avg 489	Avg 588	Avg 455	Avg 538	Avg 134	Avg 127	Avg 133	Avg 122	Avg 133	Avg 118	Avg 127
.122	.076	.112	.110	713	917	(-) -	—*	877	992	502							
.196	.206	.195	.220	520	568	558	547	519	570	601							
.244	.249	.243	.255	584	505	520	468	573	423	562							
.186	.194	.184	.205	444	514	473	510	432	547	509							
.177	.182	--	.185	477	575	485	587	447	—	496							
				Avg 547	Avg 616	Avg 507	Avg 528	Avg 569	Avg 633	Avg 534	Avg 129	Avg 136	Avg 124	Avg 126	Avg 131	Avg 138	Avg 127
.167	.165	.166	.185	479	598	433	638	423	697	538							
.240	.245	.239	.275	510	456	455	418	506	380	592							
.195	.205	.194	.265	366	407	399	395	369	413	616							
.162	.156	.159	.205	377	481	306	526	323	570	525							
.165	.162	.163	.210	404	510	353	551	354	601	574							
				Avg 434	Avg 490	Avg 389	Avg 505	Avg 395	Avg 532	Avg 589	Avg 115	Avg 122	Avg 109	Avg 124	Avg 106	Avg 127	Avg 139

10^{-4}

Effects of Orientation, Aging Time, and Temperature on the Slow-Notch-Bend Fracture Toughness of Plate from Republic Heat 3920556

Figure 12, Sheet 2 of 2

Specimen Orientation/ Aged (°F)	Method of Calculation	Fracture Toughness in-lb/in^2* Aging Time (Hrs) 4 Hrs.	8 Hrs.	16 Hrs.	24 Hrs
Longitudinal 850	Data Smoothing	-	433-502 Avg(6)467	476-511 Avg(4)497	450-478 Avg(3)461
	Bueckner	-	526-667 Avg(5)581	577-628 Avg(4)601	509-572 Avg(4)543
Transverse 850	Data Smoothing	-	512-649 Avg(10)563	-	336-388 Avg(3)367
	Bueckner	-	532-615 Avg(5)569	-	434-511 Avg(4)461
Longitudinal 900	Data Smoothing	471-523 Avg(3)502	391-627 Avg(10)496	463-543 Avg(4)506	415-517 Avg(4)476
	Bueckner	457-526 Avg(4)589	459-639 Avg(5)526	558-617 Avg(4)589	514-576 Avg(4)537
Transverse 900	Data Smoothing	425-534 Avg(3)489	449-607 Avg(10)539	-	417-529 Avg(4)476
	Bueckner	457-526 Avg(4)589	496-579 Avg(5)538	-	480-553 Avg(4)519
Longitudinal 950	Data Smoothing	477-502 Avg(3)492	408-587 Avg(8)518	487-609 Avg(3)533	463-540 Avg(3)504
	Bueckner	502-602 Avg(4)553	496-601 Avg(5)534	483-500 Avg(4)514	526-698 Avg(4)595
Transverse 950	Data Smoothing	451-543 Avg(4)496	395-455 Avg(4)417	-	470-539 Avg(4)496
	Bueckner	483-551 Avg(4)517	525-616 Avg(5)589	-	457-576 Avg(4)529

*Values in parentheses indicate number of tests in computing the average.

Summary of Plane-Strain Fracture Toughness, Plate From Republic Heat 3920556

Figure 13

Solution Annealed (1500°F - 1 hr) and Aged Conditions

Aging Cycle Temp °F	Aging Cycle Time, Hrs.	Orientation	Yield Strength 0.2% Offset, psi	Fracture Toughness W/A (in-lb/in.^{2}) Test Temperature, °F -100	Rt	200	400
850	8	Longitudinal	238	798	948	968	1321
				766	968	1231	1141
				782	958	1099	1231
		Transverse	248	577	413	722	780
				526	682	743	995
				551	547	732	8887
900	8	Longitudinal	239	745	1072	1182	1426
				840	940	1472	1410
				792	1006	1327	1418
		Transverse	244	652	786	873	852
				631	671	934	1025
				641	728	903	938
900	24	Longitudinal	228		1386		
					1701		
					1330		
					1292		
					1427		
		Transverse	233		1047		
					915		
					1084		
					991		
					1009		
950	8	Longitudinal	219	1047	1282	2004	1643
				922	1430	2212	2230
				1018	1356	2108	1936
		Transverse	218	720	1056	1044	1490
				722	1197	1220	1340
				721	1126	1132	1415

Effects of Specimens Orientation, Aging Temperature, and Test Temperature on the Precracked Impact Fracture Toughness (W/A) of Republic Heat 3960524

Figure 14

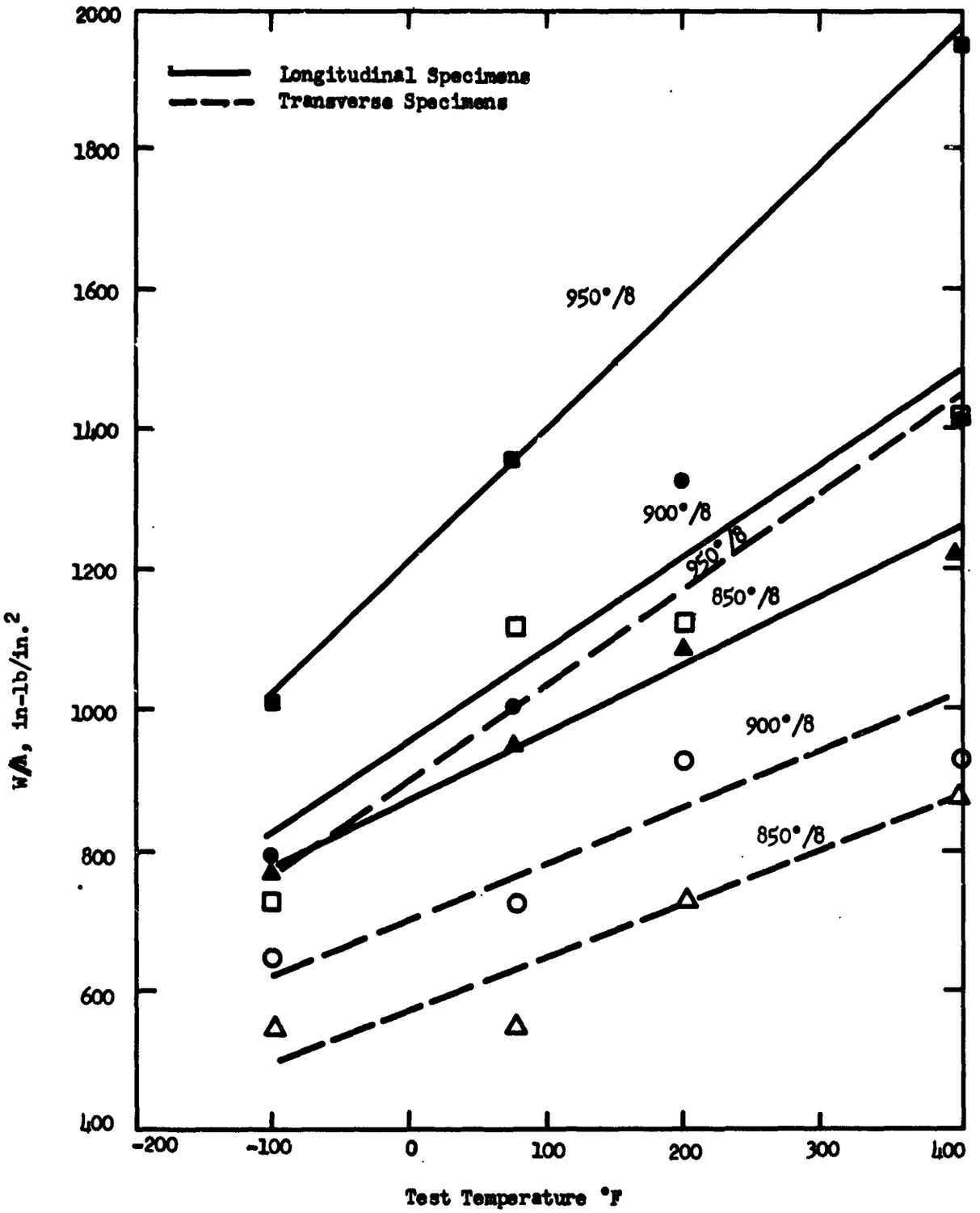

Precracked Impact Fracture Toughness (W/A) vs Test Temperature for Various Aging Cycles - Republic Heat 3960524

Figure 15

Temp. °F	Time, Hrs.	Orientation	Yield Strength 0.2% Offset, psi	-100	Rt	200	400
850	8	Longitudinal	211	1121	1417	2255	2197
				1046	1678	1491	2028
				1083	1548	1873	2112
		Transverse	214	909	1630	1752	2117
				925	1565	2309	2064
				917	1597	2030	2091
900	8	Longitudinal	218	1043	1425	1410	1774
				1012	1594	1594	2785
				1028	1509	1502	2279
		Transverse	220	891	1296	1410	1804
				894	1384	1424	2409
				893	1340	1417	2106
900	24	Longitudinal	233	917	1266	1313	1680
				983	1326	1633	1744
					1330		
				950	1307	1474	1712
		Transverse	231	1189	1606	1810	2193
				1352	1749	1987	2266
					1781		
				1270	1712	1898	2229
950	8	Longitudinal	219	924	1352	1574	1633
				806	1300	1377	1913
				865	1326	1476	1773
		Transverse	---	865	1207	1373	1655
				864	1333	1465	1666
				864	1270	1419	1660

Specimen Size .575 x .394

Effects of Specimen Orientation, Aging Temperature, and Test Temperature on the Precracked Impact Fracture Toughness (W/A) of Republic Heat 3920556

Figure 16

Element		Composition, weight percent *
C		0.025
Mn		0.08
P		0.004
S		0.006
Si		0.087
Ni		17.98
Mo		4.32
Ti		0.15
Co		7.75
Al		0.08
B	added during melting	0.003
Zr	added during melting	0.02
Ca **	added during melting	0.06

* Averaged from four locations on the plate pattern

** Added in increments of 0.02

Mill Certified Analysis of Chemical Composition, Lukens Plate
R-599-1

Figure 17

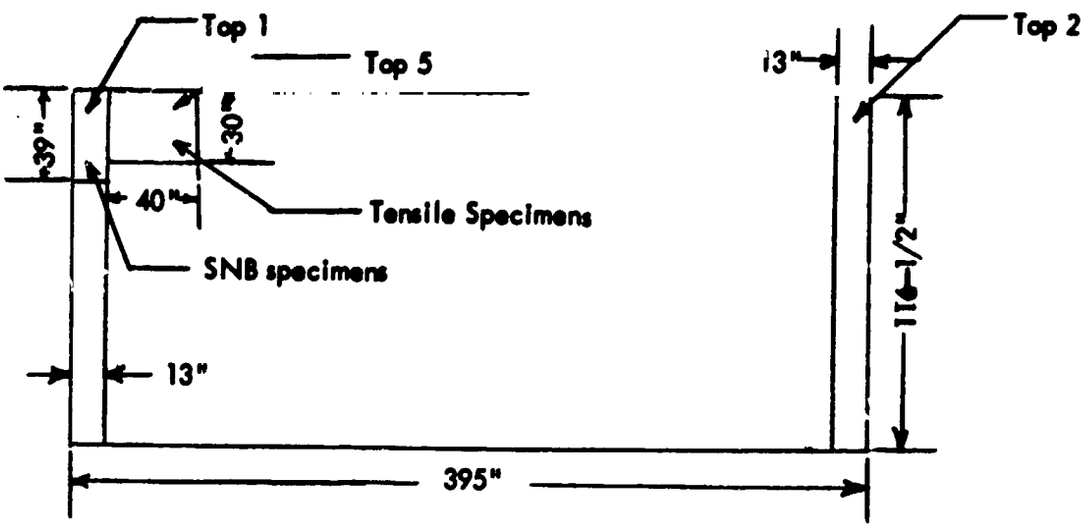

Location of Specimens, Lukens Heat R-5[illegible]-1

Figure 18

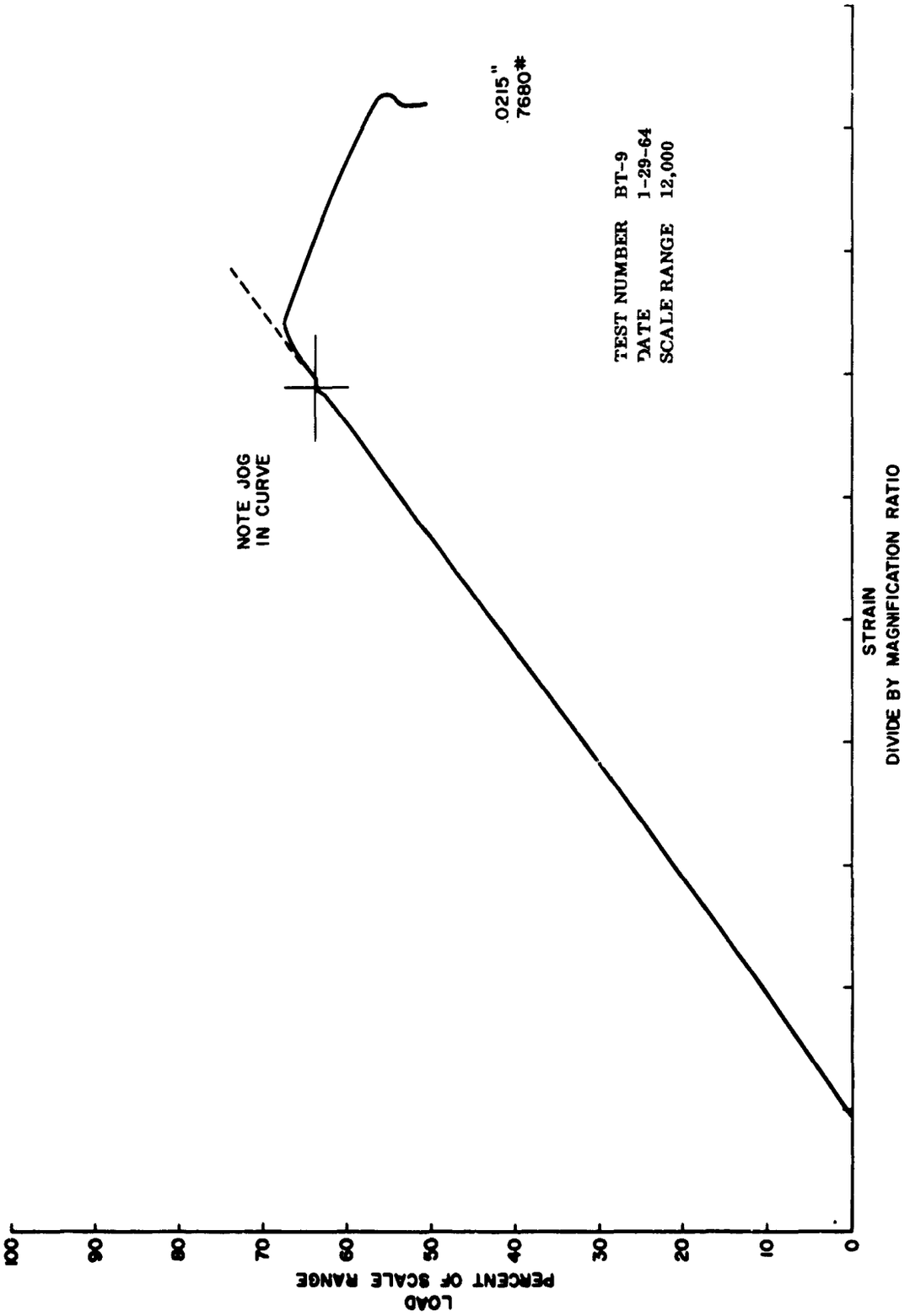

Typical Load vs Strain Curve for Slow-Notch-Bend Specimens
Tested by Sun Shipbuilding

Figure 19

Aging Cycle Temperature, °F	Time, hours	Orientation	0.2% Offset Yield Strength Ksi	Ultimate Tensile Strength Ksi	Elongation in 1 inch %	Reduction in Area %
850	4	Longitudinal	207	216	13	56
		Transverse	218	225	11	56
850	8	Longitudinal	221	227	11	55
		Transverse	232	240	10	50
850	16	Longitudinal	234	241	11	58
		Transverse	242	248	10	51
850	32	Longitudinal	239	248	10	53
		Transverse	246	257	10	51
900	2	Longitudinal	207	214	11	61
		Transverse	221	229	10	53
900	4	Longitudinal	[illegible]	230	12	60
		Transverse	232	238	10	52
900	8	Longitudinal	225	235	11	55
		Transverse	230	243	11	51
900	16	Longitudinal	226	230	11	57
		Transverse	232	243	11	51
950	2	Longitudinal	223	228	13	56
		Transverse	228	234	10	53
	4	Longitudinal	225	229	13	55
		Transverse	228	237	11	52
	8	Longitudinal	215	226	12	54
		Transverse	229	235	11	49
	16	Longitudinal	216	227	12	55
		Transverse	229	242	11	50

* Average of three specimens

Tensile Data Obtained from Lukens Plate R-599-1

Figure 20

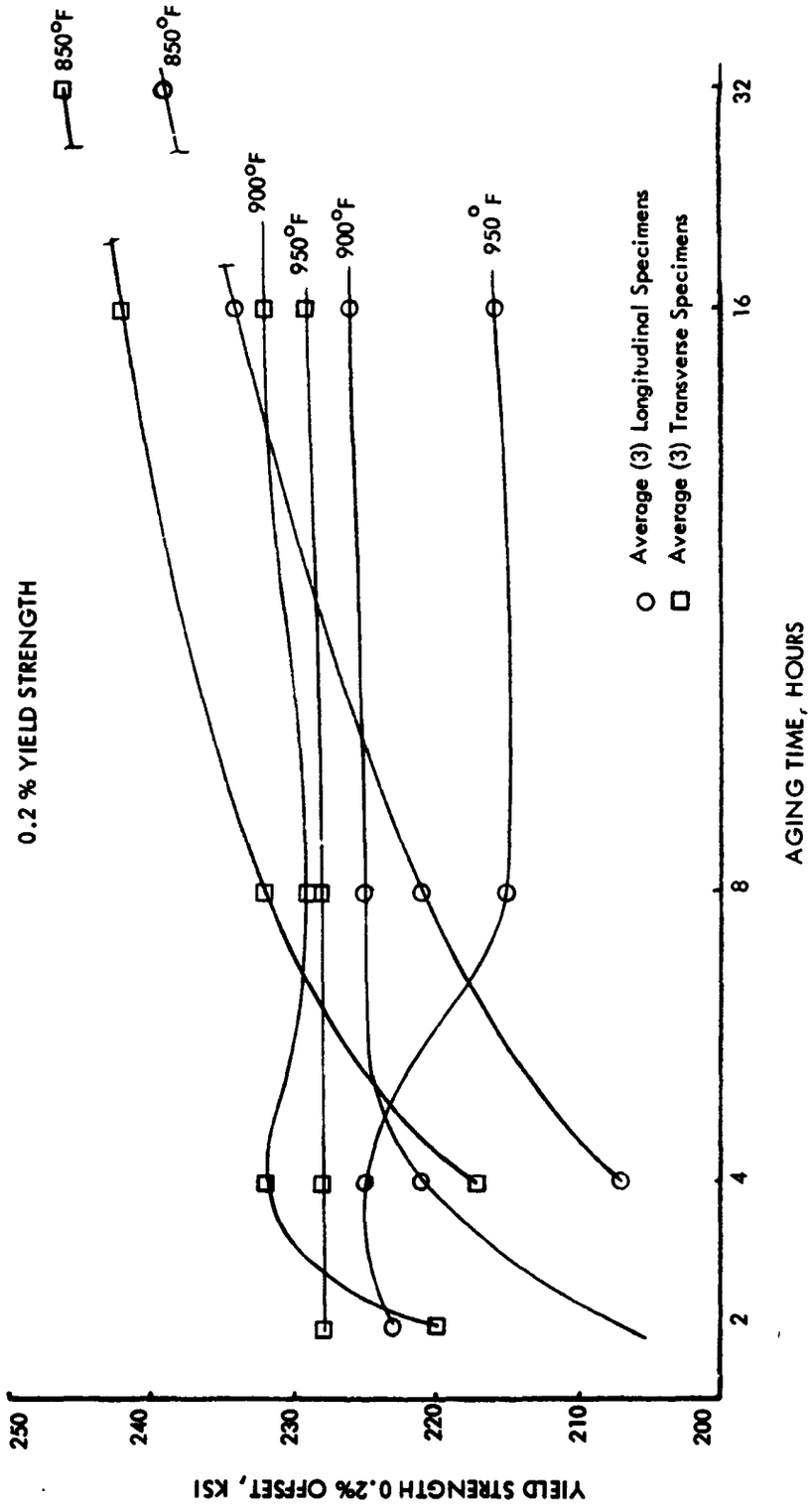

Effect of Aging Temperature and Time on the Yield Strength of Lukens Plate, Heat R-599-1

Figure 21

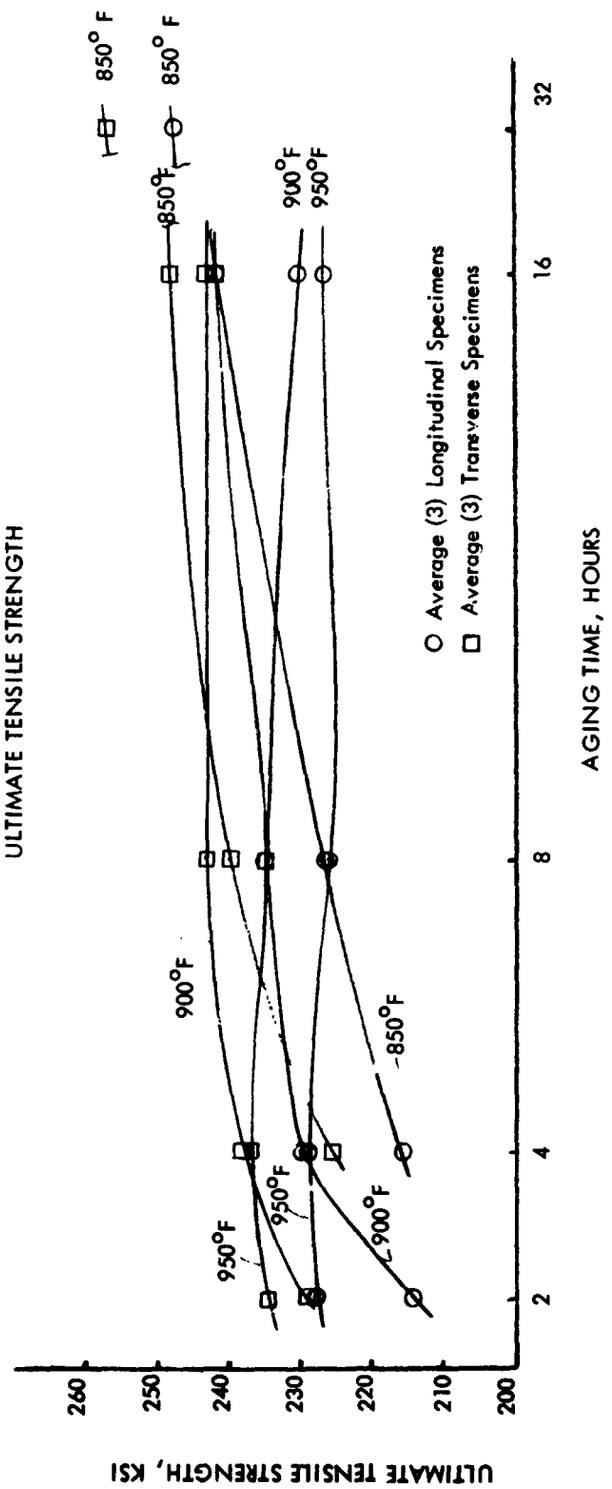

Effect of Aging Temperature and Time on the Ultimate Tensile Strength of Lukens Plate, Heat R-599-1

Figure 22

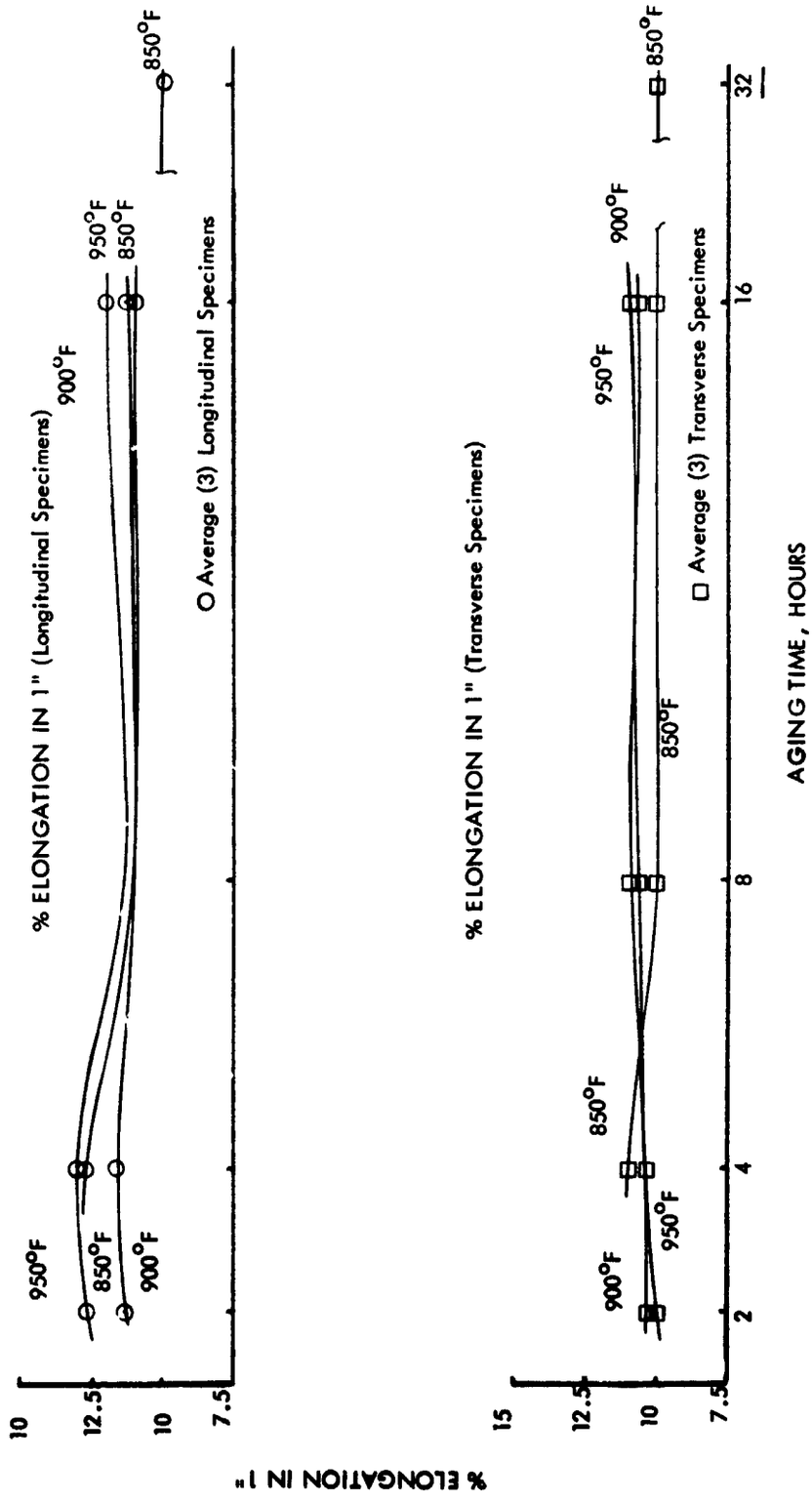

Effect of Aging Time and Temperature on the Ductility of Lukens Plate, Heat R-599-1

Figure 23

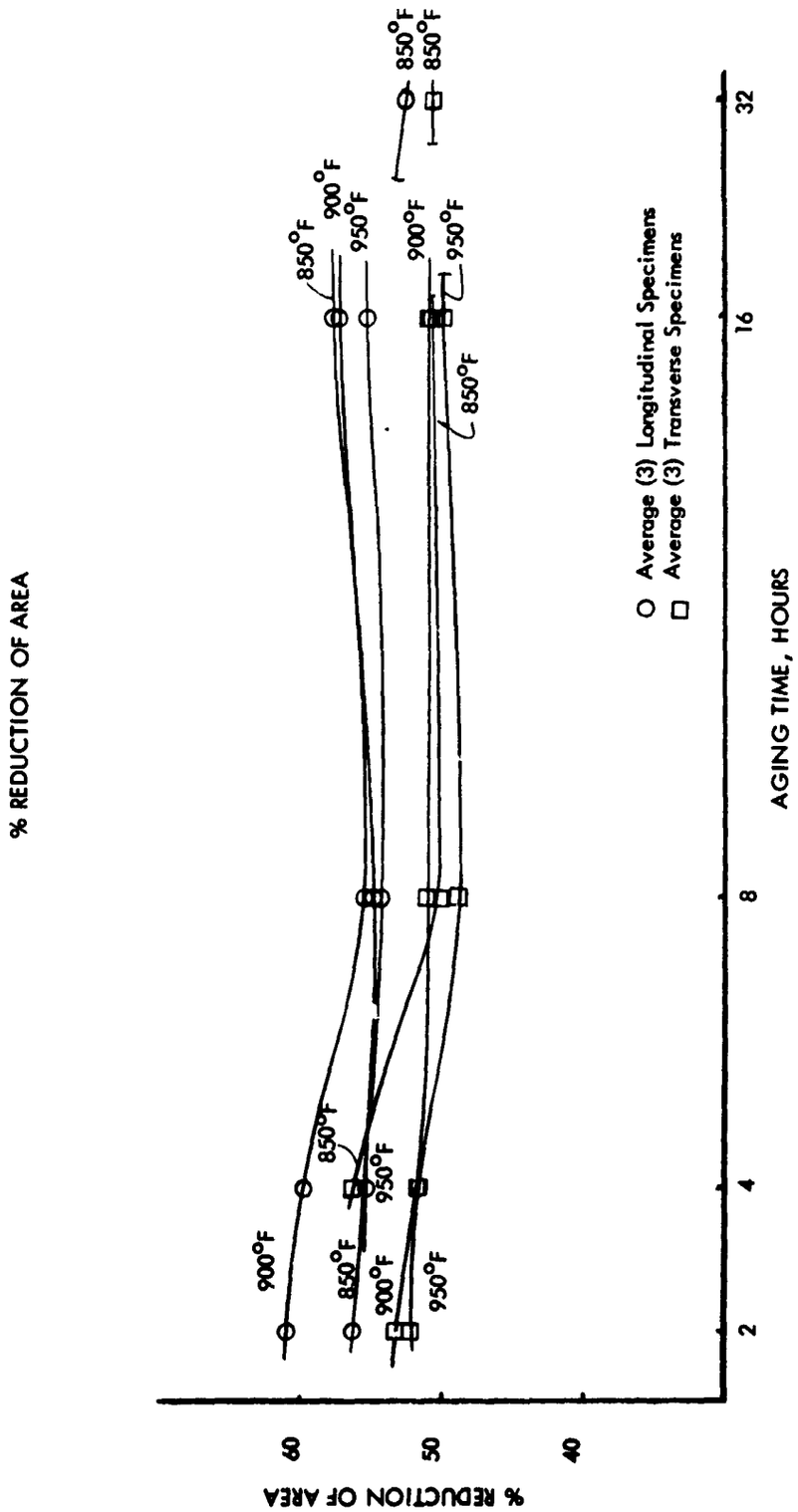

Effect of Aging Temperature and Time on the Reduction of Area of Lukens Plate, Heat R-599-1

Figure 24

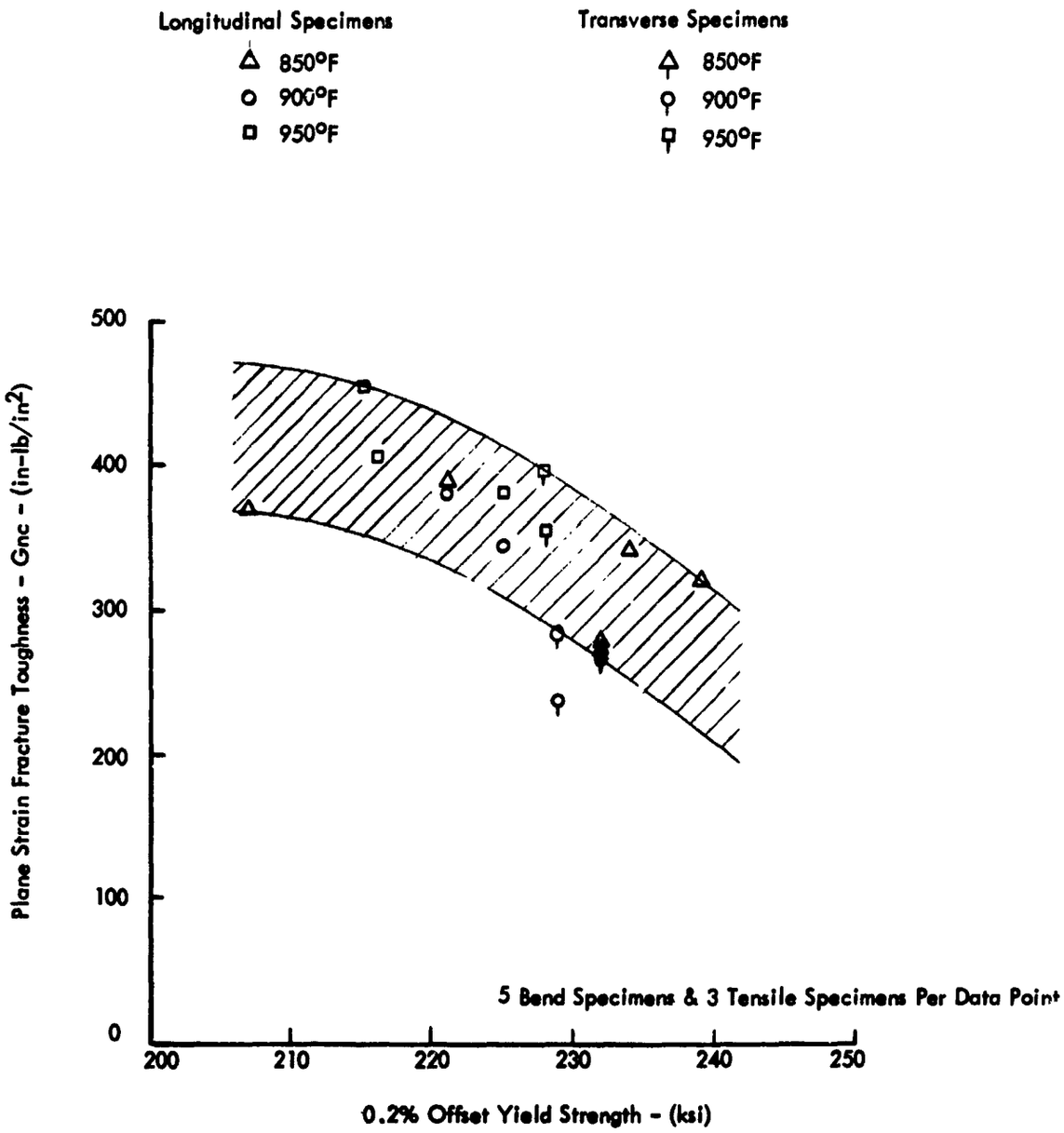

Plane-Strain Fracture Toughness vs Yield Strength for Lukens Plate Heat R-599-1

Figure 25

Effect of Aging Time and Temperature on the Plane-Strain Fracture Toughness of Lukens Plate, Heat R-599-1 Slow-Notch-Bend Specimens

Specimen Number	Aging Cycle (°F-Hrs.)	Width b-(in.)	Depth d-(in.)	$1/M \times 10^6$ (in.^{2}/lb.)	Effective a - (in.) **	Measured a - (in.) **	Proportional Load Limit (lbs.)	Maximum Load (lbs.)	Fracture Toughness Gnc (in-lb/in^2)	Fracture Toughness Gic (in-lb/in^2)	Stress Intensity Factor Knc (1000 psi $\sqrt{in}$)	Stress Intensity Factor Kic (1000 psi $\sqrt{in.}$)
* BST-1	850-8	0.598	0.600	1.690	0.1278	0.1106	7440	7620	270	274	85	86
* BST-2	850-8	0.598	0.600	1.690	0.1278	0.1142	7440	7920	270	285	85	88
* BST-3	850-8	0.599	0.599	1.700	0.1306	0.1050	7560	7800	285	266	88	85
* BST-4	850-8	0.600	0.600	1.640	0.1125	0.1009	8220	8450	285	297	88	90
* BST-5	850-8	0.599	0.599	1.750	0.1438	0.1298	6840	7200	264	287	84	88
								Average Values	275	282	86	87
* BST-6	900-4	0.598	0.598	1.700	0.1306	0.1112	7380	7680	273	275	86	86
* BST-7	900-4	0.599	0.599	1.780	0.1509	0.1378	6240	6840	235	261	80	84
* BST-8	900-4	0.599	0.600	1.700	0.1306	0.1257	7380	7240	272	317	86	92
* BST-9	900-4	0.599	0.600	1.680	0.1249	0.1176	7500	8040	267	299	85	90
* BST-10	900-4	0.599	0.597	1.760	0.1462	0.1105	7140	7440	294	256	89	83
								Average Values	268	282	85	87
* BST-11	900-8	0.599	0.598	2.390	0.2383	0.2238	5520	5220	451	494	110	116
* BST-12	900-8	0.598	0.598	1.700	0.1306	0.1090	7380	7800	273	268	86	85
* BST-13	900-8	0.600	0.599	1.680	0.1249	0.1165	7320	7800	253	283	83	87
* BST-14	900-8	0.598	0.600	1.690	0.1278	0.1225	6720	6960	221	254	77	83
* BST-15	900-8	0.599	0.600	1.650	0.1157	0.1105	7440	7680	242	273	81	86
								Average Values	288	314	87	91
BST-16	950-8	0.599	0.599	1.690	0.1278	0.1020	8830	9780	384	355	102	98
BST-17	950-8	0.598	0.600	1.660	0.1189	0.1022	9000	9650	365	364	99	99
BST-18	950-8	0.599	0.600	1.650	0.1157	0.1015	9060	9650	358	365	98	99
BST-19	950-8	0.598	0.599	1.680	0.1249	0.0970	9960	10320	472	423	113	107
BST-20	950-8	0.598	0.599	1.680	0.1249	0.1001	9240	9600	406	377	105	101
								Average Values	397	377	103	101

* Specimen fatigue cracked on SF-1U at the Vertol Division of The Boeing Company.

** NOTE: Effective "a" and Measured "a" values have an accuracy of ± 0.0010 (in.).

Figure 26, Sheet 1 of 4

Effect of Aging Time and Temperature on the Plane-Strain Fracture Toughness of Lukens Plate, Heat R-599-1 Slow-Notch-Bend Specimens

Specimen Number	Aging Cycle (°F-Hrs.)	Width b-(in.)	Depth d-(in.)	$1/M_c \times 10^6$ (in.^{2}/lb.)	Effective a - (in.) **	Measured a - (in.) **	Proportional Load Limit (lbs.)	Maximum Load (lbs.)	Fracture Toughness G_{nc} (in-lb/in^2)	Fracture Toughness G_{Ic} (in-lb/in^2)	Stress Intensity Factor K_{nc} (1000 psi $\sqrt{in}$)	Stress Intensity Factor K_{Ic} (1000 psi $\sqrt{in.}$)
BL-11	950-4	0.599	0.599	1.780	0.1509	0.0925	8750	10140	463	308	112	91
BL-12	950-4	0.599	0.599	1.746	0.1428	0.0868	8750	11760	428	286	108	88
BL-13	950-4	0.599	0.599	1.489	0.0446	0.1168	8650	8650	149	397	63	104
BL-14	950-4	0.599	0.599	2.111	0.2076	0.1720	6100	6720	400	357	104	98
BL-15	950-4	0.599	0.599	1.764	0.1472	0.1053	9000	10620	472	379	113	101
								Average Values	382	345	100	96
BL-16	950-8	0.599	0.599	1.945	0.1832	0.1102	7700	9300	494	293	116	89
BL-17	950-8	0.599	0.599	1.800	0.1554	0.0935	8650	10680	472	304	113	91
BL-18	950-8	0.599	0.599	1.797	0.1548	0.0924	9000	10680	508	325	117	94
BL-19	950-8	0.599	0.599	1.825	0.1608	0.1032	7550	9120	379	260	101	84
BL-20	950-8	0.599	0.599	1.843	0.1645	0.1307	7800	9600	420	377	106	101
								Average Values	455	312	111	92
BL-21	950-16	0.599	0.598	1.764	0.1472	0.0975	8150	10680	387	286	102	88
BL-22	950-16	0.599	0.598	1.756	0.1452	0.1059	8530	10260	416	345	106	97
BL-23	950-16	0.599	0.598	1.684	0.1261	0.0943	8890	10800	379	327	101	94
BL-24	950-16	0.597	0.597	1.679	0.1246	0.0885	8890	11880	376	308	101	91
BL-25	950-16	0.599	0.597	1.845	0.1649	0.1040	8280	10200	475	320	113	93
								Average Values	407	317	105	93
BL-26	900-4	0.599	0.599	1.747	0.1430	0.1087	8400	10200	395	343	103	96
BL-27	900-4	0.599	0.600	1.730	0.1387	0.0980	9000	10200	436	346	108	97
BL-28	900-4	0.600	0.600	1.738	0.1407	0.0940	8100	10040	359	266	98	85
BL-29	900-4	0.599	0.599	2.006	0.1929	0.1035	6120	8160	345	172	97	68
BL-30	900-4	0.599	0.599	1.622	0.1064	0.0838	9600	10200	370	331	100	94
								Average Values	381	291	101	88
BL-31	900-8	0.599	0.599	1.908	0.1768	0.1330	6750	9150	356	290	98	88
BL-32	900-8	0.599	0.598	1.803	0.1561	0.1110	7640	8250	371	293	100	89
BL-33	900-8	0.599	0.599	1.747	0.1430	0.0973	8400	9150	395	301	103	90
BL-34	900-8	0.599	0.599	2.202	0.2188	(1)	6120	6840	452	(1)	110	(1)
BL-35	900-8	0.599	C.599	1.770	0.1486	0.1125	6600	8100	257	221	83	77
								Average Values	345(2)	276(2)	96(2)	86(2)

(1) Specimen BL-34 was missing when the fatigue measurement was made.
(2) Specimen BL-34 is not included in the average.

** NOTE: Effective "a" and Measured "a" values have an accuracy of ± 0.0010 (in.)

Figure 26, Sheet 2 of 4

Specimen Number	Aging Cycle (°F-Hrs.)	Width b-(in.)	Depth d-(in.)	$1/M \times 10^6$ (in.^{2}/lb.)	Effective a - (in.) **	Measured a - (in.) **	Proportional Load Limit (lbs.)	Maximum Load (lbs.)	Fracture Toughness G_{nc} (in-lb/in^2)	Fracture Toughness G_{Ic} (in-lb/in^2)	Stress Intensity Factor K_{nc} (1000 psi $\sqrt{in}$)	Stress Intensity Factor K_{Ic} (1000 psi $\sqrt{in.}$)
BL-36	850-4	0.599	0.598	1.769	0.1483	0.0997	7450	10000	327	245	94	81
BL-37	850-4	0.600	0.598	1.758	0.1457	0.1063	7680	10140	338	280	96	87
BL-38	850-4	0.598	0.598	1.858	0.1675	0.1055	7080	8520	357	237	98	80
BL-39	850-4	0.600	0.599	1.818	0.1593	0.0946	7920	9840	410	258	105	83
BL-40	850-4	0.600	0.598	1.723	0.1369	0.0975	8880	11580	416	338	106	96
								Average Values	370	272	100	85
BL-41	850-8	0.599	0.598	1.811	0.1578	0.0922	7440	8400	358	223	98	78
BL-42	850-8	0.599	0.598	1.766	0.1476	0.1033	7800	8400	356	280	98	87
BL-43	850-8	0.600	0.599	2.333	0.2328	0.1258	5400	5520	406	170	105	68
BL-44	850-8	0.600	0.598	1.844	0.1647	0.1122	7320	7620	369	272	100	86
BL-45	850-8	0.600	0.598	1.743	0.1420	0.0869	9120	9960	460	312	111	92
								Average Values	390	251	102	82
BL-46	850-16	0.599	0.599	1.800	0.1554	0.0951	7320	7800	338	222	96	77
BL-47	850-16	0.600	0.598	1.838	0.1635	0.1090	7020	7380	336	241	95	81
BL-48	850-16	0.600	0.598	1.765	0.1474	0.0974	8160	8580	388	285	102	88
BL-49	850-16	0.600	0.599	1.789	0.1530	0.0875	7380	7800	335	205	95	74
BL-50	850-16	0.599	0.599	1.839	0.1637	0.1088	6840	7320	320	228	93	78
								Average Values	343	236	96	80
BL-51	850-32	0.600	0.598	1.930	0.1807	0.0905	6840	7560	379	184	101	70
BL-52	850-32	0.599	0.599	1.815	0.1587	0.1185	7260	7260	343	285	96	88
BL-53	850-32	0.600	0.599	2.209	0.2196	0.1967	5160	5160	323	326	93	94
*BL-54	850-32	0.599	0.599	1.800	0.1554	0.0960	7320	7920	338	225	96	78
*BL-56	850-32	0.599	0.599	1.776	0.1500	0.1130	6240	6600	233	198	79	73
								Average Values	323	244	93	81

* Specimen Fatigue Cracked on SF-1U at the Vertol Division of The Boeing Company.

** NOTE: Effective "a" and Measured "a" values have an accuracy of $\pm$ 0.0010 (in.)

Effect of Aging Time and Temperature on the Plane-Strain Fracture Toughness of Lukens Plate, Heat R-599-1 Slow-Notch-Bend Specimens

Figure 26, Sheet 3 of 4

Effect of Aging Time and Temperature on the Plane-Strain Fracture Toughness of Lukens Plate, Heat R-599-1 Slow-Notch-Bend Specimens

Specimen Number	Aging Cycle (°F-Hrs.)	Width b-(in.)	Depth d-(in.)	$1/M \times 10^6$ (in.^{2}/lb.)	Effective a - (in.) **	Measured a - (in.) **	Proportional Load Limit (lbs.)	Maximum Load (lbs.)	Fracture Toughness G_{nc} (in-lb/in^2)	Fracture Toughness G_{Ic} (in-lb/in^2)	Stress Intensity Factor K_{nc} (1000 psi $\sqrt{in}$)	Stress Intensity Factor K_{Ic} (1000 psi $\sqrt{in.}$)
*BT-1	850-8	0.599	0.596	1.660	0.1189	0.1047	8280	8640	308	325	91	94
*BT-2	850-8	0.598	0.596	1.640	0.1125	0.1033	8400	8580	300	331	90	94
*BT-3	850-8	0.598	0.600	1.660	0.1189	0.1165	7560	7800	257	301	83	90
*BT-4	850-8	0.599	0.600	1.690	0.1278	0.1105	7440	7620	269	273	85	86
*BT-5	850-8	0.599	0.600	1.750	0.1438	0.1277	6840	7000	264	278	84	87
								Average Values	280	302	87	90
*BT-6	900-4	0.598	0.600	1.870	0.1698	0.1544	6240	6360	284	310	88	91
*BT-7	900-4	0.599	0.600	1.740	0.1413	0.1372	6540	6720	236	283	80	87
*BT-8	900-4	0.599	0.600	1.690	0.1278	0.1125	7440	7800	269	279	85	87
*BT-9	900-4	0.599	0.600	1.670	0.1219	0.1107	7680	8100	273	292	86	89
*BT-10	900-4	0.599	0.600	1.700	0.1306	0.1122	7560	7680	285	287	88	88
								Average Values	270	290	85	88
*BT-11	900-8	0.598	0.600	1.650	0.1157	0.1158	7260	7380	231	276	79	86
*BT-12	900-8	0.599	0.599	1.690	0.1278	0.1125	7440	7770	269	281	85	87
*BT-13	900-8	0.599	0.600	1.680	0.1249	0.1260	6960	6960	230	283	79	87
*BT-14	900-8	0.599	0.600	1.710	0.1334	0.1383	6840	6900	240	313	80	92
*BT-15	900-8	0.599	0.600	1.650	0.1157	0.1180	7080	7410	219	268	77	85
								Average Values	238	284	80	88
BT-16	950-8	0.599	0.600	1.620	0.1057	0.0928	8880	10200	315	316	92	92
BT-17	950-8	0.598	0.600	1.600	0.0985	0.0860	9720	11200	354	348	98	97
BT-18	950-8	0.598	0.600	1.700	0.1306	0.1237	8460	9720	359	408	98	105
BT-19	950-8	0.599	0.600	1.660	0.1189	0.0875	9000	10310	364	303	99	90
BT-20	950-8	0.599	0.600	1.660	0.1189	0.0823	9360	10130	393	306	103	91
								Average Values	357	336	98	95

* Specimen Fatigue Cracked on SF-1U at the Vertol Division of The Boeing Company

** NOTE: Effective "a" and Measured "a" values have an accuracy of $\pm$ 0.0010 (in.)

Figure 26, Sheet 4 of 4

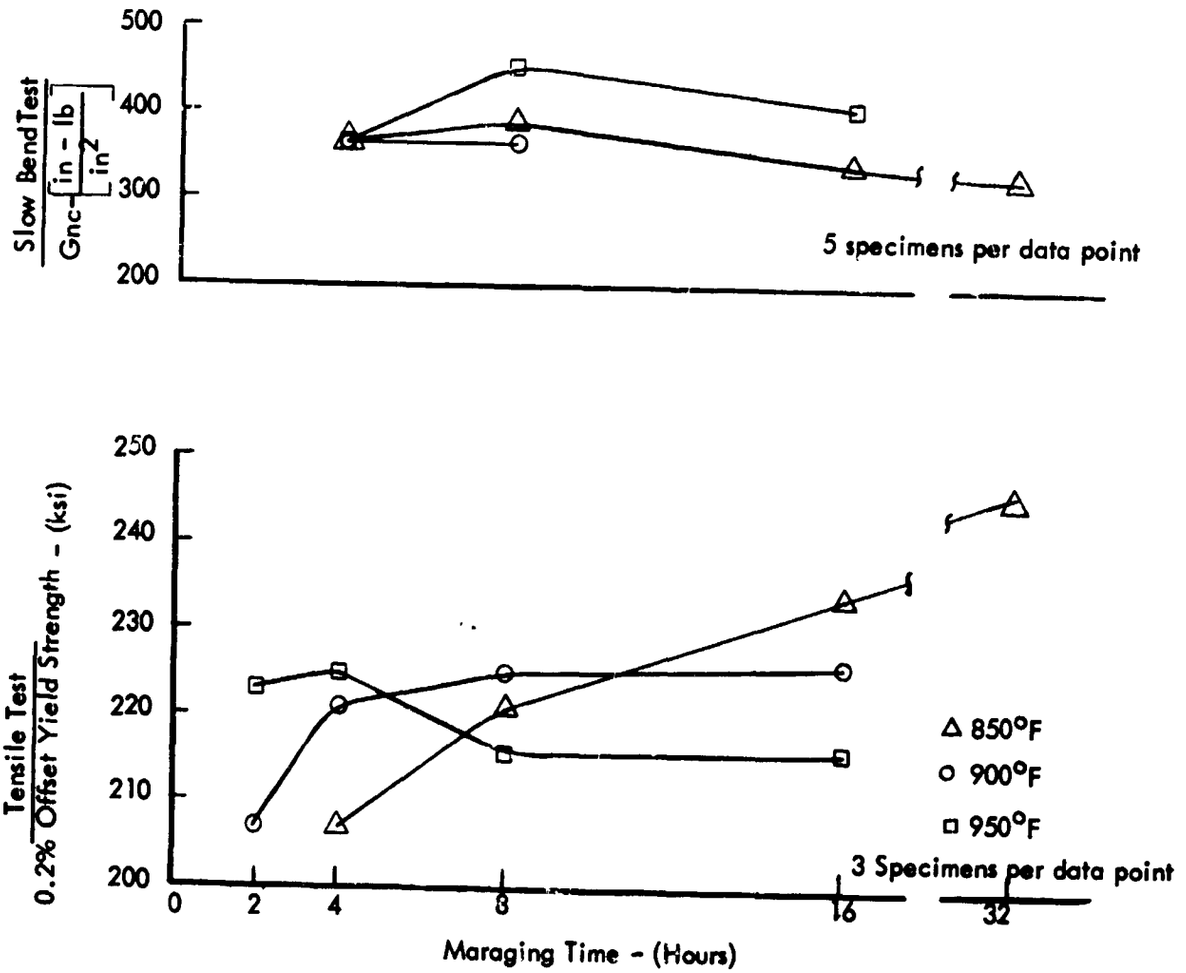

Plane-Strain Fracture Toughness and Yield Strength vs Maraging Time for Lukens Plate, Heat R-599-1 Longitudinal Test Specimens

Figure 27

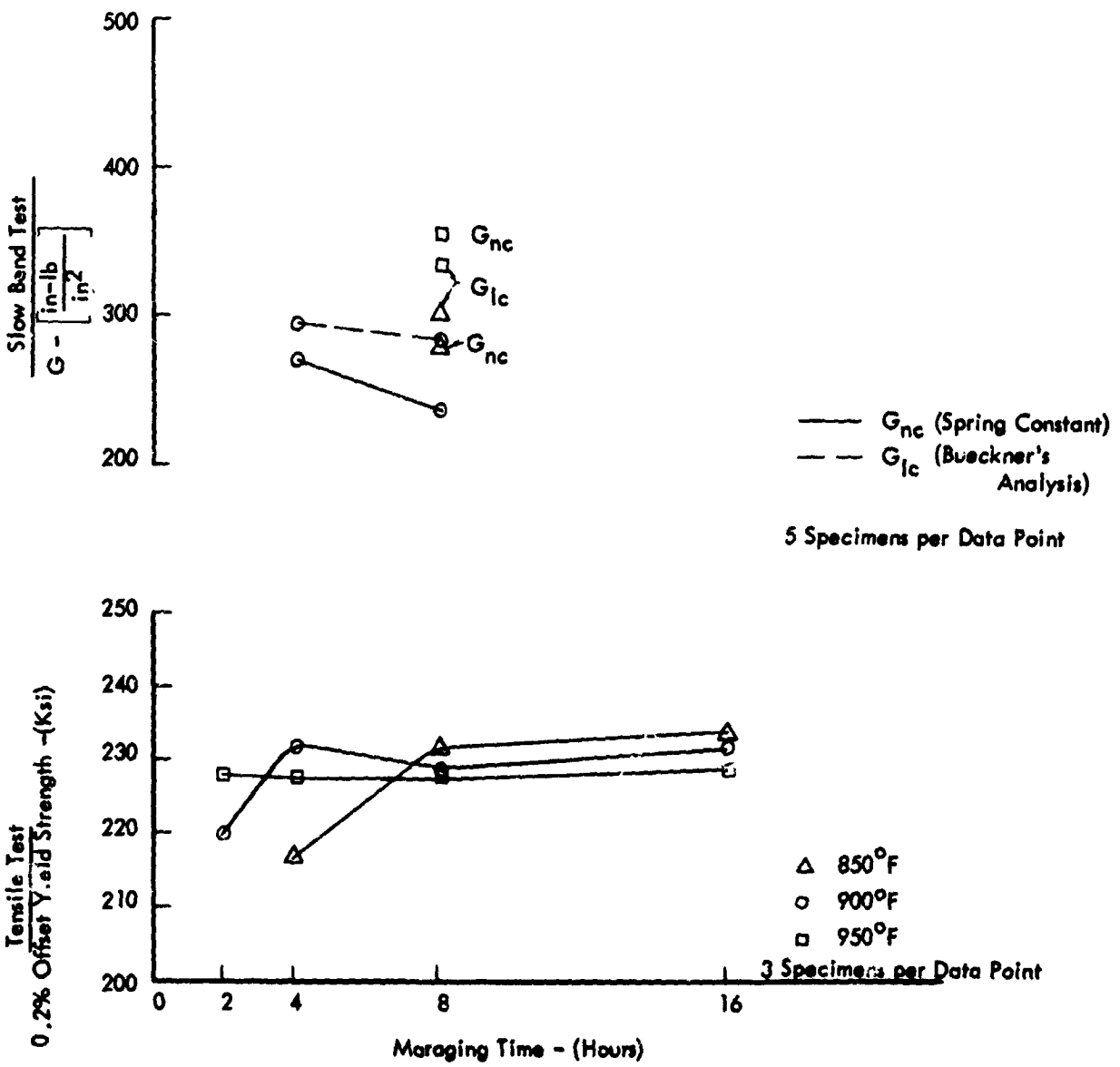

Plane-Strain Fracture Toughness and Yield Strength vs Maraging Time for Lukens Plate, Heat R-599-1 Transverse Test Specimens

Figure 28

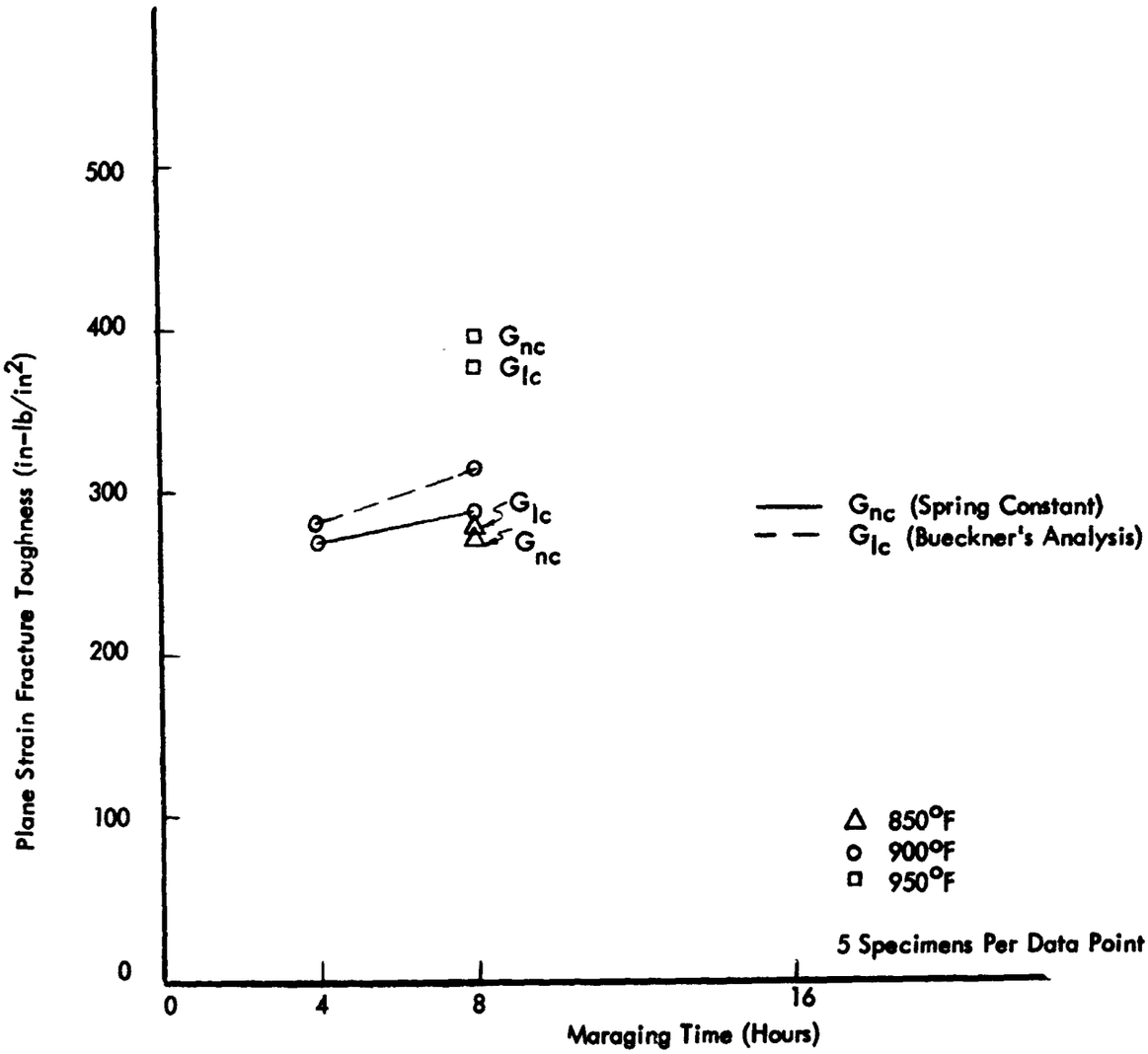

Plane-Strain Fracture Toughness and Yield Strength vs Maraging Time for Lukens Plate, Heat R-599-1 Transverse Test Specimens

Figure 29

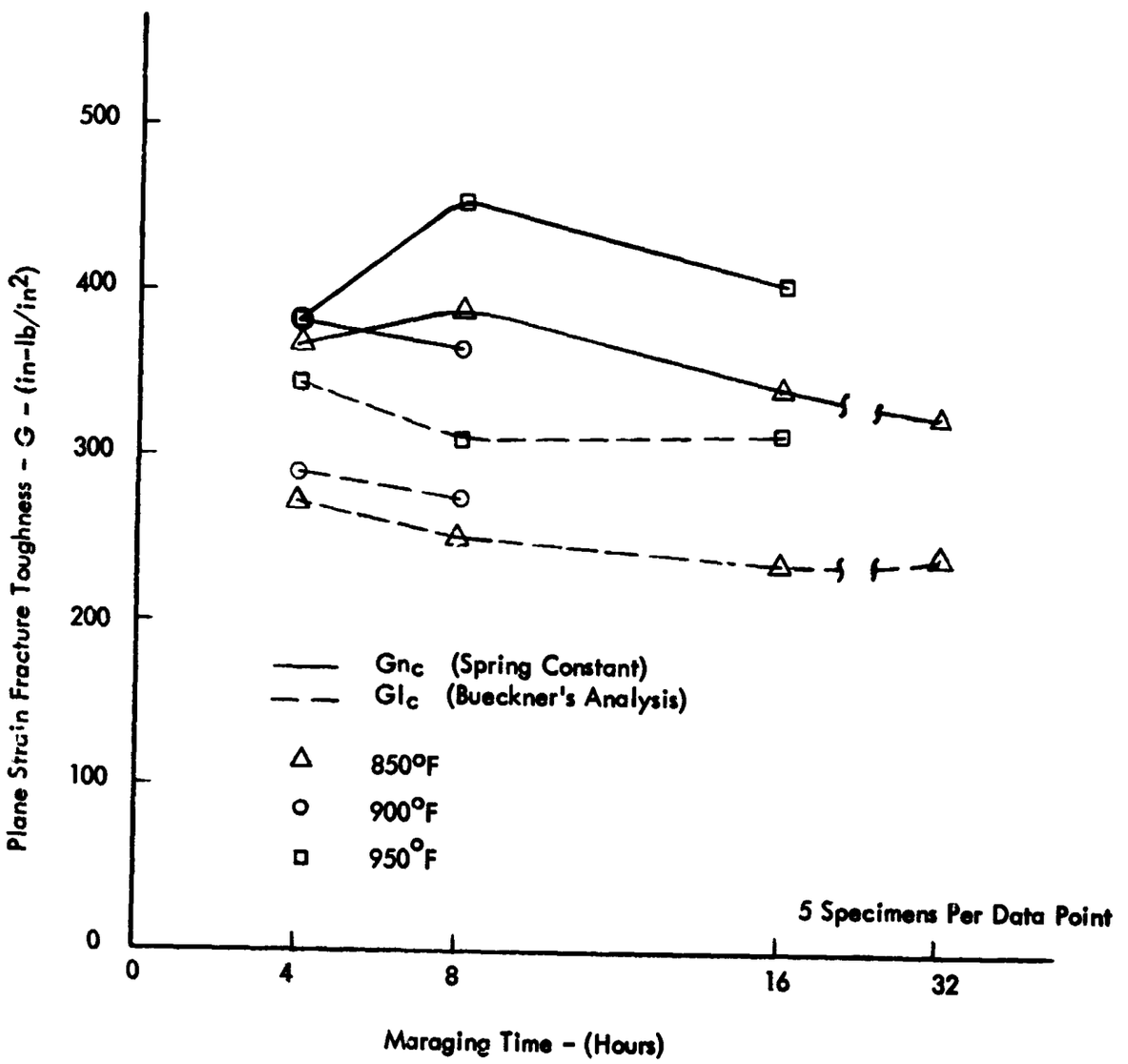

Plane-Strain Fracture Toughness vs Maraging Time for Lukens Plate, Heat R-599-1 Short Transverse Test Specimens

Figure 30

Heat No.	Plate Size, inches	Solution Annealing Temperature, °F	Aging Cycle Temperature, °F	Aging Cycle Time, hours	Orientation	Location	0.2% Offset Yield Strength ksi	Ultimate Tensile Strength ksi	Elongation in 1 Inch %	Reduction in Area %
25000-1	0.610x103x209	1500	890	4	Longitudinal	Top	216	226	11	51
					Transverse	Top	239	243	9	46
					Longitudinal	Bottom	223	228	11	53
					Transverse	Bottom	243	244	10	48
		1650			Longitudinal		216	222	10	47
					Transverse		223	229	10	51
25000-6B	0.410x85x360	1500	890	4	Longitudinal	Bottom	220	227	11	55
					Transverse	Bottom	236	244	10	47
		1650			Longitudinal		215	221	12	57
					Transverse		221	228	12	50
24998-1	0.610x80x440	1500	890	4	Longitudinal	Bottom	228	235	11	55
					Transverse	Bottom	235	242	10	46
		1650			Longitudinal		220	227	11	54
					Transverse		222	230	11	49
25000-6A	0.410x85x360	1500	890	4	Longitudinal	Top	226	232	12	57
					Transverse	Top	239	244	9	44
					Longitudinal	Middle	224	230	11	55
					Transverse	Middle	240	244	11	48
		1650			Longitudinal		209	220	12	-
					Transverse		218	225	11	-
25050-1	0.410x45x360	1500	890	4	Longitudinal		237	244	12	50
					Transverse		239	244	10	43
		1650			Longitudinal		217	224	11	46
					Transverse		220	228	11	46
25050-1A	0.410x85x360	1500	890	4	Longitudinal		233	239	13	54
					Transverse		236	243	12	49
		1650			Longitudinal		213	223	13	47
					Transverse		216	226	12	47
25064-1 (2)	0.410x80x414	1500	890	4	Longitudinal		218	232	13	-
					Transverse		239	245	12	-
		1600			Longitudinal		212	223	13	-
					Transverse		229	238	10	-
		1650			Longitudinal		211	224	13	-
					Transverse		221	234	11	-

(1) Each set of data represents the average of three tensile determinations
(2) Results reported are pilot test results with two tensile determinations made per data point

Allegheny Ludlum Comparison of Tensile Properties on Solution Annealing at 1500°F and Resolution Annealing at 1650°F

Figure 31

Heat No.	Plate Size, inches	Solution Annealing Temperature, °F	Aging Cycle Temperature, °F	Aging Cycle Time, hours	Orientation	Location	0.2% Offset Yield Strength ksi	Ultimate Tensile Strength ksi	Elongation in 1 Inch %	Reduction in Area %
25007-1	0.610x80x414	1500	890	4	Longitudinal	Bottom	219	227	10	51
					Transverse	Bottom	225	234	11	47
					Longitudinal	Middle	222	232	12	53
					Transverse	Middle	229	237	11	47
					Longitudinal	Top	222	232	12	53
					Transverse	Top	229	237	11	47
24996-1A	0.610x103x431	1500	890	4	Longitudinal		225	231	11	52
					Transverse		227	235	10	47
24999-1A	0.610x103x431	1500	890	4	Longitudinal		221	225	10	57
					Transverse		229	233	11	48
24999-1	0.510x48x431	1500	890	4	Longitudinal		220	223	12	56
					Transverse		225	230	12	50
24997-1A	0.610x103x431	1500	890	4	Longitudinal		223	230	11	56
					Transverse		225	232	10	49
24996-1	0.410x85x360	1500	890	4	Longitudinal		227	232	12	51
					Transverse		233	240	10	44

* NOTE: Each set of data represents the average of three tensile determinations

Allegheny Ludlum Comparison of Tensile Properties on Solution Annealing at 1500°F

Figure 32

Heat No.	Plate Size, Inches	Solution Annealing Temperature, °F	Aging Cycle Temperature, °F	Aging Cycle Time, Hours	Orientation	Plate Location	0.2% Offset Yield Strength ksi	Ultimate Tensile Strength ksi	Elongation in 1 inch %	Reduction in Area %
25000-1	0.610x103x209	1600	900	4	Longitudinal	Top	216	223	11	49
		1650			Longitudinal	Top	217	225	12	54
		1700			Longitudinal	Top	219	226	12	55
		1600			Transverse	Top	222	231	10	47
		1650			Transverse	Top	220	230	10	46
		1700			Transverse	Top	220	231	10	46
24998-1	0.610x80x440	1600	900	4	Longitudinal	Bottom	219	230	12	55
		1650			Longitudinal	Bottom	218	227	11	55
		1700			Longitudinal	Bottom	221	229	11	55
		1600			Transverse	Bottom	221	229	13	48
		1650			Transverse	Bottom	227	234	10	48
		1700			Transverse	Bottom	223	232	10	48
25000-6A	0.410x85x360	1600	900	4	Longitudinal	Top	219	228	12	55
		1650			Longitudinal	Top	219	227	11	55
		1700			Longitudinal	Top	221	229	11	53
		1600			Transverse	Top	226	235	12	46
		1650			Transverse	Top	229	235	10	48
		1700			Transverse	Top	227	234	10	48
25000-6B	0.410x85x360	1600	900	4	Longitudinal	Top	219	226	11	55
		1650			Longitudinal	Top	220	228	12	56
		1700			Longitudinal	Top	219	229	11	55
		1600			Transverse	Top	222	229	11	48
		1650			Transverse	Top	225	233	10	50
		1700			Transverse	Top	225	234	10	50

* Each set of data represents average data from three tensile specimens

Resolution Annealing Evaluation, Tensile Property Data Taken From Four Allegheny Plates Initially Solution Treated at 1500°F

Figure 33

Plate	Designation	Aging Cycle Temperature, °F	Aging Cycle Time, hours	Reannealing Temperature, °F	Orientation	0.2% Offset Yield Strength, ksi	W/A in-lb/in^2 at Room Temp. Except as Noted*
24998-1	IL201	900	4	1600	Longitudinal	219	* 602
	IL202	900	4	1600	Longitudinal		590
	IL203	900	4	1600	Longitudinal		589
							593 Average
25000-6A	IL210	900	4	1600	Longitudinal	219	* 496
	IL211	900	4	1600	Longitudinal		517
	IL212	900	4	1600	Longitudinal		525
							513 Average
25000-1	IL219	900	4	1600	Longitudinal	216	* 652
	IL220	900	4	1600	Longitudinal		630
	IL221	900	4	1600	Longitudinal		639
							640 Average
25000-6B	IL228	900	4	1600	Longitudinal	219	* 588
	IL229	900	4	1600	Longitudinal		561
	IL230	900	4	1600	Longitudinal		568
							572 Average
24998-1	IL204	900	4	1650	Longitudinal	218	826
	IL205	900	4	1650	Longitudinal		906
	IL206	900	4	1650	Longitudinal		839
							857 Average
25000-6A	IL213	900	4	1650	Longitudinal	219	576
	IL214	900	4	1650	Longitudinal		575
	IL215	900	4	1650	Longitudinal		544
							565 Average
25000-1	IL222	900	4	1650	Longitudinal	217	811
	IL223	900	4	1650	Longitudinal		843
	IL224	900	4	1650	Longitudinal		891
							848 Average
25000-6B	IL231	900	4	1650	Longitudinal	220	652
	IL232	900	4	1650	Longitudinal		665
	IL245	900	4	1650	Longitudinal		603
							640 Average
24998-1	IL207	900	4	1700	Longitudinal	221	763
	IL208	900	4	1700	Longitudinal		788
	IL209	900	4	1700	Longitudinal		783
							778 Average
25000-6A	IL216	900	4	1700	Longitudinal	221	525
	IL217	900	4	1700	Longitudinal		356
	IL218	900	4	1700	Longitudinal		557
							479 Average
25000-1	IL225	900	4	1700	Longitudinal	219	805
	IL226	900	4	1700	Longitudinal		819
	IL227	900	4	1700	Longitudinal		843
							822 Average
25000-6B	IL246	900	4	1700	Longitudinal	219	595
	IL247	900	4	1700	Longitudinal		649
	IL248	900	4	1700	Longitudinal		594
							613 Average

* NOTE: Temperature was -40°F

W/A Values from Impact Specimens from Crop Ends of Four Allegheny Ludlum Plates; Specimens Re-Annealed at 1600°F, and 1700°F

Figure 34

Designation	Aging Cycle Temperature, °F	Aging Cycle Time, hours	Orientation	Specimen Width, inch	W/A in-lb/in^2 -40°F	W/A in-lb/in^2 Room Temp.	W/A in-lb/in^2 + 200°F
IL291	900	4	Longitudinal	0.598		846	
IL292	900	4	Longitudinal	0.598		808	
IL293	900	4	Longitudinal	0.598		782	
IL294	900	4	Longitudinal	0.598		851	
IL295	900	4	Longitudinal	0.598		1090	
						875 Avg.	
IL296	900	8	Longitudinal	0.598		822	
IL297	900	8	Longitudinal	0.598		928	
IL298	900	8	Longitudinal	0.598		861	
IL299	900	8	Longitudinal	0.598		869	
IL300	900	8	Longitudinal	0.598		940	
						884 Avg.	
IL311	900	4	Longitudinal	0.395		865	
IL312	900	4	Longitudinal	0.395		792	
IL313	900	4	Longitudinal	0.395		841	
IL314	900	4	Longitudinal	0.394		777	
IL315	900	4	Longitudinal	0.395		753	
						806 Avg.	
IL316	900	8	Longitudinal	0.395		812	
IL317	900	8	Longitudinal	0.395		837	
IL318	900	8	Longitudinal	0.395		989	
IL319	900	8	Longitudinal	0.395		852	
IL320	900	8	Longitudinal	0.394		825	
						863 Avg.	
IL281	900	4	Longitudinal	0.598	808		
IL282	900	4	Longitudinal	0.598	769		
IL283	900	4	Longitudinal	0.598	940		
IL284	900	4	Longitudinal	0.598	774		
IL285	900	4	Longitudinal	0.598	683		
					795 Avg.		
IL301	900	4	Longitudinal	0.395	664		
IL302	900	4	Longitudinal	0.395	723		
IL303	900	4	Longitudinal	0.395	718		
IL304	900	4	Longitudinal	0.395	667		
IL305	900	4	Longitudinal	0.395	713		
					697 Avg.		
IL286	900	4	Longitudinal	0.598			1003
IL287	900	4	Longitudinal	0.599			915
IL288	900	4	Longitudinal	0.598			1121
IL289	900	4	Longitudinal	0.599			876
IL290	900	4	Longitudinal	0.598			1164
							1016 Avg.
IL306	900	4	Longitudinal	0.394			957
IL307	900	4	Longitudinal	0.395			884
IL308	900	4	Longitudinal	0.394			889
IL309	900	4	Longitudinal	0.394			971
IL310	900	4	Longitudinal	0.394			980
							936 Avg.

The Effects of Specimen Width on W/A Values, Allegheny Ludlum Plate 25000-1; All Specimens Re-Annealed at 1650°F

Figure 35

Heat No.	Plate Size, Inches	Solution Annealing Temperature, °F	Aging Cycle Temperature, °F	Aging Cycle Time, hours	Orientation	Plate Location	0.2% Offset Yield Strength ksi	Ultimate Tensile Strength ksi	Elongation in 1 Inch %	Reduction in Area %
3920781	0.410x75x250	1500	890	4	Transverse	Bottom	227	233	10	52
		1500			Transverse	Top	234	237	9	50
		1500			Longitudinal	Bottom	217	223	12	59
		1500			Longitudinal	Top	218	223	11	58
		1650			Transverse	Bottom	219	224	11	51
		1650			Transverse	Top	212	218	12	59
		1650			Longitudinal	Bottom	214	218	12	55
		1650			Longitudinal	Top	212	217	12	59
3920778	0.410x85x360	1500	890	4	Transverse	Bottom	227	234	10	54
		1500			Transverse	Top	242	244	9	53
		1500			Longitudinal	Bottom	217	225	11	58
		1500			Longitudinal	Top	227	231	10	57
		1650			Transverse	Bottom	216	225	11	51
		1650			Transverse	Top	212	221	12	54
		1650			Longitudinal	Bottom	212	220	12	55
		1650			Longitudinal	Top	209	217	13	59
3930771	0.410x85x360	1500	890	4	Transverse	Bottom	232	238	10	54
		1500			Transverse	Top	229	235	10	53
		1500			Longitudinal	Bottom	215	221	11	60
		1500			Longitudinal	Top	217	225	11	57
		1650			Transverse	Bottom	218	223	11	52
		1650			Transverse	Top	213	220	11	54
		1650			Longitudinal	Bottom	215	219	12	58
		1650			Longitudinal	Top	207	215	13	61
3951215	0.610x80x414	1650	890	4	Transverse	Top	206	216	12	56
		1650			Longitudinal	Top	208	215	12	58
		1650			Transverse	Bottom	205	213	12	57
		1650			Longitudinal	Bottom	204	212	12	59

* Each set of data represents the average of three tensile determinations

Comparison of Tensile Properties of Republic Plates
Solution Annealed at 1500°F and Resolution Annealed at 1650°F

Figure 36

Heat No.	Plate Size, Inches	Solution Annealing Temperature, °F	Aging Cycle Temperature, °F	Aging Cycle Time, Hours	Orientation	0.2% Offset Yield Strength Ksi	Ultimate Tensile Strength Ksi	Elongation in 1 inch %	Reduction in Area %
3951218A	0.610 x 104 x 431	1650	890	4	Longitudinal	* 210	220	12	57
		1675			Longitudinal	208	220	12	57
		1700			Longitudinal	212	223	12	57
		1650			Transverse	213	225	11	52
		1675			Transverse	215	225	12	52
		1700			Transverse	216	227	11	52
39608298	0.610 x 104 x 431	1650	890	4	Longitudinal	212	224	13	58
		1675			Longitudinal	211	223	13	60
		1700			Longitudinal	216	226	12	59
		1650			Transverse	220	233	12	56
		1675			Transverse	220	231	12	56
		1700			Transverse	220	231	12	56
39608278	0.610 x 104 x 431	1650	890	4	Longitudinal	210	222	12	56
		1675			Longitudinal	212	223	12	57
		1700			Longitudinal	213	224	12	58
		1650			Transverse	216	227	11	56
		1675			Transverse	219	227	11	54
		1700			Transverse	221	228	12	56
39608328	0.610 x 104 x 431	1650	890	4	Longitudinal	215	222	12	58
		1675			Longitudinal	217	224	12	60
		1700			Longitudinal	217	225	12	58
		1650			Transverse	218	226	10	53
		1675			Transverse	219	228	11	55
		1700			Transverse	221	230	12	56
39608198	0.610 x 104 x 431	1650	890	4	Longitudinal	207	216	12	57
		1675			Longitudinal	209	217	12	59
		1700			Longitudinal	213	219	11	58
		1650			Transverse	214	221	11	54
		1675			Transverse	215	222	11	54
		1700			Transverse	212	223	11	53
39608298	0.710 x 87 x 431	1650	890	4	Longitudinal	214	230	12	59
		1675			Longitudinal	212	224	12	58
		1700			Longitudinal	216	228	12	59
		1650			Transverse	218	229	11	55
		1675			Transverse	217	229	12	55
		1700			Transverse	220	232	11	55
39512198	0.710 x 87 x 431	1650	890	4	Longitudinal	205	215	11	62
		1675			Longitudinal	205	215	12	60
		1700			Longitudinal	206	216	12	62
		1650			Transverse	206	216	10	55
		1675			Transverse	208	218	10	53
		1700			Transverse	208	218	10	52

* Each set of data represents average data from two tensile specimens taken from top and bottom of each plate

Preliminary Tensile Property Data Taken from Seven Republic Plates Before Solution Annealing

Figure 37

Heat No.		1500°F RXN	1500°F Gr. Size	1550°F RXN	1550°F Gr. Size	1600°F RXN	1600°F Gr. Size	1650°F RXN	1650°F Gr. Size	1700°F RXN	1700°F Gr. Size	1750°F RXN	1750°F Gr. Size
3960832A	(T)	No	NR	No	NR	50-70%	7 - 8	90-100%	7 - 8	100%	6 - 8	100%	6 - 7
	(B)	No	NR	No	NR	50-70	7 - 8	90-100	7 - 8	100	6 - 8	100	6 - 8
3960827B	(T)	No	NR	No	NR	60-80	7 - 8	90-100	6 - 8	100	6 - 8	100	6 - 8
	(B)	No	NR	No	NR	60-80	7 - 8	90-100	6 - 8	100	6 - 8	100	6 - 8
3960819B	(T)	No	NR	No	NR	50-70	7 - 8	90-100	8	100	6 - 8	100	7
	(B)	No	NR	No	NR	50-70	7 - 8	90-100	7 - 8	100	6 - 8	100	5 - 7
3951219B	(T)	No	NR	No	NR	60-80	7 - 8	90-100	6 - 8	100	7	100	7
	(B)	No	NR	No	NR	60-80	7 - 8	90-100	6 - 8	100	7	100	7
3951218A	(T)	No	NR	No	NR	60	7 - 8	90-100	6 - 8	100	7	100	6 - 7
	(B)	No	NR	No	NR	60	7 - 8	90-100	6 - 8	100	7	100	6 - 7
3960829A	(T)	No	NR	No	NR	50-70	7 - 8	90-100	7 - 8	100	7	100	6 - 7
	(B)	No	NR	No	NR	50-70	7 - 8	90-100	7 - 8	100	7	100	6 - 7
3960829B	(T)	No	NR	No	NR	60-80	7 - 8	90-100	6 - 8	100	6 - 8	100	6 - 8
	(B)	No	NR	No	NR	60-80	7 - 8	90-100	6 - 8	100	6 - 8	100	6 - 8

RXN = Percent Recrystallization

NR = Non-Rateable

Effect of Solution-Annealing Temperature on Grain Size and Re-Crystallization on Seven Republic Plates; Performed Before Annealing

Figure 38

Heat No.	Plate Size, Inches	Solution Annealing Temperature, °F	Aging Cycle Temperature, °F	Aging Cycle Time, hours	Orientation	Plate Location	0.2% Offset Yield Strength ksi	Ultimate Tensile Strength ksi	Elongation in 1 Inch %	Reduction in Area %
50210-2	1.500x125x190	1500	890	4	Transverse	Top	* 208	217	13	52
					Longitudinal	Top	204	214	14	54
		1600			Transverse	Top	209	219	13	51
					Longitudinal	Top	208	216	13	52
		1700			Transverse	Top	212	223	13	52
					Longitudinal	Top	209	220	13	52
		1800			Transverse	Top	207	219	13	55
					Longitudinal	Top	205	217	14	55
50210-1	1.500x125x190	1500	890	4	Transverse	Top	203	213	13	53
					Longitudinal	Top	201	210	13	53
		1600			Transverse	Top	203	213	13	53
					Longitudinal	Top	201	212	13	51
		1700			Transverse	Top	212	222	13	49
					Longitudinal	Top	209	219	13	51
		1800			Transverse	Top	203	215	14	53
					Longitudinal	Top	204	214	13	54
50187-1	1.500x125x190	1500	890	4	Transverse	Top	224	232	13	54
					Longitudinal	Top	218	225	13	54
		1600			Transverse	Top	221	229	13	51
					Longitudinal	Top	218	225	13	52
		1700			Transverse	Top	214	224	13	53
					Longitudinal	Top	211	220	13	55
		1800			Transverse	Top	216	226	13	54
					Longitudinal	Top	213	224	13	54

* Each set of data represents the average of two tensile determinations

Solution Annealing Evaluation Tensile Property Data Taken From Three Cameron Plates Before Solution Annealing

Figure 39

Heat No.	Plate Size, Inches	Solution Annealing Temperature, °F	Aging Cycle Temperature, °F	Aging Cycle Time, Hours	Orientation	Plate Location	0.2% Offset Yield Strength ksi	Ultimate Tensile Strength ksi	Elongation in 1 inch %	Reduction in Area %
50210-2	1.500x125x190	1650/1700	890	4	Transverse	Top	211	221	13	53
					Longitudinal	Top	211	220	13	52
50210-1	1.500x125x190	1650/1700	890	4	Transverse	Top	212	220	12	52
					Longitudinal	Top	210	219	13	54
50187-1	1.500x125x190	1650/1700	890	4	Transverse	Top	216	224	12	53
					Longitudinal	Top	215	222	13	52

* Each set of data represents the average of three tensile determinations

Acceptance Tensile Property Data on Cameron Plates

Figure 40

Element	AGC-34316 (Limits)	Slab Section
C	0.03	0.02
Mn	0.10	0.07
P	0.025	0.008
S	0.010	0.007
Si	0.10	0.08
Ni	17.50/19.00	18.11
Mo	4.00/4.50	4.25
Co	7.00/8.00	7.82
Ti	0.05/0.25	0.17
Al	0.05/0.15	0.07

Test Methods:

C	Conductometric
Mn, Ni, Mo, Co, Ti	X-ray Spectrograph
P, Si, Al	Wet Procedure
S	Combustion

Chemical Analysis of Lukens Heat R-559

Figure 41

Original Billet Section Size, inches	Forged Test Bar Size, inches	Orientation	0.2% Offset Yield Strength ksi	Ultimate Tensile Strength ksi	Elongation in 1 inch %	Reduction in Area %
3 (Square)	1-1/8	Longitudinal (50 inches Length)	238	240	12	58
3 (Square)	1-1/8	Longitudinal (50 inches Length)	233	238	12	57
3 x 2	1-1/8	Transverse (28 inches Width)	237	240	12	59
3 x 2	1-1/8	Transverse (28 inches Width)	236	238	11	55
3 x 2	1-1/8	Short Transverse (10 inches Thick)	234	237	11	58
3 x 2	1-1/8	Short Transverse (10 inches Thick)	235	239	12	57

Tensile Test Results of Specimens Removed from Forged Test Bars

Figure 42

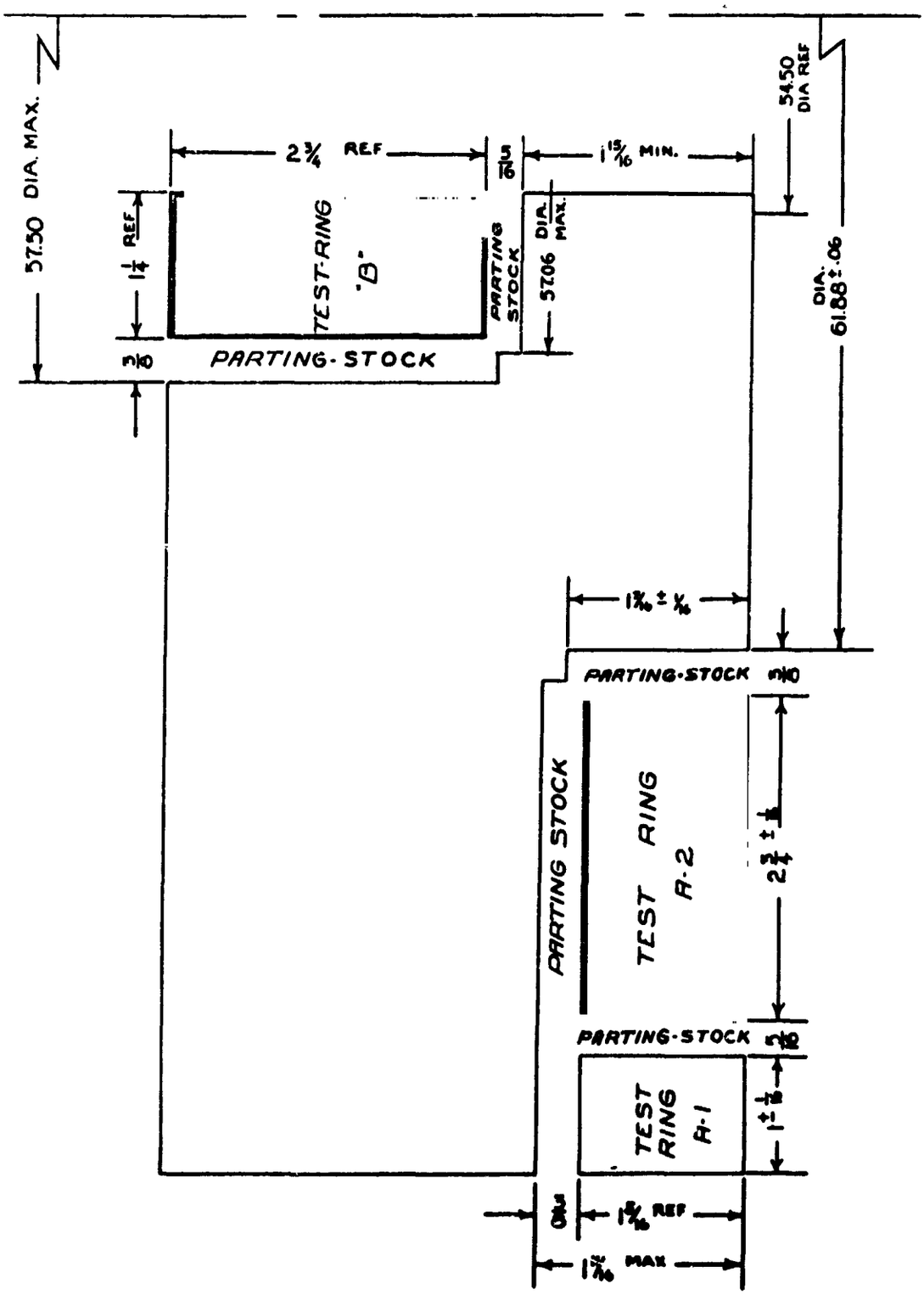

Test Ring Locations

Figure 43

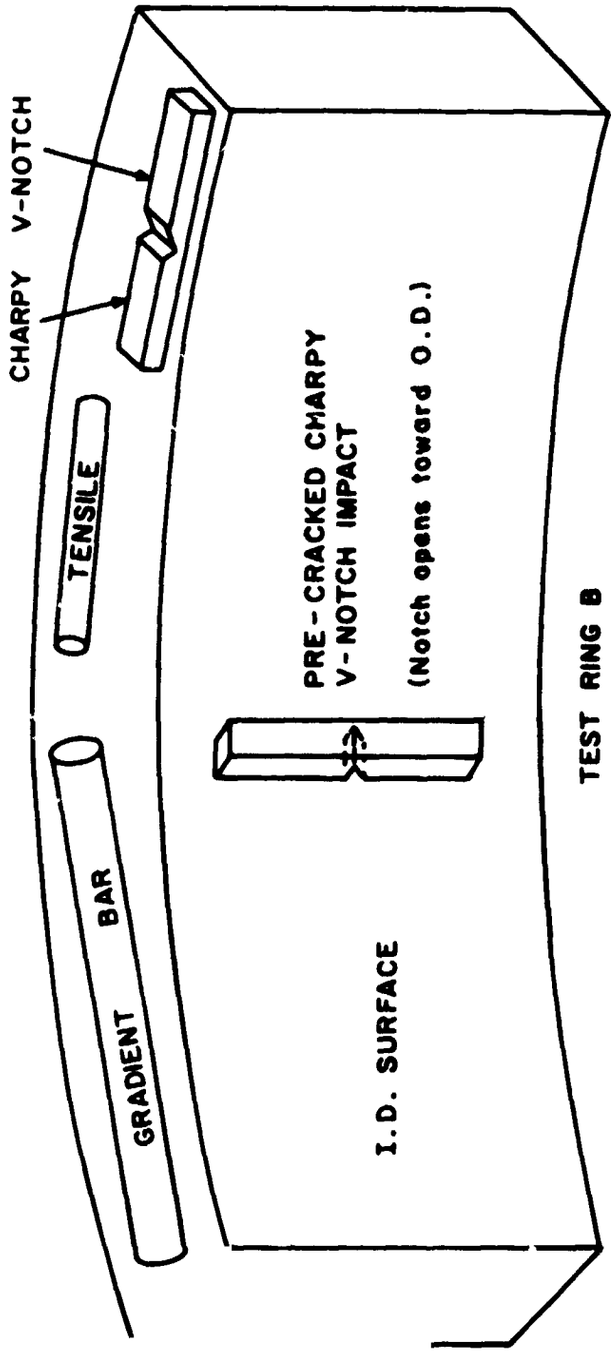

Test Specimen Orientation

Figure 44

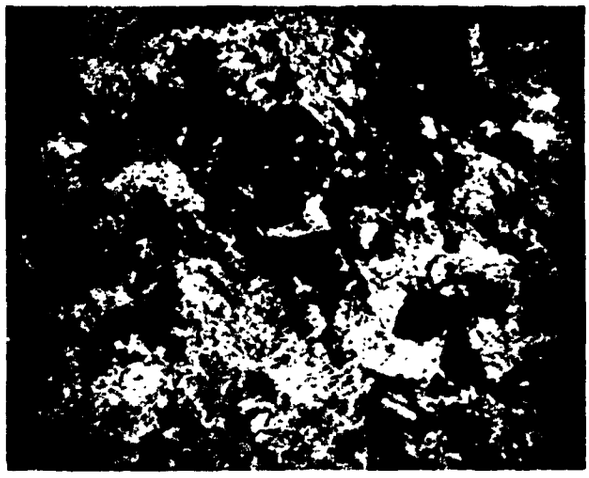

1100°F

1200°F

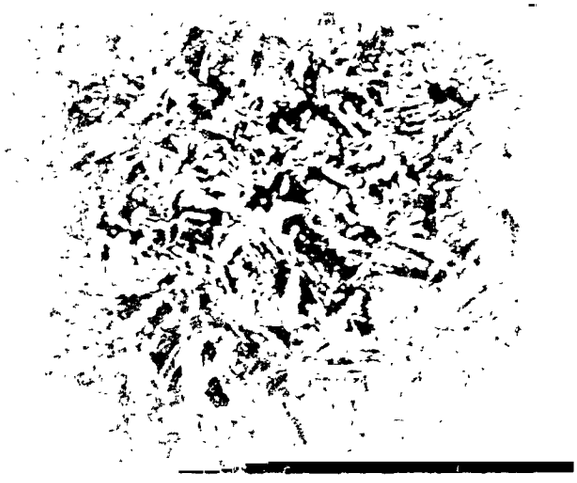

1500°F

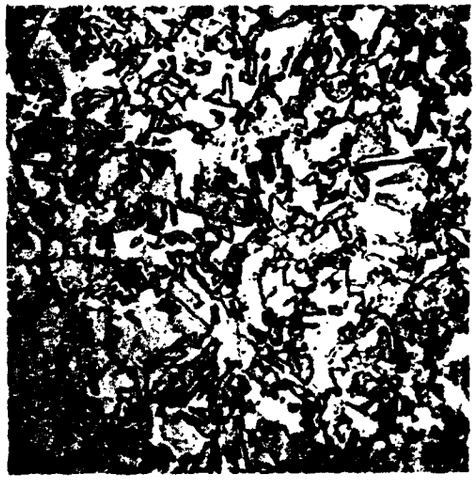

1600°F

1900°F

2000°F

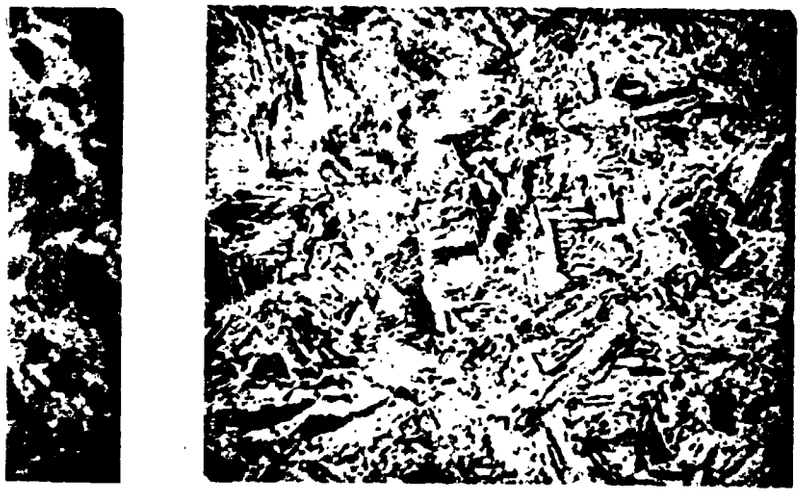

1300°F

1400°F

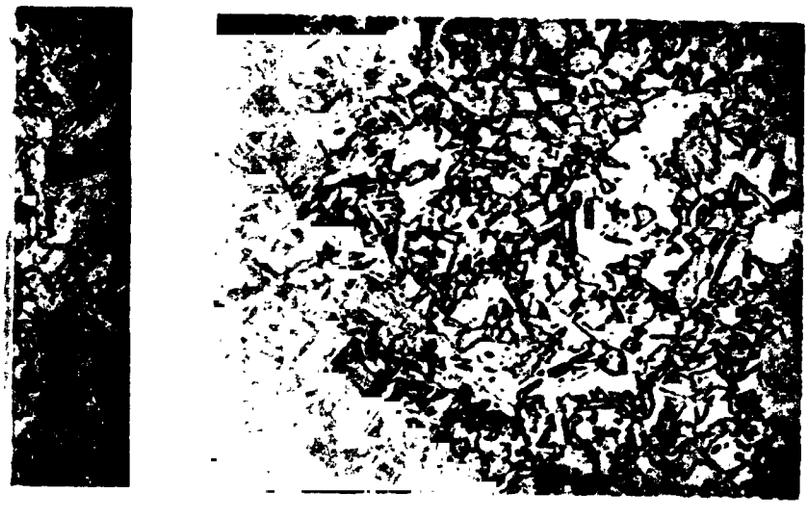

1700°F

1800°F

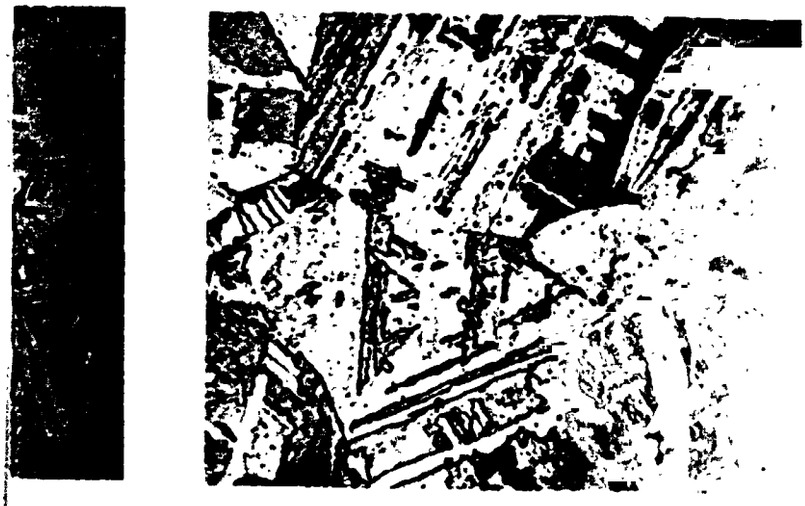

2100°F

Gradient Bar Microstructures, Magnification 100X

Figure 45

Solution Annealing Temperature °F	0.2% Offset Yield Strength ksi	Ultimate Tensile Strength ksi	Elongation in 1 Inch %	Reduction in Area %	Precracked Charpy W/A @ Room Temperature in-psi	Charpy V-Notch Impact ft-lb
1500	219.8	228.8	12	58	778	30.0
	221.2	228.8	12	58	731	30.5
					749	
1600	208.5	218.8	12	59	927	37.0
	208.1	218.8	13	61	1023	36.0
					1084	
1700	211.8	222.3	12	59	945	35.0
	211.3	222.2	12	61	936	37.0
					974	
1800	195.7	217.8	14	60	1026	40.0
	186.9	217.3	15	61	923	41.0
	199.3	219.0	13	62	933	
	201.7	224.6	12	61		
1900	214.9	227.4	13	60		33.5
	216.1	228.6	12	60		35.0
	199.1	221.4	12	61		
	198.5	220.0	13	62		

Notes:

1. Test ring machined from as-rolled ring. Test specimens cut from ring, solution annealed 5 hours at temperature indicated, and then air cooled. Aged 4 hours at 890°F, air cooled, finish machined, and tested.
2. Tensile specimens were 0.252-inch diameter x 1-inch gage length; Charpy V-notch and precracked Charpy V-notch impact specimens were 0.394-inch square; precracked Charpy V-notch impact specimens were precracked and tested at Manlabs, Inc.

Mechanical Property Data for Various Solution Annealing Temperatures

Figure 46

Aging Cycle Temperature, °F	Aging Cycle Time, hours	0.2% Offset Yield Strength ksi	Ultimate Tensile Strength, ksi	Elongation in 1 Inch %	Reduction in Area %
890	4	210.3	221.3	12	59
		209.5	221.2	12	60
		209.6	221.0	12	58
890	8	220.6	231.8	12	58
		221.3	231.9	12	58
		220.8	231.1	12	57
950	8	210.7	224.5	13	55
		210.5	225.0	13	57
		209.9	224.5	14	56
850	8	216.0	227.7	12	59
		213.8	226.6	13	60
		214.8	226.6	12	59
850	16	228.3	239.6	11	58
		228.3	239.2	12	57
		228.1	239.0	12	57

Test specimens from test ring B after ring was solution heat treated with part at 1625°F for 3 hours.

Aging Response Evaluation

Figure 47

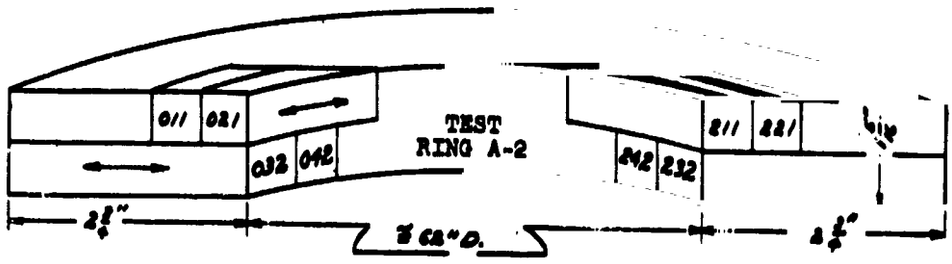

Test No.	0.2% Offset Yield Strength ksi	Ultimate Tensile Strength ksi	Elongation in 1 inch %	Reduction in Area %	Test No.	0.2% Offset Yield Strength ksi	Ultimate Tensile Strength ksi	Elongation in 1 inch %	Reduction in Area %
011	204.1	216.6	12	58	211	206.3	223.2	13	60
021	203.3	219.0	12	55	221	204.1	223.3	12	59
032	208.4	218.4	10	52	232	210.5	242.2	11	53
042	203.7	221.2	11	52	242	203.3	221.3	12	53

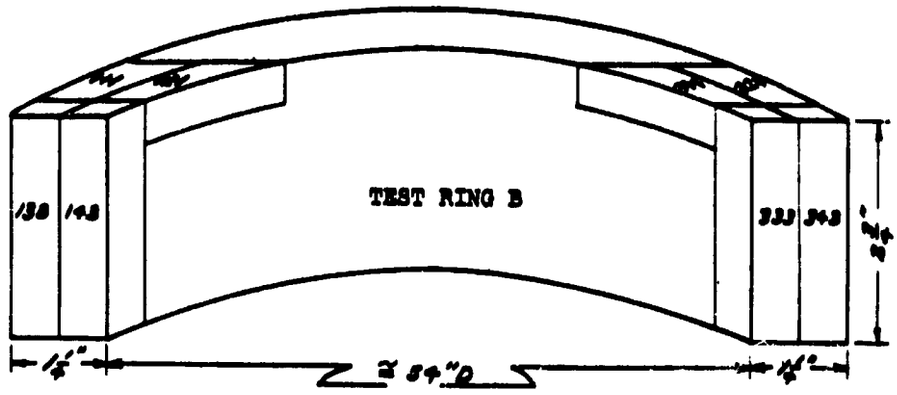

Test No.	0.2% Offset Yield Strength ksi	Ultimate Tensile Strength ksi	Elongation in 1 inch %	Reduction in Area %	Test No.	0.2% Offset Yield Strength ksi	Ultimate Tensile Strength ksi	Elongation in 1 inch %	Reduction in Area %
133	211.4	223.6	10	45	333	207.4	221.8	10	46
143	207.7	225.0	10	45	343	206.9	223.8	8	39
111	206.1	223.8	12	59	311	209.4	218.7	12	58
121	206.2	220.4	12	55	321	208.8	222.4	12	59

(0.252-inch Tensiles: 1625°F, 3 Hours, Air Cool Solution; 890°F, 4 Hours, Air Cool Age)

Room Temperature Tensile Results

Figure 48

-40°F TEST

Mark	T	DBN	E	CD	W/A (in-lb/in²)
401	0.393	0.317	5.00	0.050	572
411	0.393	0.317	6.31	0.020	649
421	0.393	0.315	5.11	0.025	538
502	0.393	0.317	4.91	0.029	520
512	0.394	0.316	6.92	0.015	609
522	0.394	0.317	5.55	0.015	560
603	0.394	0.316	4.61	0.020	474
613	0.393	0.315	4.68	0.020	485
623	0.393	0.314	4.65	0.017	478
703	0.393	0.313	5.31	0.020	554
713	0.393	0.315	5.02	0.021	522
723	0.393	0.315	4.61	0.025	485

TEST SPECIMEN ORIENTATION

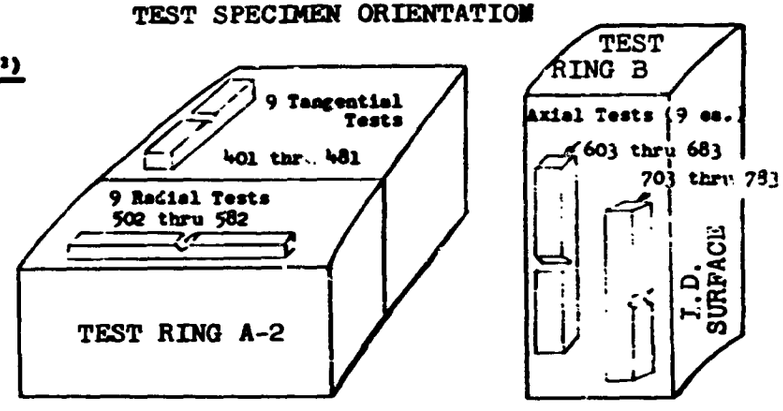

ROOM TEMPERATURE TEST

Mark	T	DBN	E	CD	W/A (in-lb/in²)
431	0.394	0.315	12.48	0.016	1271
441	0.393	0.316	11.30	0.015	1146
*451	0.394	0.316	6.15	0.092	836
532	0.394	0.315	9.71	0.013	979
542	0.394	0.316	8.68	0.016	881
552	0.393	0.316	8.46	0.018	866
633	0.394	0.315	6.37	0.024	666
643	0.393	0.316	7.09	0.020	732
653	0.393	0.314	5.68	0.020	590
733	0.393	0.316	7.22	0.019	742
743	0.393	0.317	7.34	0.020	755
753	0.393	0.317	7.86	0.015	795

*Note: Deep precrack caused smaller shear lips compared with similar specimens.

200°F TEST

Mark	T	DBN	E	CD	W/A (in-lb/in²)
461	0.393	0.313	13.97	0.016	1437
471	0.393	0.315	13.20	0.020	1367
*481	0.393	0.314	18.10	0.015	1849
562	0.394	0.315	9.19	0.030	982
572	0.394	0.313	9.02	0.022	944
582	0.394	0.314	9.39	0.025	989
663	0.394	0.315	6.86	0.100	977
673	0.394	0.316	7.98	0.019	818
683	0.394	0.314	7.69	0.020	797
763	0.393	0.313	7.52	0.100	1078
773	0.393	0.315	9.29	0.020	962
783	0.393	0.314	9.65	0.022	1009

*Note: No explanation for this high energy value.

LEGEND:
T = Specimen thickness-inches E = Energy — ft-lbs
DBN = Depth of specimen under notch-inches CD = Crack depth-inches

Precracked Charpy V-Notch Impact Test Results

Figure 49

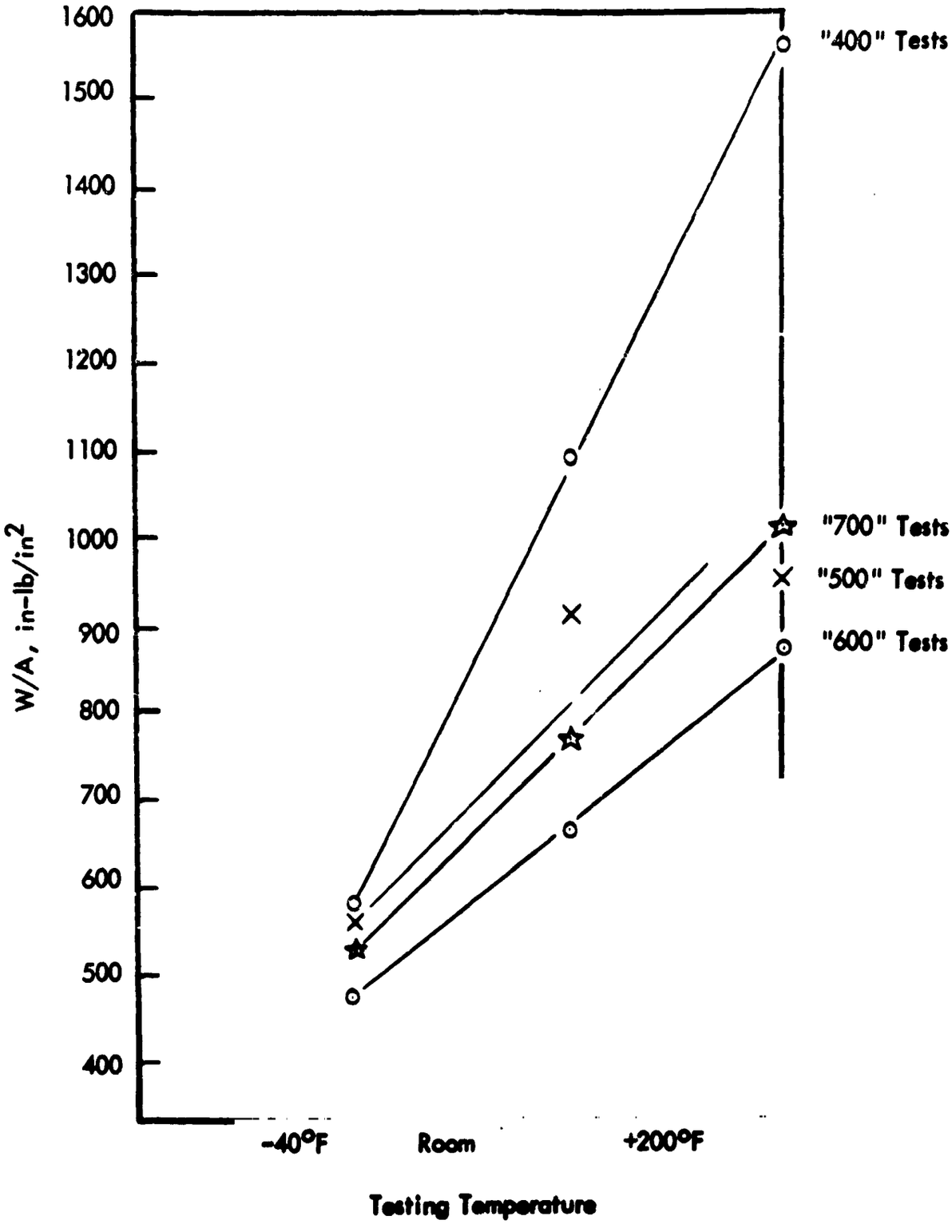

Precracked Impact Notch Toughness; Orientation and Test Temperature Effects

Figure 50

Element	AGC-34316 (Limits)	Billet
C	0.03	0.017
Mn	0.10	0.02
P	0.025	0.018
S	0.010	0.010
Si	0.10	0.02
Ni	17.50/19.00	18.20
Mo	4.00/4.50	4.45
Co	7.00/8.00	7.69
Ti	0.05/0.25	0.19
Al	0.05/0.15	0.09

Test Methods:

C	Conductometric
Mn, Ni, Mo, Co, Ti	X-ray Spectrograph
P, Si, Al	Wet Procedure
S	Combustion

Chemical Analysis of Allegheny Ludlum Heat 25005

Figure 51

TENSILE TEST DATA					PRECRACKED CHARPY V-NOTCH IMPACT DATA				
Solution Annealing Temperature °F	0.2% Offset Yield Strength ksi	Ultimate Tensile Strength ksi	Elongation in 1 Inch %	Reduction in Area %	Thickness Inches	Depth Below Notch Inch	Work ft-lb	Crack Depth Inch	W/A in-lb/in^2
1500	223.4	233.5	10	47	0.394	0.316	9.78	0.050	1120
	220.6	228.2	10	53	0.394	0.316	10.34	0.050	1184
	218.9	228.6	10	50	0.394	0.316	10.25	0.045	1152
1600	211.7	220.6	10	50	0.394	0.316	11.37	0.050	1302
	213.8	224.8	10	51	0.394	0.316	10.56	0.045	1187
	211.3	219.4	10	54	0.394	0.316	10.47	0.050	1199
1650	207.7	218.5	10	51	0.394	0.316	11.53	0.050	1320
	210.4	220.0	10	49	0.394	0.316	11.77	0.050	1348
	207.3	216.5	10	50	0.394	0.316	13.16	0.045	1479
1700	214.9	225.4	10	50	0.394	0.316	11.20	0.045	1258
	215.3	224.6	11	53	0.394	0.316	10.41	0.055	1215
	211.3	223.0	10	52	0.394	0.316	11.68	0.050	1337
1800	216.5	225.8	10	53	0.394	0.316	10.21	0.045	1147
	218.8	231.5	10	53	0.394	0.316	10.02	0.050	1147
	218.2	228.5	10	48	0.394	0.316	10.40	0.045	1169

All test specimens were annealed at indicated temperatures for 3 hours and air cooled, then aged at 890°F for 4 hours and air cooled. All specimens were tested at room temperature.

Solution Heat-Treating Evaluation, Intermediate Section

Figure 52

TENSILE TEST DATA					PRECRACKED CHARPY V-NOTCH IMPACT DATA				
Solution Annealing Temperature °F	0.2% Offset Yield Strength ksi	Ultimate Tensile Strength ksi	Elongation in 1 Inch %	Reduction in Area %	Thickness Inch	Depth Below Notch Inch	Work ft-lb	Crack Depth Inch	W/A in-lb/in^2
1500	219.9	228.3	10	46	0.393	0.314	8.11	0.030	872
	221.5	229.4	9	36	0.392	0.314	8.17	0.030	881
					0.392	0.314	7.78	0.035	853
1600	217.4	226.1	9	43	0.392	0.314	7.80	0.030	841
	216.7	228.1	10	45	0.392	0.314	6.68	0.030	720
					0.392	0.314	7.83	0.025	829
1650	212.6	222.2	10	44	0.392	0.314	8.46	0.037	935
	212.6	222.0	10	47	0.392	0.313	8.64	0.033	944
					0.392	0.313	9.35	0.035	1029
1700	215.8	225.2	10	41	0.392	0.314	8.88	0.025	941
	216.3	227.3	8	40	0.392	0.313	8.87	0.028	953
					0.392	0.314	8.89	0.035	975
1800	215.5	227.3	10	48	0.392	0.313	8.73	0.040	979
	215.1	225.2	10	48	0.392	0.314	9.10	0.042	1024
					0.392	0.313	8.14	0.035	896

All test specimens were annealed at indicated temperatures for 3 hours and air cooled, then aged at 890°F for 4 hours and air cooled. All specimens were tested at room temperature.

Solution Heat-Treating Evaluation, Exit Flange,

Figure 53

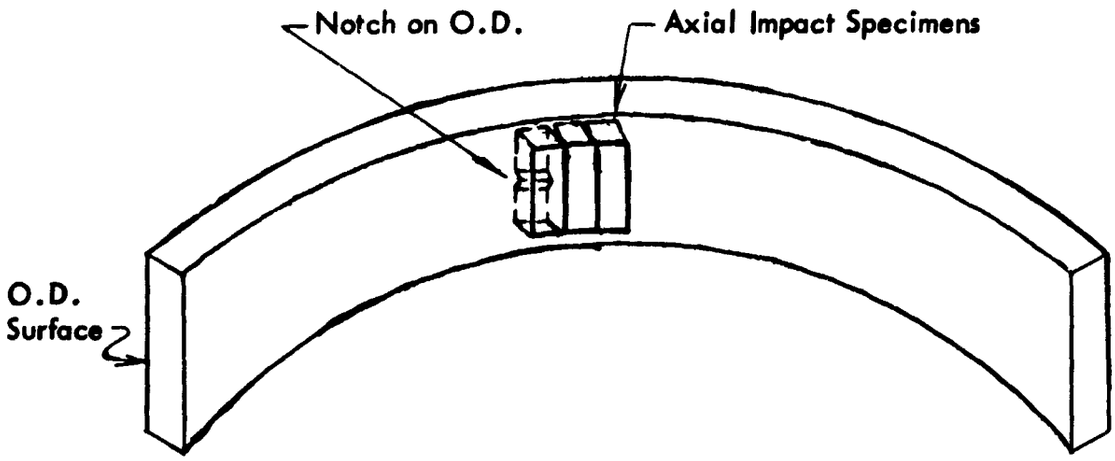

AXIAL FORGING TEST RING CFA

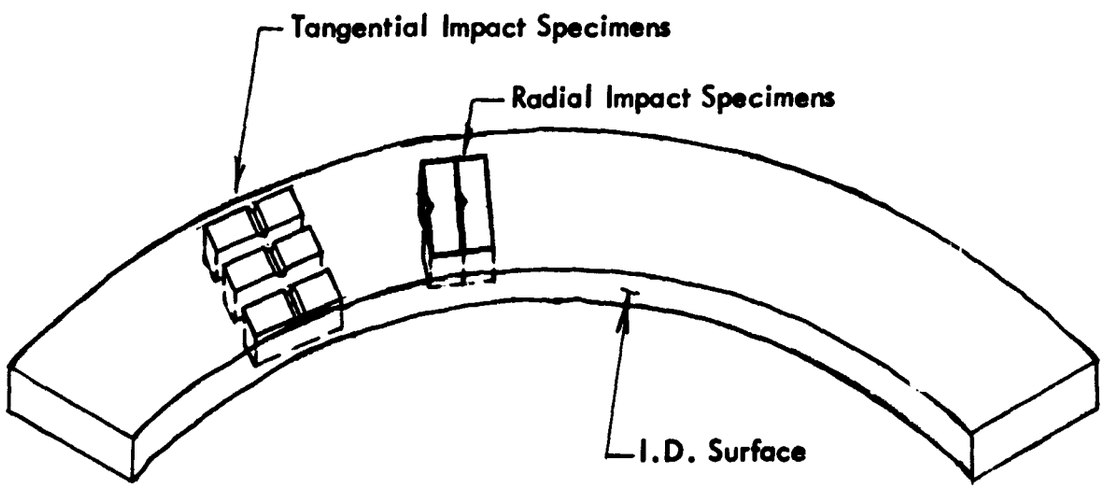

RADIAL FORGING TEST RING CFR

Axial Forging Test Ring CFA; Radial Forging Test Ring CFR

Figure 54

0° LOCATION							180° LOCATION						
Aging Cycle			0.2% Offset Yield Strength ksi	Ultimate Tensile Strength ksi	Elongation in 1 inch %	Reduction in Area %	Aging Cycle			0.2% Offset Yield Strength ksi	Ultimate Tensile Strength ksi	Elongation in 1 inch %	Reduction in Area %
Temperature, °F	Time, hours	Orientation					Temperature, °F	Time, hours	Orientation				
890	8	Tangential	221.1	229.5	9	45	890	4	Tangential	213.9	223.5	9	50
			222.4	230.8	9	47				213.8	223.9	1	54
			221.8	230.5	7	31				215.4	223.8	10	57
		Radial	223.2	231.2	8	34			Radial	203.7	217.3	10	48
			222.8	233.6	7	32				204.9	217.9	10	39
			222.2	230.8	7	29				205.5	216.9	10	49
		Axial	225.0	231.8	8	39			Axial	218.1	225.5	8	39
			223.6	233.5	8	42				216.4	225.8	10	43
			225.2	234.4	6	26				214.2	222.2	9	46
890	4	Tangential	215.0	223.2	10	51							
			214.6	224.4	10	48							
			215.1	225.0	10	46							
		Radial	215.3	223.3	10	49							
			214.8	224.2	9	44							
			215.2	226.3	9	41							
		Axial	214.8	224.1	8	39							
			219.4	229.5	8	36							
			215.6	223.1	8	44							

Axial test ring heat treated integrally with part at 1625°F for 3 hours and air cooled. Test ring parted, specimens aged at indicated temperatures and air cooled. Radial test ring removed prior to heat treatment; heat treated in place with part.

Product Test Evaluation, Intermediate Section Tensile Test Data

Figure 55

0° LOCATION								180° LOCATION							
Aging Cycle				Depth Below				Aging Cycle				Depth Below			
Temperature, °F	Time, hours	Orientation	Thickness Inch	Notch Inch	Work ft-lb	Crack Depth Inch	W/A in-lb/in^2	Temperature, °F	Time, hours	Orientation	Thickness Inch	Notch Inch	Work ft-lb	Crack Depth Inch	W/A in-lb/in^2
890	8	Tangential	0.394	0.315	9.82	0.025	1031	890	4	Tangential	0.394	0.315	10.53	0.050	1210
			0.394	0.315	8.42	0.030	900				0.394	0.315	12.70	0.095	1432
			0.394	0.315	8.92	0.035	970				0.394	0.315	10.63	0.025	1116
		Radial	0.394	0.315	8.20	0.025	861			Radial	0.394	0.313	6.73	0.030	724
			0.394	0.315	7.80	0.030	833				0.394	0.313	6.91	0.040	771
			0.394	0.315	7.82	0.030	836				0.394	0.313	7.54	0.030	811
		Axial	0.394	0.315	8.42	0.035	916			Axial	0.394	0.315	10.18	0.030	1088
			0.394	0.315	9.88	0.035	1075				0.394	0.315	9.19	0.045	1036
			0.394	0.315	9.19	0.040	1017				0.394	0.314	9.41	0.035	1027
890	4	Tangential	0.394	0.310	9.38	0.040	1058								
			0.394	0.313	10.57	0.025	1118								
			0.394	0.313	9.28	0.035	1017								
		Radial	0.394	0.313	10.94	0.030	1177								
			0.394	0.313	10.26	0.035	1124								
			0.394	0.313	8.91	0.030	959								
		Axial	0.394	0.313	9.76	0.030	1050								
			0.394	0.313	8.78	0.035	962								
			0.394	0.313	9.58	0.027	1020								

Axial test ring heat treated integrally with part at 1625°F for 3 hours and air cooled. Test ring parted, specimens aged at indicated temperatures and air cooled. Radial test ring removed prior to heat treatment, heat treated in place with part. All specimens were tested at room temperature.

Product Test Evaluation, Intermediate Section, Room Temperature Precracked Charpy V-Notch Impact Test Data

Figure 56

0° LOCATION							180° LOCATION						
Aging Cycle			0.2% Offset Yield Strength ksi	Ultimate Tensile Strength ksi	Elongation in 1 Inch %	Reduction in Area %	Aging Cycle			0.2% Offset Yield Strength ksi	Ultimate Tensile Strength %	Elongation in 1 Inch %	Reduction in Area %
Temperature, °F	Time, hours	Orientation					Temperature, °F	Time, hours	Orientation				
890	8	Tangential	221.8	231.5	11	49	890	4	Tangential	211.7	222.1	10	50
			217.9	228.1	10	47				204.1	213.9	10	45
			219.6	230.1	8	42				204.9	216.1	8	40
		Radial	215.1	225.8	4	15			Radial	201.7	211.9	7	27
			215.9	225.5	3	8				203.9	213.3	3	9
			215.5	224.9	1	3				204.1	214.1	3	11
		Axial	217.5	227.9	10	43			Axial	203.7	215.3	11	52
			218.1	229.7	10	47				202.7	213.7	10	49
			217.0	227.4	10	45				202.9	217.3	11	52
890	4	Tangential	207.3	218.2	11	52							
			203.7	213.9	9	40							
			205.9	215.6	10	46							
		Radial	202.3	212.3	3	13							
			203.5	212.9	4	18							
			203.5	213.5	2	7							
		Axial	204.7	215.7	11	50							
			204.3	215.5	10	48							
			204.3	214.7	11	49							

Axial test ring heat treated integrally with part at 1650°F for 3 hours and air cooled. Test ring parted, specimens aged at indicated temperatures and air cooled. Radial test ring removed prior to heat treatment; heat treated in place with part.

Product Test Evaluation, Exit Flange Tensile Test Data

Figure 57

0° LOCATION								180° LOCATION							
Aging Cycle															
Temperature, °F	Time, hours	Orientation	Thickness Inch	Depth Below Notch Inch	Work ft-lb	Crack Depth Inch	W/A in-lb/in^2	Temperature, °F	Time, hours	Orientation	Thickness Inch	Depth Below Notch Inch	Work ft-lb	Crack Depth Inch	W/A in-lb/in^2
890	8	Tangential	0.394	0.316	8.56	0.040	945	890	4	Tangential	0.394	0.314	10.38	0.035	1133
			0.394	0.315	8.75	0.035	952				0.394	0.314	9.88	0.035	1099
			0.394	0.315	7.17	0.030	766				0.394	0.314	9.65	0.040	1072
		Radial	0.394	0.314	5.40	0.040	600			Radial	0.394	0.313	6.21	0.035	681
			0.394	0.314	5.45	0.035	595				0.394	0.313	6.28	0.040	700
			0.394	0.314	5.93	0.030	636				0.394	0.313	6.35	0.040	708
		Axial	0.394	0.315	7.89	0.035	858			Axial	0.394	0.314	8.34	0.040	927
			0.394	0.314	8.01	0.035	875				0.394	0.314	8.48	0.035	926
			0.394	0.314	9.02	0.035	985				0.394	0.315	8.53	0.035	928
890	4	Tangential	0.394	0.315	9.97	0.045	1124								
			0.394	0.315	9.66	0.045	1089								
			0.394	0.314	8.56	0.040	951								
		Radial	0.394	0.315	6.90	0.035	751								
			0.394	0.316	7.28	0.040	804								
			0.394	0.314	6.57	0.040	730								
		Axial	0.394	0.314	10.17	0.035	1110								
			0.394	0.314	10.47	0.035	1143								
			0.394	0.314	9.76	0.040	1084								

Axial test ring heat treated integrally with part at 1650°F for 3 hours and air cooled. Test ring parted, specimens aged at indicated temperatures and air cooled. Radial test ring removed prior to heat treatment; heat treated in place with part. All specimens were tested at room temperature.

Product Test Evaluation, Exit Flange, Room Temperature Precracked Charpy V-Notch Impact Test Data

Figure 58

0° LOCATION									
Part	Aging Cycle Temperature, °F	Aging Cycle Time, hours	Test Temperature, °F	Orientation	Thickness Inch	Depth Below Notch, inch	Work ft-lb	Crack Depth Inch	W/A in-lb/in^2
Intermediate Section	890	4	-40	Tangential	0.394	0.313	11.12	0.025	1176
					0.394	0.313	8.88	0.030	956
					0.394	0.313	9.02	0.030	971
				Radial	0.394	0.315	7.05	0.035	767
					0.394	0.315	7.75	0.040	858
					0.394	0.315	7.86	0.030	840
			200	Tangential	0.394	0.315	13.19	0.030	1409
					0.394	0.315	14.19	0.035	1544
					0.394	0.315	11.38	0.040	1260
				Radial	0.394	0.313	9.42	0.030	1014
					0.394	0.313	10.41	0.035	1141
					0.394	0.313	9.71	0.030	1045
Exit Flange	890	4	-40	Tangential	0.394	0.314	8.45	0.035	923
					0.394	0.314	7.58	0.045	858
					0.394	0.314	6.36	0.035	694
				Radial	0.394	0.314	5.15	0.035	562
					0.394	0.314	5.60	0.035	611
					0.394	0.314	4.35	0.040	483
			200	Tangential	0.394	0.314	10.31	0.035	1126
					0.394	0.314	13.12	0.030	1407
					0.394	0.314	10.48	0.030	1124
				Radial	0.394	0.314	6.60	0.035	721
					0.394	0.314	7.80	0.035	852
					0.394	0.314	6.72	0.035	734

* Axial test ring heat treated integrally with part at 1625°F (for intermediate section) and 1650°F (for exit flange) for 3 hours and air cooled. Test ring parted, specimens aged at indicated temperature and air cooled. Radial test ring removed prior to heat treatment; heat treated in place with part. Specimens tested at indicated temperatures.

Product Test Evaluation, Intermediate Section and Exit Flange, Precracked Charpy V-Notch Impact Test Data

Figure 59

EXIT FLANGE				SPEC. REQUIREMENTS		INTERMEDIATE SECTION			
Ladish Co. Half of Test Ring		Customer Half of Test Ring				Ladish Co. Half of Test Ring		Customer Half of Test Ring	
Thin	Heavy	Thin	Heavy	Microcleanliness Thin	Heavy	Thin	Heavy	Thin	Heavy
-	-	-	-	A 2.0	1.5	-	-	-	-
-	-	-	-	B 2.5	1.5	-	-	-	-
-	-	-	-	C 2.0	1.5	-	-	-	-
1	1.5	1	0.5	D 2.5	2.0	1	1.5	0.5	0.5
1.5	1	1.5	1	*E 2.5	1.5	1.5	1	1	1
				Grain Size					
4-8 Predom. 6		4-8 Predom. 6		Predominantly 5 or finer as aim		4-8 Predom. 7		4-8 Predom. 7	

* E Series for Titanium Compounds

Ladish Metallurgical Department Microcleanliness
Grain Size Results
Figure 60

Elements	AGC-34313 (Limits)	Entrance Flange (Ring A-2)	Intermediate Section (Ring CFR)	Intermediate Section Ring (CFA)	Exit Flange (Ring CFR)	Exit Flange (Ring CFA)
C	0.03	0.022	0.025	0.027	0.026	0.025
Mn	0.10	0.033	0.010	0.010	0.017	0.012
P	0.025	0.008	0.002	0.005	0.008	0.002
S	0.010	0.004	0.003	0.008	0.020	0.006
Si	0.10	0.080	0.023	0.029	0.020	0.020
Ni	17.50/19.00	18.21	18.23	18.54	18.60	18.51
Mo	4.00/4.50	4.21	4.25	4.39	4.21	4.17
Co	7.00/8.00	7.34	7.61	7.65	7.61	7.60
Ti	0.05/0.25	0.19	0.19	0.19	0.19	0.20
Al	0.05/0.15	0.090	0.055	0.060	0.120	0.100

Results of Testing Conducted at Lehigh Test Laboratories

Figure 61

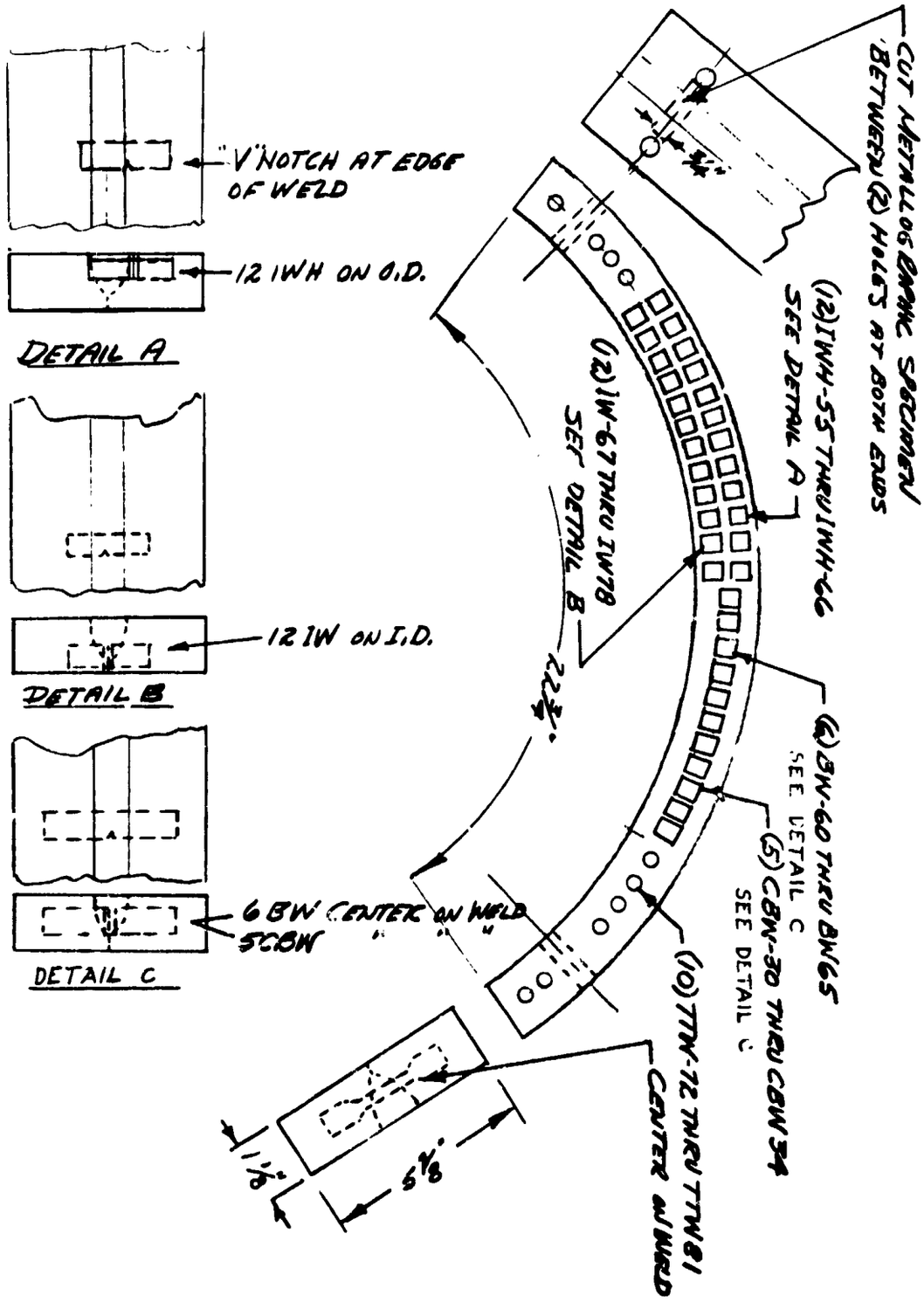

Weld Test Plate from 70-in.-dia Forging

Figure 62

Specimen No.	Aging Cycle Temperature, °F	Aging Cycle Time, hours	0.2% Offset Yield Strength ksi	Ultimate Tensile Strength ksi	Elongation in 1 inch %	Reduction in area %
TTW-72	900	4	196	201	13	65
TTW-73	900	4	195	201	13	60
TTW-74	900	4	195	201	13	60
TTW-75	900	4	194	200	12	61
TTW-77	900	8	200	207	12	60
TTW-78	900	8	200	205	13	63
TTW-79	900	8	200	206	13	63
TTW-80	900	8	206	211	12	60
TTW-81	900	8	196	201	12	62

Report of Tensile Properties (0.250-in.-Round Tensile Specimens), Weld Metal Evaluation - 70.5-in. Flange Material Weld Wire; Armetco Heat 08436

Figure 63

Specimen No.	Notch Location	Aging Cycle Temperature, °F	Aging Cycle Time, hours	Test Temperature °F		W/A in-lb/in²
603 (Ladish Des.)	Parent Metal	890	4	-40		474
613	Parent Metal	890	4	-40		485
623	Parent Metal	890	4	-40		478
					Avg.	479
633	Parent Metal	890	4	RT		666
643	Parent Metal	890	4	RT		732
653	Parent Metal	890	4	RT		590
					Avg.	663
663	Parent Metal	890	4	200		977
673	Parent Metal	890	4	200		818
683	Parent Metal	890	4	200		797
					Avg.	864
IW-67 (Sun Des.)	Weld	900	4	-40		1892
IW-68**	Weld	900	4	-40		2267
					Avg.	2080
IW-70	Weld	900	4	RT		2645*
IW-71	Weld	900	4	RT		3003
					Avg.	2824
IW-75**	Weld	900	4	200		2909
IW-76	Weld	900	4	200		3011
					Avg.	2960
IW-69**	Weld	900	8	-40		1548
IW-74**	Weld	900	8	-40		1956
					Avg.	1752
IW-72	Weld	900	8	RT		2424
IW-73	Weld	900	8	RT		2203
					Avg.	2314
IW-77	Weld	900	8	200		2650
IW-78	Weld	900	8	200		2608
					Avg.	2629
IWH-55**	HAZ	900	4	-40		626
IWH-56**	HAZ	900	4	-40		730
					Avg.	678
IWH-58	HAZ	900	4	RT		872
IWH-59	HAZ	900	4	RT		827
					Avg.	850
IWH-63**	HAZ	900	4	200		1147
IWH-64	HAZ	900	4	200		1243
					Avg.	1195
IWH-57**	HAZ	900	8	-40		667
IWH-62**	HAZ	900	8	-40		606
					Avg.	636
IWH-60	HAZ	900	8	RT		1175
IWH-61	HAZ	900	8	RT		856
					Avg.	1016
IWH-65	HAZ	900	8	200		1172
IWH-66	HAZ	900	8	200		958
					Avg.	1065

* Hit twice before failure
** Specimen width 0.380 inch

Fracture Toughness (W/A) Values for Impact Specimens from Entrance Flange for 120-SS Nozzle Shell (Lukens Heat R-559) Welded with Armetco Heat 08436 Wire

Figure 64

Specimen No.	Aging Cycle Temperature, °F	Aging Cycle Time, hours		*G_{nc} in-lb/in^2	*Knc (1000 psi $\sqrt{in}$)
BW-60	900	4		216	76.3
BW-61	900	4		272	85.7
BW-62	900	4		232	79.1
			Avg.	240	80.4
BW-63	900	8		309	91.3
BW-64	900	8		225	77.9
BW-65	900	8		319	92.7
			Avg.	284	87.3

* From calibration curve

Fracture Toughness (G_{nc}) Values for Slow-Notch-Bend Specimens from Entrance Flange for 120-SS Nozzle (Lukens Heat R-559) Welded With Armetco Heat 08436 Wire

Figure 65

MICROHARDNESS TRAVERSE SUMMARY
(KNOOP HARDNESS NUMBERS)
(500 GM LOAD)

RANGE OF HARDNESS RESULTS (Max. - Min. Values)					
			Across Top of Weld		
Condition	HUB *	HAZ **	WELD	HUB	HUB
As-welded	356-378(22)	410-415(5)	334-404(70)	387-400(13)	361-388(27)
Maraged (900°F/8 Hr.)	437-474(37)	496-503(7)	435-491(56)	491-532(41)	450-496(46)
			Across Middle of Weld		
As-welded	348-384(36)	374-413(39)	354-394(40)	378-388(10)	352-388(36)
Maraged (900°F/8 Hr.)	490-522(32)	493-532(39)	442-487(45)	487-509(22)	470-485(15)
			Across Bottom of Weld		
As-welded	340-396(56)	371-381(10)	364-413(49)	376-379(3)	340-384(44)
Maraged (900°F/8 Hr.)	461-503(42)	474-481(7)	454-496(42)	474-511(37)	456-496(40)

NOTES

Numbers in parentheses represent difference between maximum and minimum values

WELD: Based on 7 to 26 indents at 0.040-inch intervals

HAZ: Based on 2 to 5 indents at 0.040-inch intervals

HUB: Based on 4 to 6 indents at 0.040-inch intervals

* Weld heat-unaffected base (base metal) = HUB
** Weld heat-affected zone (base metal) = HAZ

Weld in Forged Test Ring
Figure 66

MICROHARDNESS TRAVERSE SUMMARY
(KNOOP HARDNESS NUMBERS)
(500 GM LOAD)

AVERAGE HARDNESS RESULTS					
			Across Top of Weld		
Condition	HUB*	HAZ**	WELD	HAZ	HUB
As-welded	366	413	384	397	375
Maraged (900°F/8 Hr.)	459	502	461	509	473
			Across Middle of Weld		
As-welded	363	394	349	384	369
Maraged (900°F/8 Hr.)	508	512	459	499	479
			Across Bottom of Weld		
As-welded	364	376	399	384	358
Maraged (900°F/8 Hr.)	482	478	475	489	478

NOTES

WELD: Based on 7 to 26 indents at 0.040-inch intervals

HAZ: Based on 2 to 5 indents at 0.040-inch intervals

HUB: Based on 4 to 6 indents at 0.040-inch intervals

* Weld heat-unaffected base (base metal) = HUB
** Weld heat affected zone (base metal) = HAZ

Weld in Forged Test Ring

Figure 67

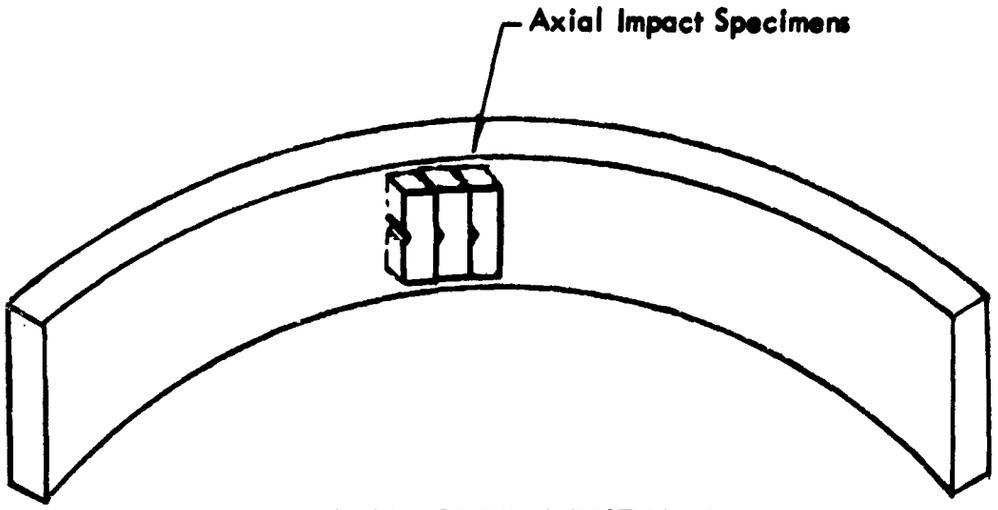

AXIAL FORGING TEST RING

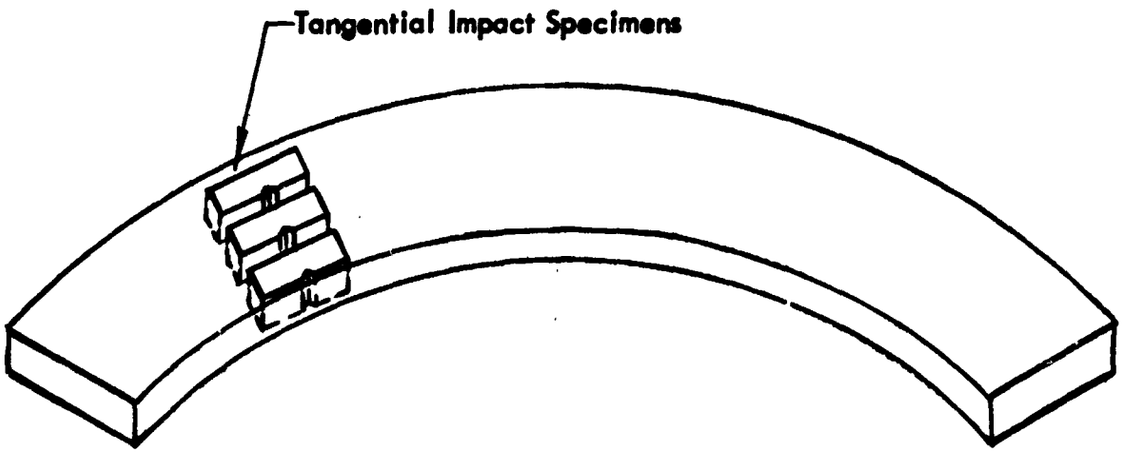

RADIAL FORGING TEST RING

Precracked Impact Specimens for Maraging with Nozzle Shell

Figure 68

Forging	Test Ring	Orientation	0.2% Offset Yield Strength ksi	Ultimate Tensile Strength, ksi	Elongation in 1 Inch %	Reduction in Area %
Entrance Flange	A-2	Tangential	230.0	238.0	11	51.7
			232.5	240.0	12	52.2
			233.0	240.0	12	52.0
		Avg.	232	239	12	52
Entrance Flange	B	Axial	230.0	239.0	11	42.9
			232.0	241.0	9	38.5
			234.0	242.0	10	40.8
		Avg.	232	241	10	41
Intermediate Section	CFR	Tangential	230.0	240.0	8	34.6
			232.0	240.0	8	33.4
			230.0	237.0	11	42.0
		Avg.	231	239	9	37
Intermediate Section	CFA	Axial	229.0	232.0	9	32.5
			232.5	244.0	5	21.8
			236.0	242.0	4	16.8
		Avg.	233	239	6	24
Exit Flange	CFR	Tangential	230.0	238.5	10	39.6
			230.0	240.5	10	40.2
			233.0	240.0	10	44.5
		Avg.	231	240	10	41
Exit Flange	CFA	Axial	230.0	239.5	9	38.4
			229.0	239.5	9	28.1
			230.0	240.5	9	39.0
		Avg.	230	240	9	35

Test Results of Tensile Specimens Maraged with the 120-SS Nozzle Shell

Figure 69

Forging	Test Ring	Orientation	W/A at Room Temperature in-lb/in^2
Entrance Flange	A-2	Tangential	728 732 736 Avg. 732
Entrance Flange	B	Axial	516 478 451 Avg. 482
Intermediate Section	CFR	Tangential	758 812 820 Avg. 797
Intermediate Section	CFA	Axial	614 606 643 Avg. 621
Exit Flange	CFR	Tangential	733 752 784 Avg. 756
Exit Flange	CFA	Axial	635 638 637 Avg. 637

Test Results of Precracked Impact Specimens Maraged with The 120-SS Nozzle Shell

Figure 70

Heat No.[b]	Composition, Weight percent[a]									
	C	Mn	Si	Ni	Co	Mo	Ti	Al	P	S
3920556	0.02	0.05	0.08	17.68	7.9	4.2	0.16	0.16	0.008	0.006
Specified Limits, Max.	0.03	0.10	0.10	17.5/19.0	7.0/8.0	4.0/4.5	0.05/0.25	0.05/0.15	.0025	0.01

(a) Mill certified analysis checked by AGC.
(b) Vacuum arc remelted material supplied by Republic Steel Corporation.

Composition of 18%-Nickel Maraging Steel Bar Stock

Figure 71

Etchant - Marbles Magnification - 100X

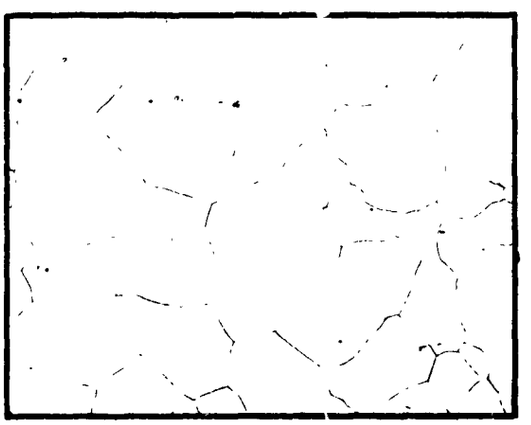

Etchant - 10% Chromic Magnification - 100X

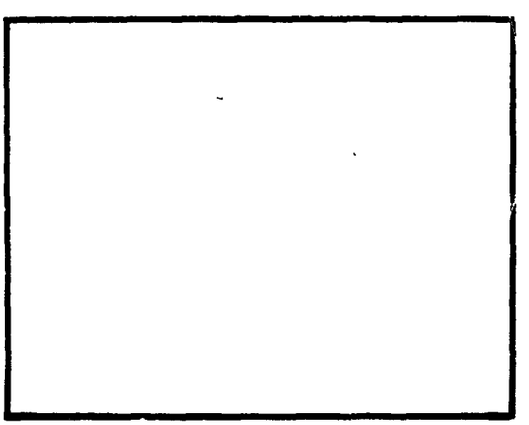

Unetched Magnification - 100X

Typical Microstructure, Grain Size and Inclusion Content of 2.5-in.-thick Bar Stock from Republic Heat 3920556

Figure 72

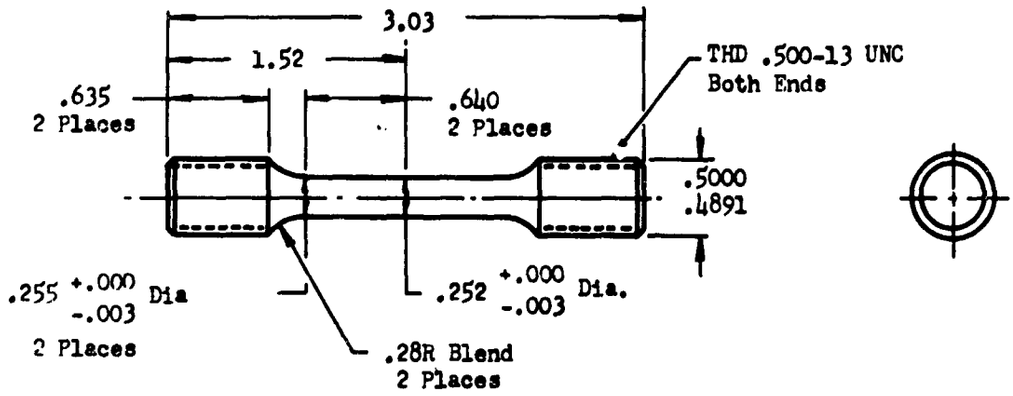

Tensile Specimen

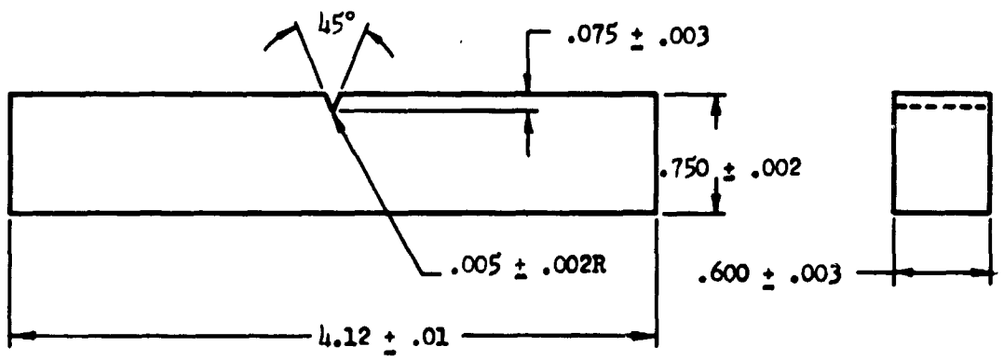

Slow-Notch-Bend Specimen

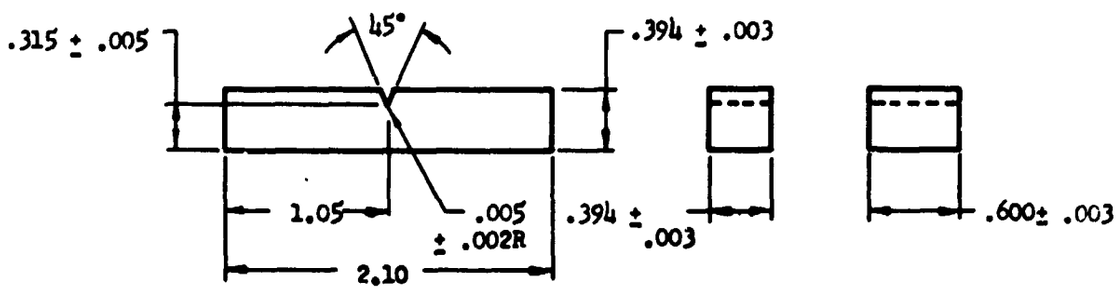

Precrack Charpy Impact Specimen

Test Specimens

Figure 73

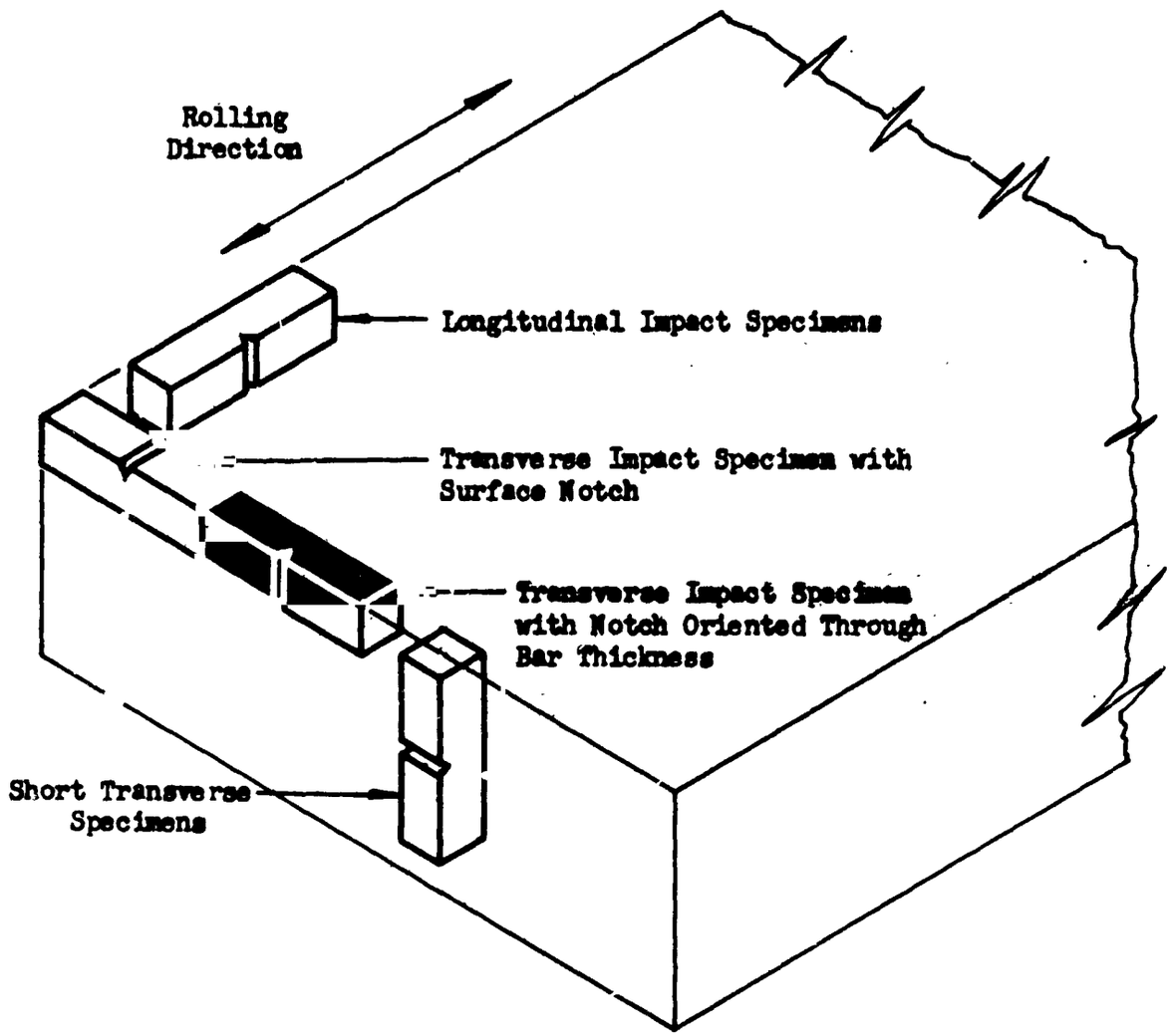

Orientation of Specimens Taken from 2-1/2 by 8-in. Bar Stock, Republic Heat 3920556, 18%-Nickel Maraging Steel

Figure 74

Aging Cycle °F	Hr.	Orientation		Yield Strength at 0.2% Offset, ksi	Ultimate Tensile Strength, ksi	Elongation in 1 in. %	Reduction of Area, %
900	8	Longitudinal		219	231	12.0	58.1
				217	231	11.6	58.8
				221	235	12.8	58.8
			Avg.	219	232	12.1	58.7
		Transverse		219	233	11.5	51.3
				219	233	10.5	53.1
				218	232	11.1	52.1
			Avg.	219	233	11.0	52.2
900	16	Longitudinal		220	235	12.8	58.5
				219	233	12.4	58.8
				220	233	12.9	59.4
			Avg.	220	233	12.7	58.9
		Transverse		215	233	10.9	48.7
				218	236	12.0	54.7
				220	234	11.3	48.7
			Avg.	218	234	11.4	50.7

Effects of Aging Time and Temperature and Specimen Orientation on the Tensile Properties of Republic Heat 3920556, Grade 200, 2-1/2-in.-thick 18%-Nickel Maraging Steel Bar Stock

Figure 75

Aging Cycle °F	Hr.	Orientation	0.2% Offset Yield Strength, ksi		W/A in-lb/in^2 Test Temperature, °F -100	RT	200	384
900	8	Longitudinal	219		821	1133	1998	2091
					835	1082	1620	2041
				Avg.	828	1108	1809	2066
900	8	Transverse	219		699	1340	1351	1365
					713	1633	1330	1836
				Avg.	706	1487	1341	1646
900	8	Transverse**	219		599	1053	1170	1182
					576	1055	1098	—
				Avg.	588	1054	1134	1182
900	8	Short Transverse	-		569	1065	1062	1366
					618	—	1148	1240
				Avg.	594	1065	1105	1303
900	16	Longitudinal	220		895	1262	1672	1998
					883	1016	1621	1951
				Avg.	889	1139	1647	1970
900	16	Transverse*	218		671	1393	1461	1265
					633	1138	1263	1188
				Avg.	652	1288	1362	1242
900	16	Transverse**	218		708	844	1081	1092
					683	927	1142	1262
				Avg.	969	886	1113	1177
900	16	Short Transverse	-		630	933	936	1405
					654	715	1048	1250
				Avg.	642	824	992	1328

* Notch located in surface of bar.
** Notch located through the thickness of bar.

Effects of Aging Time and Temperature and Orientation of the Precracked Charpy Impact Fracture Toughness of Republic Heat 3920556, Grade 200, 2-1/2-in.-thick, 18%-Nickel Maraging Steel Bar Stock

Figure 76

Specimen Number	Aging Cycle °F - hr	Specimen Orientation	.2% Offset Yield (ksi)	Width b (in)	Depth d (in)	Proportional Limit Load (L) (lbs.)	Proportional Limit Defle.(e) (in.)	Maximum Load (L) (lbs)	eb/L in²/lb. x 10⁻⁸	Notch + Crack Depth Effective a_1(1)	a_2(2)	a_3(3)	a_4(4)
RB 22	900-8	Long.	219	.588	.754	9150	.0234	10670	150	.221	.214	.223	.214
RB 23				.577	.750	9400	.0237	10760	145	.207	.201	.205	.201
RB 24				.577	.753	9100	.0243	10220	154	.231	.224	.235	.223
RB 25				.576	.752	10200	.0237	11780	134	(6)	(6)	.170	.170
RB 26				.575	.752	9900	.0239	11670	142	.185	.183	.185	.184
RB 32	900-8	Trans.	219	.577	.752	6700	.0165	8550	142	.196	.192	.194	.192
RB 33				.576	.737	7800	.0199	8530	148	.211	.204	.210	.205
RB 34				.576	.735	11600	.0241	13450	120	(6)	(6)	.106	.122
RB 35				.576	.739	7800	.0204	8420	152	.222	.214	.224	.215
RB 36				.574	.751	9525	.0204	10530	123	.109	(6)	.112	.126
RB 42	900-8	Trans. (Surface Notch)	219	.576	.752	6450	.0217	7490	194	.298	.307	.300	.308
RB 43				.575	.751	10000	.0230	10840	133	(6)	(6)	.164	.165
RB 44				.575	.752	6100	.0179	7850	169	.265	.262	.263	.264
RB 45				.575	.752	9950	.0230	10800	133	(6)	(6)	.167	.167
RB 46				.577	.753	9475	.0214	10900	130	(6)	(6)	.157	.159
RB 27	900-16	Long.	220	.577	.752	9100	.0206	12450	131	(6)	(6)	.158	.160
RB 28				.575	.752	8025	.0185	10560	133	(6)	(6)	.166	.166
RB 29				.577	.751	7400	.0202	8900	158	.239	.234	.243	.23[illegible]
RB 30				.577	.752	8000	.0194	9830	140	.189	.186	.188	.18[illegible]
RB 31				.577	.752	8800	.0222	10470	139	.207	.201	.205	.20[illegible]
RB 37	900-16	Trans.	218	.576	.740	7300	.0196	7950	155	.232	.226	.236	.22[illegible]
RB 38				.576	.752	7490	.0181	8560	136	.186	.184	.186	.18[illegible]
RB 39				.576	.751	8725	.0194	9980	128	(6)	(6)	.148	.15[illegible]
RB 40				.576	.751	6950	.0179	7850	148	.215	.208	.216	.20[illegible]
RB 41				.576	.752	8850	.0199	9830	130	(6)	(6)	.154	.15[illegible]
RB 47	900-16	Trans. (Surface Notch)	218	.576	.752	9500	.0220	10210	134	(6)	(6)	.168	.16[illegible]
RB 48				.574	.752	10180	.0221	10740	124	(6)	(6)	.132	.14[illegible]
RB 49				.577	.752	9410	.0205	10770	126	(6)	(6)	.137	.14[illegible]
RB 50				.576	.752	9200	.0213	9960	135	(6)	(6)	.168	.16[illegible]
RB 51				.575	.753	8560	.0197	9680	132	(6)	(6)	.165	.16[illegible]

(1) Five-point curve fitting using first run calibration data.
(2) Five-point curve fitting using second run calibration data.
(3) Four-point curve fitting using first run calibration data.
(4) Four-point curve fitting using second run calibration data.
(5) Bueckner's Analysis.
(6) Denotes values of Notch + Effective Crack Depth less than 0.176 inches.

77-1

	Measured a_o(5) (in)	Plane-Strain Fracture Toughness (in.-lb/in.^{2}) G_{nc_1}(1)	G_{nc_2}(2)	G_{nc_3}(3)	G_{nc_4}(4)	G_{Ic}(5)	Stress Intensity Factor (ksi $\sqrt{in.}$) K_{nc_1}(1)	K_{nc_2}(2)	K_{nc_3}(3)	K_{nc_4}(4)	K_{Ic}(5)
	.232	485	441	465	448	494					
	.238	387	463	415	488	582					
	.263	513	471	534	459	650					
	.222	---	---	441	529	598					
	.226	446	500	421	523	583					
		Avg 458	Avg 469	Avg 455	Avg 489	Avg 582	Avg 118	Avg 119	Avg 117	Avg 122	Avg 131
	.238	226	230	196	243	292					
	.212	348	324	304	339	354					
	.132	---	---	413	532	380					
	.234	368	334	356	340	419					
	.171	---	496	306	385	354					
		Avg 314	Avg 346	Avg 315	Avg 368	Avg 360	Avg 98	Avg 103	Avg 98	Avg 106	Avg 104
1	.333	545	484	551	474	561					
1	.203	---	---	423	502	496					
1	.290	342	259	303	254	364					
7	.193	---	---	420	501	449					
9	.200	---	---	370	436	426					
		Avg 444	Avg 372	Avg 413	Avg 434	Avg 459	Avg 116	Avg 106	Avg 112	Avg 115	Avg 118
0	.180	---	---	342	404	333					
5	.217	---	---	273	324	356					
3	.267	352	326	367	309	449					
5	.240	301	325	275	342	423					
1	.234	427	406	365	428	488					
		Avg 360	Avg 352	Avg 324	Avg 361	Avg 410	Avg 104	Avg 117	Avg 99	Avg 104	Avg 112
5	.237	333	307	348	297	373					
4	.228	258	286	241	299	338					
2	.196	---	---	303	359	355					
3	.255	284	260	256	270	362					
7	.211	---	---	319	378	411					
		Avg 291	Avg 284	Avg 293	Avg 321	Avg 368	Avg 94	Avg 93	Avg 94	Avg 99	Avg 106
9	.203	---	---	382	357	444					
0	.171	---	---	383	463	389					
4	.188	---	---	333	400	382					
9	.212	---	---	358	428	448					
5	.214	---	---	310	368	393	---	---			
				Avg 353	Avg 403	Avg 411			Avg 117	Avg 111	Avg 112

Effects of Orientation, Aging Time, and Temperature on the Slow-Notch Bend Fracture Toughness of Republic Heat 3920556, 2-1/2-in.-thick Bar Stock

Figure 77-2

Aging Cycle °F - Hr	Specimen Orientation	0.2% Offset Yield Strength, ksi	Fracture Toughness (in-lb/in.^{2}) 2.5" Thick Bar Stock: Spring Constant	2.5" Thick Bar Stock: Bueckner	.6" Thick Plate: Spring Constant	.6" Thick Plate: Bueckner
900-8	Longitudinal	219	387-534 Avg(18)470	494-650 Avg(5)582	391-627 Avg(10)496	459-639 Avg(5)526
	Transverse	219	196-532 Avg(17)338	292-419 Avg(5)360	449-607 Avg(10)539	496-579 Avg(5)538
	Transverse*	219	254-502 Avg(10)381	364-561 Avg(5)459	-	-
900-16	Longitudinal	220	273-428 Avg(16)348	333-488 Avg(5)410	463-543 Avg(4)506	558-617 Avg(4)589
	Transverse	218	241-378 Avg(16)300	338-411 Avg(5)368	-	-
	Transverse*	218	310-463 Avg(18)378	382-448 Avg(5)411	-	-

*Notch located in surface of bar stock

Plane Strain Fracture Toughness of Republic Heat 3920556, Grade 200, 2-1/2-in.-thick, 18%-Nickel Maraging Steel Bar Stock

Figure 78

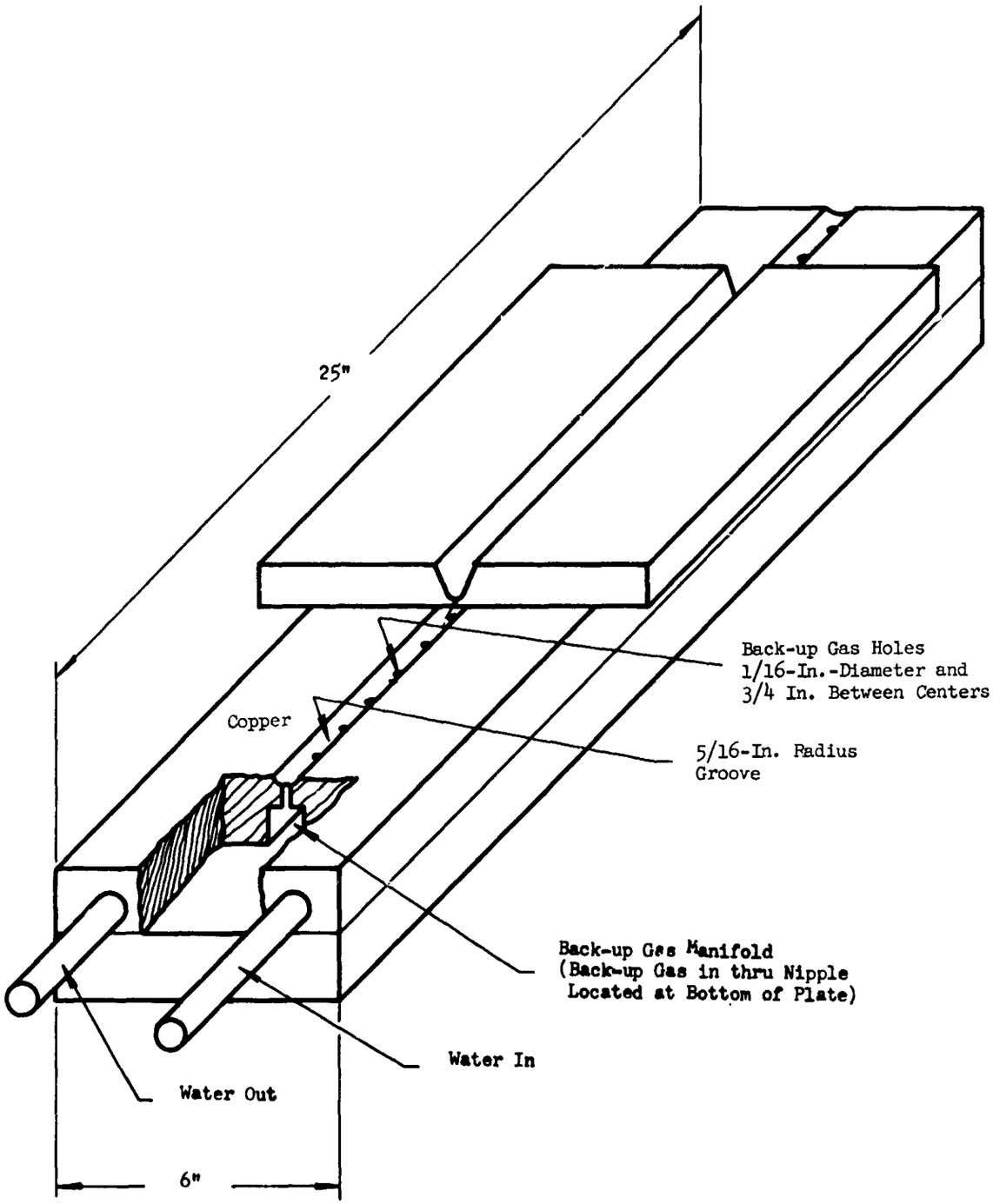

Welding Fixture

Figure 79

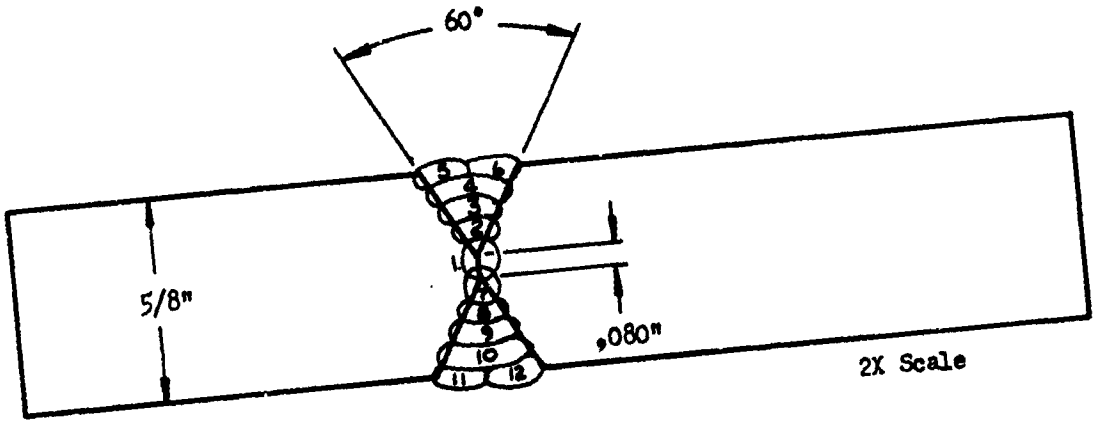

VIEW SHOWING DOUBLE VEE WELD JOINT

Pass (a) No.	Amps	Volts	Travel I.P.M.	Wire (b) Speed	Torch Gas c.f.h. A*	Torch Gas c.f.h. He*	Back-Up Gas A* c.f.h.
1	325	10	8	8	8.5	35	15
2	250	10	8	20			
3	225	11	20	25			
4	225	11	20	25			
5	230	11	20	25			
6	230	11	20	25			
7	250	10	20	10			
8	240	11	20	25			
9	240	11	20	25			
10	240	11	20	25			
11	240	11	20	25	8.5	35	15
12	240	11	20	25			

* "A" = Argon; He = Helium

(a) 1/8-inch diameter thoriated tungsten electrode

(b) 1/16-inch diameter filler wire

Weld Joint Design and Welding Conditions for Double-V Joint, 18%-Nickel Maraging Steel Plate Material

Figure 80

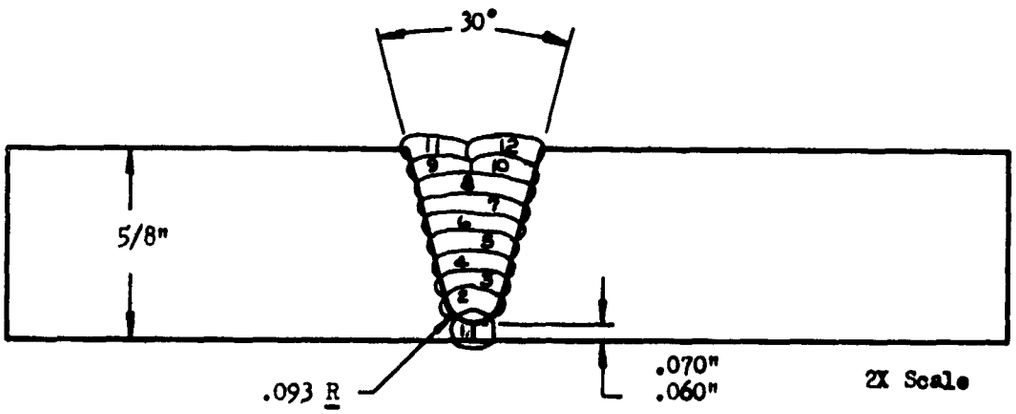

VIEW SHOWING SINGLE "U" WELD JOINT

Pass(a) No.	Amps	Volts	Travel I.P.M.	Wire (b) I.P.M.	Torch Gas c.f.h. A* He*	Back-Up Gas A* c.f.h.
1	100	9	8	10	10	15
2	150	9		10		
3	195	9		20		
4	200	10		20		
5	200			20		
6	225			30		
7						
8						
99						
10						
11						
12						

* "A" = Argon; He = Helium

(a) 1/8-inch diameter thoriated tungsten electrode
(b) 1/16-inch diameter filler wire

Weld-Joint Design and Welding Conditions for Single-U Joint, 18%-Nickel Maraging Steel Plate Material

Figure 81

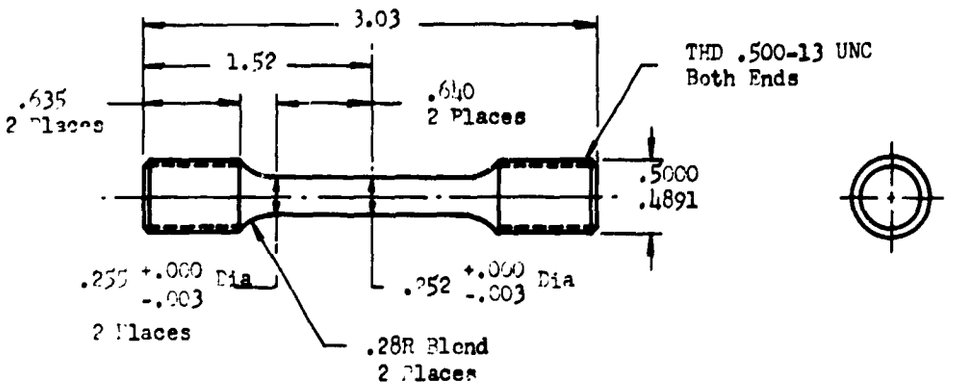

Tensile Specimen

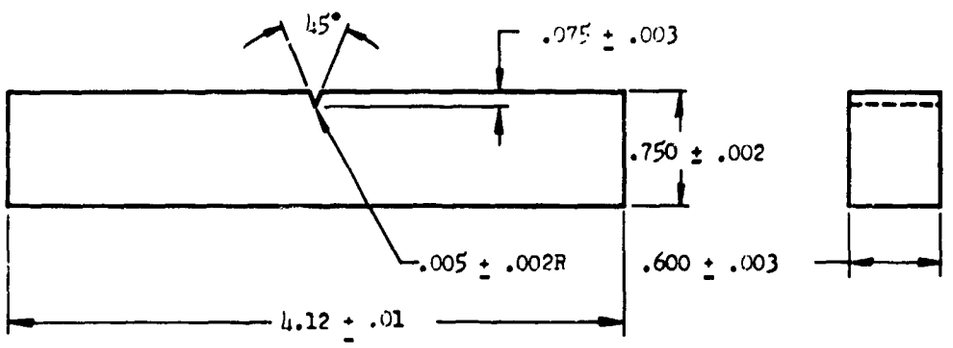

Slow-Notch-Bend Specimen

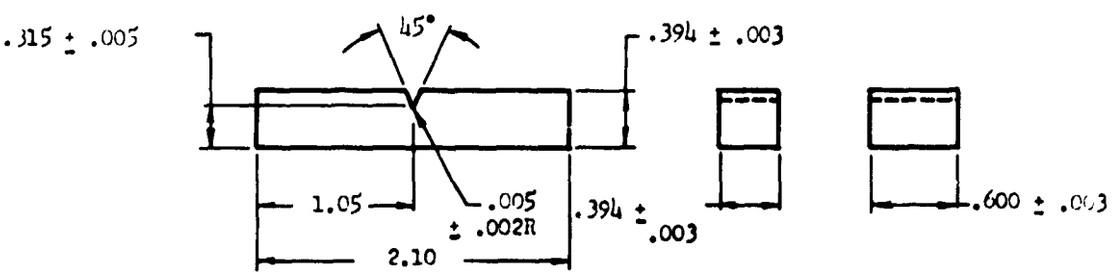

Precracked Charpy Impact Specimen

Precracked Charpy Impact Specimen

Figure 82

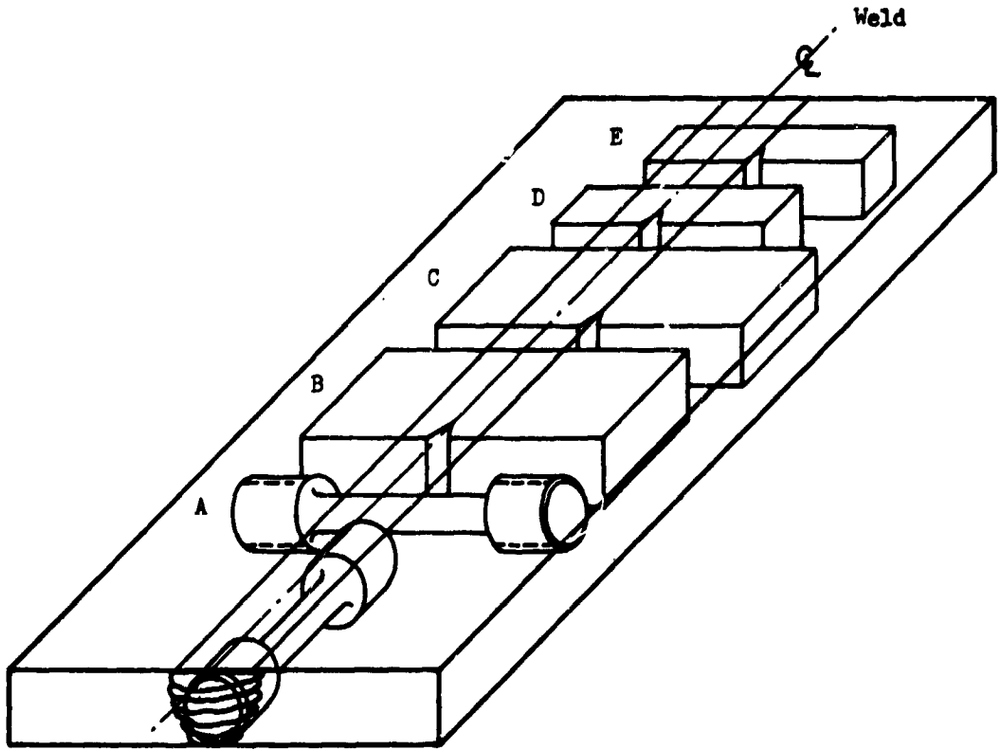

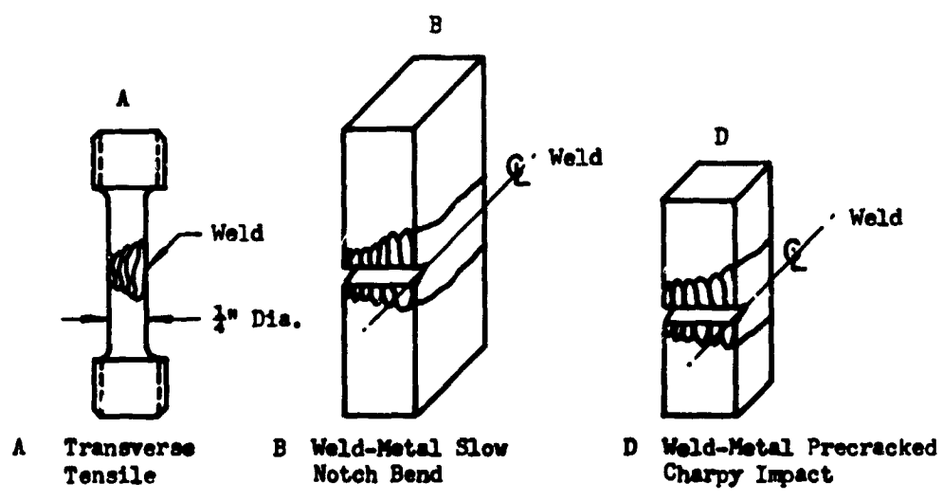

Orientation of Weld-Joint Test Specimens

Figure 83

Designations (Heat No)	Composition, wt per cent									
	C	Ni	Co	Mo	Ti	Al	Mn	P	S	Si
					Filler Wires					
06887	0.041	18.3	7.9	4.1	0.34	0.07	0.03	0.005	0.006	0.047
07496	0.026	18.4	8.0	4.2	0.35	0.06	0.02	0.005	0.007	0.033
3-4428-.39 Ti	0.019	18.8	7.14	4.1	0.34	0.09	0.02	0.009	0.008	0.03
3-4428-.31 Ti	0.010	18.4	7.15	4.4	0.29	0.09	0.02	0.008	0.008	0.04
INCO	0.003	18.7	4.2	3.7	0.50	0.30	0.02	0.004	0.004	0.020
					Base Metals					
3960524	0.026	19.0	9.0	3.5	0.22	0.07	0.06	0.005	0.008	0.05
3920556	0.02	17.68	7.9	4.2	0.16	0.16	0.05	0.008	0.006	0.08

Filler Wire and Base Metal Compositions

Figure 84

Filler Wire*	Joint Design	0.2 Percent Offset Yield Strength ksi	Ult. Tensile Strength, ksi	Elongation in 1 incn %	Reduction in Area, %
		Longitudinal Specimens			
06887	Double "V"	221	234	10.3	44.5
		220	233	11.8	51.2
		220.5 Ave	233.5 Ave	11.0 Ave	47.9 Ave
07495	Double "V"	217	235	10.0	51.9
		220	230	12.1	41.1
		218.5 Ave	232.5 Ave	11.0 Ave	46.5 Ave
34428-.39 Ti	Double "V"	218	225	13.7	53.5
		219	224	13.1	51.2
		218 Ave	224.3 Ave	13.6 Ave	52.3 Ave
34428-.31 Ti	Double "V"	215	225	13.9	54.0
		214	224	13.0	53.0
		216	224	12.6	50.5
		215 Ave	224.3 Ave	13.1 Ave	52.5 Ave
Inco	Double "V"	196.0	224.2	12.5	58.8
		202.6	224.3	14.0	55.3
		215.3	223.8	14.0	54.6
		206.8 e	224.1 Ave	13.5 Ave	55.7 Ave
06887	Single "U"	229	243	8.8	44.5
		232	243	10.0	43.4
		230.5 Ave	243 Ave	9.4 Ave	44.0 Ave
07495	Single "U"	226	239	8.6	38.5
		226	238	9.2	38.9
		226 Ave	238.5 Ave	8.9 Ave	38.7 Ave
34428-.31 Ti	Single "U"	218	227	15.1	54.6
		212	225	15.2	56.7
		215 Ave	226 Ave	15.1 Ave	55.6 Ave

*Refer to Fig. 86 for weld wire and weld deposit chemical composition

Longitudinal Tensile Properties of Welded Joints in Republic Heat 3960524, 18%-Nickel Maraging Steel Plate After Aging at 900°F for 8 hr

Figure 85

Filler Wire Designation	Material	Joint Design	Composition, wt% Ni	Co	Mo	Ti
06887	Wire	-	18.3	7.9	4.1	0.34
06887	Weld Metal	Double V	18.5	8.8	3.8	0.24
06887	Weld Metal	Single U	18.5	8.7	3.8	0.28
07495	Wire	-	18.4	8.0	4.2	0.35
07495	Weld Metal	Double V	18.5	8.8	3.5	0.24
07495	Weld Metal	Single U	18.0	8.5	3.8	0.26
34428-.39 Ti	Wire	-	18.8	7.4	4.1	0.34
34428-.39 Ti	Weld Metal	Double V	18.3	8.9	3.8	0.27
34428-.31 Ti	Wire	-	18.4	7.5	4.4	0.29
34428-.31 Ti	Weld Metal	Double V	18.2	8.7	3.8	0.25
34428-.31 Ti	Weld Metal	Single U	18.8	8.7	4.0	0.28
Inco	Wire	-	18.2	4.3	3.5	0.45
Inco	Weld Metal	Double V	18.5	4.4	3.2	0.37
Base Metal - Republic Heat 3960524		-	19.0	9.0	3.5	0.22

Composition of Weld Metals Obtained in TIG-Welded Republic Heat 3960524, Grade 200, 0.6-in.-thick 18%-Nickel Maraging Steel Plate with Five Filler Wires

Figure 86

Aging Temperature* and Time		0.2% Offset Yield Strength, ksi	Ultimate Tensile Strength, ksi	Elongation in 1-in., %	Reduction in Area, %
850°F/4 hr		206.6	219.2	15.3	56.7
		206.5	217.6	16.5	55.6
		211.2	220.5	16.0	56.7
	Avg.	204.7	219.1	16.0	56.7
850°F/8 hr		219.0	228.2	14.3	53.2
		215.7	227.6	14.3	56.9
		217.2	227.8	----	56.9
	Avg.	217.3	227.8	14.3	55.0
850°F/16 hr		217.7	228.9	14.4	59.5
		223.6	234.8	13.8	45.3
		223.1	233.1	----	50.6
	Avg.	221.4	232.2	14.1	50.6
900°F/2 hr		205.3	220.0	14.4	56.4
		209.2	220.3	16.0	57.9
		209.1	220.2	14.8	54.2
	Avg.	207.8	220.2	15.0	56.1
900°F/4 hrs		217.1	227.6	13.1	52.2
		215.8	225.8	14.5	58.4
		215.8	225.8	15.0	55.0
	Avg.	216.2	226.6	14.2	55.2
900°F/8 hrs		215.7	223.0	16.0	58.7
		214.7	226.8	15.8	53.5
		216.5	228.4	16.4	54.6
	Avg.	215.9	226.0	16.0	55.6
950°F/2 hrs		209.2	220.5	16.5	55.9
		199.3	223.8	16.7	53.6
		214.7	222.1	16.3	54.4
	Avg.	207.7	222.1	16.5	54.8
950°F/4 hrs		216.9	223.8	16.1	48.6
		215.7	225.0	18.7	57.0
		215.1	223.6	19.8	56.0
	Avg.	215.9	224.1	18.2	54.1
950°F/8 hrs		205.9	216.4	22.5	54.5
		205.2	216.3	22.5	55.2
		210.5	217.1	22.7	57.4
	Avg.	207.2	216.6	22.6	55.7

*As-welded and aged condition.

Effects of Aging Temperature and Time on the Longitudinal Tensile Properties of Welded Joints in Republic Heat 3960524, 18%-Nickel Maraging Steel Plate Made with 07495 Filler and a Double-V Joint Design

Figure 87

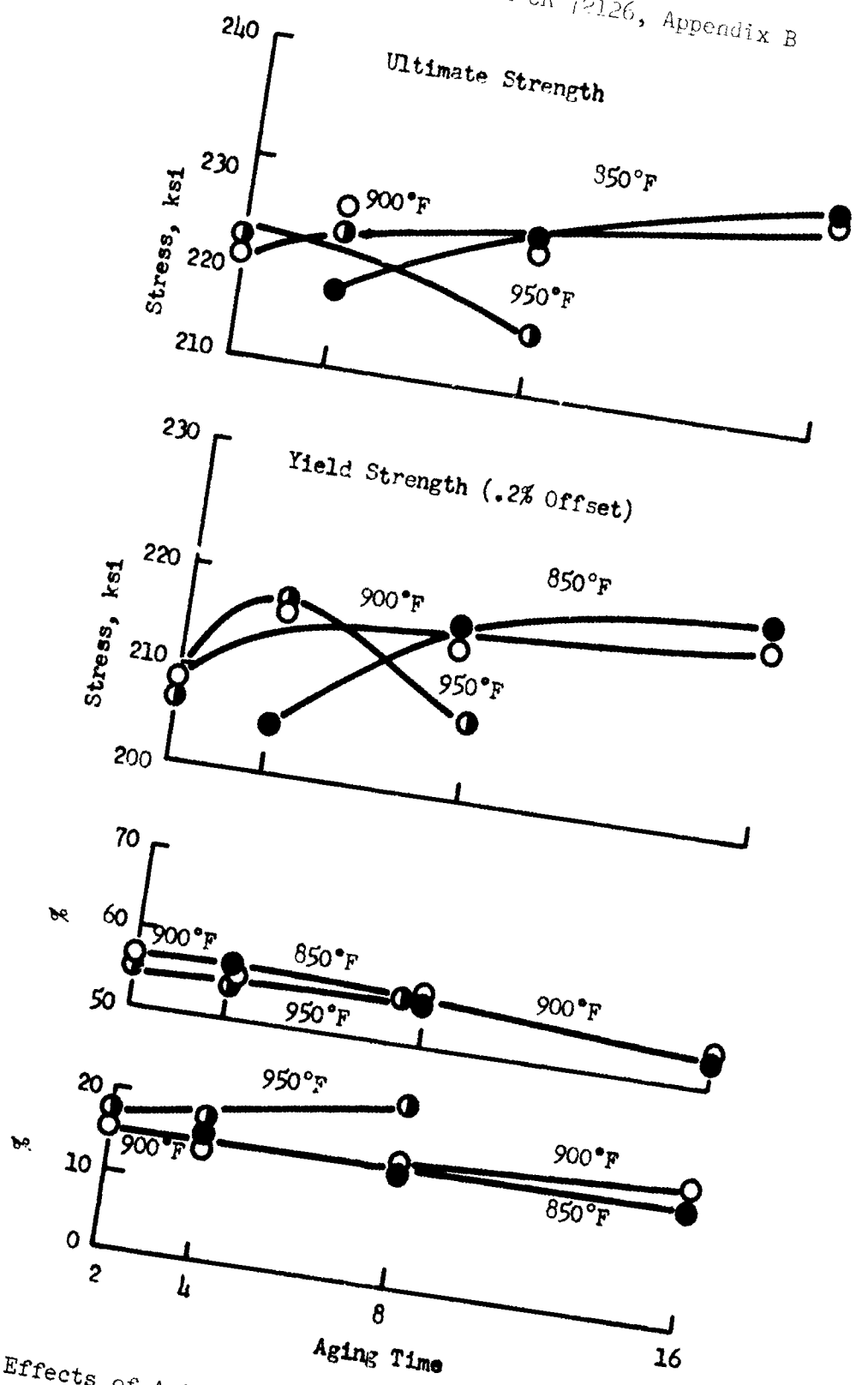

Effects of Aging Time and Temperature on the Longitudinal Tensile Properties of Weld Metals Deposited with Filler Wire 07495 in Republic Heat 3960524, 18%-Nickel Maraging Steel Plate Material

Figure 88

Aging Temp[1] and Time	Joint Design	Yield Strength 0.2% Offset ksi	Ult. Tensile Strength ksi	Elongation in 1 in. %	Reduction in Area %
850°F/8 hrs	Double V	212	225	13.3	53.4
		212	226	14.0	56.6
		212 Ave	226 Ave	13.7 Ave	57.5 Ave
	Single U	207	218	11.7	57.1
		208	219	11.8	49.9
		206	217	13.0	58.0
		207 Ave	218 Ave	12.1 Ave	55.0 Ave
900°F/8 hrs	Double V	215	225	13.9	54.0
		214	224	13.0	53.0
		216	224	12.6	50.5
		215 Ave	224 Ave	13.1 Ave	52.5 Ave
	Single U	213	223	11.2	52.5
		212	223	13.4	55.2
		210	222	13.4	57.4
		212 Ave	223 Ave	12.3 Ave	55.0 Ave
950°F/8 hrs	Double V	207	217	14.5	55.6
		207	217	16.1	58.7
		207 Ave	217 Ave	15.3 Ave	57.2 Ave
	Single U	203	216	14.3	57.4
		203	215	13.1	54.7
		204	215	14.0	56.4
		203 Ave	215 Ave	13.6 Ave	56.1 Ave

(1) As-Welded and Aged Condition

Effects of Aging Temperature and Time on the Longitudinal Tensile Properties of Welded Joints in Republic Heat 3960524, Grade 200, 0.6-in.-thick, 18%-Nickel Maraging Steel Plate Made with 34428-0.31 Ti Filler Wire and Double-V and Single-U Joint Designs

Figure 89

Aging Temp and Time	Filler Wire	Joint Design	Ultimate Tensile Strength, ksi	Location of Failure[a]
850°F/8 hrs.	07495	Double V	229	W
			223	W
			223	W
			225 Ave.	
	34428-.31	Double V	215	W
			222	W
			219 Ave.	
		Single U	218	W
			219	W
			218	
			219 Ave.	
900°F/8 nrs	07495	Double V	221	W, HAZ
			223	W, HAZ
			222	W, HAZ
			222 Ave.	
	34428-.31 Ti	Double V	218	W, HAZ
			221	W, HAZ
			219 Ave.	
	34428-.31 Ti	Single U	219	W
			220	W, HAZ
			219	W. HAZ
			219 Ave.	
950°F/8 hrs	07495		210	W, HAZ
			212	W, HAZ
			213	W, HAZ
			212 Ave.	
	34428-.31 Ti		215	W, HAZ
			217	W, HAZ
			216 Ave.	
	34428-.31 Ti	Single U	213	W, HAZ
			217	W, HAZ
			217	W, HAZ
			215 Ave.	

(a) W - Weld Metal
HAZ - Heat Affected Zone

Ultimate Tensile Strength and Failure Locations of Transverse Weld Tensile Specimens from Weldments in Republic Heat 3960524, Grade 200, 0.6-in.-thick, 18%-Nickel Maraging Steel Plate Made with 07495 and 34428-.31 Ti Filler Wires and Double-V and Single-U Joint Design

Figure 90

Aging Cycle* °F	Aging Cycle* Hr	Notch Location	0.2% Offset Yield Strength, ksi		W/A (In.-lb/In.^{2})** Test Temperature, °F +200	RT	-40
850	8	Weld Metal	217		821	583	432
					628	507	321
				Avg.	724	545	376
		Heat-Affected Zone**			1097	759	743
					1080	930	741
				Avg.	1088	844	742
900	4	Weld Metal	216		622	782	423
					633	694	433
				Avg.	627	738	428
		Heat-Affected Zone			1214	1068	870
					1052	1304	1088
				Avg.	1133	1186	978
900	8	Weld Metal	216		660	560	367
					570	704	402
				Avg.	615	632	384
		Heat-Affected Zone			766	921	635
					798	770	620
				Avg.	782	845	627
950	8	Weld Metal	207		817	766	514
					700	750	552
				Avg.	758	758	533
		HAZ			1209	869	925
					1090	1054	310
				Avg.	1148	961	867

* As-welded and aged.
**These values obtained with a 0.600 by 0.394-in. specimen.

Precracked Impact Fracture Toughness of Weld Metal and Heat Affected Zones of Weldments Made in Republic Heat 3960524, Grade 200, 0.6-in.-thick, 18%-Nickel Maraging Steel Plate With 07495 Filler Wire and Double-V Joint

Figure 91

Aging Cycle* °F	Hr	Notch Location	0.2% Offset Yield Strength, ksi		W/A (In-lb/In.^{2})** Test Temperature, °F +200	RT	-40
850	8	Weld Metal	212		922	808	536
						710	528
				Avg.		759	532
		Heat Affected Zone			871	995	826
						909	795
				Avg.		952	810
900	8	Weld Metal	215		770	677	523
						737	579
				Avg.		707	551
		Heat Affected Zone			1703	1068	752
						982	889
				Avg.		1025	820
950	8	Weld Metal	207		856	879	600
						795	625
				Avg.		837	612
		Heat Affected Zone			1422	1068	1018
						1134	1089
				Avg.		1106	1053

* As-welded and aged.
** These values obtained with a .600 by .394-in. specimen.

Precracked Impact Fracture Toughness of TIG Weldments Made in Republic Heat 3960524, Grade 200, 0.6-in.-thick, 18%-Nickel Maraging Steel Plate With 34428-0.31 Ti Filler Wire and Double-V Joint

Figure 92

Aging Cycle* °F	Hr	Notch Location	0.2% Offset Yield Strength, ksi		W/A (in-lb/in^2)** Test Temperature, °F -40	RT	200
850	8	Weld Metal	207		655	876	1122
					698	766	1106
				Avg.	676	821	1114
850	8	Heat-Affected Zone	-		907	1234	1513
					944	1167	1284
				Avg.	926	1200	1398
900	8	Weld Metal	212		643	803	901
					662	862	859
				Avg.	652	832	880
900	8	Heat-Affected Zone	-		944	1333	1483
					1024	1235	1384
				Avg.	984	1284	1434
950	8	Weld Metal	203		643	832	953
					658	849	1103
				Avg.	650	840	1028
950	8	Heat-Affected Zone	-		1264	1485	1553
					1162	1505	1599
				Avg.	1213	1495	1576

* As-welded and aged
** These values obtained with a 0.575 by 0.394-in. specimen.

Precracked Charpy Impact Fracture Toughness of TIG Weldments Made in Republic Heat 3960524, Grade 200, 0.6-in.-thick, 18%-Nickel Maraging Steel Plate with Filler Wire 34428-.31 Ti and Single-U Joint

Figure 93

Aging Cycle[1] °F	Hr	0.2% Offset Yield Strength, ksi		W/A in.-lb/in.^{2},[2] Test Temperature, °F -40	RT	200
850	8	-		588	1028	1180
				558	913	1127
			Avg.	573	970	1153
900	4	-		718	1102	1334
				718	1293	1525
			Avg.	718	1197	1429
900	8	207[3]		642	1047	1036
				709	1007	987
			Avg.	675	1027	1011
950	8	-		798	1178	1138
				856	1252	1218
			Avg.	827	1215	1178

(1) As-welded and aged.
(2) These values obtained with a 0.575 by 0.394-in. specimen.
(3) This yield strength value was obtained with a double-V joint configuration and Republic heat 3960524 base plate.

Precracked Charpy Impact Fracture Toughness of TIG Weld Metal Deposited in Republic Heat 3920556, Grade 200, 0.6-in.-thick, 18%-Nickel Maraging Steel Plate With Inco Filler Wire and Single-U Joint

Figure 94

Specimen Number	Aging Cycle °F - hr	Notch Location	.2% Offset Yield (ksi)	Width b (in.)	Depth d (in.)	Proportional Limit Load (L) (lb)	Proportional Limit Deflec. (e) (in.)	Maximum Load (L) (lb)	eb/L (in.^{2}/lb)x10^{-8}	a_1(in.
61	850-8	Weld Metal	217	.575	.750	6930(5)	.01766	7620	147	.226
62				.575	.750	6400	.01900	6405	171	.272
63				.575	.750	7000	.01749	7710	144	.216
64				.575	.750	6150	.01540	6675	144	.216
65				.575	.751	5000	.01730	5660	199	.311
71	900-4	Weld Metal	216	.575	.750	5800	.01726	5985	171	.272
72				.575	.751	6000	.01436	6785	138	.198
73				.574	.751	6300	.01436	7230	131	.172
74				.575	.749	5250(5)	.01140	7200	125	.144
75				.575	.750	5600(5)	.01481	6245	152	.235
81	900-8	Heat-Affected Zone	-	.575	.751	6700		8060		
82				.575	.750	9300		9760		
83				.575	.751	8200(5)		9660		
84				.575	.750	7800		8620		
85				.575	.751	7800(5)		10155		
91	950-8	Heat-Affected Zone	-	.575	.749	7900		9090		
92				.575	.749	8350		9330		
93				.575	.749	7350		9335		
94				.575	.749	9100		10395		
95				.575	.750	7700		9955		

(1) Rawe's Analysis; Calibration Curve Constants: $Q = 13.50 \times 10^{-6}$; $R = -60.00 \times 10^{-6}$; $S = 150.00 \times 10^{-6}$

(2) Least Square Statistical Analysis; Curve Equation $\hat{y} = 1.09 \times 10^{-6} + 1.39\, a \times 10^{-6} - 7.82\, a^2 \times 10^{-6} + 4.09\, a^3 \times 10^{-5}$

(3) 5-Point Fitting

(4) Bueckner's Analysis

(5) Pop-in Valves

Notch + Crack Depth Effective		Measured	Plane-Strain Fracture Toughness (in. lb/in.^{2})				Stress Intensity Factor 1000 psi $\sqrt{\text{in.}}$			
a_1(in.)(1)	a_2(in.)(2)	a_3(in.)(3)	a_o(in.)(4)	G_{nc_1}(1)	G_{nc_2}(2)	G_{nc_3}(3)	G_{Ic}(4)	K_{nc_1}(1)	K_{nc_2}(2)	K_{nc_3}(3)	K_{Ic}(4)
	.222	.218	.275	276	289	265	425				
	.271	.276	.315	378	380	403	491				
	.215	.210	.270	258	274	258	417				
	.216	.211	.290	199	213	200	375				
	.310	.312	.330	342	315	322	333	—	—	—	—
				Avg 291	Avg 294	Avg 289	Avg 408	Avg 94	Avg 95	Avg 94	Avg 111
	.271	.276	.300	310	314	333	360				
	.197	.193	.280	160	167	173	329				
	.172	.172	.250	143	140	175	288				
	.141	.154	.235	81	68	116	180				
	.235	.233	.280	199	214	190	288	—	—	—	—
				Avg 179	Avg 181	Avg 197	Avg 289	Avg 74	Avg 74	Avg 77	Avg 94
			.235				289				
			.205				439				
			.195				312				
			.225				364				
			.215				333				—
			.220				Avg 347				Avg 103
			.225				361				
			.235				420				
			.225				352				
			.230				499				
							369				—
							Avg 400				Avg 110

Slow-Notch-Bend Fracture Toughness of Weldments Made in Republic Heat 3960524 with 07495 Filler Wire and Double-V Joints

Figure 95

Specimen Number	Aging Cycle °F - hr	Notch Location	.2% Offset Yield (ksi)	Width b (in.)	Depth d (in.)	Proportional Limit Load (L) (lb)	Proportional Limit Deflec. (e) (in.)	Maximum Load (L) (lb)	(in.
229	850-8	Weld Metal	207	.545	.746	6000	.0174	7040	158
230				.546	.746	5200	.0169	6540	177
231				.544	.746	5150	.0184	5960	194
232				.545	.744	5250	.0163	6390	169
233				.545	.746	5300	.0167	6400	172
234	900-8	Weld Metal	212	.544	.746	5200	.0171	5895	179
235				.543	.746	5800	.0186	6200	174
236				.547	.750	7000	.0224	7350	175
237				.547	.750	5100	.0176	6330	189
239	950-8	Weld Metal	203	.547	.750	5600	.0190	6770	186
241				.546	.750	6100	.0173	7490	155
242				.547	.750	4700	.0163	5910	190
243				.547	.750	5425	.0186	6690	188
214	850-8	Heat-Affected Zone		.545	.746	5300		6450	
215				.545	.746	5700		7400	
216				.545	.746	5600		6340	
217				.546	.746	5400		6640	
218				.545	.746	5850		7220	
219	900-8	Heat-Affected Zone		.545	.746	5300		6550	
220				.546	.745	6900		8405	
221				.545	.746	5550		7255	
222				.546	.746	6300		8390	
223				.544	.746	5000		6100	
224	950-8	Heat-Affected Zone		.545	.746	5600		7330	
225				.546	.746	5700		8575	
226				.545	.746	5900		7750	
227				.544	.746	6350		8730	
228				.545	.745	6400		8160	

(1) Rawe's Method; Calibration Curve Constants: $Q = 17.42 \times 10$; $R = -85.00 \times 10^{-2}$; $S = 208.33 \times 10^{-6}$
(2) Five-Point Curve Fittings
(3) Least-Squares Statistical Method; Curve Equation: $y = 1.1 \times 10^{-6} - 2.07a \times 10^{-6} + 1.74a^2 \times 10^{-5}$
(4) Buckner's Method

96-1

Notch + Crack Depth				Plane-Strain Fracture Toughness (in.lb/in.^{2})				Stress Intensity Factor 1000 psi $\sqrt{in.}$			
	Effective		Measured								
a_1(in.)	a_2(in.)(2)	a_3(in.)(3)	a_o(in.)(4)	G_{nc_1}(1)	G_{nc_2}(2)	G_{nc_3}(3)	G_{Ic}(4)	K_{nc_1}(1)	K_{nc_2}(2)	K_{nc_3}(3)	K_{Ic}(4)
.256	.254	.250	.260	375	333	402	324				
.281	.288	.277	.300	369	418	344	330				
.300	.304	.299	.316	448	461	373	368				
.272	.276	.266	.286	342	350	334	308				
.276	.280	.270	.296	364	382	346	334				
				Avg 380	Avg 389	Avg 360	Avg 333	Avg 107	Avg 109	Avg 104	Avg 101
.284	.289	.279	.308	384	432	350	353				
.278	.283	.273	.298	450	490	424	409				
.279	.285	.274	.310	652	718	612	625				
.294	.299	.292	.324	408	445	352	369				
				Avg 474	Avg 521	Avg 435	Avg 439	Avg 120	Avg 126	Avg 115	Avg 116
.292	.296	.288	.323	481	531	417	441				
.251	.248	.245	.266	365	319	403	341				
.296	.300	.293	.345	354	379	300	369				
.282	.298	.290	.326	405	502	394	423				
				Avg 401	Avg 433	Avg 379	Avg 394	Avg 110	Avg 115	Avg 107	Avg 109
			.350				504				
			.322				470				
			.372				666				
			.353				533				
			.319				484				
							Avg 531				Avg 127
			.336				452				
			.300				581				
			.341				515				
			.304				499				
			.368				517				
							Avg 513				Avg 125
			.331				486				
			.309				425				
			.335				556				
			.306				519				
			.322				597				
							Avg 517				Avg 125

Slow-Notch-Bend Fracture Toughness of Weldments Made in Republic Heat 3960524 with 34428-.31 Ti Filler Wire and Single-U Joints

Figure 96

Specimen Number	Aging Cycle °F - hr	Notch Location	.2% Offset Yield (ksi)	Width b (in.)	Depth d (in.)	Proportional Limit Load (L) (lb)	Proportional Limit Deflec. (e) (in.)	Maximum Load (L) (lb)	eb/L (in.^{2}/lb)x10^{-8}	a_1(
105	850-8	Weld Metal	212	.575	.748	7500	.0194	7840	149	.
106				.575	.736	7100	.0194	8040	156	.
107				.575	.748	7650	.0201	8110	151	.
108	900-8	Weld Metal	215	.576	.732	7900	.0198	8220	144	
109				.575	.748	7500	.0190	7640	146	
110				.575	.748	7600	.0186	7780	141	
111	950-8	Weld Metal	207	.575	.748	9500	.0220	9850	133	
112				.575	.748	7000	.0184	7440	151	
113				.575	.748	8300	.0207	9180	143	
114	850-8	Heat-Affected Zone		.575	.748	10700		11920		
115				.575	.748	7500		8850		
116				.575	.748	10050		10740		
117	900-8	Heat Affected Zone		.576	.743	10250		10450		
118				.575	.748	8400		9350		
119				.575	.738	11250		12575		
120	950-8	Heat-Affected Zone		.575	.747	7250		7800		
121				.575	.748	6650		8500		
122				.575	.748	6500		9650		

(1) Rawe's Method; Calibration Curve Constants: $Q = 17.42 \times 10$; $R = -85.00 \times 10^{-6}$; $S = 208.33 \times 10^{-6}$
(2) Five-Point Curve Fittings
(3) Least-Squares Statistical Method; Curve Equation: $\hat{y} = 1.1 \times 10^{-6} - 2.07a \times 10^{-6} + 1.74a^2 \times 10^{-5}$
(4) Buechner's Method

Notch+Crack Depth				Plane-Strain Fracture Toughness (in. lb/in.^{2})				Stress Intensity Factor 1000 psi $\sqrt{\text{in.}}$			
	Effective		Measured								
in.)(1)	a_2(in.)(2)	a_3(in.)(3)	a_o(in.)(4)	G_{nc_1}(1)	G_{nc_2}(2)	G_{nc_3}(3)	G_{Ic}(4)	K_{nc_1}(1)	K_{nc_2}(2)	K_{nc_3}(3)	K_{Ic}(4)
.240	.237	.236	.215	442	402	521	314				
.253	.253	.249	.240	456	409	502	373				
.244	.241	.239	.230	480	428	554	369				
				Avg 444	Avg 410	Avg 526	Avg 352	Avg 116	Avg 111	Avg 126	Avg 103
.229	.228	.228	.195	434	436	552	325				
.234	.230	.230	.225	414	395	506	341				
.222	.221	.222	.225	374	405	494	350				
				Avg 409	Avg 41[illegible]	Avg 517	Avg 339	Avg 111	Avg 112	Avg 125	Avg 101
.201	.207	.208	.170	473	651	705	342				
.244	.241	.239	.250	402	359	464	362				
.226	.226	.227	.210	465	482	606	369				
				Avg 447	Avg 497	Avg 592	Avg 358	Avg 118	Avg 123	Avg 134	Avg 104
			.185				496				
			.270				485				
			.215				564				
							Avg 515				Avg 125
			.180				448				
			.275				632				
			.170				510				
							Avg 530				Avg 127
			.300				574				
			.320				560				
			.260				337				
							Avg 490				Avg 122

Slow-Notch-Bend Fracture Toughness of Weldments Made in Republic Heat 3960524 with 34428-.31 Ti Filler Wire and Double-V Joints

Figure 97 -2

Specimen Number	Aging Cycle °F	hr	Width b (in.)	Depth d (in.)	Proportional Limit Load (L) (lb)	Proportional Limit Deflec. (e) (in.)	Maximum Load (L) (lb)	Notch Plus Crack Depth Measured a_o (in.)	Plain-Strain Fracture Toughness in. lb/in.^{2} G_{Ic}	Stress Intensity Factor 1000 ksi $\sqrt{\text{in.}}$ K_{Ic}
I 1	850	8	.575	.750	6000	.0216	6970	.351	567	
I 2			.575	.749	6700	.0194	8615	.302	491	
I 3			.575	.750	6250	.0196	7230	.321	490	
I 4			.575	.750	7050	.0224	7865	.319	614	
I 5			.575	.750	9700	.0238	10490	.234	605	
									AVG. 553	130
I 6	900	4	.576	.750	8200	.0236	10350	.250	489	
I 7			.575	.750	5900	.0198	7240	.328	460	
I 8			.575	.750	7050	.0220	7850	.299	528	
I 9			.575	.750	3050	.0232	3945	.481	-	
I 10			.575	.749	6700	.0211	8040	.311	525	
									AVG. 500	123
I 11	900	8	.575	.750	5900	.0181	7675	.307	392	
I 12			.575	.749	9000	.0219	9660	.223	480	
I 13			.575	.749	6600	.0203	7195	.292	442	
I 14			.575	.749	7500	.0219	7365	.296	588	
I 15			.575	.750	7500	.0205	8110	.245	394	
									AVG. 459	118
I 16	950	8	.575	.748	6450	.0211	7280	.311	491	
I 17			.574	.748	7300	.0200	8305	.260	427	
I 18			.575	.750	6950	.0196	7805	.274	424	
I 19			.575	.749	7350	.0211	7870	.278	492	
I 20			.574	.748	6700	.0179	8080	.244	318	
									AVG. 430	112

Slow-Notch-Bend Fracture Toughness of Weldments Made in Republic Heat 3960524 with Inco Filler Wire and Single-U Joints

Figure 98

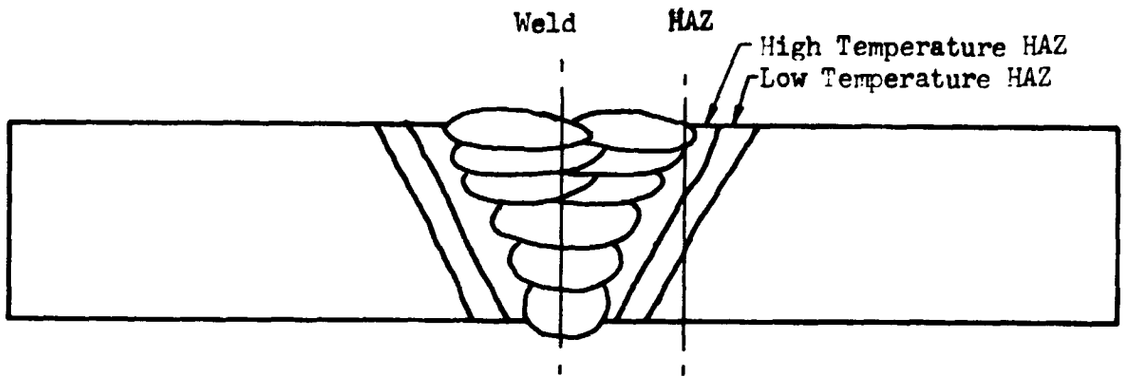

SINGLE-U WELDS

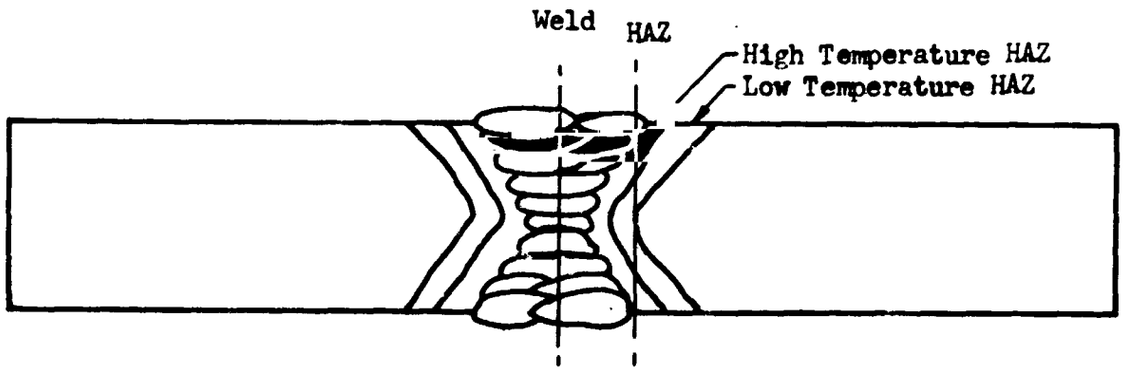

DOUBLE "V" WELDS

Notch Locations for Weld and Heat Affected Zone Slow-Notch-Bend and Precracked Charpy Impact Test Specimens

Figure 99

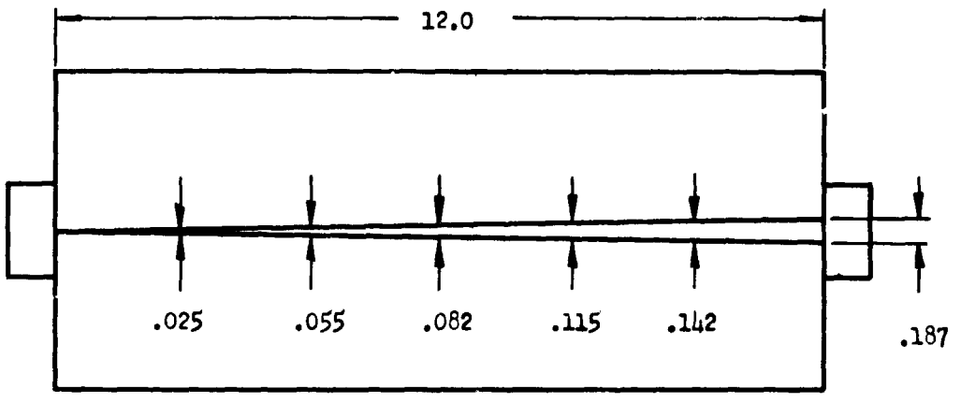

View Showing Typical Gap Weld Plate Set-Up

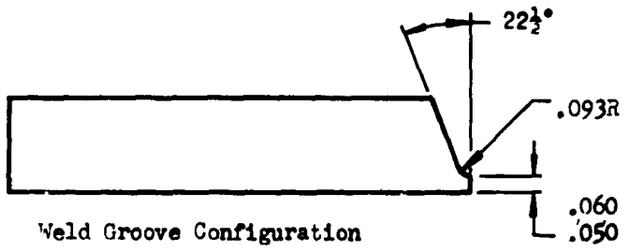

Weld Groove Configuration

Plate No.	Amps	Volts	Travel I.P.M.	Wire I.P.M.	Burn-Thru Gap - Inches	Root Thick. Inches
1	125	7.5	8	8	.065	.055 - .055
2	125	8	8	8	.035	.041 - .052
3	115	7.5	6	8	.045	.051 - .056
4	115	7.5	6	14	.070	.055 - .055
5	115	7.5	6	16	.100	.055 - .056

Weld-Joint Design and Welding Conditions for Single-U Joint Gap-Weld Test, 18%-Nickel Maraging Steel Plate Material

Figure 100

Aging Cycle Temp, °F	Aging Cycle Time, hr	Specimen Orientation	0.2% Offset Yield Strength, ksi	Ultimate Strength, ksi	Elongation in 1 in., %	Reduction of Area, %	Location of Failure
900	8	Longitudinal	225	240	10.9	51.0	-
			226	242	9.5	48.4	-
			226	237	10.8	52.3	-
		Avg	224	240	10.6	50.5	
900	8	Transverse	231	236	9.9	51.0	HAZ
			226	232	10.0	55.0	HAZ
			226	231	9.8	54.8	HAZ
		Avg	228	233	9.9	53.6	

* HAZ = Heat-affected zone

Tensile Properties of Weldments Made in Republic Heat 3920556 with 07495 Filler Wire, 0.070-in.-wide Root Gap, and Single-U Joints

Figure 101

Aging Cycle Temp, °F	Aging Cycle Time, hr	Notch Location	0.2% Offset Yield Strength, ksi		W/A in.-lb/in.^{2}* Test Temperature, °F -40	RT	200
900	8	WM	224		587	773	743
					580	768	699
				Avg	584	770	721
900	8	HAZ	---		1329	1890	1661
					1444	1667	1660
				Avg	1386	1778	1661

* Values were obtained with 0.575 x 0.394-in. specimens.
WM = Weld Metal
HAZ = Heat-affected Zone

Precracked Impact Fracture Toughness of Weldments Made in Republic Heat 3920556 with 07495 Filler Wire, 0.070-in.-wide Root Gap, and Single-U Joints

Figure 102

Specimen Number	Aging Cycle °F - Hr	Notch Location	.2% Offset Yield (ksi)	Width b (in.)	Depth d (in.)	Proportional Limit Load (L) (lbs)	Proportional Limit Deflect. (e) (in.)	Maximum Load (lbs)	eb/L in.^{2}/lb x 10^{-8}
WE 8	900-8	Weld	224	.575	.749	6200	.0202	6370	187
WE 9				.576	.750	8200	.0190	8220	133
WE 10				.575	.750	4350	.0165	5275	218
WE 11				.575	.750	6050	.0169	6760	160
WE 12	900-8	Heat-Affected Zone		.575	.750	8900	.0243	10760	157
WE 13				.575	.750	7200	.0228	8150	182
WE 14				.575	.750	4300	.0219	5460	293
WE 15				.576	.749	8900	.0253	9730	164
WE 16				.575	.750	8450	.0245	9315	167

(1) Five-Point Curve Fitting
(2) Least Squares Statistical Method; Curve Equation: $= 1.09 \times 10^{-6} + 1.41 \times 10^{-6}\ a - 7.93 \times 10^{-6}\ a^2 + 4.10 \times 10^{-5}\ a^3$
(3) Bueckner's Method

Notch Plus Crack Depth			Plane Strain Fracture Toughness in-lb/in.^{2}			Stress Intensity Factor 1000 psi in.		
Effective		Measured						
a_1(in.)(1)	a_2(in.)(2)	a_3(in.)(3)	G_{nc_1}(1)	G_{nc_2}(2)	G_{Ic}(3)	K_{nc_1}(1)	K_{nc_2}(2)	K_{Ic}(3)
.298	.295	.351	435	433	610			
.180	.182	.210	304	265	355			
.330	.331	.385	269	292	387			
.255	.253	.276			326			
			Avg. 336	Avg. 330	Avg. 419	Avg. 101	Avg. 100	Avg. 113
		.264						
		.312			640			
		.435			607			
		.272			695			
		.273			622			
					Avg. 641			Avg. 139

Slow-Notch-Bend Fracture Toughness of Weld Metal and Heat-Affected Zone, Republic Heat 3920556, Grade 200, Vacuum-Arc Remelted, 18%-Nickel Maraging Steel Plate, 07495 Filler Wire, and Single-U Joint with 0.070-in. Root Gap

Figure 103 -2

Weld Wire Heat No.	Composition, wt %										Gas Analysis, ppm		
	C	Mn	P	S	Si	Ni	Mo	Ti	Co	Al	H	O	N
34428	0.018	0.02	-	0.004	0.02	18.2	4.0	0.31	7.6	0.08			
34481	0.014	0.01	0.005	0.006	0.01	18.4	3.6	0.26	7.73	0.08	1.0	25	6
08436	0.01	0.02	0.003	0.006	0.01	17.90	3.63	0.25	7.77	0.04	3.7	13	37
63343	0.02	0.01	0.005	0.005	0.01	18.1	3.70	0.29	7.70	0.06	5	45	25

Plate No.	Composition, wt %*										Added during melting		
	C	Mn	P	S	Si	Ni	Mo	Ti	Co	Al	B	Zr	Ca**
R-599-1	0.025	0.08	0.004	0.006	0.087	17.98	4.32	0.15	7.75	0.08	0.003	0.02	0.06
R-600-1	0.015	0.04	0.006	0.008	0.04	17.96	4.32	0.19	7.56	0.07	0.003	0.02	0.06
R-600-1A	0.017	0.04	0.007	0.010	0.04	18.10	4.24	0.20	7.58	0.07	0.003	0.02	0.06
25000-1	0.020	0.020	0.005	0.008	0.013	18.47	4.15	0.21	7.74	0.064			

* Averaged from six locations on the plate.
** Added in increments of 0.02.

Mill Certified Analysis on Chemical Composition of Weld Wire: Mill Certified Chemical Analyses

Figure 104

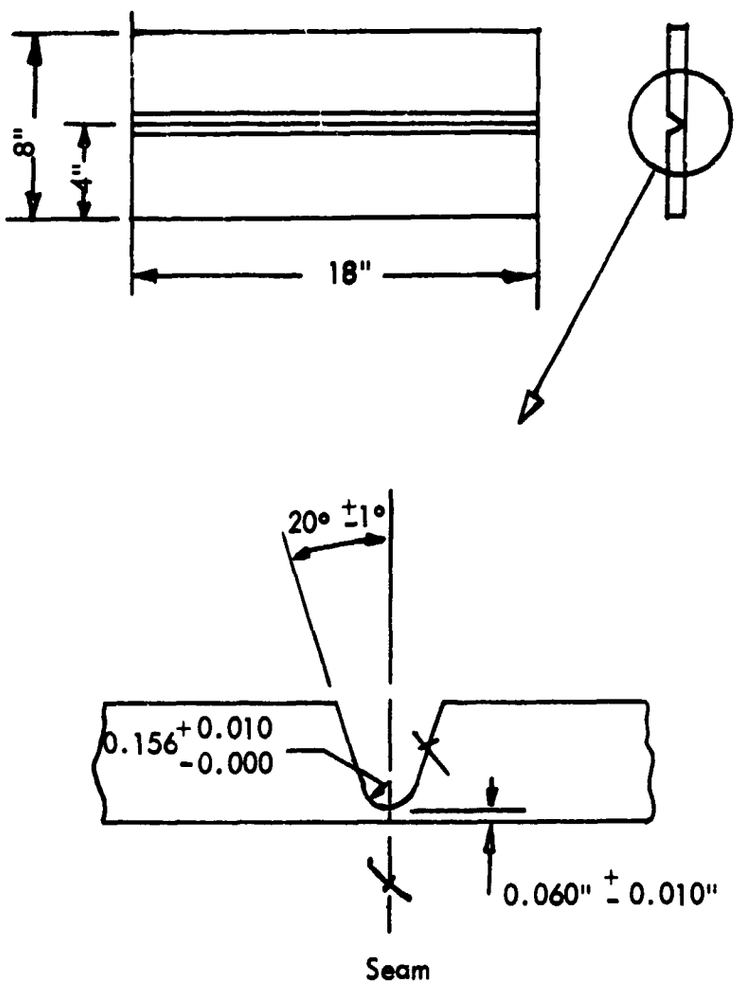

Joint Detail for Weld Test Plates

Figure 105

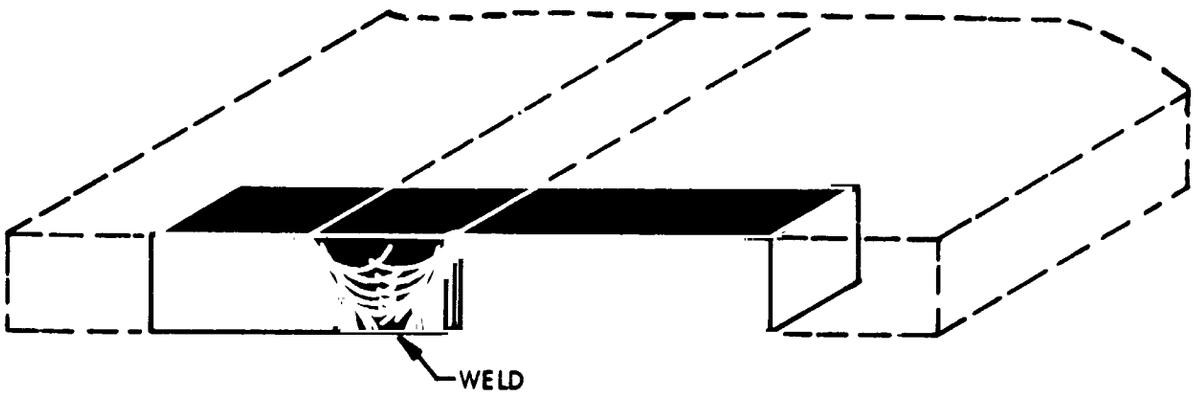

Locations of Notches for Weld Heat-Affected-Zone Slow-Notch Bend Specimens, Calibration Bars, and Precracked Impact Specimens

Figure 106

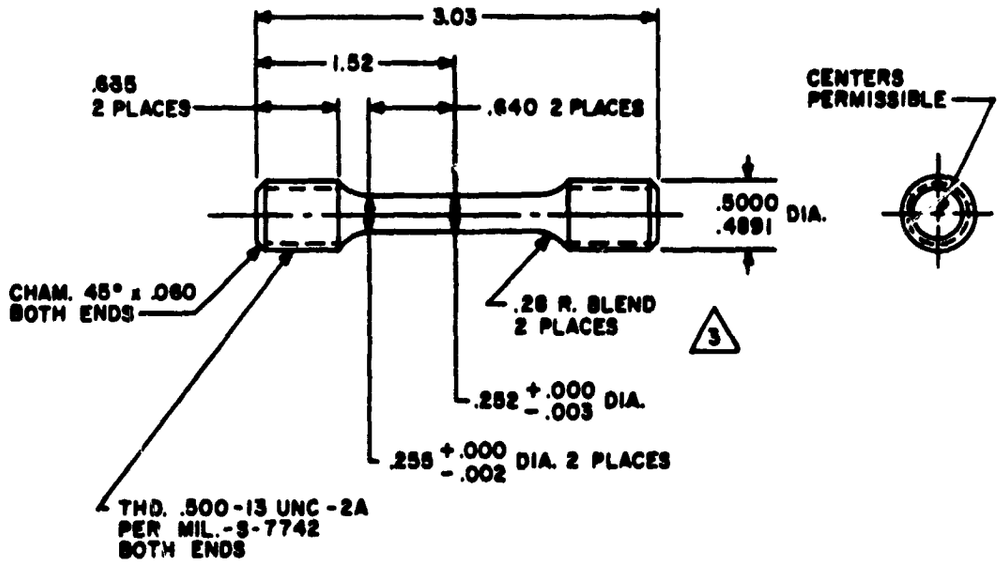

Tensile Specimen, 0.250-in. Round

Figure 107

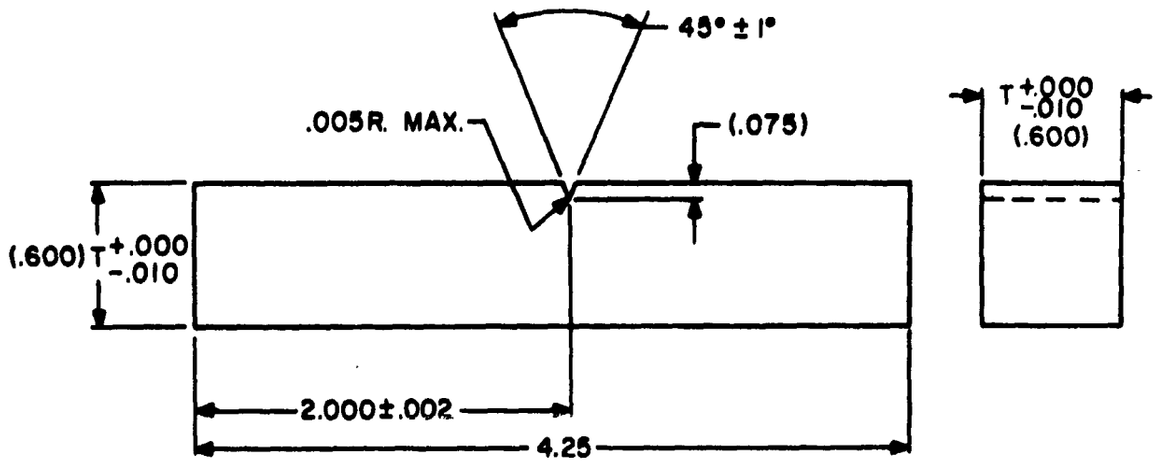

T = MINIMUM PLATE GAUGE THICKNESS

Slow-Notch-Bend Specimen

Figure 108

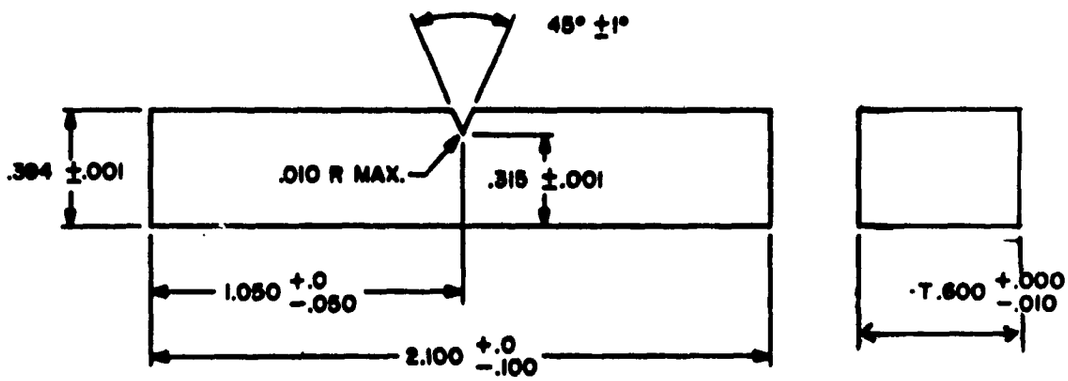

T = MINIMUM PLATE GAUGE THICKNESS

Charpy V-Notch Impact Specimen

Figure 109

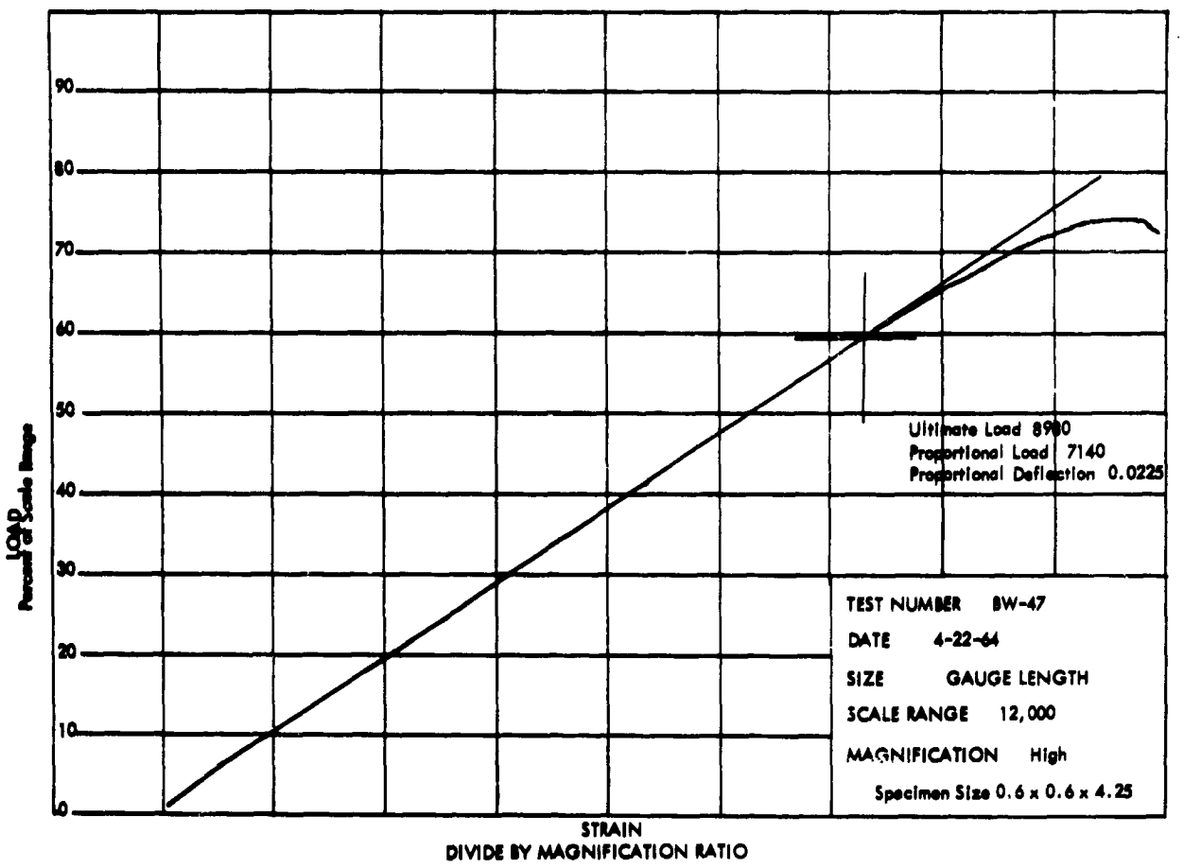

Load Deflection Curve Showing Deviation from Linearity

Figure 110

Aging Cycle Temperature, °F	Aging Cycle Time, hours	Orientation	0.2% Offset Yield Strength, ksi	Ultimate Tensile Strength, ksi	Elongation in 1 inch, %	Reduction in Area, %
850	8	Longitudinal	206	215	12	50
850	8	Longitudinal	206	215	12	54
850	8	Longitudinal	209	218	12	48
			207 Avg.			
850	8	Transverse	214	217	11	50
850	8	Transverse	212	217	11	54
850	8	Transverse	212	217	11	56
			213 Avg.			
900	4	Transverse	214	219	11	54
900	4	Transverse	214	218	11	52
900	4	Transverse	214	219	11	54
			214 Avg.			
900	8	Longitudinal	211	220	14	39
900	8	Longitudinal	211	219	13	38
900	8	Longitudinal	211	221	12	38
			211 Avg.			
900	8	Transverse	220	224	11	46
900	8	Transverse	220	225	14	55
900	8	Transverse	220	225	12	53
			220 Avg.			
950	8	Transverse	211	219	2	5
950	8	Transverse	208	220	13	51
950	8	Transverse	212	221	12	54
			210 Avg.			

NOTE: Specimens broke in weld metal

Tensile Test Data Obtained from Lukens Plate R-599-1 and Special Metals Weld Wire 34428

Figure 111

Aging Cycle Temperature, °F	Aging Cycle Time, hours	Orientation	0.2% Offset Yield Strength, ksi	Ultimate Tensile Strength, ksi	Elongation in 1 inch, %	Reduction in Area, %
900	8	Transverse	199	208	11	48
900	8	Transverse	202	208	11	50
900	8	Transverse	202	209	11	44
900	8	Transverse	196	206	11	49
900	8	Transverse	199	203	13	53
900	8	Transverse	187	195	15	63
900	8	Transverse	197	206	14	53
900	8	Transverse	187	194	14	60
900	8	Transverse	199 196 Average	207	15	57

NOTE: Specimens fractured in heat affected zone

Tensile Test Data Obtained from Lukens Plate R-599-1 and Special Metals Weld Wire 34428

Figure 112

Specimen Number	Aging Cycle °F-Hr	Width b, in	Depth d, in	$1/M \times 10^6$ in^2/lb	Effective a, in *	Measured a, in *	Proportional Load Limit, lb	Maximum Load, lb	Fracture Toughness G_{nc} in-lb/in^2	Fracture Toughness G_{Ic} in-lb/in^2	Stress Intensity Factor K_{nc} 1000 psi$\sqrt{in}$	Stress Intensity Factor K_{Ic} 1000 psi $\sqrt{in}$
AUTOMATIC WELDS												
BTW-1	950-8	0.597	0.597	1.806	0.1346	0.1162	8760	9180	562	413	129	111
BTW-2	950-8	0.597	0.597	1.809	0.1352	0.1248	7920	8700	462	372	117	105
BTW-3	950-8	0.597	0.597	1.875	0.1470	0.1335	7800	8320	504	397	123	109
BTW-4	950-8	0.597	0.595	1.760	0.1254	0.1199	7800	9050	404	346	109	102
BTW-5	950-8	0.597	0.597	1.604	0.0837	0.1302	9120	8610	329	524	99	125
								Average Values	452	410	115	110
BTW-6	900-8	0.598	0.597	1.847	0.1422	0.1410	6960	7230	382	342	107	101
BTW-7	900-8	0.598	0.598	1.812	0.1358	0.1265	7260	8018	389	315	108	96
BTW-8	900-8	0.593	0.596	2.055	0.1739	0.1648	6060	6480	394	342	108	101
BTW-9	900-8	0.597	0.597	1.945	0.1583	0.1577	6600	6680	401	369	109	105
BTW-10	900-8	0.590	0.597	1.833	0.1397	0.1303	7080	7600	396	324	108	97
								Average Values	392	338	108	101
BTW-11	900-4	0.597	0.597	1.880	0.1479	0.1379	7620	7920	485	398	120	101
BTW-12	900-4	0.597	0.597	1.805	0.1344	0.1283	7440	8400	405	341	110	101
BTW-13	900-4	0.597	0.597	2.009	0.1676	0.1715	6240	6800	390	380	108	106
BTW-14	900-4	0.597	0.595	1.927	0.1555	0.1531	6660	7110	398	363	109	104
BTW-15	900-4	0.597	0.598	1.846	0.1420	0.1331	7440	8040	437	357	114	103
								Average Values	423	368	112	105
BTW-16	850-8	0.596	0.598	1.800	0.1335	0.1088	8940	10200	581	396	131	108
BTW-17	850-8	0.597	0.598	1.813	0.1360	0.1234	7740	9090	445	347	115	102
BTW-18	850-8	0.597	0.598	1.949	0.1589	0.1550	7200	7560	480	423	120	112
BTW-19	850-8	0.597	0.598	1.837	0.1404	0.1320	7800	8650	472	388	118	107
BTW-20	850-8	0.597	0.597	1.835	0.1400	0.1285	8460	8880	554	442	128	114
								Average Values	506	399	123	101
MANUAL WELDS												
BTW-22	900-8	0.594	0.596	1.897	0.1507	0.1515	6420	7150	357	333	103	100
BTW-23	900-8	0.594	0.596	1.907	0.1523	0.1280	6540	6960	376	267	106	89
BTW-24	900-8	0.595	0.596	1.903	0.1517	0.1700	5160	8640	232	260	83	88
BTW-25	900-8	0.590	0.596	1.912	0.1531	0.1835	5400	7200	262	332	88	100
BTW-26	900-8	0.590	0.596	1.762	0.1258	0.1217	7200	9120	354	306	103	95
BTW-27	900-8	0.594	0.596	2.180	0.1894	0.2232	5040	6000	309	424	95	112
BTW-28	900-8	0.594	0.596	1.768	0.1271	0.1213	8400	8820	482	409	119	110
BTW-29	900-8	0.595	0.596	1.887	0.1479	0.1587	6780	7800	387	399	107	109
								Average Values	345	341	101	101

* NOTE: Effective "a" and measured "a" values have an accuracy of ± 0.0010 inch.

Effect of Aging Time and Temperature on the Plane-Strain Fracture Toughness of Welds Made with Lukens Plate R-599-1 and Special Metals Weld Wire 34428; Slow-Notch-Bend Specimens

Figure 113

Aging Cycle Temperature, °F	Aging Cycle Time, hours	Orientation	0.2% Offset Yield Strength, ksi	Ultimate Tensile Strength, ksi	Elongation in 1 inch, %	Reduction in Area, %
900	4	Longitudinal	202	210	12	56
900	4	Longitudinal	206	212	12	52
900	4	Longitudinal	206	212	12	56
			205 Avg.			
900	4	Transverse	206	213	12	58
900	4	Transverse	209	215	12	60
900	4	Transverse	212	215	12	58
			209 Avg.			
900	8	Longitudinal	206	216	12	56
900	8	Longitudinal	212	215	13	60
900	8	Longitudinal	217	224	11	53
			212 Avg.			
900	8	Transverse	218	222	11	52
900	8	Transverse	218	222	11	56
900	8	Transverse	218	221	11	48
			218 Avg.			
900	8	Transverse	212	217	10	54
900	8	Transverse	212	217	10	54
900	8	Transverse	215	219	11	59
900	8	Transverse	214	218	11	59
900	8	Transverse	214	217	11	54
900	8	Transverse	212	215	10	51
			213 Avg.			
Maraged with First 36-Inch PETV		Transverse	208	214	12	52
Maraged with First 36-Inch PETV		Transverse	205	211	12	55
Maraged with First 36-Inch PETV		Transverse	208	211	12	54
			207 Avg.			
Maraged with First 36-Inch PETV Repair Procedure 1		Transverse	209	214	12	58
Maraged with First 36-Inch PETV Repair Procedure 1		Transverse	212	214	11	54
Maraged with First 36-Inch PETV Repair Procedure 1		Transverse	208	213	12	53
			210 Avg.			

NOTE: All specimens broke in weld metal

Tensile Test Data Obtained from Lukens Plate R-600-1 and Special Metals Weld Wire 34481

Figure 114

Aging Cycle Temperature, °F	Aging Cycle Time, hours	Orientation	0.2% Offset Yield Strength, ksi	Ultimate Tensile Strength, ksi	Elongation in 1 inch, %	Reduction in Area, %
900	4	Transverse	203	208	11	76
900	4	Transverse	205	210	11	57
900	4	Transverse	205	210	10	59
900	4	Transverse	205	210	12	59
			205 Avg.			
900	8	Longitudinal	208	214	11	55
900	8	Longitudinal	202	212	12	57
900	8	Longitudinal	202	213	12	55
			204 Avg.			
900	8	Transverse	209	214	12	76
900	8	Transverse	211	214	11	57
900	8	Transverse	208	214	11	57
900	8	Transverse	209	212	12	56
			209 Avg.			

NOTE: All specimens broke in weld metal

Tensile Test Data Obtained from Lukens Plate R-600-1A and Armetco Weld Wire 08436

Figure 115

Specimen Number	Aging Cycle °F, Hr	Width b, in	Depth d, in	1/M x 10^6 in^2/lb	Effective a, in*	Measured a, in*	Proportional Load Limit, lb	Maximum Load, lb	Fracture Toughness Gnc in-lb/in^2	Fracture Toughness Glc in-lb/in^2	Stress Intensity Factor Knc 1000 psi $\sqrt{in}$	Stress Intensity Factor Klc 1000 psi $\sqrt{in}$
AUTOMATIC WELDS												
BW-30	900-4	0.599	0.600	1.852	0.1295	0.1387	7440	9060	291	372	93	105
BW-31	900-4	0.600	0.600	1.852	0.1295	0.1200	7740	9850	314	326	96	98
BW-32	900-4	0.599	0.600	1.704	0.0777	0.0992	9840	13700	279	419	91	111
BW-33	900-4	0.599	0.600	1.923	0.1466	0.1509	6840	8350	296	358	93	103
BW-34	900-4	0.599	0.600	1.819	0.1203	0.1290	7560	9130	272	345	90	102
								Average Values	291	364	93	104
BW-35	900-8	0.600	0.600	1.852	0.1295	0.1333	7440	8400	290	349	93	102
BW-36	900-8	0.600	0.600	1.819	0.1203	0.1311	7560	8720	271	352	90	102
BW-37	900-8	0.600	0.600	1.822	0.1211	0.1258	7560	8720	273	332	90	100
BW-38	900-8	0.600	0.600	1.766	0.1032	0.1192	7800	8900	238	328	84	98
BW-39	900-8	0.600	0.600	1.808	0.1170	0.1268	7440	8860	253	325	87	98
								Average Values	265	337	89	100
WELD HEAT AFFECTED ZONE												
BWH-1	900-4	0.600	0.594	1.939	0.1538	0.1380	6180	6640	266	265	89	89
BWH-2	900-4	0.600	0.600	1.861	0.1364	0.1250	6600	7120	240	251	84	86
BWH-3	900-4	0.600	0.600	1.786	0.1141	0.1185	7200	7580	201	277	78	91
BWH-4	900-4	0.600	0.600	1.783	0.1130	0.1123	7560	7910	218	286	81	92
BWH-5	900-4	0.600	0.600	1.827	0.1272	0.1287	6720	7050	217	271	80	89
								Average Values	228	270	82	89
BWH-6	900-8	0.599	0.600	1.834	0.1292	0.1333	7500	8120	279	356	91	103
BWH-7	900-8	0.600	0.600	1.830	0.1281	0.1382	7200	8040	252	345	87	102
BWH-8	900-8	0.600	0.600	1.830	0.1281	0.1391	7200	8130	252	348	87	102
BWH-9	900-8	0.600	0.600	1.906	0.1469	0.1600	6600	7300	277	365	91	104
BWH-10	900-8	0.600	0.600	1.822	0.1257	0.1264	7560	8590	268	334	89	100
								Average Values	266	350	89	102

* NOTE: Effective "a" and measured "a" values have an accuracy of ± 0.0010 inch.

Effect of Aging Time and Temperature on the Plane-Strain Fracture Toughness of Welds and Weld Heat-Affected Zone of Lukens Plate R-600-1 and Special Metals Weld Wire 34481; Slow-Notch-Bend Specimens

Figure 116

Effect of Aging Time and Temperature on the Plane-Strain Fracture Toughness of Welds and Weld Heat-Affected Zone of Lukens Plate R-600-1A and Armetco Weld Wire 08436; Slow Notch Bend Specimens

Figure 117

Specimen Number	Aging Cycle °F, Hr	Width b, in	Depth d, in	1/M x 10^6 in^2/lb	Effective a, in*	Measured a, in*	Proportional Load Limit, lbs	Maximum Load, lb	Fracture Toughness Gnc in-lb/in^2	Fracture Toughness Glc in-lb/in^2	Stress Intensity Factor Knc 1000 psi, $\sqrt{in}$	Stress Intensity Factor Klc 1000 psi, $\sqrt{in}$
AUTOMATIC WELDS												
SW-40	900-4	0.599	0.599	1.833	0.1247	0.1080	7680	10400	227	270	82	90
SW-41	900-4	0.598	0.599	1.849	0.1302	0.1100	7860	10520	263	290	88	93
SW-42	900-4	0.598	0.598	1.840	0.1272	0.1160	7800	10400	246	307	85	95
SW-43	900-4	0.598	0.598	1.863	0.1347	0.1220	7800	10200	279	326	91	98
SW-44	900-4	0.598	0.598	1.883	0.1405	0.1320	7620	9660	292	345	93	101
								Average Values	262	306	88	95
SW-45	900-8	0.598	0.598	1.859	0.1334	0.1320	7560	9100	257	339	87	100
SW-46	900-8	0.598	0.599	1.875	0.1382	0.1270	7080	8580	243	281	85	91
SW-47	900-8	0.598	0.598	1.884	0.1408	0.1360	7140	8900	258	315	87	97
SW-48	900-8	0.597	0.597	1.836	0.1258	0.1220	7500	9200	223	305	82	95
SW-49	900-8	0.597	0.597	1.913	0.1483	0.1450	7020	8800	280	337	91	100
								Average Values	252	316	86	97
WELD HEAT AFFECTED ZONE												
SWH-11	900-4	0.596	0.597	1.834	0.1229	0.1270	7800	9080	332	348	109	102
SWH-12	900-4	0.599	0.600	1.824	0.1203	0.1110	7980	9440	337	299	100	94
SWH-13	900-4	0.599	0.600	1.785	0.1096	0.0980	7920	9440	302	257	94	87
SWH-14	900-4	0.599	0.599	1.845	0.1257	0.1120	7920	9340	347	300	102	94
SWH-15	900-4	0.599	0.599	1.831	0.1222	0.0970	8880	9960	423	321	112	98
								Average Values	348	305	102	95
SWH-16	900-8	0.599	0.599	1.827	0.1211	0.1150	8460	9780	381	353	106	102
SWH-17	900-8	0.599	0.599	1.831	0.1222	0.1070	8340	9380	373	316	105	97
SWH-18	900-8	0.598	0.599	1.856	0.1285	0.1170	7860	9500	351	312	102	96
SWH-19	900-8	0.599	0.599	1.787	0.1101	0.1130	8580	10140	356	356	103	103
SWH-20	900-8	0.599	0.599	1.791	0.1113	0.1200	8760	10100	375	399	106	109
								Average Values	367	347	105	101

* NOTE: Effective "a" and measured "a" values have an accuracy of ± 0.0010 inch.

Aging Cycle		Orientation	Notch Location	W/A, in-lb/in^2			
Temperature, °F	Time, hours			-40°F	RT	200°F	
900	4	Transverse	Weld	1128	1306	1397	
				1206	1380	1390	
				1197	1343	1394	Avg.
900	8	Transverse	Weld	857	1067	1253	
				935	935	1181	
				896	1001	1217	Avg.
900	4	Transverse	HAZ *	698	805	883	
				720	805	833	
				709	805	833	Avg.
900	8	Transverse	HAZ	675	726	832	
				684	799	809	
				680	762	820	Avg.

* HAZ - Heat affected zone

NOTE: The corresponding 0.2% offset yield strength at a maraging cycle of 900°F-4 hours is 209 ksi.

The corresponding 0.2% offset yield strength at a maraging cycle of 900°F-8 hours is 218 ksi.

Specimen size: 0.394 inch depth x 0.600-inch wide x 2.10 inch length

Plane-Stress Fracture Toughness of Welds Made With Lukens Plate R-600-1 and Special Metals Weld Wire 34481

Figure 118

Aging Cycle Temperature, °F	Aging Cycle Time, hours	Orientation	Notch Location	W/A, in-lb/in² -40°F	RT	200°F	
900	4	Transverse	Weld	1210	1479	1687	
				1145	1509	1615	
				1178	1494	1651	Avg.
900	8	Transverse	Weld	992	1328	1629	
				1011	1312	1400	
				1002	1320	1515	Avg.
900	4	Transverse	HAZ *	882	1396	1367	
				962	1460	1357	
				922	1428	1362	Avg.
900	8	Transverse	HAZ	992	1273	1256	
				1161	1303	1190	
				1076	1288	1223	Avg.

* HAZ - Heat affected zone

NOTE: The corresponding 0.2% offset yield strength at a maraging cycle of 900°F-4 hours is 205 ksi.

The corresponding 0.2% offset yield strength at a maraging cycle of 900°F-8 hours is 209 ksi.

Specimen size: 0.394 inch depth x 0.600-inch wide x 2.10 inch length

Plane-Stress Fracture Toughness of Welds Made With Lukens Plate R-600-1A and Armetco Weld Wire 08436

Figure 119

Aging Cycle Temperature, °F	Aging Cycle Time, hours	Orientation		0.2% Offset Yield Strength ksi	Ultimate Tensile Strength ksi	Elongation in 1 Inch %	Reduction in Area %
850	4	Transverse		197	204	11	51
				197	204	10	58
				197	205	11	61
			Avg	197	204	11	57
850	8	Transverse		209	214	11	58
				203	210	12	60
				209	213	12	58
			Avg	207	212	12	59
850	16	Transverse		214	219	12	57
				212	218	11	55
				212	218	11	56
			Avg	213	218	11	56
900	4	Longitudinal		208	216	10	56
				211	220	11	54
				208	219	11	57
			Avg	209	218	11	56
900	4	Transverse		204	210	11	56
				204	211	11	60
				208	214	15	58
			Avg	205	212	12	58
900	8	Longitudinal		215	224	13	55
				208	216	12	57
				208	217	11	54
			Avg	210	219	12	55
900	8	Transverse		212	217	11	56
				211	218	10	52
				211	216	11	67
			Avg	211	217	11	58
900	16	Transverse		209	218	12	57
				208	218	11	56
				208	219	11	51
			Avg	208	218	11	55
925	4	Longitudinal		206	214	12	54
				205	214	12	54
				206	213	12	58
			Avg	206	214	12	56
925	4	Transverse		209	215	11	57
				209	215	12	56
				208	214	11	55
			Avg	209	215	11	56
925	8	Longitudinal		205	214	12	54
				205	215	13	53
				206	214	12	52
			Avg	205	214	12	53
925	8	Transverse		212	220	11	55
				211	218	11	54
				212	219	12	54
			Avg	212	218	11	54
950	4	Transverse		196	208	9	51
				202	212	12	53
				202	212	14	55
			Avg	200*	210	12	53
950	8	Transverse		197	207	10	54
				194	204	10	54
				199	209	12	54
			Avg	196*	207	11	54
950	16	Transverse		189	202	12	60
				189	202	11	57
				191	202	11	56
			Avg.	190*	202	11	58
Managed with Second 36-Inch PETV		Transverse		215	222	12	53
				218	223	11	54
				215	221	11	47
			Avg	216	222	11	51
Managed with Second 36-Inch PETV (Manual Repair Weld)		Transverse		212	217	11	56
				212	218	10	48
				206	210	10	58
			Avg	210	215	10	54

* Specimens broke through weld heat affected zone. All other specimens broke in weld metal

Tensile Test Data Obtained from Welds Made With 260-SL-1 Plate and Special Metals Weld Wire 63343

Figure 120

Specimen Number	Aging Cycle °F, Hr	Width b, in	Depth d, in	$1/M \times 10^6$ in^2/lb	Effective a, in*	Measured a, in*	Proportional Load Limit, lb	Maximum Load, lb		Fracture Toughness Gnc in-lb/in^2	Fracture Toughness Glc in-lb/in^2	Stress Intensity Factor Knc 1000 psi $\sqrt{in}$	Stress Intensity Factor Klc 1000 psi $\sqrt{in}$
DBW-1	850-8	0.591	0.594	2.255	0.1851	0.2130	4140	5580		168	242	71	85
DBW-2	850-8	0.591	0.594	2.449	0.2103	0.2220	4320	5360		231	289	83	93
DBW-3	850-8	0.592	0.597	2.466	0.2123	0.2560	3840	4960		185	314	74	96
DBW-4	850-8	0.593	0.593	2.336	0.1964	0.2280	4440	5520		212	325	79	98
DBW-5	850-8	0.592	0.595	2.635	0.2299	0.2470	4020	4880		241	319	85	97
									Avg.	208	297	78	94
DBW-6	900-4	0.593	0.593	2.208	0.1781	0.1640	5100	7000		239	225	84	82
DBW-7	900-4	0.593	0.594	2.620	0.2284	0.2480	3960	4860		230	314	83	97
DBW-8	900-4	0.593	0.593	2.511	0.2173	0.2240	4320	5340		245	295	85	94
DBW-9	900-4	0.591	0.594	2.189	0.1751	0.2120	4860	6060		214	330	80	99
DBW-10	900-4	0.593	0.594	2.360	0.1995	0.2240	4320	4940		207	292	78	93
									Avg.	227	291	82	93
DBW-11	900-8	0.593	0.593	2.339	0.1968	0.2350	4260	4980		196	321	76	98
DBW-12	900-8	0.592	0.594	2.003	0.1419	0.1720	5820	6700		241	316	84	97
DBW-13	900-8	0.591	0.593	2.180	0.1737	0.2100	5160	6000		238	368	84	104
DBW-14	900-8	0.592	0.592	2.003	0.1419	0.1770	5700	6480		231	324	83	98
DBW-15	900-8	0.593	0.593	2.141	0.1673	0.1690	4680	5380		185	199	74	77
									Avg.	218	306	80	95
DBW-16	950-8	0.592	0.593	2.472	0.2130	0.2140	4620	5660		270	306	89	95
DBW-17	950-8	0.591	0.594	2.499	0.2160	0.2050	4800	5720		301	300	94	94
DBW-18	950-8	0.593	0.590	2.681	0.2342	0.2520	4200	5400		274	383	90	107
DBW-19	950-8	0.588	0.594	2.387	0.2029	0.2050	5220	6580		317	359	97	103
DBW-20	950-8	0.592	0.593	2.294	0.1907	0.2190	5340	6640		293	430	93	113
									Avg.	291	356	93	102
BW-75	Managed with	0.596	0.596	2.309	0.1927	0.1990	4800	5240		238	273	84	90
BW-76	Second 36-inch	0.593	0.594	2.116	0.1630	0.2010	5520	6420		249	379	86	106
BW-77	PETV	0.598	0.595	2.374	0.2013	0.2320	4860	5340		262	391	88	108
									Avg.	250	348	86	101

* NOTE: Effective "a" and measured "a" values have an accuracy of $\pm$ 0.0010 inch.

Effect of Aging Time and Temperature on the Plane-Strain Fracture Toughness of Welds Made with Allegheny Ludlum Plate 25000-1 and Special Metals Weld Wire 63343 Slow-Notch-Bend Specimens

Figure 121

Specimen Number	Aging Cycle °F, Hr	Width b, in	Depth d, in	Measured a, in *	Proportional Load Limit, lb	Maximum Load, lb	Fracture Toughness G_{Ic} in-lb/in^2	Nominal Stress At Root of Notch **
DBW-11	900-8	0.593	0.593	0.2350	4260	4980	321	252
DBW-12	900-8	0.592	0.594	0.1720	5820	6700	316	248
DBW-13	900-8	0.591	0.593	0.2100	5160	6000	368	268
DBW-14	900-8	0.592	0.592	0.1770	5700	6480	324	251
DBW-15	900-8	0.593	0.593	0.1690	4680	5380	199	196
						Avg.	306	245
GBW-1	900-8	0.595	0.868	0.191	14100	15000	388	232
GBW-2	900-8	0.592	0.868	0.186	14100	14850	377	230
GBW-3	900-8	0.598	0.868	0.176	16350	16900	462	257
GBW-4	900-8	0.600	0.868	0.186	14400	15250	383	232
GBW-5	900-8	0.599	0.869	0.208	13000	13450	448	245
						Avg	412	239
GBW-6	900-8	0.600	0.999	0.253	18000	20150	497	243
GBW-7	900-8	0.598	0.999	0.205	18600	22050	400	222
GBW-8	900-8	0.598	0.999	0.250	17250	19700	450	232
GBW-9	900-8	0.595	0.999	0.183	19800	23950	401	225
GBW-10	900-8	0.598	0.998	0.180	19800	24300	398	225
						Avg	429	229

* "a" measured accuracy ± 0.001

** Nominal stress $\frac{(4.5)\,P}{B\,(D-a)^2}$

Effect of Specimen Depth on the Plane-Strain Fracture Toughness of Welds Made with Special Metals Weld Wire Heat 63343; Slow-Notch Bend Specimens

Figure 122

Specimen Number	Aging Cycle °F, Hr	Width b, in	Depth d, in	$1/M \times 10^6$ in^2/lb	Effective a, in*	Measured a, in*	Proportional Load Limit, lb	Maximum Load, lb	Fracture Toughness Gnc in-lb/in^2	Fracture Toughness Glc in-lb/in^2	Stress Intensity Factor Knc 1000 psi, $\sqrt{in}$	Stress Intensity Factor Klc 1000 psi, $\sqrt{in}$
DBWH-1	900-4	0.594	0.600	2.243	0.1986	0.2280	5640	6080	286	491	92	121
DBWH-2	900-4	0.594	0.599	2.176	0.1878	0.2020	5760	6620	284	398	92	109
DBWH-3	900-4	0.596	0.599	2.118	0.1780	0.1990	5880	6720	279	400	91	109
DBWH-4	900-4	0.596	0.600	2.063	0.1681	0.1870	6240	7060	298	397	94	109
DBWH-5	900-4	0.594	0.600	2.111	0.1767	0.1950	5880	6400	279	384	91	107
								Average Values	285	414	92	111
DBWH-6	900-8	0.597	0.600	1.931	0.1419	0.1680	7080	7790	326	422	98	112
DBWH-7	900-8	0.595	0.600	2.098	0.1744	0.1750	6240	5890	310	354	96	102
DBWH-8	900-8	0.593	0.600	1.939	0.1436	0.1670	6240	[illegible]	259	329	88	99
DBWH-9	900-8	0.589	0.600	2.194	0.1908	0.1940	5880	[illegible]	305	387	95	107
DBWH-10	900-8	0.589	0.600	2.360	0.2163	0.2080	5340	5680	283	366	92	104
								Average Values	297	371	94	105

* NOTE: Effective "a" and measured "a" values have an accuracy of ± 0.0010 inch.

Plane-Strain Fracture Toughness of the Weld Heat-Affected Zone, Allegheny Ludlum Plate 25000-1 and Special Metals Weld Wire 63343; Slow-Notch Bend Specimens

Figure 123

Aging Cycle Temperature, °F	Aging Cycle Time, hours	Orientation	Notch Location	0.2% Offset Yield Strength ksi	W/A, in-lb/in^2 -40°F	W/A, in-lb/in^2 RT	W/A, in-lb/in^2 200°F
850	8	Transverse	Weld	207	806	1327	1509
					839	1432	1412
					860	1322	1190
					Avg. 835	1360	1370
900	4	Transverse	Weld	205	890	1464	1692
					867	1211	1337
					875	1312	1252
					Avg. 877	1329	1427
900	4	Transverse	HAZ*		736	1021	1140
					737	960	1121
					Avg. 736	990	1130
900	8	Transverse	Weld	211	828	1145	1062
					816	1038	1058
					801	1038	1430
					Avg. 815	1074	1183
900	8	Transverse	HAZ*		848	1037	896
					881	-	1331
					Avg. 864	1037	1114
950	8	Transverse	Weld	197	952	1332	1730
					900	1214	1431
					885	1268	1341
					Avg. 912	1271	1501
Maraged with second 36-inch PETV		Transverse	Weld	216		947	
		Auto				775	
						720	
					Avg.	814	
						880	
		Manual		210		821	
						1055	
					Avg.	919	
Maraged with second 36-inch PETV		Transverse	HAZ*			825	
		Auto				964	
						1034	
					Avg.	941	
						1082	
		Manual				954	
						1062	
					Avg.	1033	

* Heat affected zone

NOTE: The corresponding 0.2% offset yield strengths are averages of three specimens unless otherwise specified.

Plane-Stress Fracture Toughness of Welds Made with 260-SL-1 Plate and Special Metals Weld Wire 63343

Figure 124

Plate	Weld Wire	Aging Cycle Temperature, °F	Aging Cycle Time, hours	Type of Repair	0.2% Offset Yield Strength ksi	Ultimate Tensile Strength ksi	Elong. in 2 Inch %	Reduction in Area %
				Repair Procedure 1				
R-600-1	34481	900	4	auto & manual	200	210	3	5
R-600-1	34481	900	4	auto & manual	210	215	12	47
R-600-1A	34481	900	8	auto & manual	217	220	10	28
R-600-1A	34481	900	8	auto & manual	218	222	10	33
R-600-1A	34481	900	8	auto	216	218	11	49
				Repair Procedure 2				
R-600-1A	08436	900	4	manual	201	203	11	43
R-600-1A	08436	900	4	manual	200	204	12	51
*R-600-1A	08436	900	4	manual	206	213	12/5*	57/18*
*R-600-1A	08436	900	4	manual	197	206	11	57
				Repair Procedure 3				
R-604-1A	08436	900	4	manual	210	216	11	49
R-604-1A	08436	900	4	manual	211	216	8	29

* Average shown for three 1/4-inch round tensile specimens

* 1 specimen only

NOTE: Flat tensile specimen size 8 inches long 2 inches x 0.5 inches x T gage
All tensile specimens broke in weld metal.

Flat Tensile Test Data Obtained from Repair Welds Made with Lukens R-600 and 604 Plate and Weld Wire Heats 34481 and 08436

Figure 125

Repair Procedure 1							
Aging Cycle				W/A, in-lb/in^2			
Temperature, °F	Time, hours	Orientation	Notch Location	-40°F	RT	200°F	
900	4	Transverse	Weld	1003	1392	1464	
				982	1783	1503	
				992	1592	1484	Avg.
900	4	Transverse	HAZ **	675	985	968	
				700	1031	861	
				819	1028	985	
				731	1015	938	Avg.
900	4	Transverse	Weld	1304*	1207*	1707*	
				1038*	1306*	1906*	
				1171*	1256*	1806*	Avg.
Maraged with First 36-Inch PETV		Transverse	Weld		2055		
					1896		
					1688		
					1880	Avg.	
Maraged with First 36-Inch PETV		Transverse	Weld		1310*		
					1345*		
					1618*		
					1424*	Avg.	

NOTE: The corresponding 0.2% offset yield strength at a maraging cycle of 900°F-4 hours is 205 ksi. The corresponding 0.2% offset yield strength for specimens maraged with the first 36-inch PETV is 210 ksi.

* Manual Repair Area

** Heat Affected Zone

Plane-Stress Fracture Toughness of Welds Made with Lukens Plate R-600-1 and Special Metals Weld Wire 34481

Figure 126

(KNOOP HARDNESS NUMBERS)
(500 GM LOAD)

AVERAGE HARDNESS RESULTS					
			Across Top of Weld		
Condition	HUB *	HAZ **	WELD	HAZ	HUB
As-welded	385	348	337	359	361
Maraged (900°F/8 Hr.)	528	480	484	438	521
			Across Middle of Weld		
As-welded	369	256	241	267	-
Maraged (900°F/8 Hr.)	532	476	455	447	495
			Across Bottom of Weld		
As-welded	371	356	358	364	358
Maraged (900°F/8 Hr.)	529	459	461	473	525

NOTES

WELD: Based on 8 to 23 indents at 0.040-inch intervals

HAZ: Based on 4 to 13 indents at 0.020-inch intervals

HUB: Based on 4 to 12 indents at 0.020-inch intervals

* Weld heat-unaffected base (base metal) = HUB
** Weld heat-affected zone (base metal) = HAZ

Microhardness Transverse Summary; Manual Repair in Automatic TIG Weld

Figure 127, Sheet 1 of 4

(KNOOP HARDNESS NUMBERS)
(500 GM LOAD)

RANGE OF HARDNESS RESULTS (Max. - Min. Values)					
			Across Top of Weld		
Condition	HUB *	HAZ **	WELD	HAZ	HUB
As-welded	377-396(19)	340-361(21)	297-400(103)	316-377(61)	356-367(11)
Maraged (900°F/8 Hr.)	509-546(37)	441-495(54)	440-520 (80)	380-474(94)	509-530(21)
			Across Middle of Weld		
As-welded	340-400(60)	184-326(142)	126-351(125)	180-338(158)	106-376(270)
Maraged (900°F/8 Hr.)	505-575(70)	423-509(86)	412-482(70)	386-482(96)	460-556(96)
			Across Bottom of Weld		
As-welded	329-420(91)	318-380(62)	334-380(46)	286-405(119)	331-386(55)
Maraged (900°F/8 Hr.)	495-552(57)	394-495(101)	439-485(46)	368-526(158)	512-533(21)

NOTES

Numbers in parentheses represent difference between maximum and minimum values

WELD: Based on 8 to 23 indents at 0.040-inch intervals

HAZ: Based on 4 to 13 indents at 0.020-inch intervals

HUB: Based on 4 to 12 indents at 0.020-inch intervals

* Weld heat-unaffected base (base metal) = HUB
** Weld heat-affected zone (base metal) = HAZ

Microhardness Transverse Summary; Manual Repair in Automatic TIG Weld

Figure 127, Sheet 2 of 4

(KNOOP HARDNESS NUMBERS)
(500 GM LOAD)

AVERAGE HARDNESS RESULTS					
			Across Top of Weld		
Condition	HUB *	HAZ**	WELD	HAZ	HUB
As-welded	313	243	276	324	293
Maraged (900°F/8 Hr.)	493	460	477	455	486
			Across Middle of Weld		
As-welded	347	337	290	344	372
Maraged (900°F/8 Hr.)	500	411	401	410	506
			Across Bottom of Weld		
As-welded	341	330	286	304	308
Maraged (900°F/8 Hr.)	471	364	399	401	443

NOTES

WELD: Based on 6 to 23 indents at 0.040-inch intervals

HAZ: Based on 3 to 8 indents at 0.020-inch intervals

HUB: Based on 4 to 5 indents at 0.020-inch intervals

* Weld heat-unaffected base (base metal) = HUB
** Weld heat-affected zone (base metal) = HAZ

Microhardness Transverse Summary; Manual Repair in Automatic TIG Weld

Figure 127, Sheet 3 of 4

(KNOOP HARDNESS NUMBERS)
(500 GM LOAD)

RANGE OF HARDNESS RESULTS (Max. - Min. Values)					
		Across Top of Weld			
Condition	HUB *	HAZ **	WELD	HAZ	HUB
As-welded	191-356(165)	132-304(172)	131-384(253)	300-359(59)	246-334(88)
Maraged (900°F/8 Hr.)	490-495(5)	440-483(43)	473-555(82)	415-512(97)	476-503(27)
		Across Middle of Weld			
As-welded	331-370(39)	304-376(72)	239-350(111)	260-386(126)	298-406(8)
Maraged (900°F/8 Hr.)	484-521(47)	386-420(34)	380-439(59)	396-432(36)	487-525(38)
		Across Bottom of Weld			
As-welded	309-386(77)	240-395(155)	213-329(116)	244-379(135)	154-366(212)
Maraged (900°F/8 Hr.)	448-500(52)	348-380(32)	380-413(33)	367-435(68)	418-468(50)

NOTES

Numbers in parentheses represent difference between maximum and minimum values

WELD: Based on 6 to 23 indents at 0.040-inch intervals

HAZ: Based on 3 to 8 indents at 0.020-inch intervals

HUB: Based on 4 to 5 indents at 0.020-inch intervals

* Weld heat-unaffected base (base metal) = HUB
** Weld heat affected zone (base metal) = HAZ

Microhardness Transverse Summary; Manual Repair in Automatic TIG Weld

Figure 127, Sheet 4 of 4

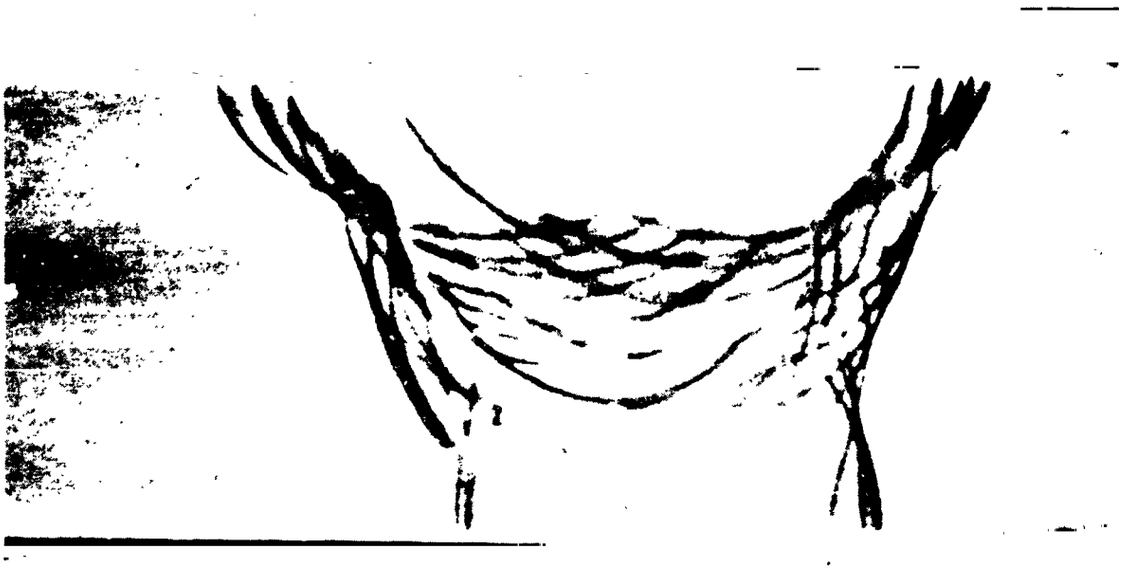

MANUAL REPAIR TO AUTOMATIC WELD WT-40-1
R-600-1A PLATE 2X

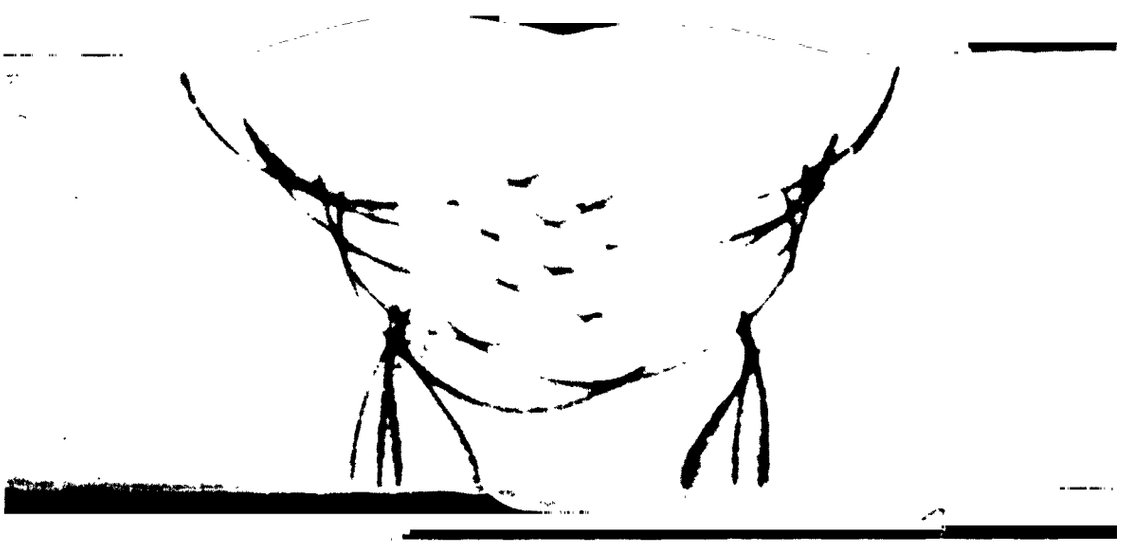

ALL MANUAL WELD WT-51-5947
R-599-1 PLATE 2X

Microphotographs of Weldments

Figure 128

Repair Procedure 2

Aging Cycle Temperature, °F	Aging Cycle Time, hours	Orientation	Notch Location	W/A, in-lb/in^2 -40°F	W/A, in-lb/in^2 RT	W/A, in-lb/in^2 200°F
900	4	Transverse	Weld	1167	1801	1695
				1179	1325	1858
			Avg.	1173	1563	1777
900	4	Transverse	HAZ*	642	860	699
				524	786	796
			Avg.	583	823	748

* HAZ - Heat affected zone

NOTE: The corresponding 0.2% offset yield strength at a maragir.g cycle of 900°F - 4 Hours is 201 ksi.

Plane-Stress Fracture Toughness of Welds Made with Lukens Plate R-600-1A and Armetco Weld Wire 08436

Figure 129

(MANUAL REPAIR WELDS)

Repair Procedure 3

Aging Cycle		Orientation	Notch Location	W/A, in-lb/in^2		
Temperature, °F	Time, hours			-40°F	R.T.	200°F
900	4	Transverse	Weld	1011	1335	1906
				1006	1782	1579
			Average	1008	1558	1742
900	4	Transverse	HAZ*	974	1382	1308
				1160	1351	1279
			Average	1067	1366	1294

* HAZ - Heat affected zone

NOTE: The corresponding 0.2% offset yield strength at a maraging cycle of 900°F-4 hours is 210 ksi

Plane-Stress Fracture Toughness of Welds Made with Lukens Plate R-604-1 and Armetco Weld Wire, Heat 08436

Figure 130

"REPRODUCIBILITY OF THE ORIGINAL PAGE IS POOR."

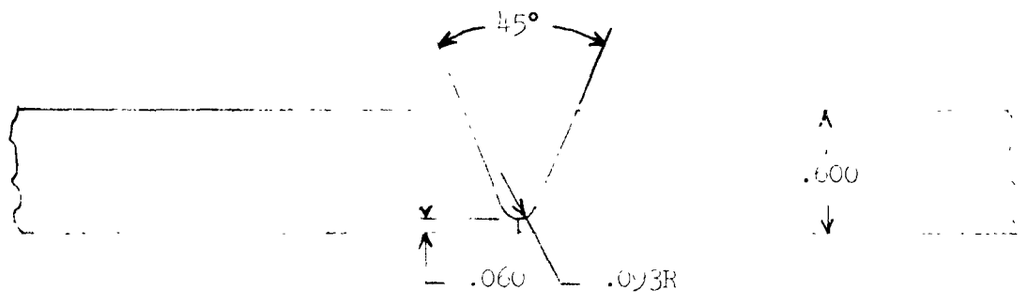

Single U

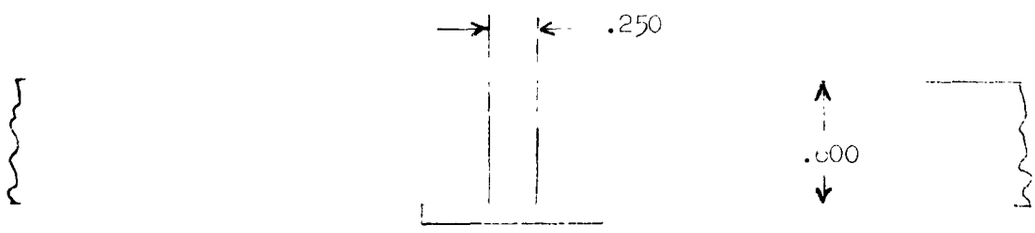

Square Butt

Joint Configurations Used to Determine the Tensile Properties and Fracture Toughness of Original Welds in Grade 200, 18%-Nickel Maraging Steel

Figure 131

Etch: Ammonium Persulphate Mag. 5X

"U" Joint

Etch: Ammonium Persulphate Mag: 5X

Narrow Gap

Typical Macrostructure of TIG Weldments Processed with a Conventional-U and Narrow-Gap Joint Designs

Figure 132

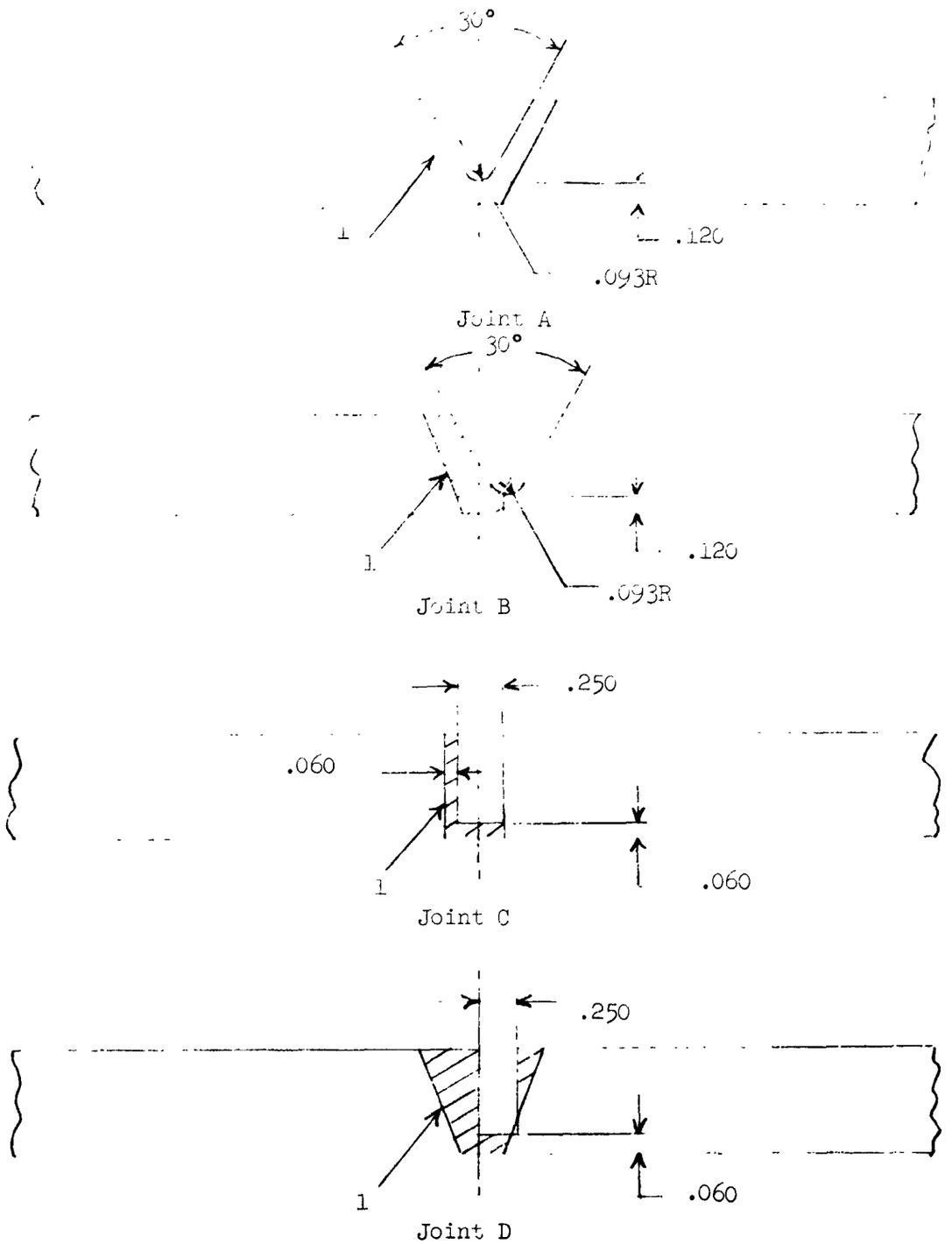

1 Shaded portion represents fusion zone of original weld deposit.

Joint Configurations and Locations Used to Determine The Tensile Properties and Fracture Toughness of Repair Welds in Grade 200, 18%-Nickel Maraging Steel (Heat 3920556) Made with Filler Wire from Heat 34482

Figure 133

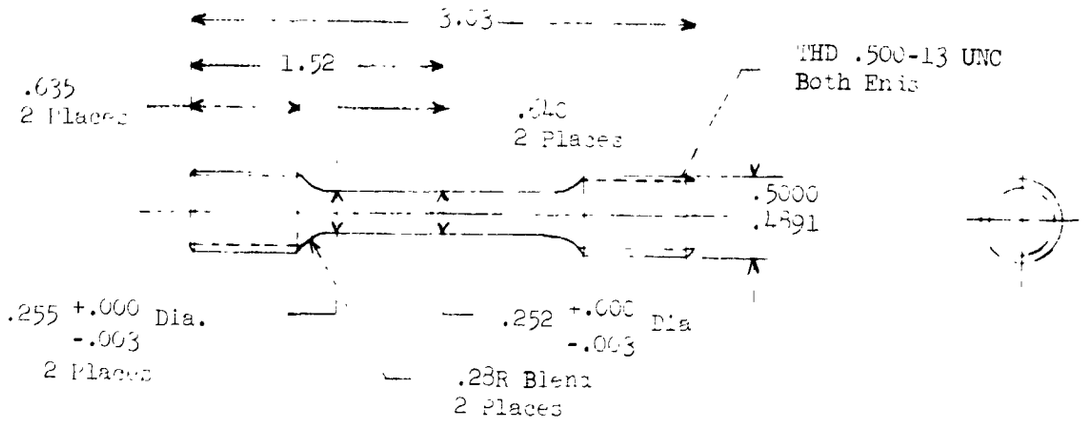

Tensile Specimen

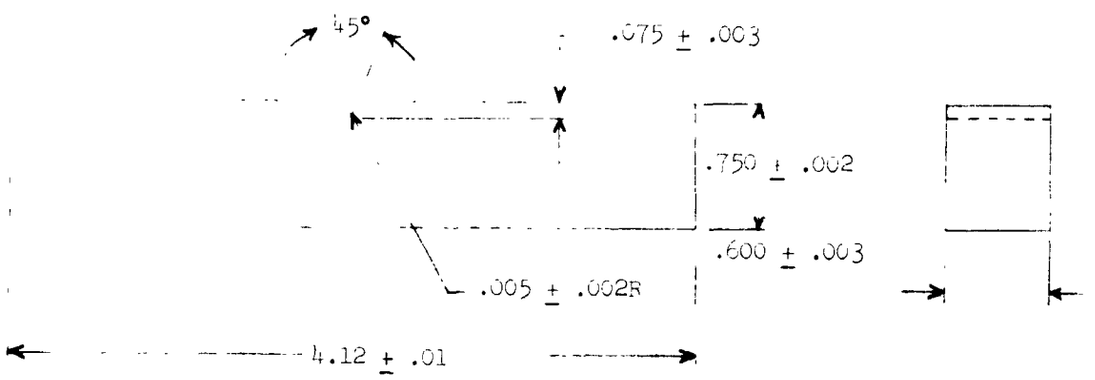

Slow-Notch-Bend Specimen

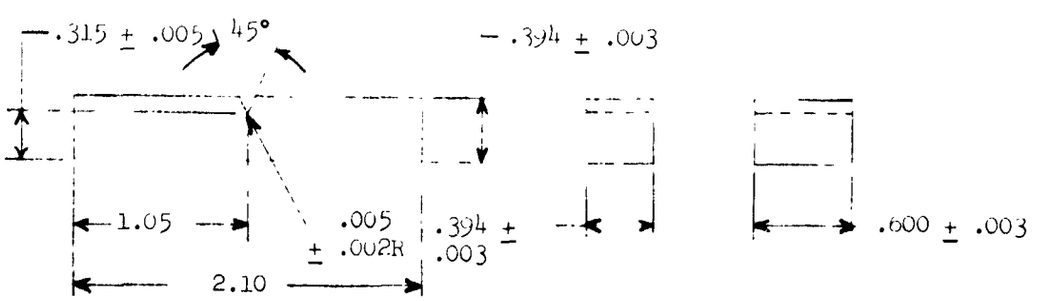

Precracked Charpy Impact Specimen

Tensile, Slow-Notch-Bend, and Precracked Charpy Impact Test Specimens

Figure 134

Heat Number	Composition, wt%									
	C	Mn	Si	Ni	Co	Mo	Ti	Al	P	S
					Parent Metal					
3920556	0.02	0.05	0.08	17.68	7.9	4.2	0.16	0.16	0.008	0.006
Specified (AGC 34315)	0.03	0.10	0.10	17.5	7.0	4.0	0.05	0.05	0.025	0.01
Limits	Max	Max	Max	19.0	8.0	4.5	0.25	0.15	Max	Max
					Filler Wire					
34482	0.02	0.01	0.007	18.2	7.65	3.53	0.24	0.1	0.003	0.003
Specified (AGC 34326)	0.03	0.10	0.01	17.5	7.5	3.6	0.26	0.10	0.01	0.01
Limits	Max	Max	Max	18.5	8.0	3.8	0.03	Added	Max	Max

Composition of Republic Heat 3920556, 18%-Nickel Maraging Steel Plate and Heat 34482 Filler Wire

Figure 135

Aging Treatment No. of Cycles	Temp. of	Time, hr	Orientation	0.2% Offset Yield Strength ksi	Ultimate Tensile Strength, ksi	Elongation in 1-in., %	Reduction of Area, %
2	900	8	Longitudinal	223	233	10.7	60.4
				220	231	10.6	58.6
				223	231	11.2	59.0
			Avg.	222	232	10.8	59.0
2	900	8	Transverse	228	237	10.7	58.4
				229	236	10.1	58.6
				228	236	10.3	58.6
			Avg.	228	236	10.3	58.5
1	900	8	Longitudinal	218	228	11.5	60.8
				217	228	11.5	62.5
				219	227	11.1	60.7
			Avg.	218	228	11.3	61.3
1	900	8	T ansverse	220	232	11.4	59.0
				221	234	11.4	59.1
				221	234	12.0	59.1
			Avg.	221	233	11.6	59.1
1	900	16	Longitudinal	223	235	11.9	60.8
				223	235	11.9	60.8
				223	235	11.2	57.5
			Avg	223	235	11.7	59.7
1	900	16	Transverse	222	234	12.6	60.1
				224	235	11.7	62.5
				222	236	12.9	61.0
			Avg.	223	235	12.4	61.2

Effects of Double-Aging treatment on the Tensile Properties of 0.6-in.-Thick Republic Heat 3920556, Grade 200, 18%-Nickel Maraging Steel Plate

Figure 136

Aging Cycle °F	Aging Cycle Hr.	No. of Cycles	Orientation	0.2% Offset Yield Strength, ksi	W/A in.-lb/in^2 Test Temperature, °F -100	-40	RT	2000
900	8	2	Longitudinal	222	-	1328	1393	1470
					-	1134	1445	1494
				Avg.	-	1231	1419	1481
900	8	2	Transverse	228	-	851	958	1064
					-	892	1086	1044
				Avg.	-	872	1022	1054
900	8	1	Longitudinal		1043	-	1425	1410
					1012	-	1594	1594
				Avg.	1028	-	1509	1502
900	8	1	Transverse	220	891	-	1296	1410
					894	-	1384	1424
				Avg.	893	-	1340	1417

Precracked Charpy Impact Fracture Toughness of 0.5-in.-Thick Republic Heat 3920556, Grade 200, 18%-Nickel Maraging Steel Plate After Two Aging Treatments at 900°F for 8 hr

Figure 137

Aging Cycle °F - hr	Number of Aging Cycles	Specimen Orientation	.2% Offset Yield (ksi)	Width b (in.)	Depth d (in.)	Proportional Limit Load (L) (lb)	Maximum Load (L) (lb)	Crack Depth a(in.)	Plain-Strain Fracture Toughness in-lb/in^2 G_{Ic} (1)	Stress Intensity Factor, ksi in K_{Ic} (1)
900 - 8	2	Transverse	228	.576	.750	7700	10755	.217	329	
				.574	.751	7400	3625	.258	424	
				.570	.751	9300	10975	.195	408	
				.576	.744	7950	8950	.237	445	
				.575	.751	9200	10275	.023	420	
									Avg 400	Avg 110
900 - 8	2	Longitudinal	222	.575	.750	7900	9725	.233	398	
				.576	.742	9150	11720	.194	406	
				.565	.751	8520	9770	.234	480	
				.575	.751	8750	9900	.250	555	
				.575	.751	8750	9755	.238	505	
									Avg 469	Avg 119
900 - 8	1	Longitudinal	218	.575	.749	10300	11000	.225	639	
				.576	.749	9500	11400	.210	479	
				.576	.749	9300	11240	.210	459	
				.576	.749	6500	7740	.310	489	
				.576	.749	8600	9760	.255	562	
									Avg 526	Avg 126
900 - 8	1	Transverse	220	.578	.751	8750	9500	.245	528	
				.578	.751	9200	9490	.242	570	
				.577	.751	9750	10250	.210	496	
				.578	.751	8000	8325	.265	515	
				.577	.751	8600	8950	.260	579	
									Avg 538	Avg 127

(1) From Bueckner's Equation

Effects of Double-Aging Treatment and Specimen Orientation of Plane-Strain Fracture Toughness of Republic Heat 3920556 Grade 200, 18%-Nickel Maraging Steel Plate; Slow-Notch-Bend Test

Figure 138

Aging Treatment*							
No. of Cycles	Temp. of	Time, hr.	Orientation	.2% Offset Yield Strength, ksi	Ultimate Tensile Strength, ksi	Elongation in 1-in., %	Reduction of Area, %
1	900	8	Transverse	214	220	10.8	59.0
				215	220	11.2	60.4
				212	218	11.0	61.2
			Avg.	214	219	11.0	60.3
			Longitudinal	207	216	11.7	61.4
				204	215	11.8	60.8
				206	219	11.5	60.0
			Avg.	206	217	11.7	60.8
2	900	8	Transverse	211	218	9.0	58.5
				211	219	11.5	61.1
				212	220	11.4	61.5
			Avg.	211	219	10.6	60.4
			Longitudinal	210	215	12.1	61.1
				208	218	12.2	63.1
				207	217	11.5	57.2
			Avg.	208	217	11.9	60.5

* As-welded and aged.

Effects of Double-Aging Treatments on the Tensile Properties of TIG Weldments Deposited in 0.6-in.-Thick Republic Heat 3920556, Grade 200, 18%-Nickel Maraging Steel Plate with Heat 34482 Filler Wire and Sinble-U Joint Configuration

Figure 139

Aging Cycle			Weld Metal Fracture Toughness W/A, in-lb, in^2	
			Number of Aging Cycles	
Temperature, °F	Time, hr		1	2
900	8		1538	1348
			1465	1423
			1602	1371
			1479	1340
			1419	1488
		Average	1499	1404

Effects of Double-Aging Treatments on the Room Temperature Precracked Impact Fracture Toughness of Weld Metals Deposited with a Single-U Joint Configuration and Filler Wire 34482 in 0.6-in.-Thick Republic Heat 3920556, Grade 200, 18%-Nickel Maraging Steel Plate

Figure 140

	Aging Cycle °F	Aging Cycle hr	No. of Aging Cycles	.2% Offset Yield Strength, ksi	Width b, (in)	Depth d (in)	Prop. Limit Load (lb)	Max. Load (lb)	Measured Crack Depth a, (in)	Stress Intensity Factor 1000 psi, in K_{IC} (1)	Stress Intensity Factor 1000 psi, in K_{IC} (2)	Plane Strain Fracture Toughness in-lb/in.^{2} G_{IC} (1)	Plane Strain Fracture Toughness in-lb/in.^{2} G_{IC} (2)
1	900	8	2	206	.578	.751	7200	10350	.255	106	106	371	371
2					.578	.751	6300	8400	.310	113	113	427	423
3					.578	.750	7600	10760	.256	112	112	419	419
4					.578	.751	7650	10980	.258	114	113	428	428
5					.578	.751	7580	11180	.235	103	103	353	356
									Average	109	109	399	399
6	900	8	1	206	.578	.749	7050	10050	.265	108	108	389	387
7	(Single Aging)				.578	.751	6750	9430	.288	112	111	417	413
8					.577	.751	8300	10980	.233	112	113	418	423
9					.578	.751	8350	11110	.236	114	115	433	437
10					.578	.751	8200	10410	.270	128	127	541	538
									Average	115	115	439	439

(1) Bueckner Analysis
(2) Kies Analysis

Effects of Double-Aging Treatments on the Slow-Notch-Bend Fracture Toughness of Weld Metals Deposited with a Single-U Joint Configuration and Filler Wire 34482 in 0.6-in.-Thick Republic Heat 3920556, Grade 200, 18%-Nickel, Maraging Steel Plate

Figure 141

Material Condition	Notch Location		Impact Toughness, W/A (in-lb/in.^{2})
Solution annealed base metal aged at 900°F for 8 hr after welding	HAZ		1769
			1637
			1794
			1740
			1741
			1815
		Avg.	1745
Solution annealed base metal double aged at 900°F for 8 hr after welding	HAZ		2197
			1812
			2113
			1939
			1888
			2238
		Avg	2031

Effects of Double-Aging Treatments on the Room Temperature Precracked Impact Fracture Toughness of Heat-Affected Zones of Weldments Made with a Square-Butt Joint Design and Filler Wire 34882 in 0.6-in.-Thick Republic Heat 3920556, Grade 200, 18%-Nickel Maraging Steel Plate

Figure 142

Material Condition	Notch Location	Width b in.	Depth d in.	Prop. Limit Load lb.	Max. Load lb.	Crack Depth a in.	Stress Intensity Factor 1000 psi$\sqrt{in.}$ K_{Ic}(1)	K_{Ic}(2)	Critical Crack Extension Force in-lb/in^2 G_{Ic}(1)	G_{Ic}(2)
Solution annealed base metal aged at 900°F for 8 hrs after welding	HAZ	.598	.751	9500	11,480	.257	136	136	612	612
		.601	.751	8350	10,230	.294	136	135	617	611
		.601	.751	8050	10,495	.285	127	126	537	532
		.601	.751	10200	12,200	.236	134	134	595	601
						Avg.	133	133	590	589
Solution annealed base metal double-aged at 900°F for 3 hrs after welding.	HAZ	.601	.751	8700	10,110	.280	135	134	604	599
		.601	.751	10200	12,400	.213	122	124	496	509
		.601	.751	9000	10,950	.263	131	131	569	568
		.601	751	8000	10.030	.306	136	136	619	612
		.601	.751	7800	11,210	.271	117	116	454	452
						Avg.	126	126	548	548

(1) Bueckner analysis
(2) Kies analysis

Effects of Double-Aging Treatments on the Slow-Notch-Bend Fracture Toughness of Heat Affected Zones of Weldments Made with a Square-Butt Joint Design and Filler Wire 34482 in 0.6-in.-Thick Republic Heat 3920556, Grade 200, 18%-Nickel, Maraging Steel Plate

Figure 143

Materials	Condition*	0.2% Offset Yield Strength	K_{IC} ksi in.	Critical Flaw Length, in. Flaw Condiguration Depth/Length .1	.5
Base Metal					
Longitudinal	Single Aged	218	126	0.74	0.38
Longitudinal	Double Aged	222	119	0.64	0.33
Transverse	Single Aged	221	127	0.74	0.38
Transverse	Double Aged	228	110	0.52	0.26
Weld Metal					
Original Weld	Single Aged	206	115	0.69	0.36
Original Weld	Double Aged	208	109	0.61	0.31
Heat-Affected Zone					
Original Weld	Single Aged	210	133	0.89	0.46
Original Weld	Double Aged	210	126	0.80	0.42

* 900°F for 8-hr aging cycle

Effects of Double-Aging Treatments on the Critical Flaw Length of Weldments Prepared in 0.6-in.-Thick Republic Heat 3920556, 18%-Nickel Maraging Steel Plate with Filler Wire 34482

Figure 144

Prior to Welding °F	Prior to Welding hr	After Welding °F	After Welding hr	0.2% Offset Yield Strength, ksi	Ultimate Tensile Strength, ksi	Elongation in 1 in., %	Reduction of Area, %	Location of Failure
900	8	900	8	229	236	11.1	54.1	Weld Metal
				229	236	11.6	58.4	Weld Metal
				228	236	11.4	53.6	Weld Metal
		Average		229	236	11.4	55.3	

Transverse Tensile Properties of Weldments Made with Filler Wire 07495 and Single-U Joints in Previously Aged Plate from Republic Heat 392056, Grade 200, 18%-Nickel Maraging Steel

Figure 145

Material Condition	Notch Location		Impact Toughness, W/A (in-lb/in^2)
Base metal aged before welding and reaged at 900°F for 8 hr after welding.	HAZ		1416
			1778
			1862
			1858
			1461
		Avg.	1675
Solution annealed base metal aged at 900°F for 8 hr after welding	HAZ		1769
			1637
			1794
			1740
			1714
			1815
		Avg.	1745

Effects of Aging the Base Metal Prior to Welding on the Room Temperature Precracked Impact Fracture Toughness of Heat-Affected Zones of Weldments Made with a Square-Butt Joint Design and Filler Wire 34482 in 0.6-in.-thick Republic Heat 3920556, Grade 200, 18%-Nickel Maraging Steel Plate

Figure 146

Material Condition	Notch Location	Width b in.	Depth d in.	Prop. Limit Load lb.	Max. Load lb.	Crack Depth a in.	Stress Intensity Factor 1000 psi$\sqrt{\text{in.}}$ $K_{IC}(1)$	$K_{IC}(2)$	Critical Crack Extension Force in-lb/in^2 $G_{IC}(1)$	$G_{IC}(2)$
Base metal aged before welding and reaged at 900°F for 8 hrs after welding	HAZ	.602	.751	9350	10,990	.259	134	133	594	594
		.601	.751	9750	11,950	.233	125	127	531	538
		.601	.751	8650	11,260	.241	116	116	445	448
		.601	.751	8800	10,495	.267	130	129	561	559
		.602	.751	8100	10,460	.271	121	121	488	485
						Avg.	126	126	524	525
Solution annealed base metal aged at 900°F for 8 hrs after welding	HAZ	.598	.751	9500	11,480	.257	136	136	612	612
		.601	.751	8350	10,230	.294	136	135	617	611
		.601	.751	8050	10,495	.285	127	126	537	532
		.601	.751	10200	12,200	.236	134	134	595	601
						Avg.	133	133	590	589

Effects of Aging the Base Metal Prior to Welding on the Slow-Notch Bend Fracture Toughness of Heat Affected Zone of Weldments Made with a Square-Butt Joint Design and Filler Wire 34482 in 0.6-in.-Thick Republic Heat 3920556, Grade 200, Maraging Steel Plate

Figure 147

Joint Configuration	Material Condition		0.2% Offset Yield Strength ksi	Ultimate Tensile Strength ksi	Elongation in./in., %	Reduction of Area, %
A	Welded, repaired and aged at 900°F for 8 hr.		212	218	9.5	46.3
			215	220	13.0	57.3
		Avg.	214	219	11.2	52.1
A	Welded, aged at 900°F for 8 hr, repaired and re-aged at 900°F for 8 hr.		216	222	10.4	47.5
			216(1)	221(1)	1.9(1)	4.5(1)
			217	223	12.1	63.4
		Avg.	216	222	11.3	55.5
B	Welded, repaired and aged at 900°F for 8 hr.		211	217	12.3	54.2
			210	216	12.3	54.2
			211	217	12.7	61.5
		Avg.	211	217	12.4	56.7
B	Welded, aged, at 900°F for 8 hr, repaired, and reaged at 900°F for 8 hr.		211	216	13.5	60.8
			212	218	12.4	58.3
			212	217	13.0	55.8
		Avg.	212	217	13.0	58.3
	Original weld aged at 900°F for 8 hr.		214	220	10.8	59.0
			215	220	11.2	60.4
			212	218	11.0	61.2
		Avg.	214	219	11.0	60.3

(1) Specimen contained defect, elongation and reduction of area values were not used in calculating averages.

Transverse Tensile Properties of Repair Welds Made in 0.6-in. Thick Republic Heat 3920556, Grade 200, 18%-Nickel Maraging Steel Plate with Filler Wire 34482 and a Single-U Joint Configuration

Figure 148

Joint Configuration	Material Condition		W/A in.-lb/in^2 Test Temperature, °F -40	RT	200
C	Welded repaired and aged at 900°F for 8 hr.		1,707	1,562	1,930
			1,450	1,573	1,914
		Avg.	1,579	1,569	1,922
C	Welded, aged at 900°F for 8 hr, repaired and reaged at 900°F for 8 hr.		2,005	2,564	2,408
			2,028	2,056	2,425
		Avg.	2,017	2,310	2,417
D	Welded, repaired and aged at 900°F for 8 hr.		1,288	2,000	2,352
			1,238	1,847	2,007
		Avg.	1,263	1,924	2,180
D	Welded, aged at 900°F for 8 hr, repaired and reaged at 900°F for 8 hr.		1,085	1,381	1,967
			1,331	1,378	1,534
		Avg.	1,208	1,380	1,751

Precracked Charpy Impact Fracture Toughness of Repair-Weld Heat-Affected Zones in 0.6-in.-Thick Republic Heat 3920556, Grade 200, 18%-Nickel Maraging Steel Plate with Filler Wire 34482

Figure 149

Joint Configuration	Process	Width b (in)	Crack Depth a (in)	Max. Load (lb)	Prop. Limit Load (lb)	K_{IC} (1) ksi$\sqrt{\text{in.}}$	G_{IC} (1) in-lb/in^2
C	Welded, repaired,	.559	.233	11,020	8,500	118.9	470
	and aged at	.559	.242	10,510	8,275	119.8	477
	900°F for 8 hr.	.559	.215	11,240	9,900	128.9	552
		.559	.254	9,580	6,200	94.0	294
		.559	.225	11,110	7,900	107.0	381
	Avg.					113.7	435
C	Welded, aged,	.559	.280	9,962	6,200	103.6	357
	at 900°F for	.559	.224	10,668	6,800	91.8	280
	8 hr, and reaged	.559	.245	10,395	5,900	86.4	248
	at 900°F for 8	.559	.230	11,680	7,450	103.0	352
	hr	.559	.197	12,645	8,200	99.2	327
	Avg.					96.8	315
D	Welded, repaired,	.559	.247	9,015	7,700	113.7	430
	and aged at 900°F	.559	.204	11,460	8,875	110.5	406
	for 8 hr.	.559	.269	9,430	7,200	115.5	444
		.559	.247	10,120	7,000	103.3	355
		.559	.284	9,350	7,200	122.2	496
	Avg.					113.0	426
D	Welded, aged,	.559	.215	10,863	7,700	100.3	352
	at 900°F for	.559	.259	9,583	6,920	106.9	380
	8 hr, repaired	.559	.259	9,657	7,475	115.5	443
	and reaged.	.559	.204	12,100	8,130	101.2	341
		.559	.264	8,915	6,320	99.5	329
	Avg.					104.7	369

(1) Bueckner Analysis.

Slow-Notch-Bend Fracture of Repair-Weld Heat Affected Zones in 0.6-in.-Thick Republic Heat 3920556, Grade 200, 18%-Nickel Maraging Joint Configuration Steel Plate with Filler Wire 34482

Figure 150

Joint Configuration	Material Condition	0.2% Offset Yield Strength, ksi	Ultimate Tensile Strength, ksi	Elongation in 1-in., %	Reduction of Area, %
A	Welded, repaired, and aged at 900°F for 8 hr.	210	219	12.2	55.4
		209	218	12.2	--
		201	218	12.0	49.9
	Avg.	207	218	12.1	52.6

Longitudinal Tensile Properties of Repair Weld Metals Deposited in 0.6-in.-Thick Republic Heat 3920556, Grade 200, 18%-Nickel Maraging Steel Plate with Filler Wire 34482

Figure 151

Joint Configuration	Material Condition	Test Temperature, °F		Fracture Toughness W/A (in. lb/in.^{2})
A	Welded, repaired, and aged at 900°F for 8 hr.	-40		1227
				1048
			Avg.	1138
		Room Temperature		1315
				1565
			Avg.	1440
		+200		1849
				1531
			Avg.	1690

Precracked Charpy Impact Fracture Toughness of Repair Weld Metals Deposited in 0.6-in.-Thick Republic Heat 3920556, Grade 200, 18%-Nickel Maraging Steel Plate with Filler Wire 34482

Figure 152

Joint Configuration	Material Condition	Width b (in)	Depth d (in)	Prop. Limit Load (lb)	Max. Load (lb)	Crack Depth a (in)	Fracture Toughness(1) K_{IC} (ksi in)	Fracture Toughness(1) G_{IC} (in lb/in.^{2})
A	Welded, repaired and aged at 900°F for 8 hr.	.575	.750	7000	8207	.2691	109	395
		.575	.750	8550	10829	.2095	107	385
		.575	.750	7580	9353	.2613	115	437
		.575	.750	6700	8505	.2719	105	369
		.575	.750	8660	9789	.2440	123	505
						Average	112	418

(1) Bueckner Analysis

Slow-Notch-Bend Fracture Toughness of Repair Weld Metal Deposited in 0.6-in.-Thick Republic Heat 3920556, Grade 200, 18%-Nickel Maraging Steel Plate with Filler Wire Heat 34482

Figure 153

Materials	Condition	0.2% Offset Yield Strength, ksi	K_{IC} ksi$\sqrt{\text{in.}}$	Critical Flaw Length, in. Flaw Configuration Depth/Length .1	.5
Base Metal					
Longitudinal	Single Aged	218	126	0.74	0.38
Longitudinal	Double Aged	222	119	0.64	0.33
Transverse	Single Aged	221	127	0.74	0.38
Transverse	Double Aged	228	110	0.52	0.26
Weld Metal					
Original Weld	Single Aged	206	115	0.69	0.36
Original Weld	Double Aged	208	109	0.61	0.31
Repair Weld	Single Aged	207	112	0.65	0.34
Heat-Affected Zone					
Original Weld	Single Aged*	210**	133	0.89	0.46
Original Weld	Double Aged*	210**	126	0.80	0.42
Repair Weld:					
In Aged Plate	Single Aged*	210**	126	0.80	0.42
In As-Welded HAZ	Single Aged*	210**	113	0.65	0.33
In Aged HAZ	Single Aged*	210**	97	0.44	0.25
In As-Welded Weld Metal	Single Aged*	210**	113	0.65	0.33
In Aged Weld Metal	Single Aged*	210**	104	0.55	0.28

* 900°F for 8 hr.
** Assumed value for yield strength of all heat-affected zones.

Summary of Slow-Notch-Bend Fracture Toughness Data of Grade 200, 18%-Nickel Maraging Steel Plate, Weldments, and Repair Weldments

Figure 154

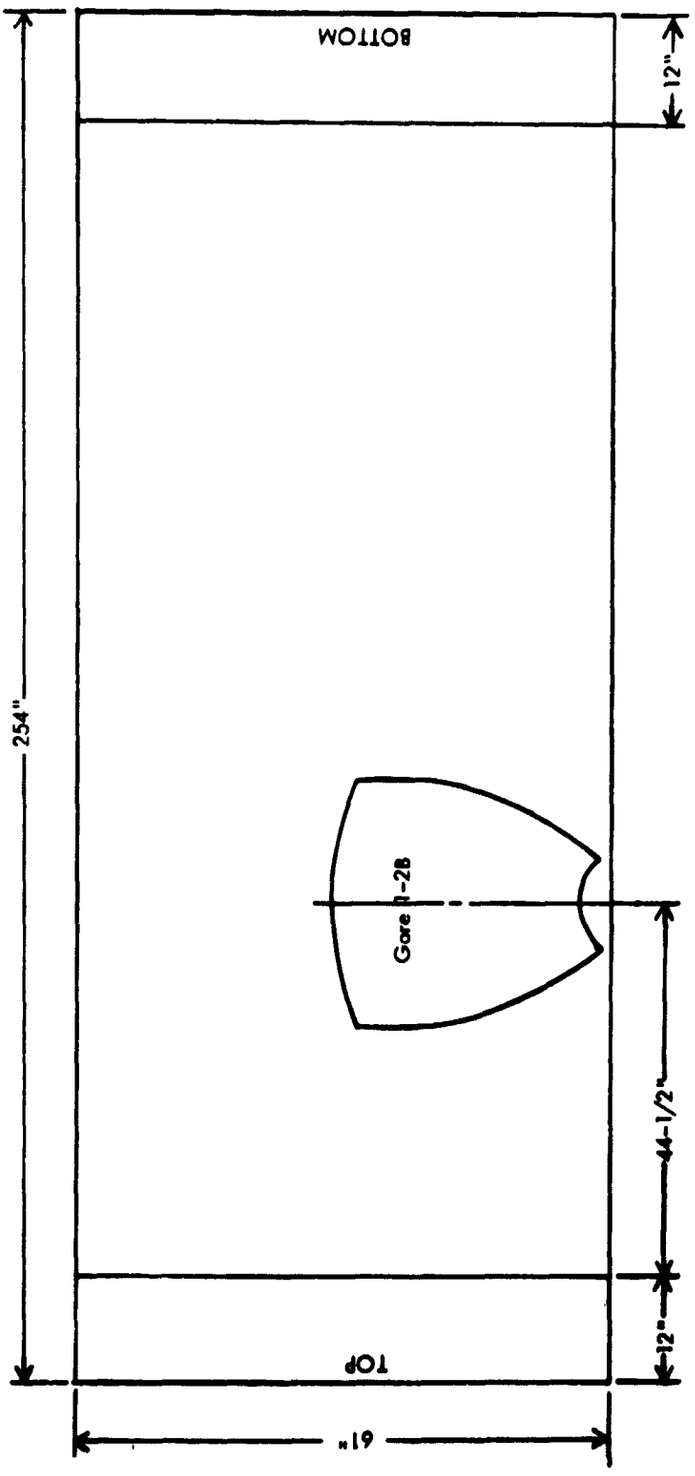

Layout of Gore-1-2B on Plate R-600-1A

Figure 155

Element	Composition, weight percent*
C	0.016
Mn	0.04
P	0.07
S	0.010
Si	0.04
Ni	18.10
Mo	4.24
Ti	0.20
Co	7.59
Al	0.07
B	0.003
Zr	0.02
Ca	0.06**

* Averaged from six locations on the plate pattern

** Added in increments of 0.02

Mill Certified Chemical Analysis of Lukens Plate R-600-1A

Figure 156

Aging Cycle Temperature, °F	Aging Cycle Time, hours	Orientation	0.2% Offset Yield Strength (1) ksi (1) Formed	0.2% Offset Yield Strength (1) ksi (1) Parent	Ultimate Tensile Strength ksi Formed	Ultimate Tensile Strength ksi Parent	Elongation in 1 Inch % Formed	Elongation in 1 Inch % Parent	Reduction in Area % Formed	Reduction in Area % Parent	Plane Stress Fracture Toughness W/A, in-lb/in² (2) −40°F Formed	−40°F Parent	Room Temperature Formed	Room Temperature Parent	+200°F Formed	+200°F Parent	Plane Strain Fracture Toughness G_{nc}, in-lb/in² (3) Formed	Plane Strain Fracture Toughness G_{nc}, in-lb/in² (3) Parent
900	8	Longitudinal	-	231	-	230	-	11	-	56	-	662	-	942	-	892	-	238
		Transverse	-	242	-	249	-	10	-	46	-	732	-	522	-	544	-	197
900	4	Longitudinal	219	228*	225	235*	11	12*	58	53*	642	1011*	914	1121*	1090	1374*	283	330
		Transverse	229	235*	234	243*	10	11*	49	51*	550	781*	724	610*	822	735*	236	215
		Short Transverse									556	742*	868	913*	995	1009*	-	218
900/4 Managed with First 36" PETV		Longitudinal	-	226	-	235	-	11	-	49								
		Transverse	-	235	-	244	-	10	-	49								
1675 (Anneal)	1	Longitudinal	213	228*	227	235*	12	12*	54	53*	938	1011*	1289	1121*	1402	1374*	294	330
900	4	Transverse	216	235*	229	243*	10	11*	47	51*	846	781*	953	610*	1020	735*	226	215
		Short Transverse									902	742*	1097	913*	1202	1009*	-	218

* Represents bottom end of plate

(1) Average of three specimens per data point

(2) Minimum of two specimens per data point

(3) Average of five specimens per data point

Comparison of Strength and Toughness Data for Plate R-600-1A and Formed Material from Core 1-2B

Figure 157

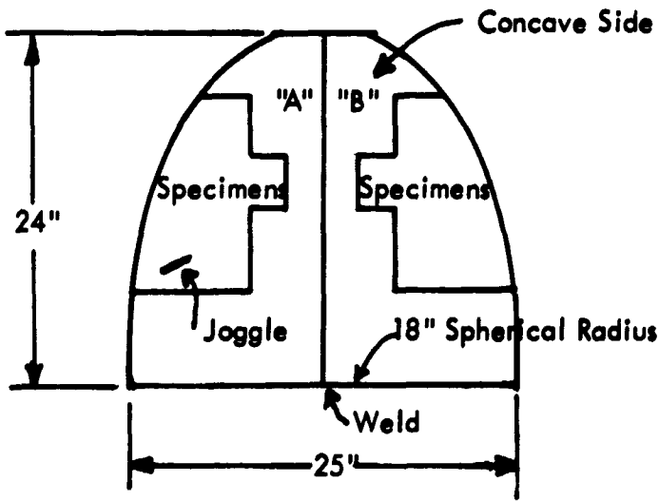

Layout of Gore 1-2B

Figure 158

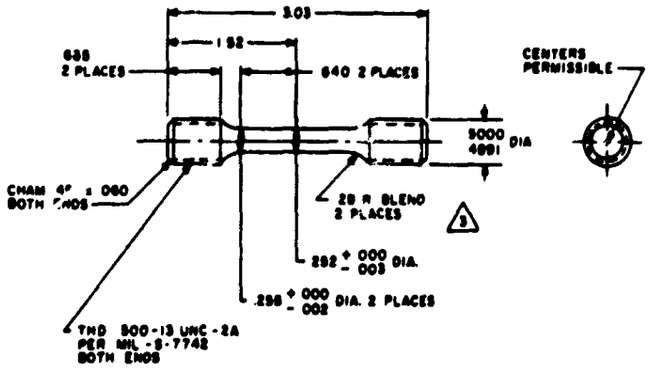

0.250-INCH ROUND TENSILE SPECIMEN

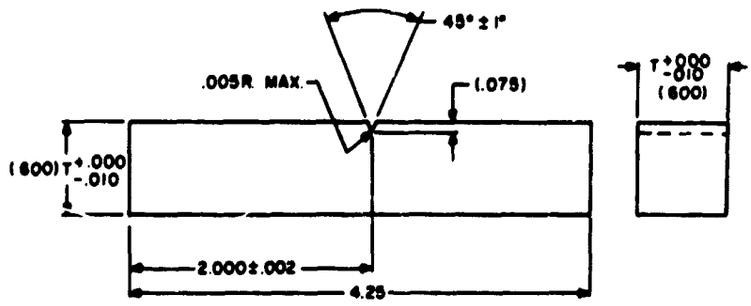

T = MINIMUM PLATE GAUGE THICKNESS

SLOW NOTCH BEND SPECIMEN

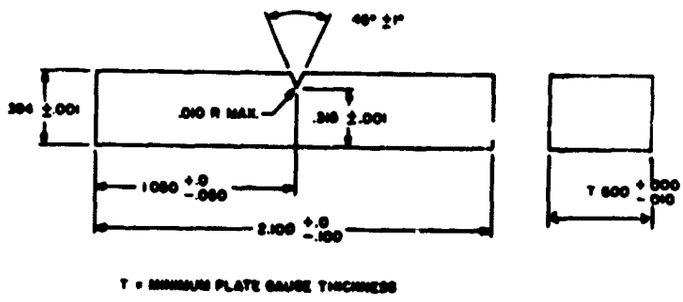

T = MINIMUM PLATE GAUGE THICKNESS

CHARPY TYPE VEE NOTCH IMPACT SPECIMEN

Specimen Configurations and Dimensions

Figure 159

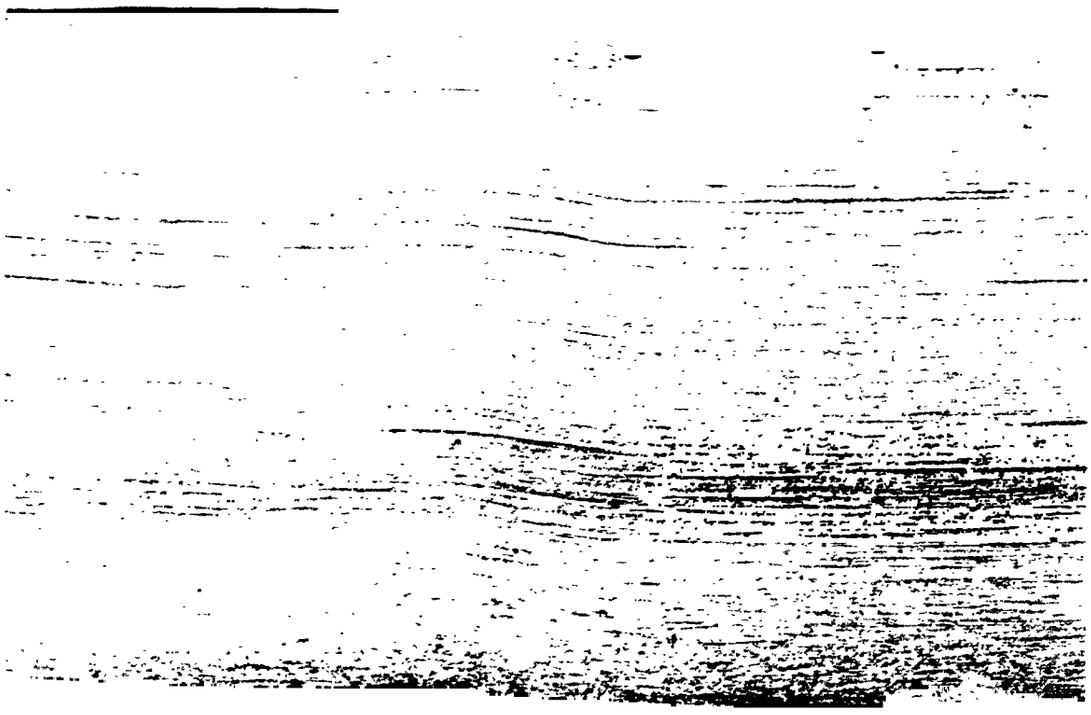

50 Percent Hydrochloric Acid 6X

Photomicrograph of a Cross-Section of Gore Segment 1-2B Through Joggle

Figure 160

Knoop Hardness Numbers (500 gm. load) Indents Each 0.010 Inch

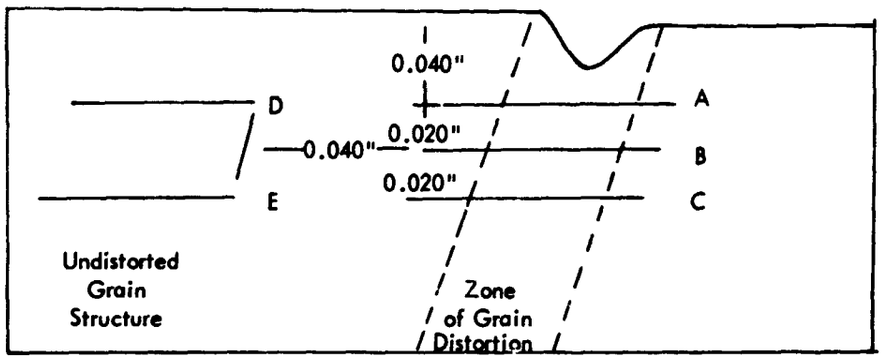

Sketch Showing Location of Microhardness Traverses

Joggled Zone of Grain Distortion

Traverse A		Traverse B		Traverse C	
As-Received	Maraged*	As-Received	Maraged*	As-Received	Maraged*
325	456	319	492	335	474
296	477	332	470	338	485
338	454	335	445	307	454
325	450	334	474	349	480
340	470	335	477	345	474
347	474	338	463	362	443
340	480	340	474	340	477
338	506	325	480	352	467
334	446	317	496	349	477
323	462	347	509	335	470

Undistorted Grain Structure

Traverse D		Traverse E	
As-Received	Maraged*	As-Received	Maraged*
325	426	327	456
319	456	325	467
328		332	510
320	454	296	480
334	450	323	485
332	443	340	485
294	467	323	477
307	462	327	470
319	489	332	489
304	474	338	480

*900°F/4 hours

Microhardness Transverse Results

Figure 161

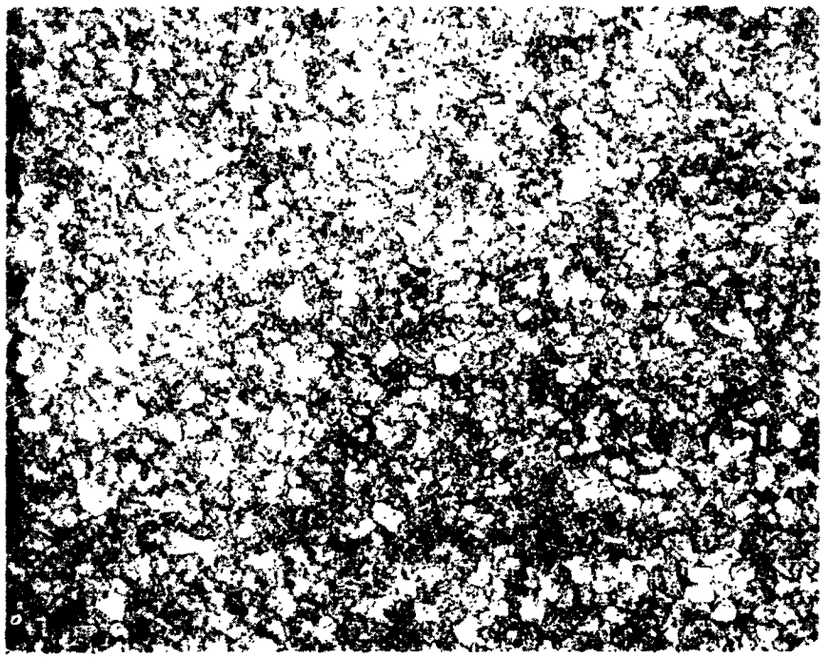

10 Percent Chromic Acid Etch (Electrolytic) 100 X

Photomicrography of Resolution Annealed Material from Plate R-600-1A

Figure 162

Vertical Flanging Press Being Used for Cold Weld Straightening

Figure 163

Aging Cycle Temperature, °F	Time, hours	Orientation	0.2% Offset Yield Strength ksi	Ultimate Tensile Strength ksi	Elongation in 1 Inch %	Reduction in Area %
900	4	Longitudinal	217	223	12	54
			233	239	11	49
			225 Avg.			
900	4	Transverse	209	213	10	51
			209	213	11	53
			212	216	10	48
			210 Avg.			
900*	4	Longitudinal	202	210	12	56
			206	212	12	52
			206	212	12	56
			205 Avg.			
900*	4	Transverse	206	213	12	58
			209	215	12	60
			212	215	12	58
			209 Avg.			

* These tensile specimens were machined from flat weld test plates, made with Lukens Plate R-600-1 and Special Metals Weld Wire, Heat No. 34481.

Tensile Test Data Obtained from Straightened Welds Made with Lukens Plate R-600-1A and Special Metals Weld Wire 34481

Figure 164

Test Temperature	FLAT WELD PLATES	COLD FORMED AND STRAIGHTENED WELD PLATES
	W/A Values, in-lb/in^2	
	Notch in Weld	
-40°F	1197	1204
R.T.	1343	1513
200°F	1394	1682
	Notch in HAZ*	
-40°F	922	1114
R.T.	1427	1397
200°F	1362	1280
	G_{nc} (in-lb/in^2)	
	Notch in Weld	
	291	292
	Notch in HAZ*	
	348	371

* HAZ - Heat affected zone

A Comparison of Plane-Strain and Plane-Stress Fracture Toughness Values, Lukens Plate R-600-1A and Special Metals Weld Wire 34481

Figure 165

Specimen Number	Aging Cycle °F/ Hr	Width b, in	Depth d, in	$1/M \times 10^6$ in^2/lb	Effective a, in*	Measured a, in	Proportional Load Limit, lb	Maximum Load, lb	Fracture Toughness Gnc in-lb/in²	Fracture Toughness Glc in-lb/in²	Stress Intensity Factor Knc 1000 psi, $\sqrt{in}$	Stress Intensity Factor Klc 1000 psi, $\sqrt{in}$
BW-70	900/4	0.594	0.596	2.011	0.1619		5700	7800	263		88	
BW-71	900/4	0.595	0.597	2.025	0.1643		5700	7860	266		89	
BW-72	900/4	0.597	0.597	2.022	0.1638		5520	8020	247		86	
BW-73	900/4	0.597	0.597	2.011	0.1619		5760	7940	266		89	
BW-74	900/4	0.597	0.597	2.257	0.2004		6480	9060	415		111	
								Average Values	292		92	
BWH-34	900/4	0.596	0.597	2.078	0.1744		5880	7740	321		97	
BWH-35	900/4	0.598	0.597	2.013	0.1640		6240	7880	323		98	
BWH-36	900/4	0.596	0.597	1.936	0.1500		7080	8620	360		103	
BWH-37	900/4	0.598	0.597	.993	0.1606		7200	8080	415		111	
BWH-38	900/4	0.595	0.597	2.052	0.1704		6960	7560	433		113	
								Average Values	371		105	

NOTE: (1) Measured "a", G_{Ic}, and K_{Ic} are not included because all specimens developed highly irregular fatigue cracks.

(2) G_{nc} and K_{nc} are based on calibration bars that were maraged at 900°F for 4 hours.

* NOTE: Effective "a" values have an accuracy of $\pm$ 0.0010 inch.

Effect of Cold Straightening of the Plane-Strain Fracture Toughness of Welds Made with Lukens Plate R-600-1A and Special Metals Weld Wire 34481, Slow-Notch Bend Specimens

Figure 166

Aging Cycle		Orientation	Notch Location	W/A, in-lb/in^2		
Temperature, °F	Time, hours			-40°F	R.T.	200°F
900	4	Transverse	Weld	1239	1570	1657
				1169	1456	1707
			Average	1204	1513	1682
900	4	Transverse	HAZ	1258	1100	1316
				970	1694	1244
			Average	1114	1397	1280

NOTE: The corresponding 0.2% offset yield strength at a maraging cycle of 900°F-4 hours is 210 ksi.

Plane-Stress Fracture of Straightened Weldments Made with Lukens Plate R-600-1A and Special Metals Weld Wire 34481

Figure 167

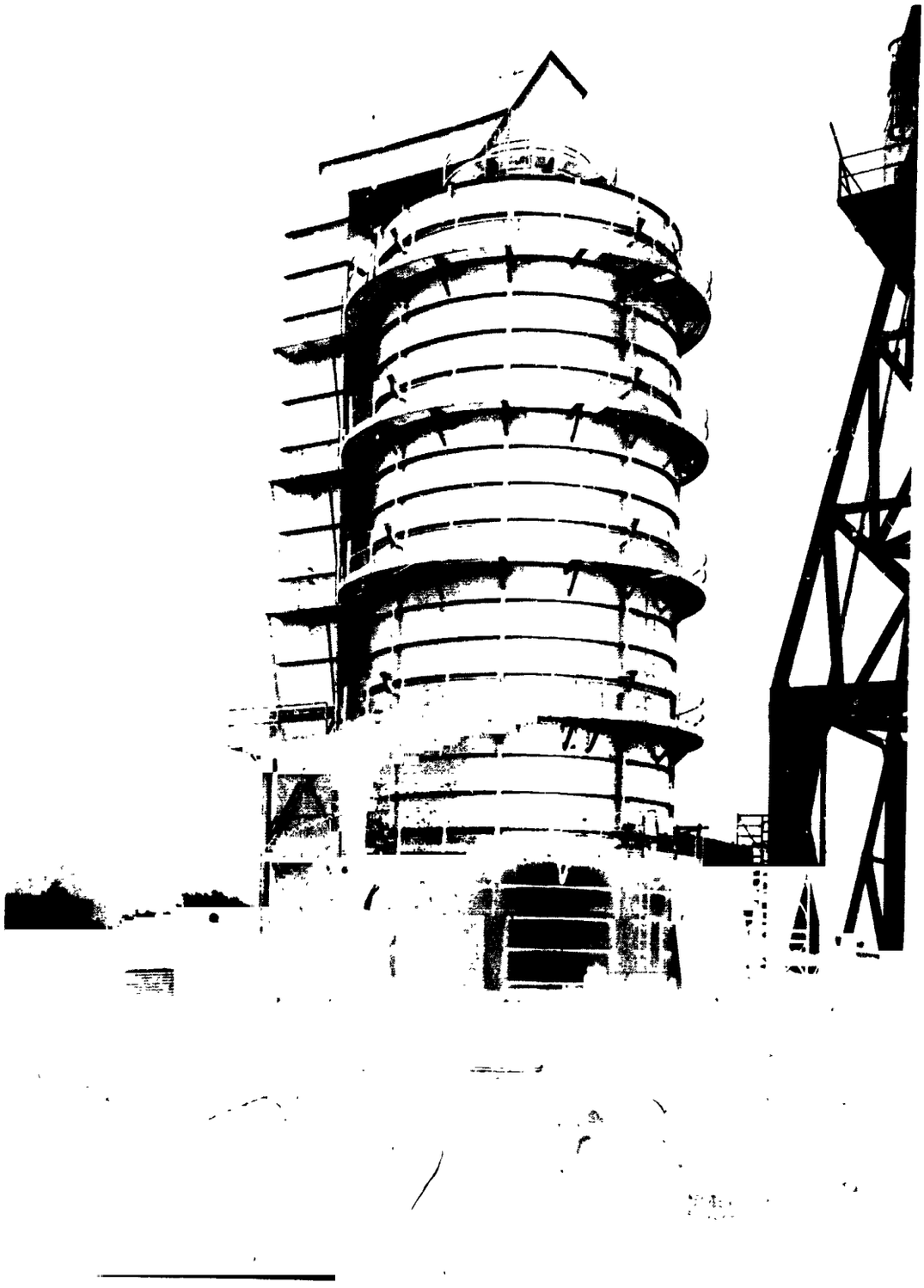

Assembled Furnace for Maraging 270-in.-dia Chamber

Figure 168

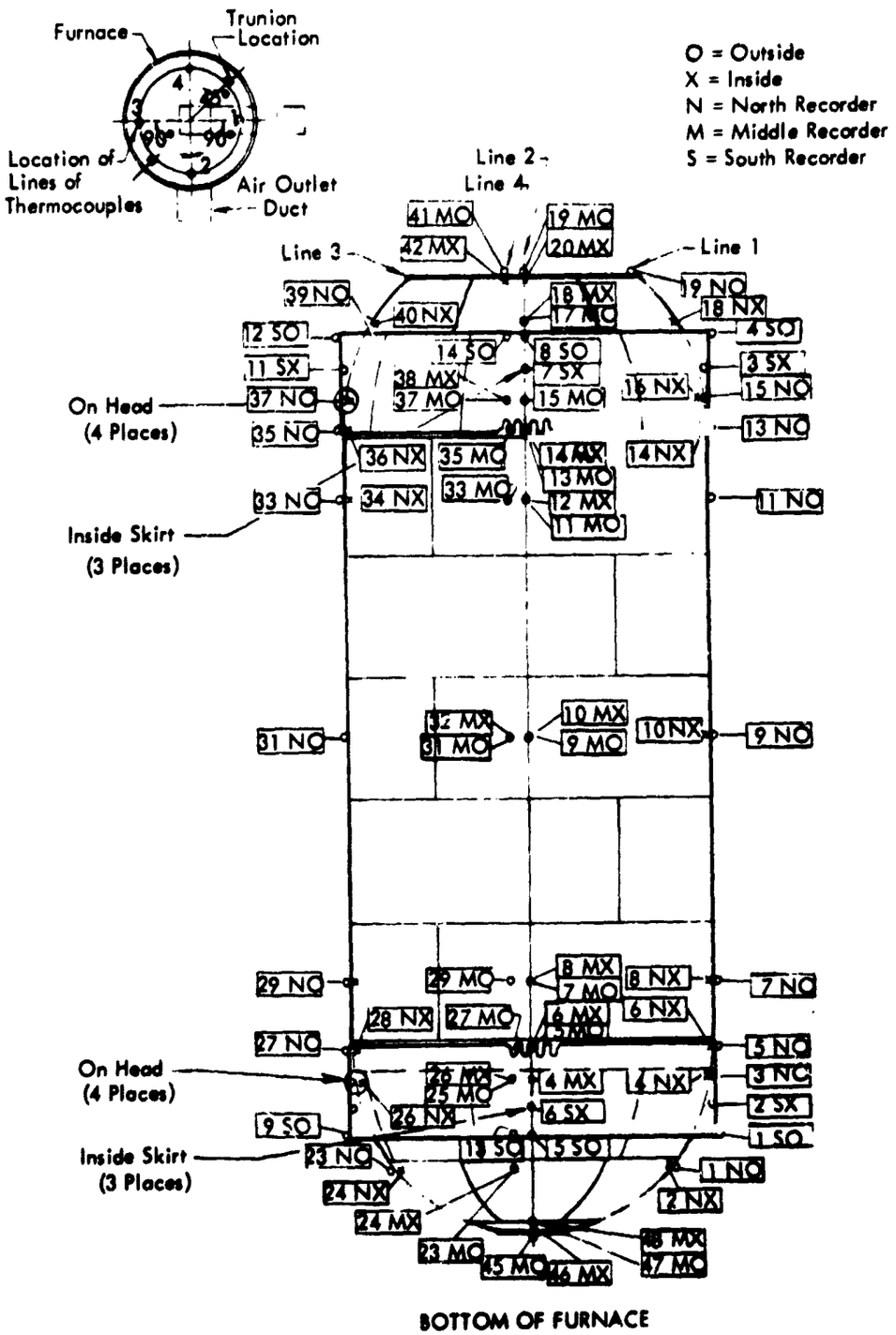

Thermocouple Recording Points, 280-in.-dia Case

Figure 169

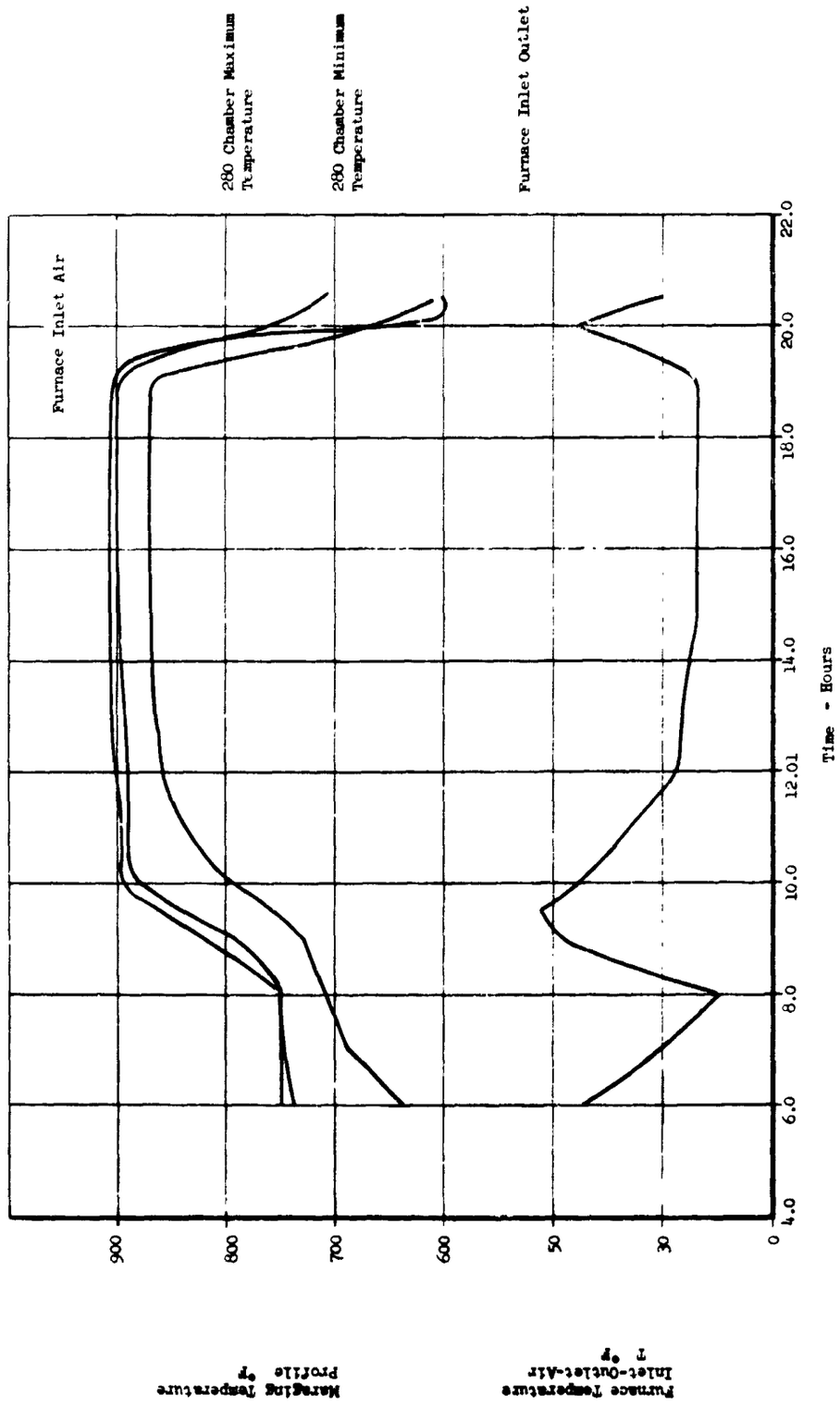

260 Chamber Maraging Demonstration

Figure 170

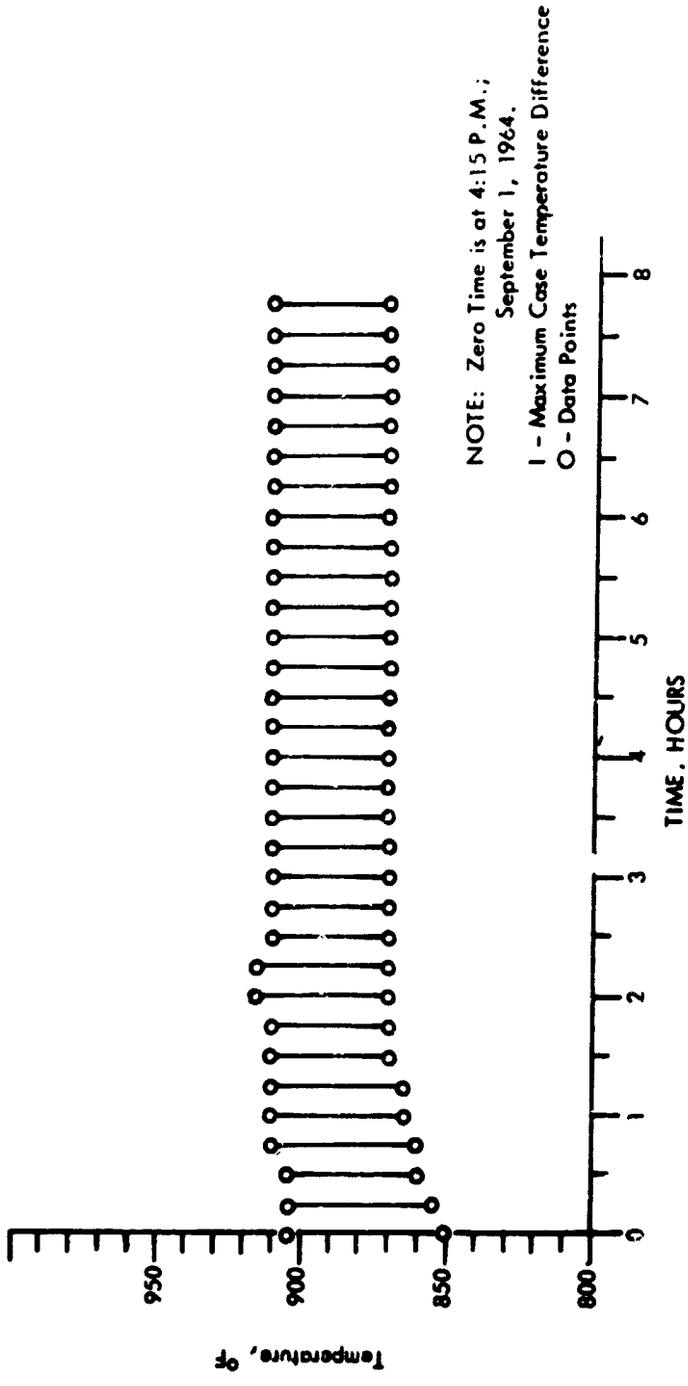

Maximum and Minimum Case Temperature During Maraging Cycle

Figure 171

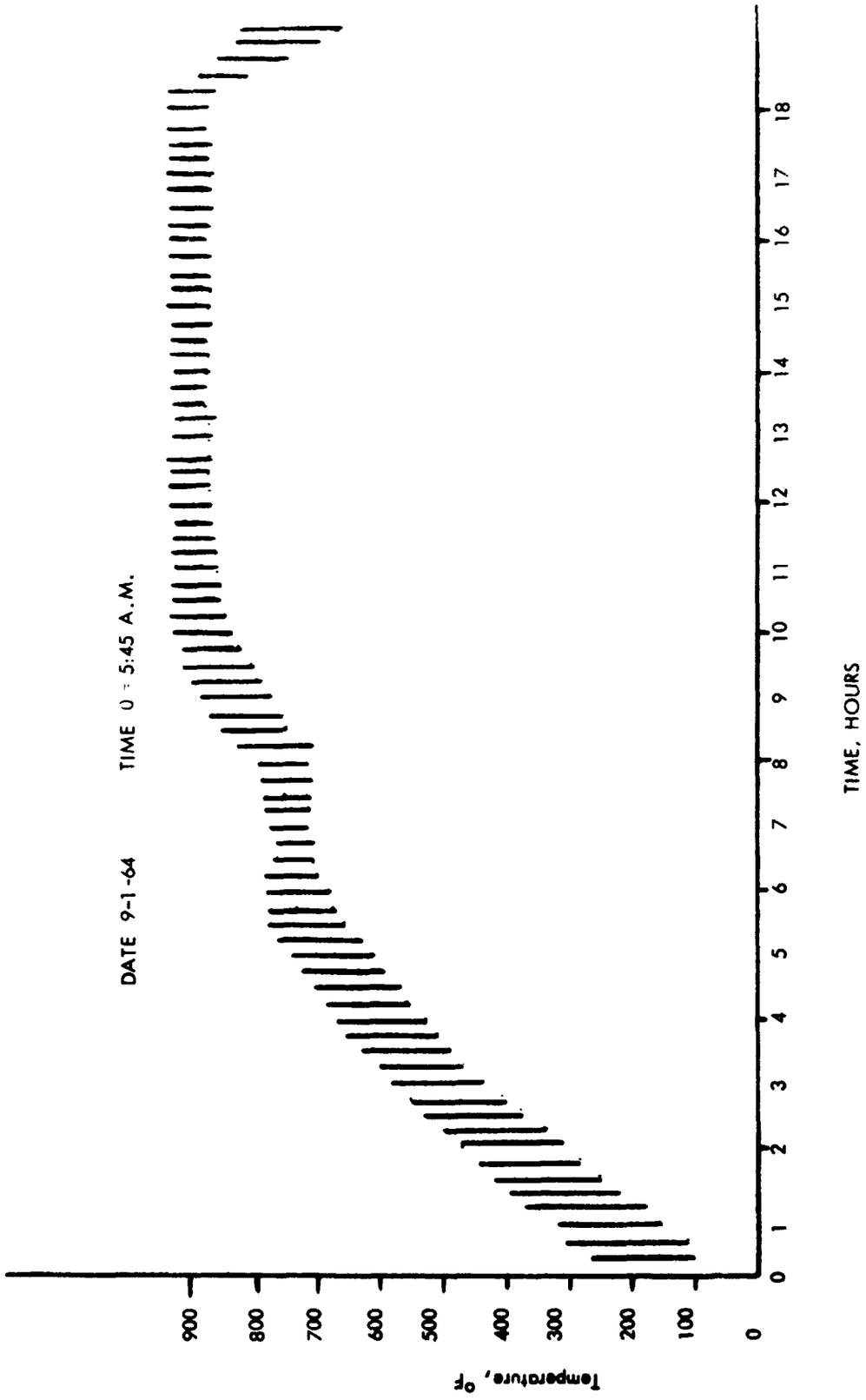

Greatest Temperature Difference for Case

Figure 172

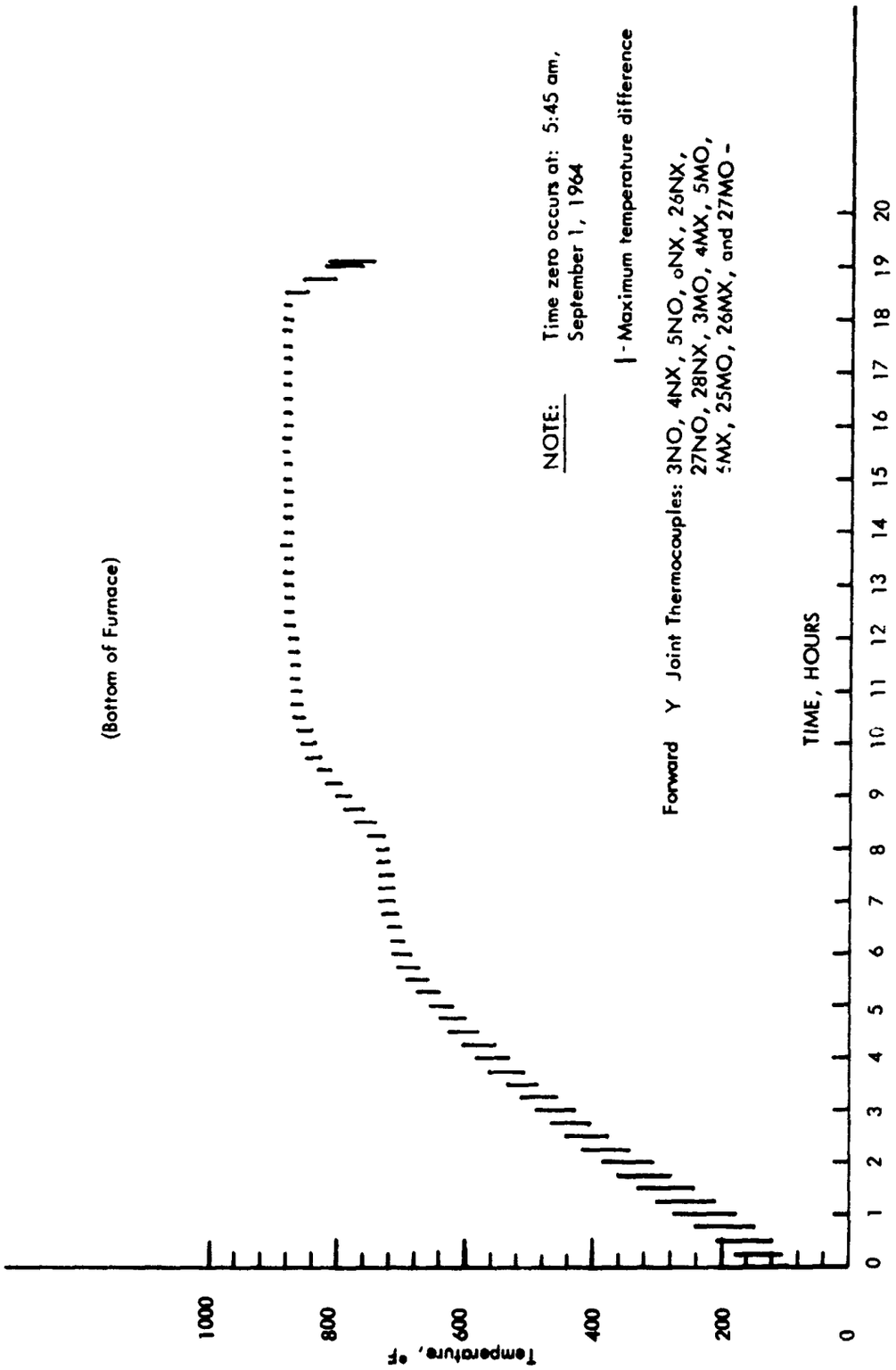

Temperature Extremes vs Time, Forward Y-Joint Location

Figure 173

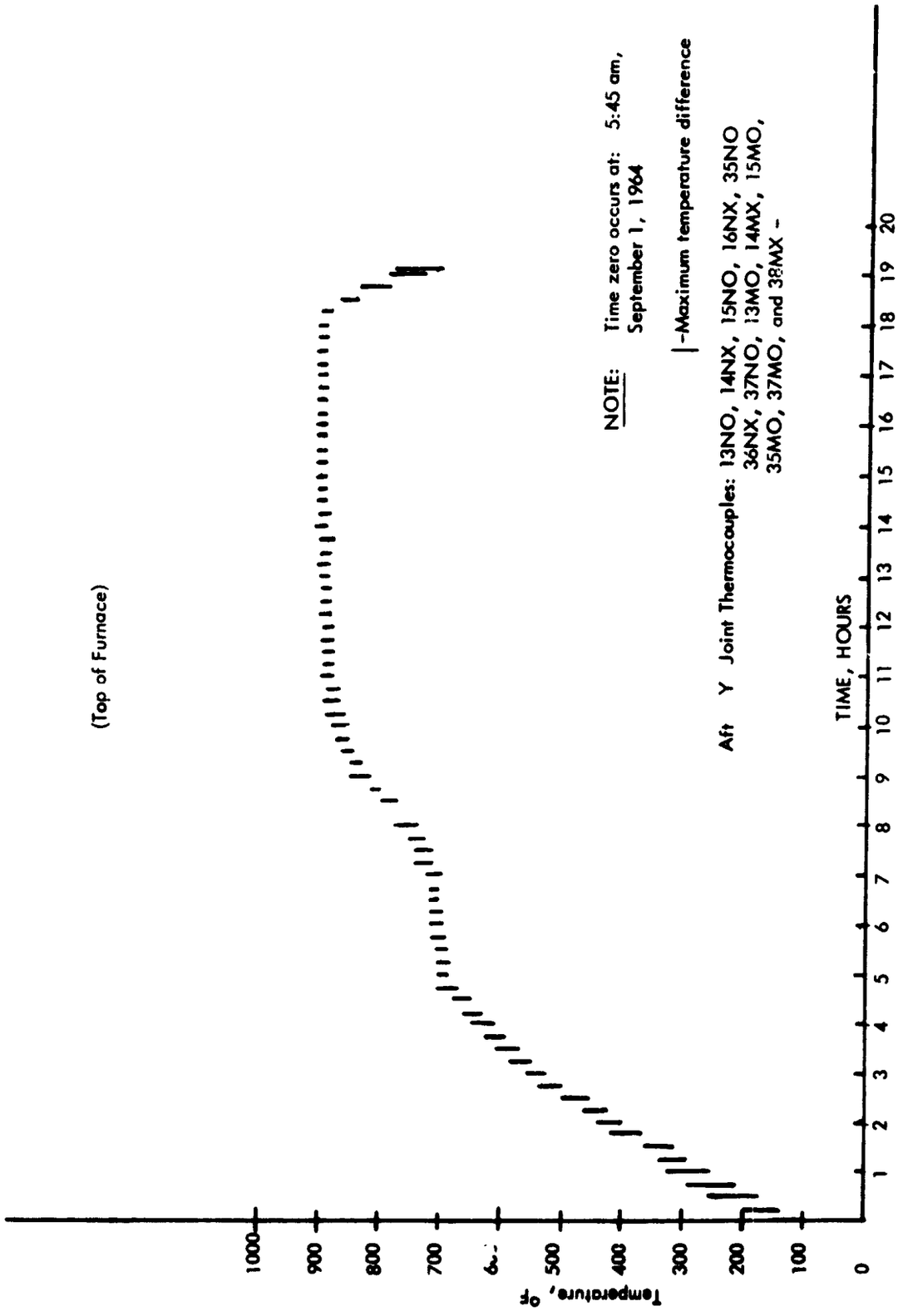

Temperature Extremes vs Time, Aft Y-Joint Location

Figure 174

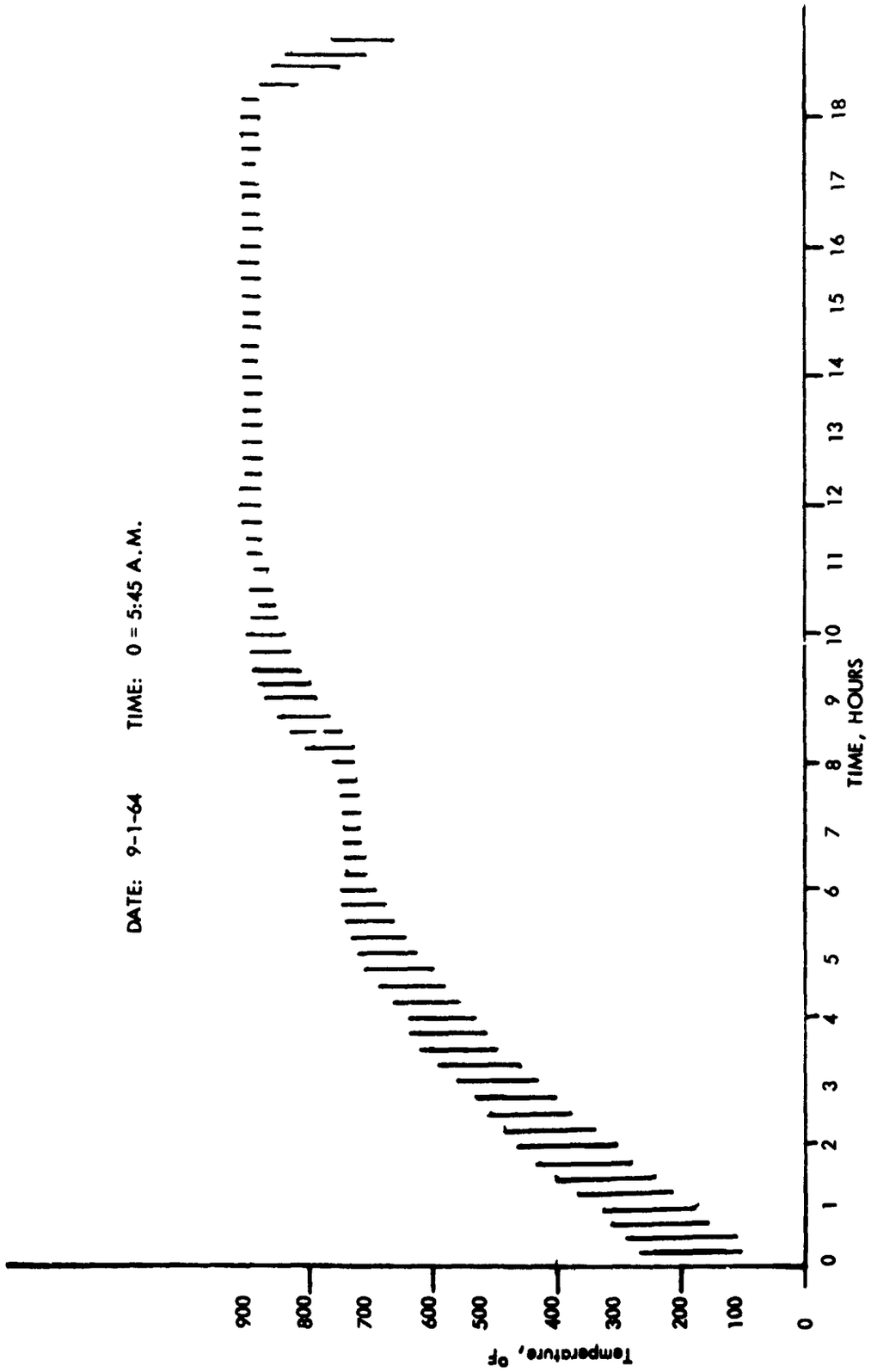

Greatest Temperature Difference for Line 3

Figure 175

Letter Code	Heat No.	Thickness, in.	260-SL-1 Component
A	24996-1A	0.610	Cylinder 1C-A
B	24997-1A	0.610	Cylinder 1C-B
C	24999-1A	0.610	Cylinder 2C-A
M	25000-6A	0.410	Upper Gores 1 through 4
P	25050-1	0.410	Lower Gore 10
H	25064-1	0.410	Lower Gores 1 through 5
EE	3960819-B	0.610	Cylinder 3C-B
FF	3960829-B	0.610	Cylinder 2C-B
-	63343	-	Weld Wire
Fwd Y	--	-	Fwd Y-Ring Forging
Aft Y	--	-	Aft Y-Ring Forging

Identification of Plates Selected for the Complete Profile Maraging Study for 260-SL-1 Material

Figure 176

Maraging Cycle: All specimens heated to 900°F @ 100°F/hr; held at 900°F for 8 hours, and cooled @ 250°F/hr.

Material	0.2% Offset Yield Strength ksi	Ultimate Tensile Strength ksi	Elongation in 1 inch %	Reduction in Area %	M.C. Baseline Yield Strength* ksi	Change ksi
Plate A	244	248	10	51	236	+ 8
Plate B	242	247	10	52	225	+17
Plate C	244	248	10	49	230	+14
Plate M	232	240	10	50	221	+11
Plate P	234	241	10	52	228	+ 6
Plate H	233	243	10	55	224	+ 9
Plate EE	227	236	10	53	217	+10
Plate FF	233	241	11	57	220	+13
Fwd. "Y"	220	230	11	55	213	+ 7
Aft. "Y"	228	235	12	58	218	+10
63343 Auto Weld	224	229	9	44	211	+13

NOTE: 63343 data average of five specimens transverse to weld. All other data average of three longitudinal or circumferential specimens.

* Average of two plate locations-Material Characterization data for 900°F/8 hour heat treatment

260-SL-1 Material Characterization Tensile Data for a Complete Profile Maraging Cycle

Figure 177

Material	G_{nc}, in-lb/in^2	*Baseline G_{nc}, in-lb/in^2		Significant Change
		Loc. 1	Loc. 2	
Plate A	188	196	212	none
Plate B	209	202	239	none
Plate C	195	279	275	down 30%
Plate M	198	168	196	none
Plate P	293	235	263	up 10-20%
Plate H	351	380	436	down 10-20%
Plate EE	325	350	377	down 10-20%
Plate FF	276	332	356	down 10-20%
Aft Y	374	423		down 10%
Fwd Y	398	357		up 10%
63343 auto weld	282 (G_{Ic})	412 (G_{Ic})		down 30%

* Baseline from Material Characterization data for 900°F/8 hour maraging cycle

260-SL-1 Material Characterization G_{nc} Data for a Full Profile Maraging Cycle

Figure 178

PLATE M

Heat-Up Rate, °F/hr	Cool-Down Rate, °F/hr	0.2% Offset Yield Strength, ksi	Ultimate Tensile Strength ksi	Elongation in 1 in. %	Reduction in Area, %
400	Ambient Air	225	235	11	52
400	200	228	236	10	52
800	Ambient Air	221	230	10	53

PLATE A

400	Ambient Air	235	242	11	52
*	Ambient Air	236	241	11	52

63343 AUTOMATIC WELDS

400	Ambient Air	211	220	--	55
400	250	218	226	--	49
800	Ambient Air	214	222	--	52

NOTE: All data average of three tensile specimens.
Elongations not reported for weld specimens since all but one specimen broke outside gage marks in the weld heat-affected zone.
Maraging Cycle: All specimens were maraged at 900°F for 8 hr; heat-up and cool-down rates were as shown above.
* Original material characterization data.

Effect of Heat-Up and Cool-Down Rates on Tensile Properties Of Plate M, Plate A, and 63343 Automatic Welds

Figure 179

Maraging Cycle: All specimens heated to the hold temperatures shown below @ 100°F/hour, held 8 hours at temperature, and cooled @ 250°F/hour.

PLATE M						
Hold Temperature °F/hour	0.2% Offset Yield Strength ksi	Ultimate Tensile Strength ksi	Elongation in 1 inch %	Reduction in Area %	M.C. Baseline Yield Strength ksi	Change ksi
800	208	218	12	53	--	--
850	223	232	11	54	212	+11
900	233	242	11	52	221	+12
950	213	228	12	54	206	+ 7
63343 Automatic Welds						
800	199	208	11	55	--	--
850	210	219	10	51	207	+ 3
900	221	228	9	49	211	+10
950	213	222	12	52	202	+11

NOTE: 900°F Plate M baseline data average of six tensile specimens from two plate locations; all other data average of three tensile specimens.

All but two weld specimens failed in weld metal.

Effect of Hold Temperature on Tensile Properties of Plate M and 63343 Automatic Welds

Figure 180

Maraging Cycle: All specimens heated to the temperatures shown below @100°F/hour and immediately cooled in ambient air.

Temperature °F	0.2% Offset Yield Strength ksi	Ultimate Tensile Strength ksi	Elongation in 1 inch %	Reduction in Area %
Solution Annealed	121	143	15	71
700	140	158	16	69
800	155	171	16	66
850	164	178	15	64
900	185	197	13	61
950	190	201	13	61

NOTE: Solution annealed data average of two tensile specimens; all others average of three tensile specimens.

Change in Strength of Plate M During Heat-Up to the Maraging Temperature

Figure 181

Heat Number	Composition, wt %									
	C	Mn	Si	Ni	Co	Mo	Ti	Al	P	S
					Parent Metal					
3920556	0.02	0.05	0.08	17.68	7.9	4.2	0.16	0.16	0.008	0.006
Specified (AGC-34315)	0.03	0.10	0.10	17.5	7.0	4.0	0.05	0.05	0.025	0.01
Limits	Max.	Max.	Max.	19.0	8.0	4.5	0.25	0.15	Max.	Max.
					Filler Wire					
34482	0.02	0.01	0.007	18.2	7.65	3.53	0.24	0.1	0.003	0.003
Specified (AGC-34326)	0.03	0.10	0.01	17.5	7.5	3.6	0.26	0.10	0.01	0.01
Limits	Max.	Max.	Max.	18.5	8.0	3.8	0.30	Added	Max.	Max.

Composition of Republic Heat 3920556, 18%-Nickel Maraging Steel Plate and Filler Wire 34482

Figure 182

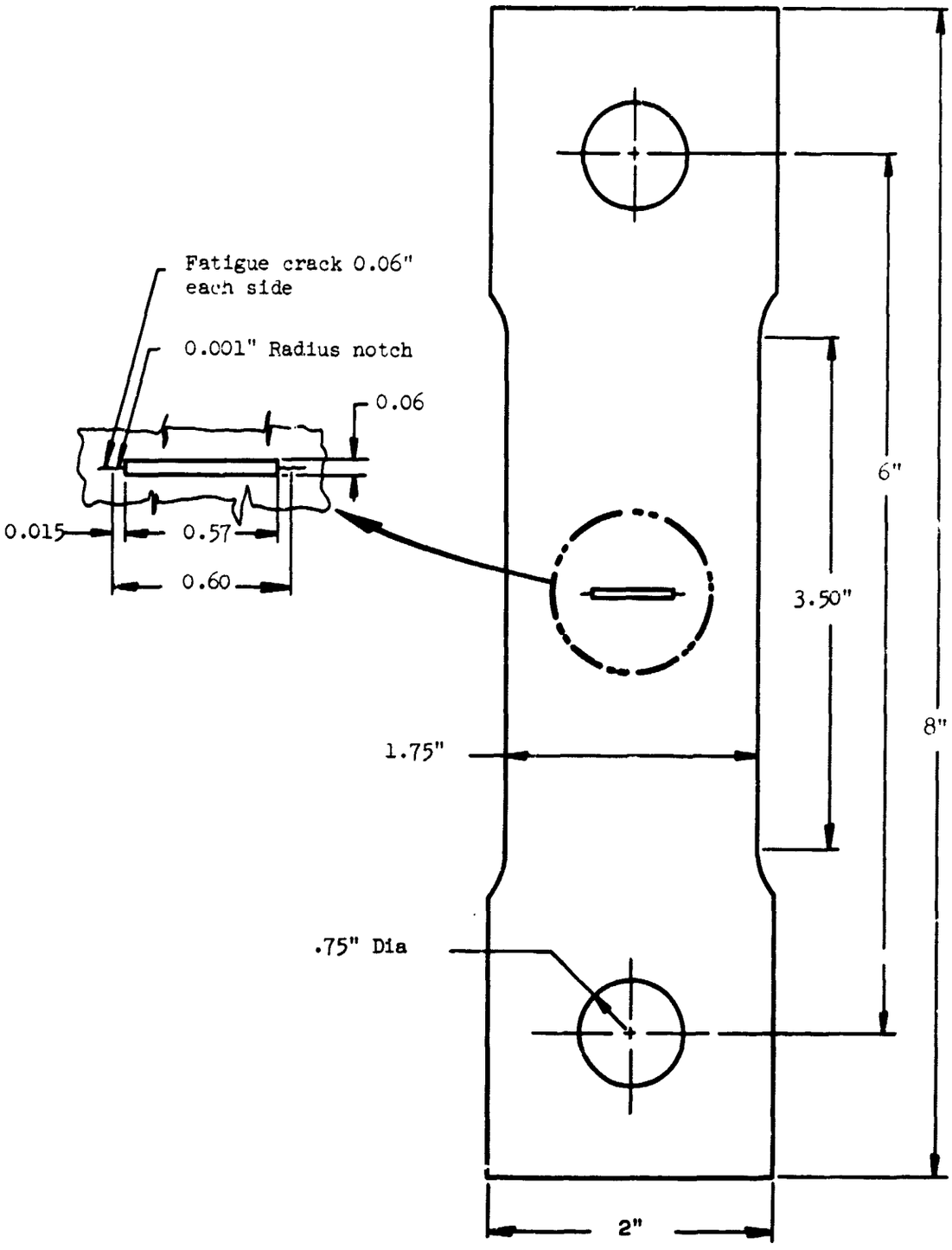

Fatigue Cracked Stress-Corrosion Specimen

Figure 183

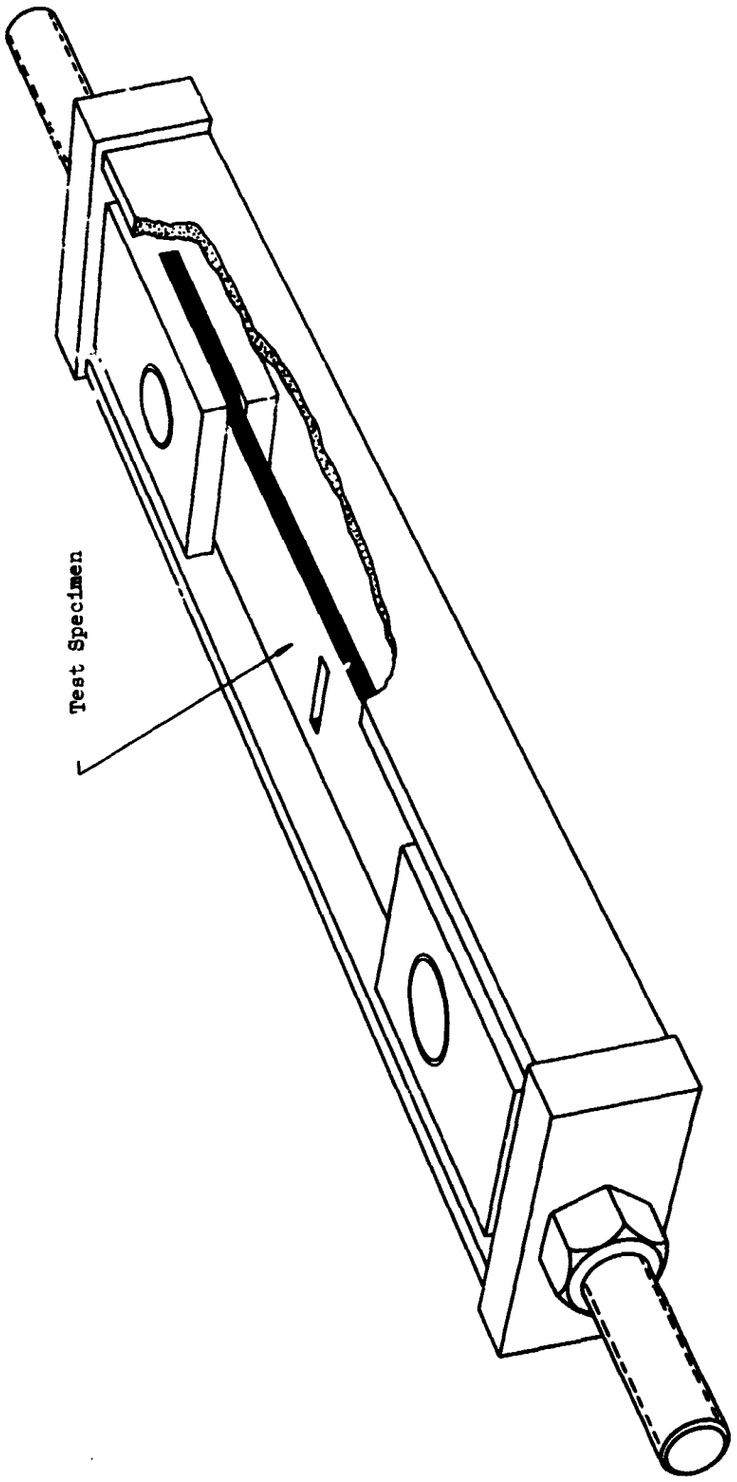

Stress-Corrosion Test Fixture

Figure 184

Material	Orientation	Thickness, in.	Width, in.	Maximum Load, lb	Crack Length, in.	Net Area[1] in.^{2}		Ultimate Tensile Strength, ksi
Base Metal[2]	Longitudinal	0.061	1.75	13,100	0.744	0.062		211
		0.062	1.75	13,200	0.748	0.063		210
		0.057	1.75	11,850	0.763	0.057		207
							Avg.	210
Base Metal[2]	Transverse	0.060	1.75	11,800	0.780	0.058		200
		0.057	1.75	12,000	0.753	0.057		201
		0.058	1.75	12,050	0.747	0.058		204
							Avg.	202
Weld Metal[3]	Transverse	0.0615	1.756	12,300	0.722	0.0636		193
		0.0615	1.748	12,150	0.722	0.0631		193
		0.0615	1.752	13,100	0.722	0.0642		204
							Avg.	197

(1) Based on uncracked area.
(2) Aged 900°F-8 hr.
(3) As-welded and aged 900°F-8 hr.

Center-Notched Tensile Properties of Republic Heat 3920556 Grade 200, 18%-Nickel Maraging Steel Plate and Weld Deposited with Filler Wire 34482

Figure 185

Material(1)	Number of Specimens	Orientation	Environment(2)	Applied Stress	Exposure Time (Days)	Failure
Base Metal	3	Longitudinal	1% $NaCr_2O_7;2H_2O$	170	45	No(3)
Base Metal	3	Transverse	1% $NaCr_2O_7;2H_2O$	170	45	No(3)
Weld Metal	3	Transverse	1% $NaCr_2O_7;2H_2O$	170	45	No(3)
Base Metal	3	Longitudinal	2% $NaCr_2O_7;2H_2O$	170	45	No(3)
Base Metal	3	Transverse	2% $NaCr_2O_7;2H_2O$	170	45	No(3)
Weld Metal	3	Transverse	2% $NaCr_2O_7;2H_2O$	170	45	No(3)
Base Metal	3	Longitudinal	Distilled Water	170	45	No(3)
Base Metal	3	Transverse	Distilled Water	170	45	No(3)
Weld Metal	3	Transverse	Distilled Water	170	15, 16, 20	Yes(3)

(1) Republic heat 3920556 base metal; Weld metal deposited with heat 34482 filler wire; all specimens aged at 900°F for 8 hr.
(2) Immersed continuously; solution pH adjusted to 7.3 by adding sodium hydroxide.
(3) Net stress

Effects of Sodium Dichromate Inhibitor on the Stress-Corrosion Susceptibility of Grade 200, 18%-Nickel Maraging Steel Plate and Weldments

Figure 186

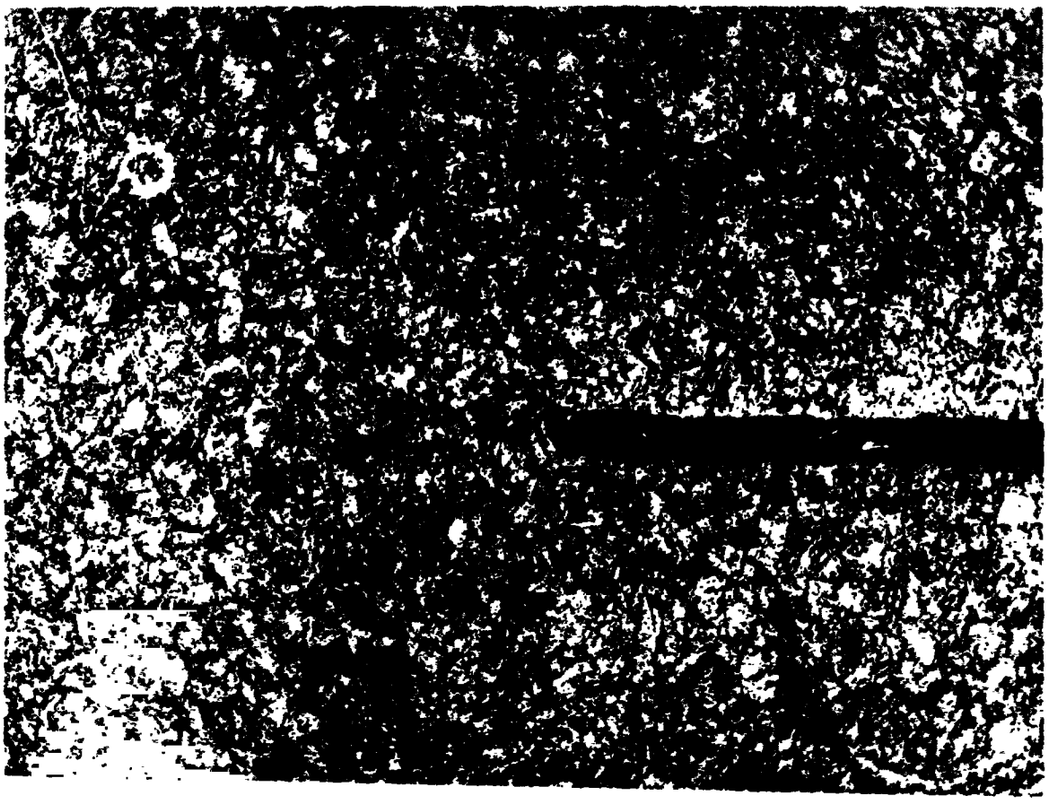

Intergranular Cracking Observed in Center-Notch Tensile Specimen Prepared from 0.6-in.-Thick Republic Heat 3920556, Grade 200, 18%-Nickel Maraging Steel Plate and Subjected to a Sustained Tensile Load of 170 ksi while Immersed in 1% Sodium Dichromate Solution for 45 Days

Figure 187

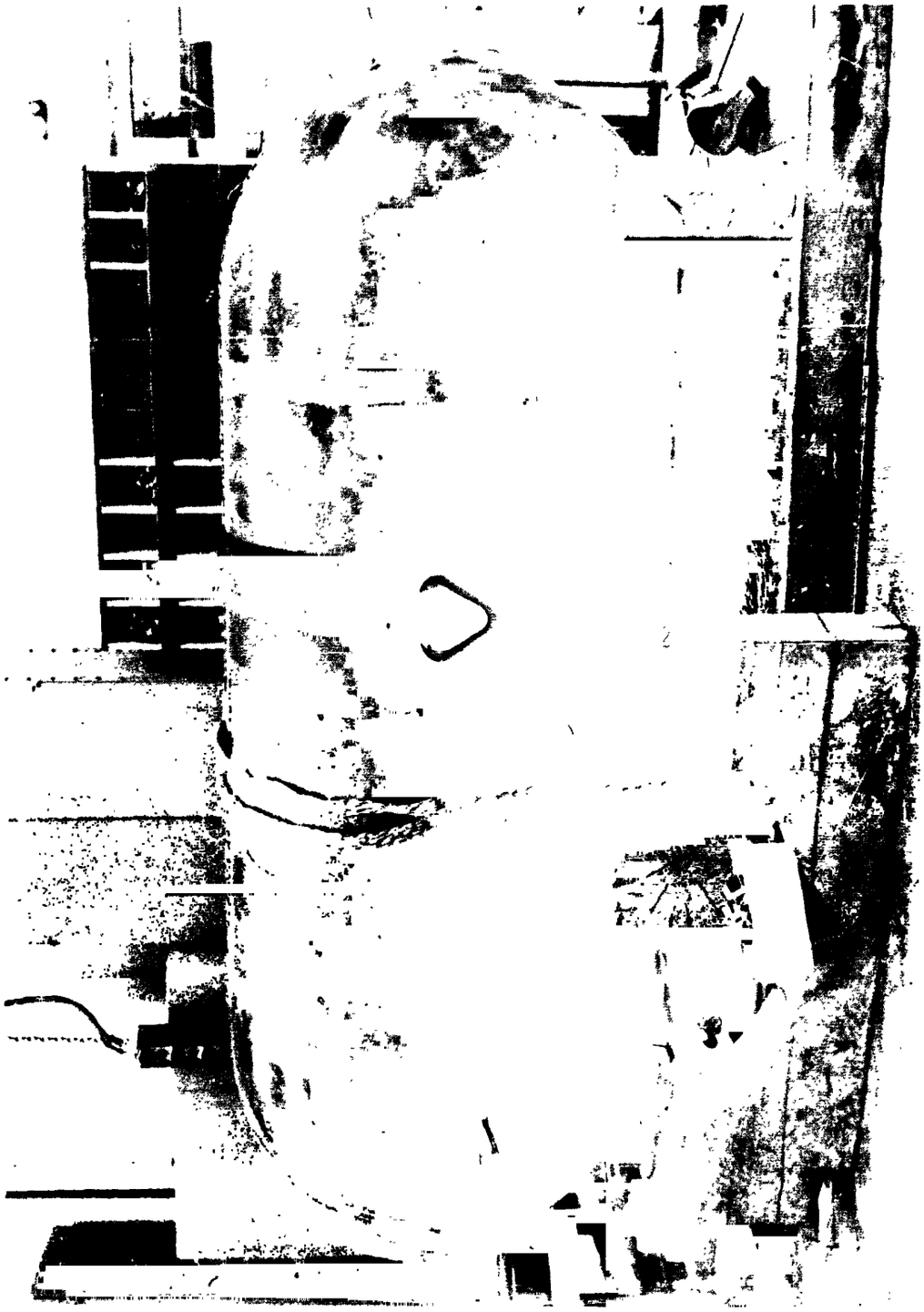

Process Evaluation Test Vehicle (PETV)

Figure 188

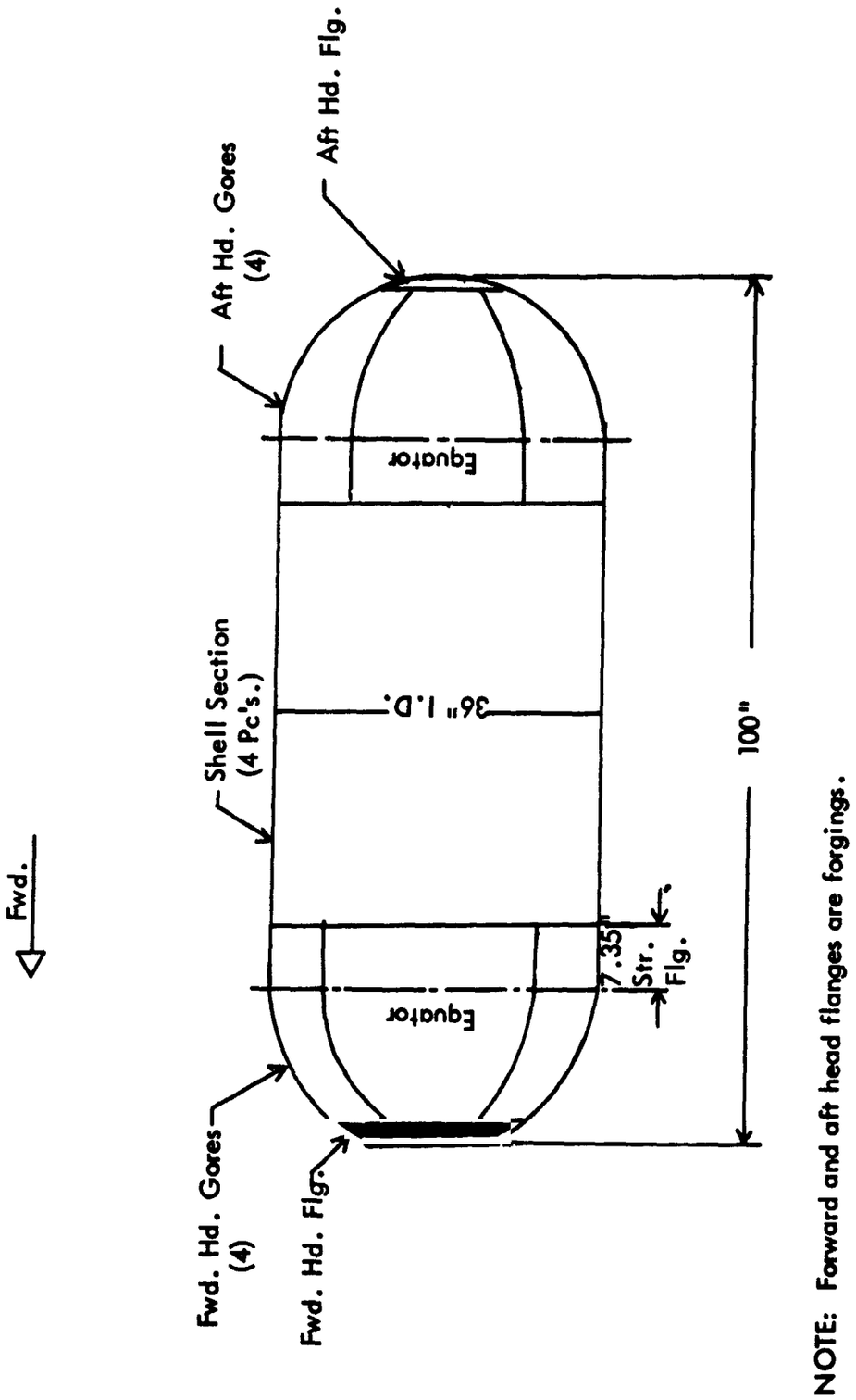

Configuration of PETV 1

Figure 189

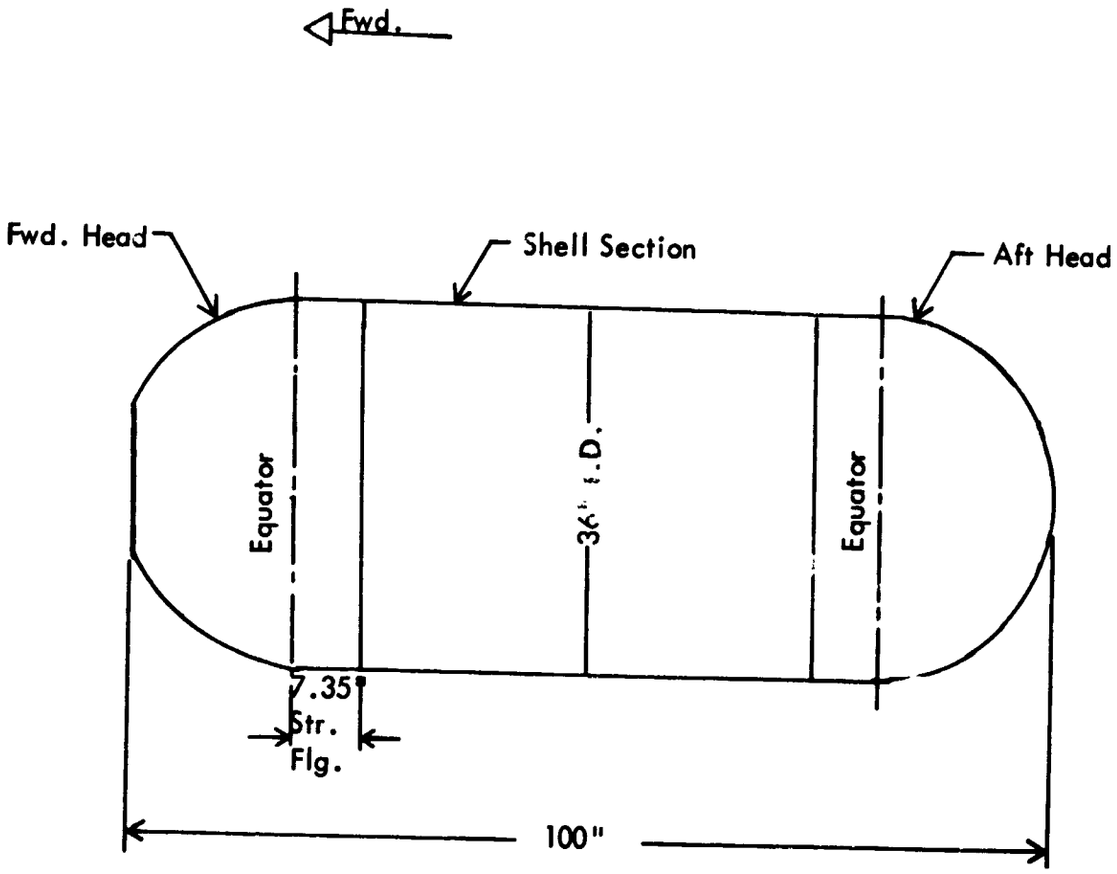

Configuration of PETV 2

Figure 190

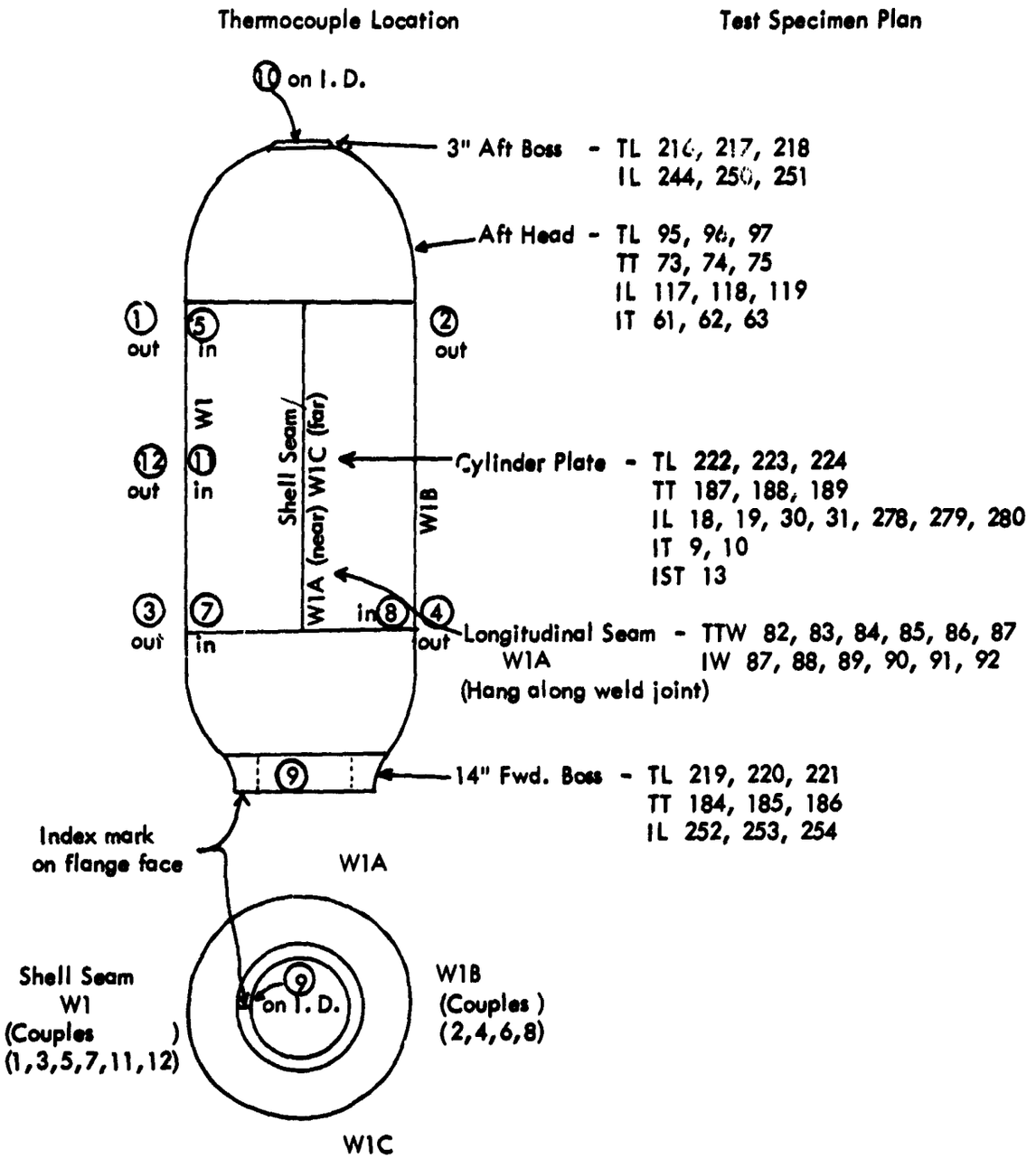

Thercocouple Location and Material Test Specimens for PETV 1

Figure 191

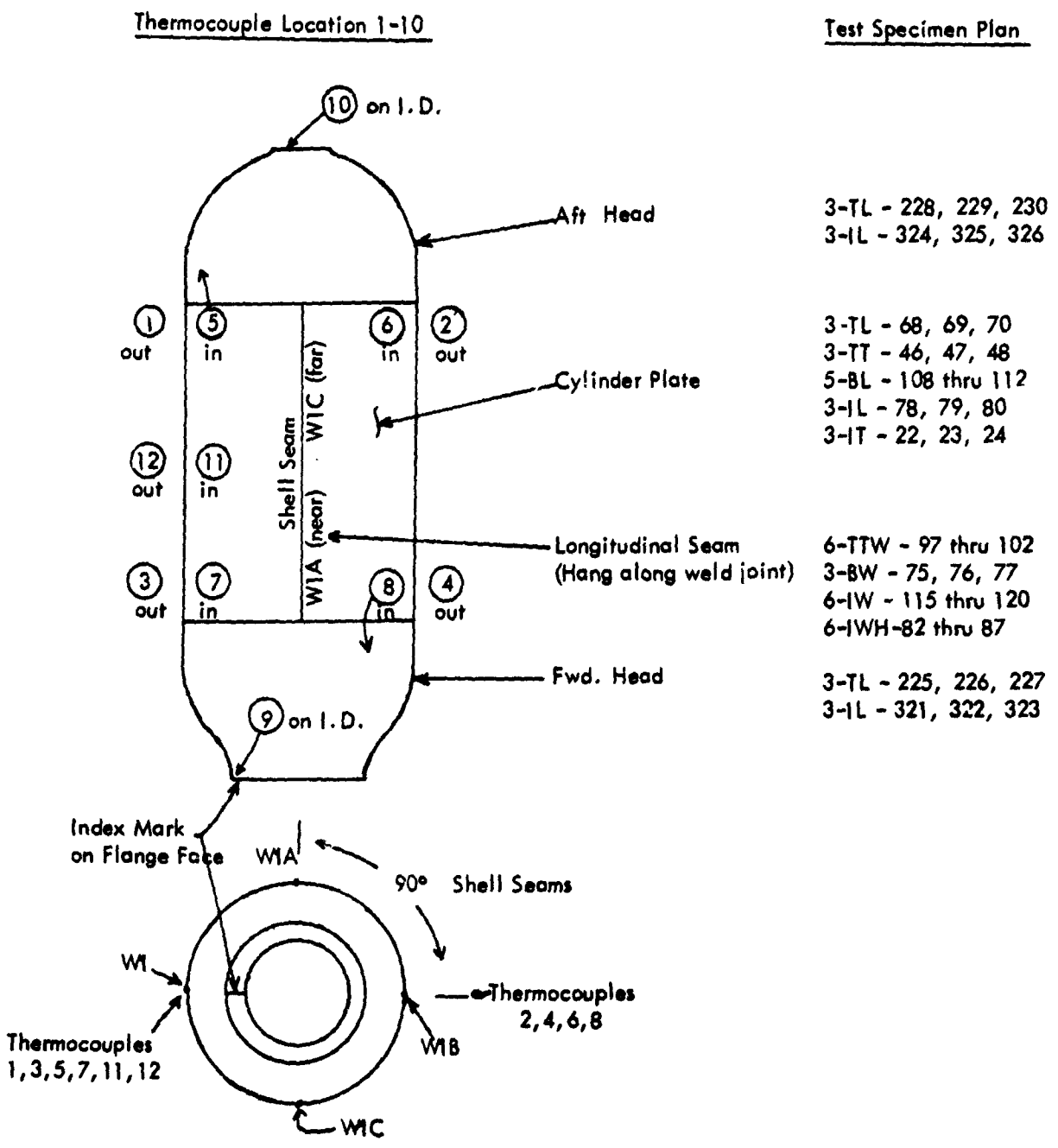

Thermocouple Location and Material Test Specimens for PETV 2

Figure 192

Material Represented	Orientation	0.2% Offset Yield Strength ksi	Ultimate Tensile Strength ksi	Elongation in 1 inch %	Reduction in Area %
Cylinder Plate (R-600-1)	Longitudinal	224.0	229.5	12	52.0
		227.0	237.0	12	54.2
		227.0	236.0	11	57.4
	Avg.	226	234	12	54
Cylinder Plate (R-600-1)	Transverse	241.5	246.5	11	52.5
		241.5	246.5	12	53.5
		241.5	246.0	10	49.7
	Avg.	241.5	246	11	52
Heads (R-600-1A)	Longitudinal	226.5	236.0	11	52.5
		224.0	232.0	12	60.5
		226.5	236.0	11	56.8
	Avg.	226	235	11	57
Heads (R-600-1A)	Transverse	236.0	245.0	10	47.5
		236.0	242.0	10	50.9
		234.0	244.0	11	49.1
	Avg.	235	244	10	49
14-Inch Flange	Tangential	212.0	224.0	12	53.2
		215.0	227.0	12	52.5
		211.0	213.0	11	49.1
	Avg.	213	221	12	52
14-Inch Flange	Axial	209.0	224.0	11	48.1
		218.0	228.0	11	46.9
		217.5	228.0	11	45.2
	Avg.	215	227	11	47
3-Inch Flange	Tangential	217.0	227.0	11	53.1
		217.0	226.0	11	51.8
		218.0	228.0	12	55.8
	Avg.	217	227	11	54

Test Results of Tensile Specimens Maraged with PETV 1

Figure 193

Material Represented	Orientation	W/A at Room Temperature in-lb/in^2
Cylinder Plate (R-600-1)	Longitudinal	813
		847
		831
		850
		640
		659
		810
		Average 779
Cylinder Plate (R-600-1)	Trans[illegible]	701
		838
		Average 770
Heads (R-600-1A)	Longitudinal	1258
		1222
		1114
		Average 1198
Heads (R-600-1A)	Transverse	742
		826
		932
		Average 833
14-Inch Flange	Longitudinal	712
		755
		723
		Average 730
3-Inch Flange	Longitudinal	711
		857
		791
		Average 786

Test Results of Precracked Impact Specimens Maraged with PETV 1

Figure 194

Material	Orientation	Yield Strength, ksi	Tensile Strength, ksi	Elongation in 1-in., %	Reduction in Area, %
34481	Transverse	209	214	12	57.5
		212	214	11	53.6
		208	213	12	53.1
		208	214	12	52.2
		205	211	12	55.2
		208	211	12	54.0

Test Results of Tensile Specimens Managed with PETV 1

Figure 195

Material Represented	Orientation	0.2% Offset Yield Strength ksi	Ultimate Tensile Strength ksi	Elongation in 1 inch %	Reduction in Area %
Cylinder Plate	Longitudinal	224.0	232.0	11	54.8
		223.5	232.5	11	55.3
		229.5	238.0	12	56.0
		Avg. 226	234	11	55
Cylinder Plate	Transverse	233.5	241.5	10	49.1
		233.5	242.5	10	46.3
		236.0	243.0	9	45.8
		Avg. 234	242	10	47
Forward Head	Tangential	218.0	228.0	12	55.8
		218.0	228.0	11	54.2
		215.0	226.0	11	47.5
		Avg. 217	227	11	53
Aft Head	Tangential	218.0	228.5	12	51.9
		217.0	226.0	12	57.2
		218.0	227.5	12	56.8
		Avg. 218	227	12	55

Test Results of Tensile Specimens Maraged with PETV 2

Figure 196

Material Represented	Orientation	Width b, in	Depth d, in	$1/M \times 10^6$ in^2/lb	Effective a, in *	Proportional Load Limit, lb	Fracture Toughness G_{nc} $in\text{-}lb/in^2$	Stress Intensity Factor K_{nc} $1000\ psi\sqrt{in}$
Cylinder Plate	Longitudinal	0.596	0.597	2.176	0.1894	5040	240	84
Cylinder Plate	Longitudinal	0.597	0.597	2.184	0.1906	5220	259	88
Cylinder Plate	Longitudinal	0.597	0.597	2.180	0.1900	5340	270	89
Cylinder Plate	Longitudinal	0.596	0.598	2.096	0.1768	5460	251	86
Cylinder Plate	Longitudinal	0.597	0.597	2.047	0.1683	6240	304	95
						Average	265	89

* NOTE: Effective "a" values have an accuracy of $\pm$ 0.0010 inch.

Test Results of Slow-Notch-Bend Specimens Maraged with PETV 2

Figure 197

Material Represented	Orientation	W/A at Room Temperature in-lb/in^2
Cylinder Plate	Longitudinal	613
		676
		689
		Average 659
Cylinder Plate	Transverse	487
		467
		487
		Average 480
Forward Head	Tangential	1112
		1166
		1140
		Average 1139
Aft Head	Tangential	1003
		1126
		1117
		Average 1082

Test Results of Precracked Impact Specimens Maraged with PETV 2

Figure 198

(Specimens Prepared from Wire 63343 and Plate 25000-1)

Tensile Specimens

Orientation	0.2% Yield Strength, ksi	Tensile Strength, ksi	Elongation in 1 in., %	Reduction in Area, %
Transverse to weld	215.5	222.0	12	52.6
(Automatic)	218.0	223.5	11	54.2
	215.5	221.5	11	46.9
Transverse to weld	212.0	217.0	11	55.8
(Manual repair)	212.0	218.0	10	47.5
	206.0	210.0	10	57.8

Precracked Impact Specimens

Material	Orientation	W/A at Room Temperature, in.-lb/sq in.
Longitudinal weld	Weld metal	947
		775
		720
Longitudinal weld	HAZ	825
		964
		1034
Manual weld	Weld metal	880
		821
		1055
Manual weld	HAZ	1082
		954
		1062

Test Results of Weldment Specimens Maraged with PETV 2

Figure 199

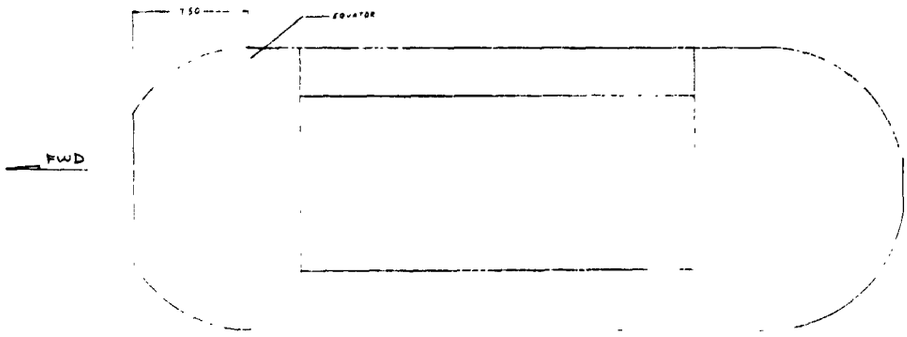

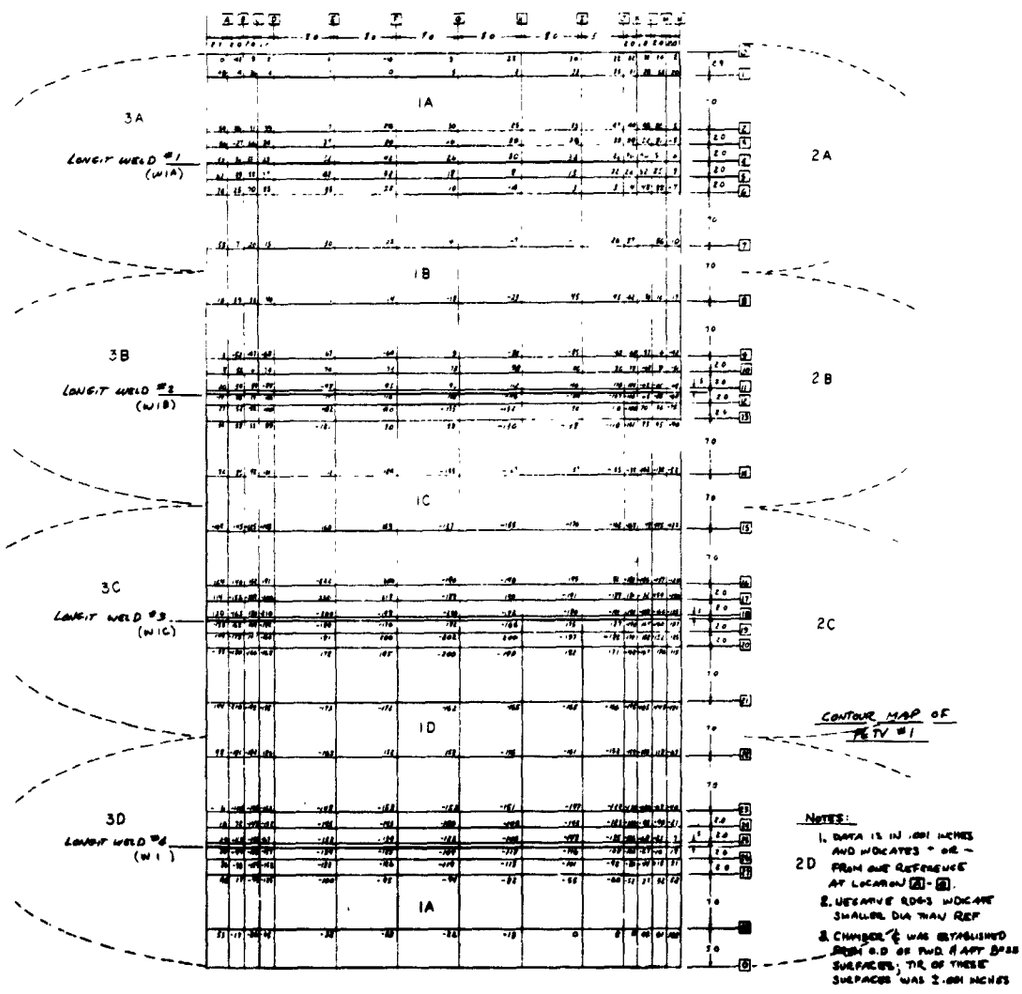

Out-of-Round Measurements, Weld Identification, and Chamber Section for PETV 1

Figure 200

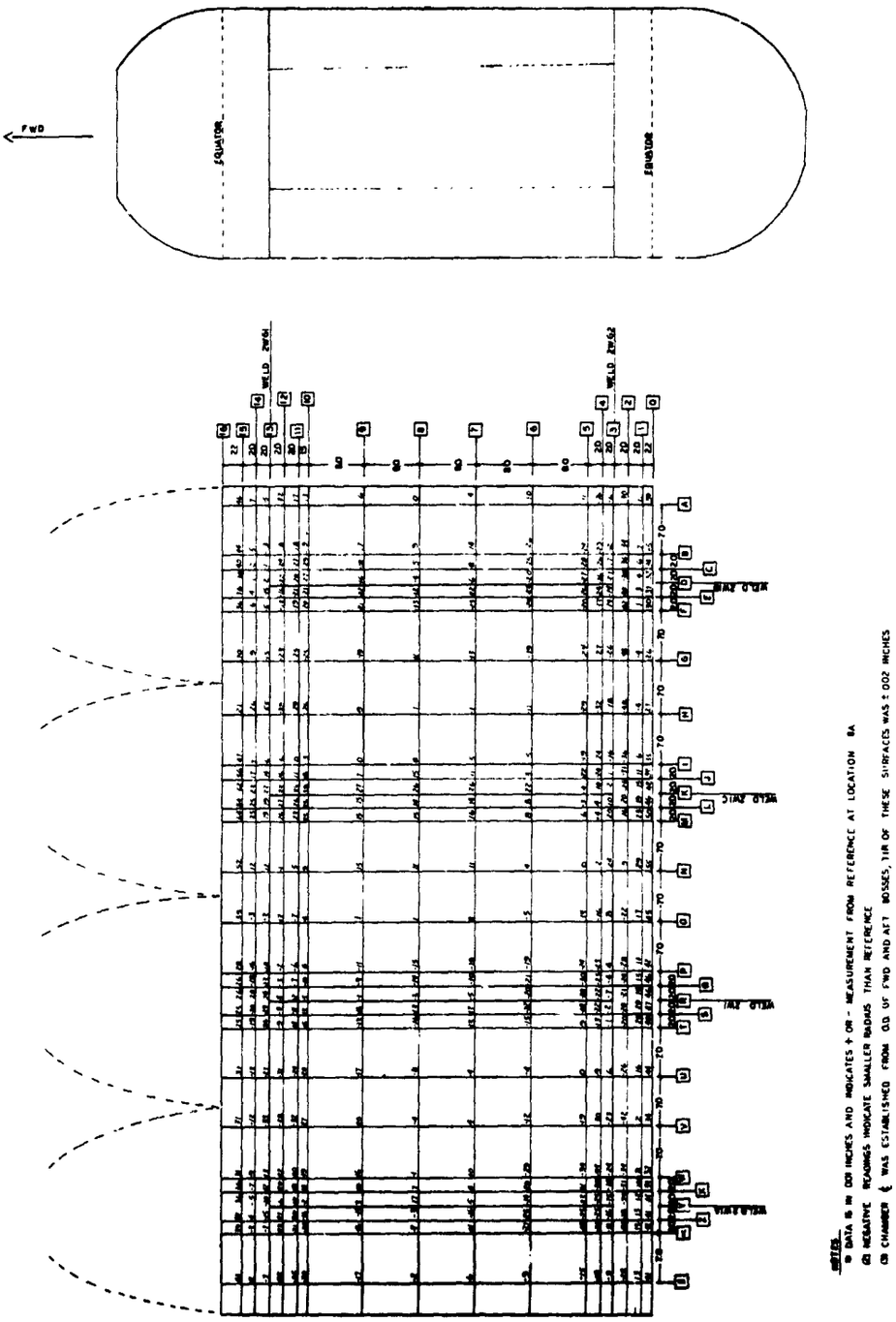

Out-of-Round Measurements, Weld Identification, and Chamber Sections for PETV 2

Figure 201

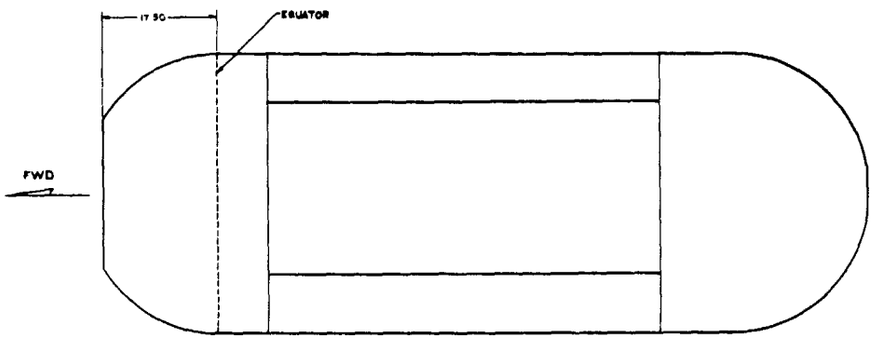

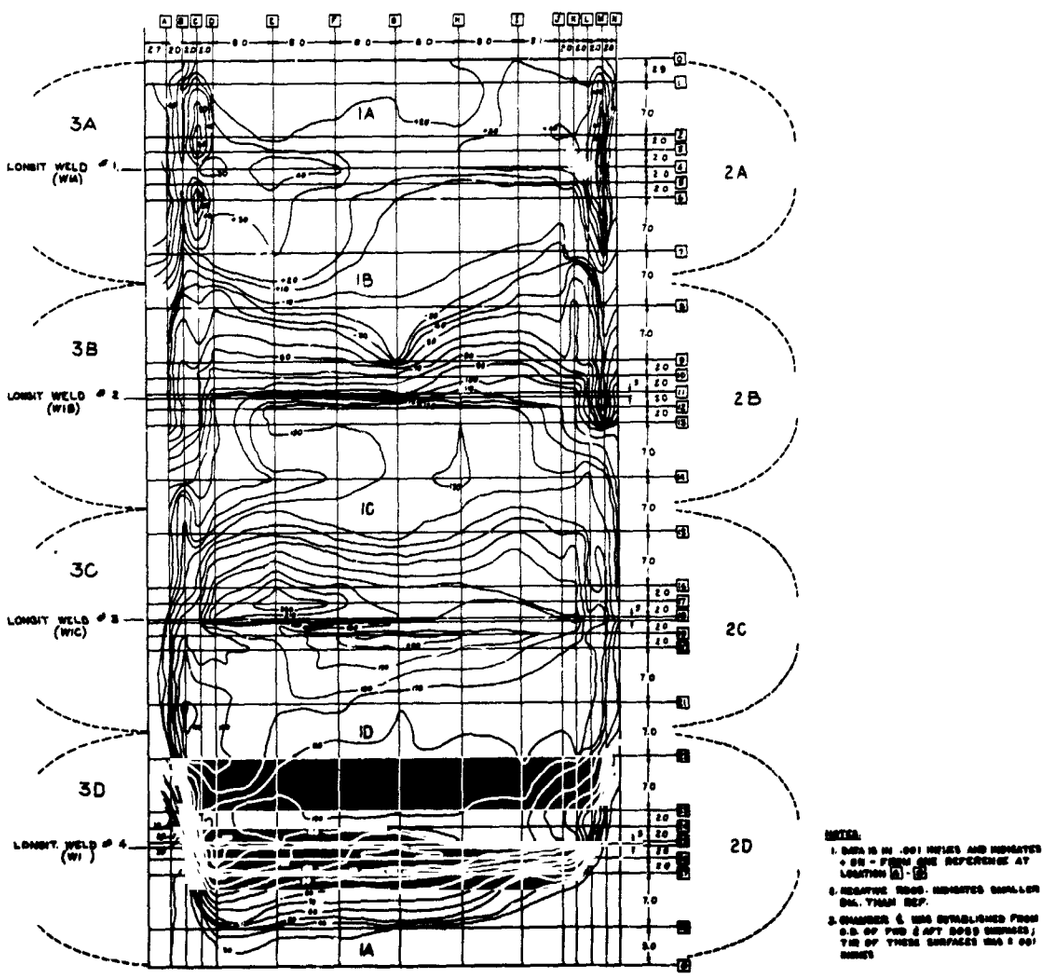

Contour Map of PETV 1

Figure 202

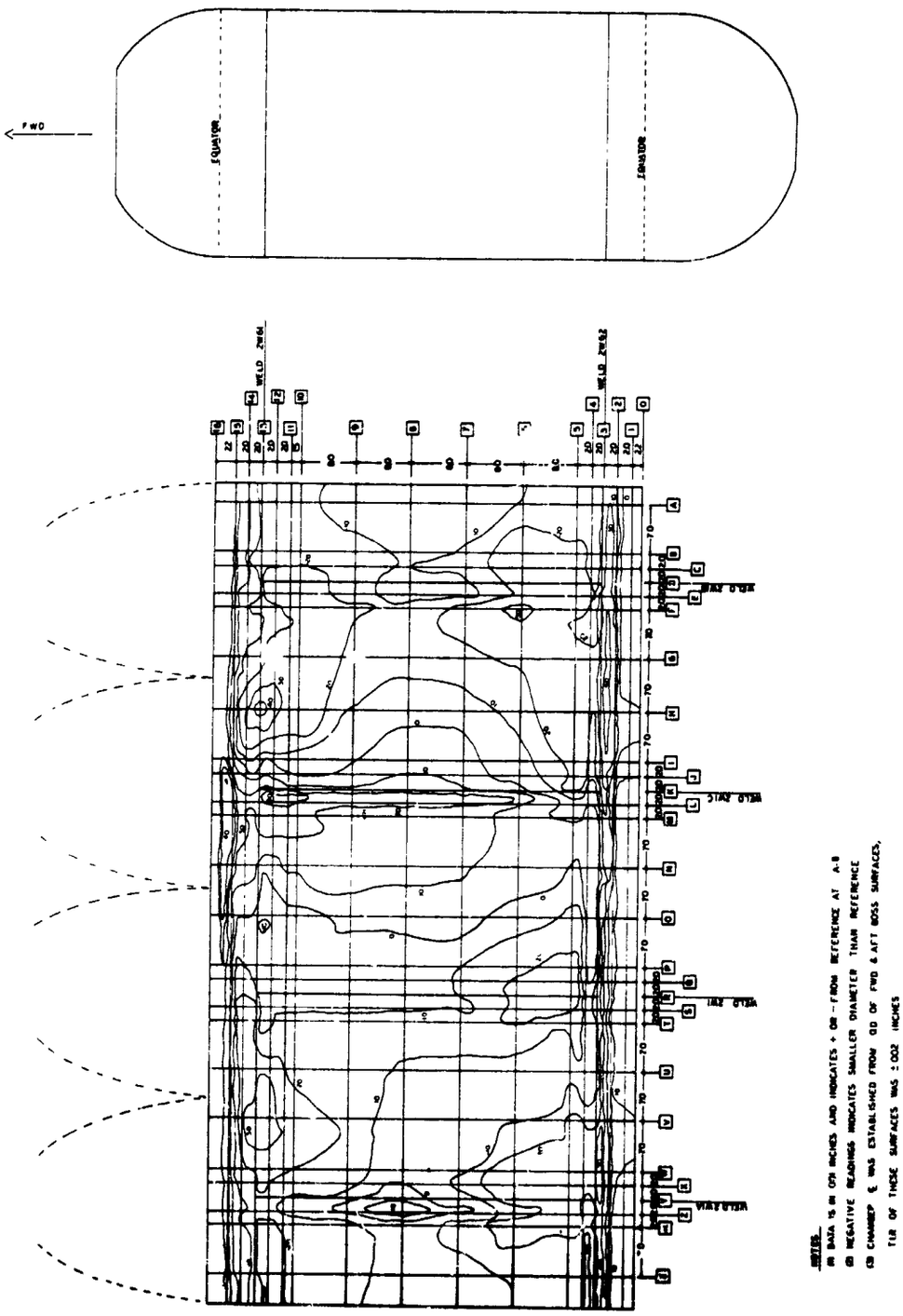

Contour Map of PETV 2

Figure 203

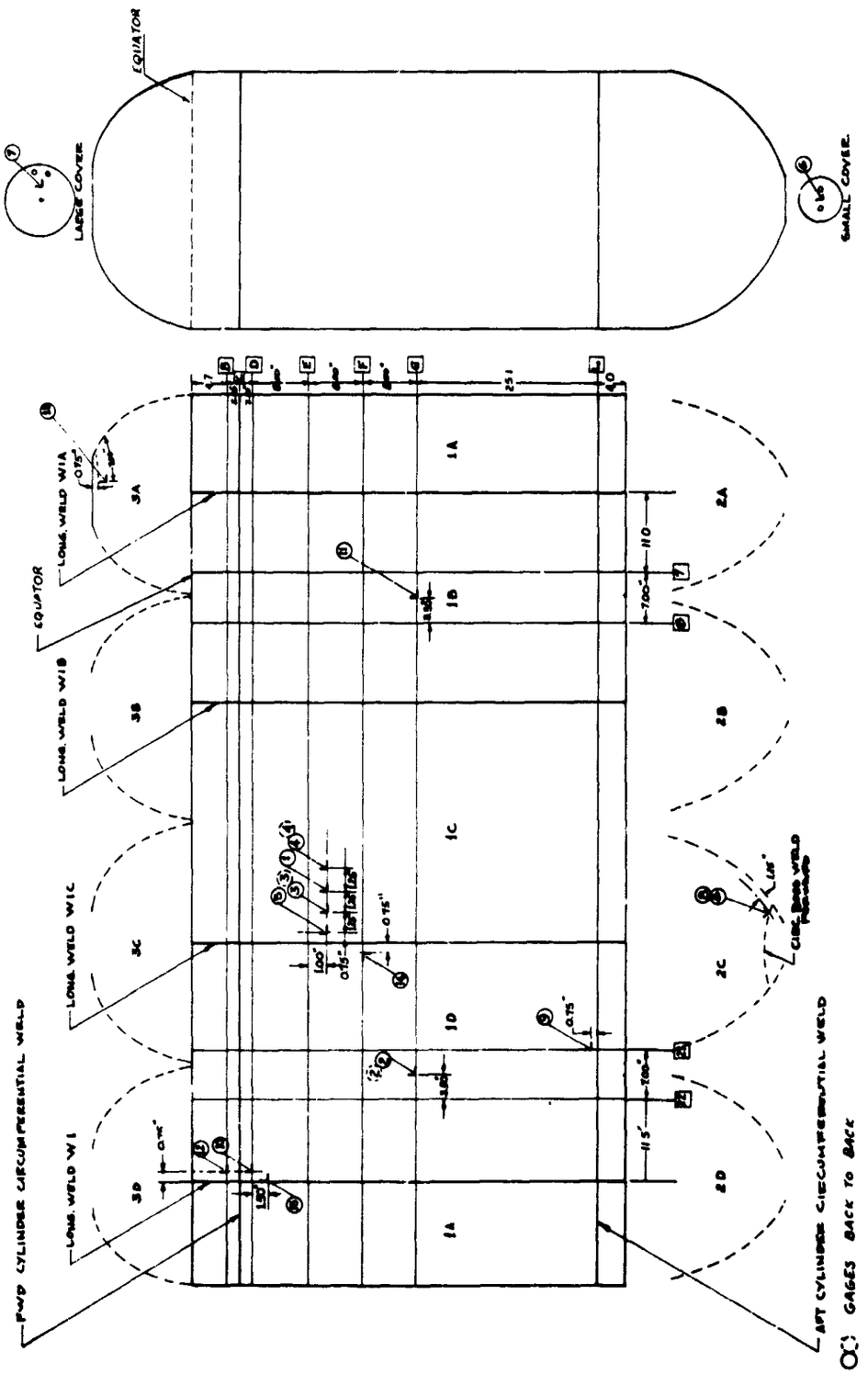

Strain Gage Locations on PETV 1

Figure 204

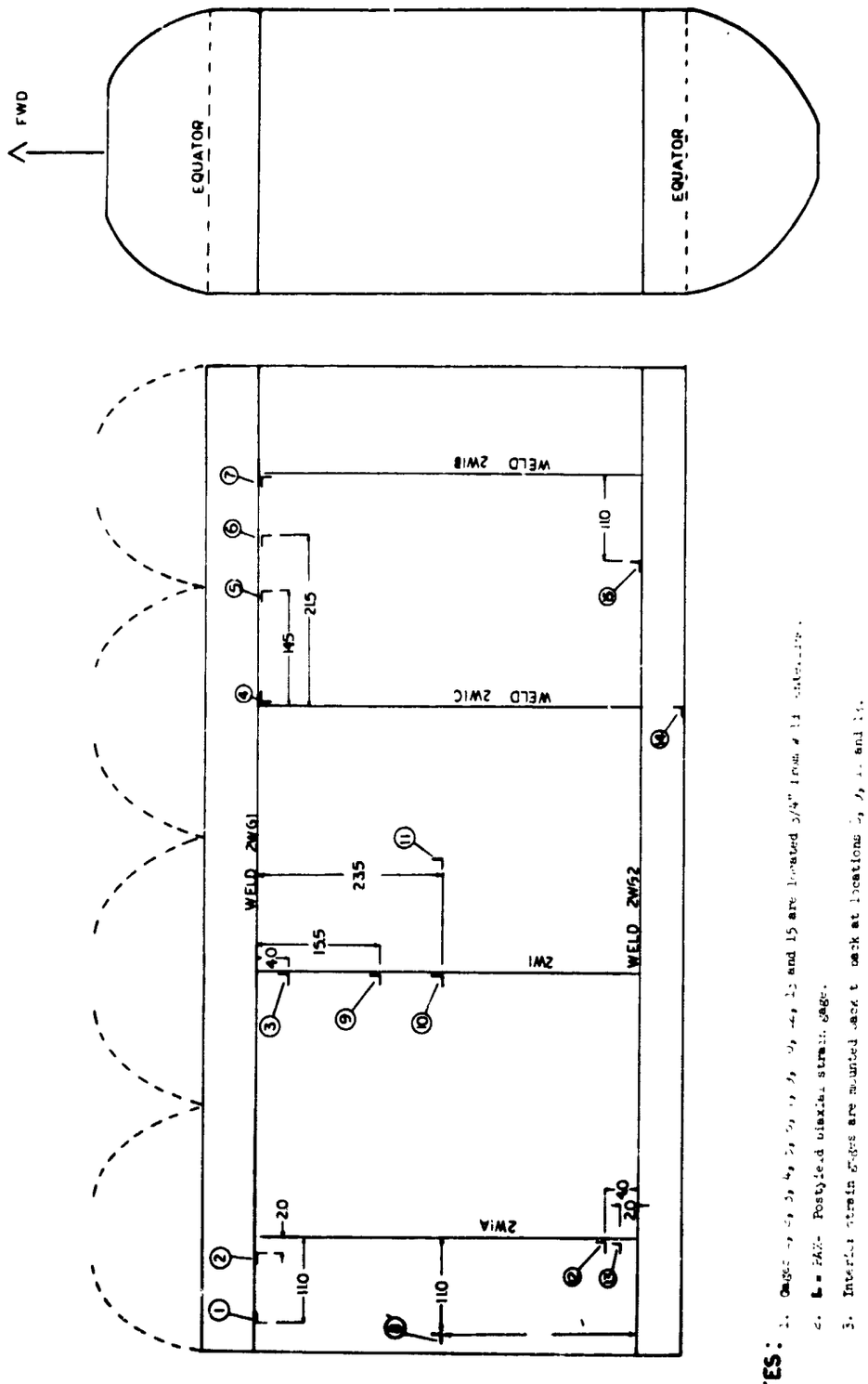

NOTES:

1. Gages [illegible] and 15 are located 3/4" from [illegible]
2. [illegible] - Postyield biaxial strain gage.
3. Interior strain gages are mounted back to back at locations [illegible] and [illegible].

Strain Gage Locations on PETV 2

Figure 205

PETV No. 1

Strain Gage Location No.	Steel Thickness at Strain Gage Location, in.	Basis for Selection
1	0.635	Center of maximum flat spot
3	0.640	Ridge of maximum flat spot
4	0.630	Ridge of maximum flat spot
5	0.645	Heat affected zone adj. to max flat spot
2	0.660	Control gage on cylindrical portion removed from welds
6	--	Measure strain on aft closure
7	--	Measure strain on fwd closure
8	--	Mismatch of aft head gores
9	0.645	Heat affected zone of aft circumferential weld-discrepand weld area
10	0.660	Heat affected zone on weld W1-secondary flat
11	0.655	Gage on cylindrical portion removed from welds
12	0.640	Heat affected zone on weld W1-Cylinder-head transition area
13	--	Weld rework area on forward head circumferential boss weld
14	0.660	Flat spot in heat affected zone of weld W1C
15	--	Area of excessive weld repair

NOTE: Interior strain gages mounted at Locations No. 2, 3, 4, and 8 were utilized in determining bending in these areas.

PETV No. 2

1	0.630	Weld repair area
2	0.635	Weld repair area
3	0.645	Weld deviation area
4	0.645	Weld deviation area
5	0.645	Weld deviation area
6	0.640	Weld deviation area
7	0.645	Weld deviation area
8	0.645	Control gage
9	0.640	Weld deviation area
10	0.640	Weld deviation area
11	0.640	Control gage
12	0.640	Weld deviation area
13	0.640	Weld deviation area
14	0.705	Steep thickness gradient
15	0.640	Weld deviation area

NOTE: Interior and exterior strain gages were mounted at Locations No. 8, 9, 11, and 13. All gages except No. 14 were located on the cylindrical portion of the chamber.

Strain Gage Locations Summary for 36-in.-dia PETV's

Figure 206

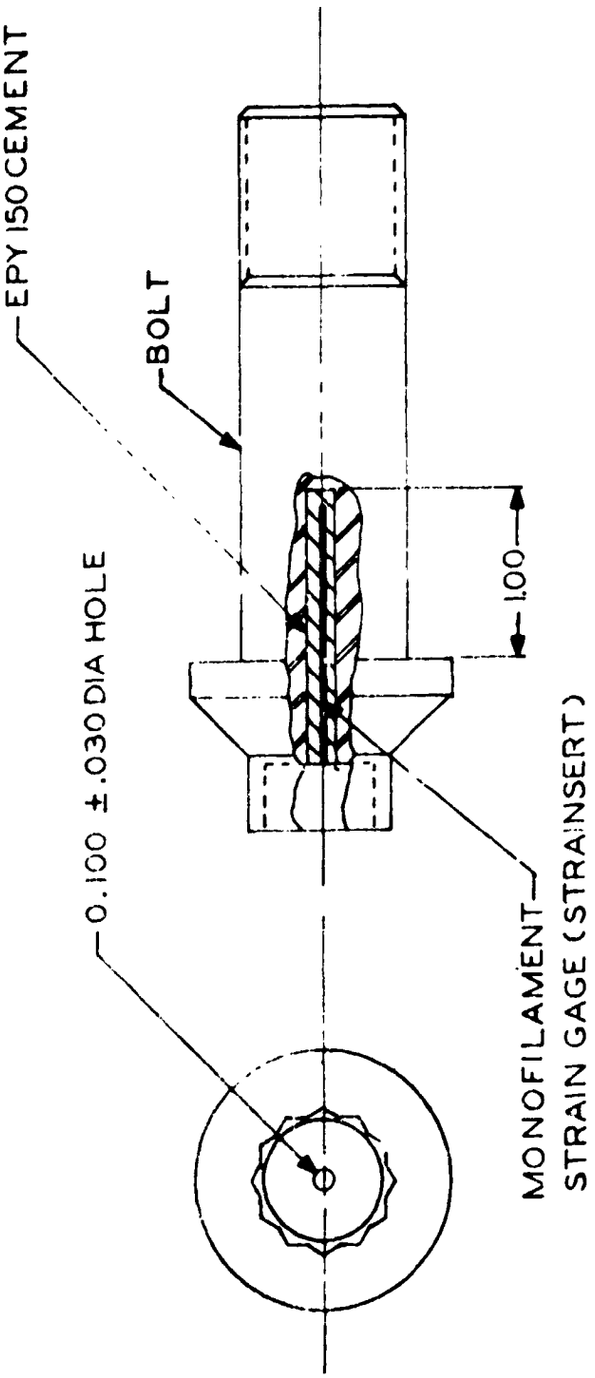

Typical Bolt Strain Gage (Strainsert) Installation

Figure 207

Test Setup Showing Chamber and Protective Netting

Figure 208

Test Setup Showing Forward Portion of Chamber and Wooden Test Stand

Figure 209

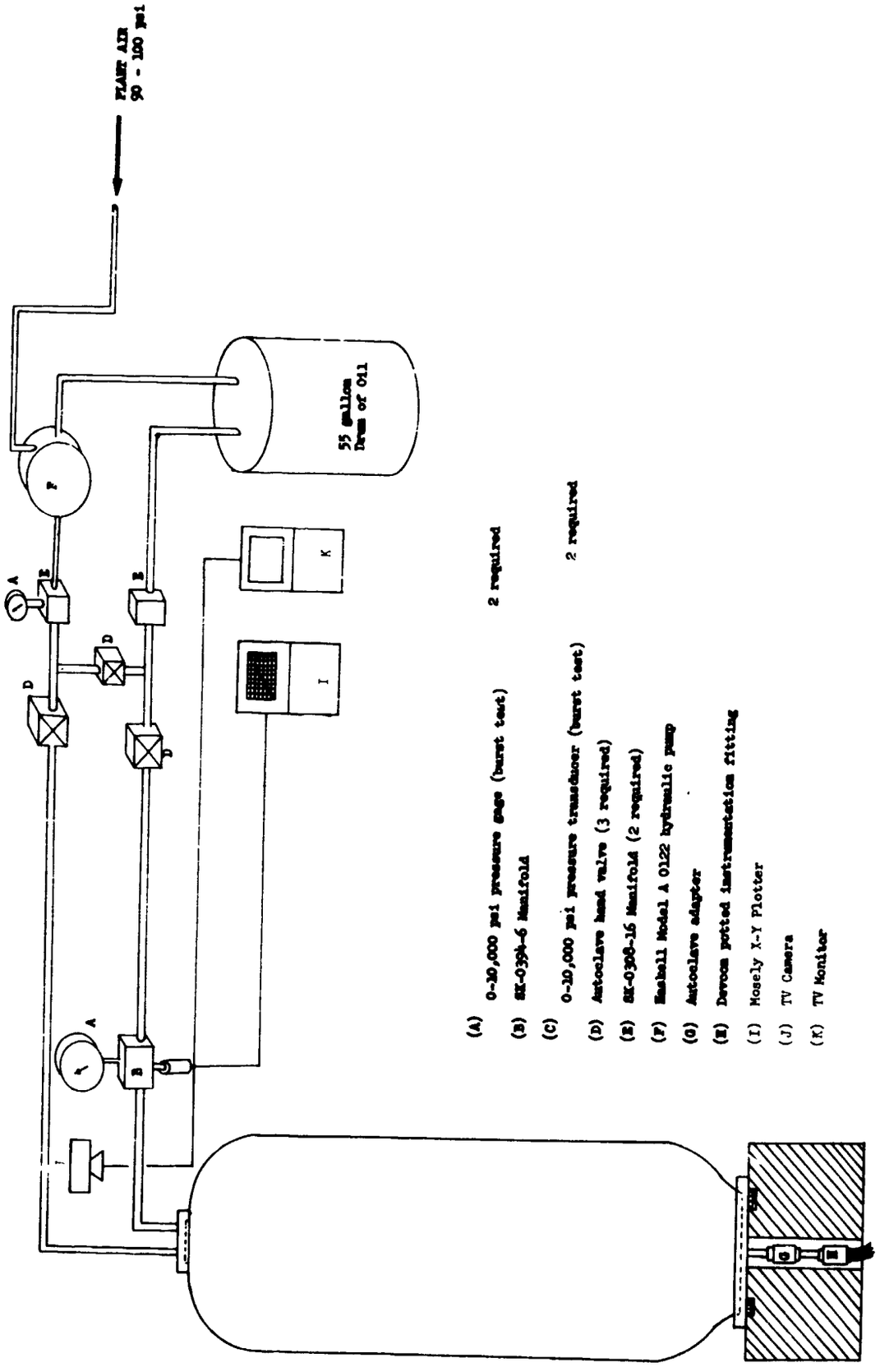

Hydraulic Schematic for PETV

Figure 210

PETV 1 after Burst

Figure 211

PETV 1 after Burst

Figure 212

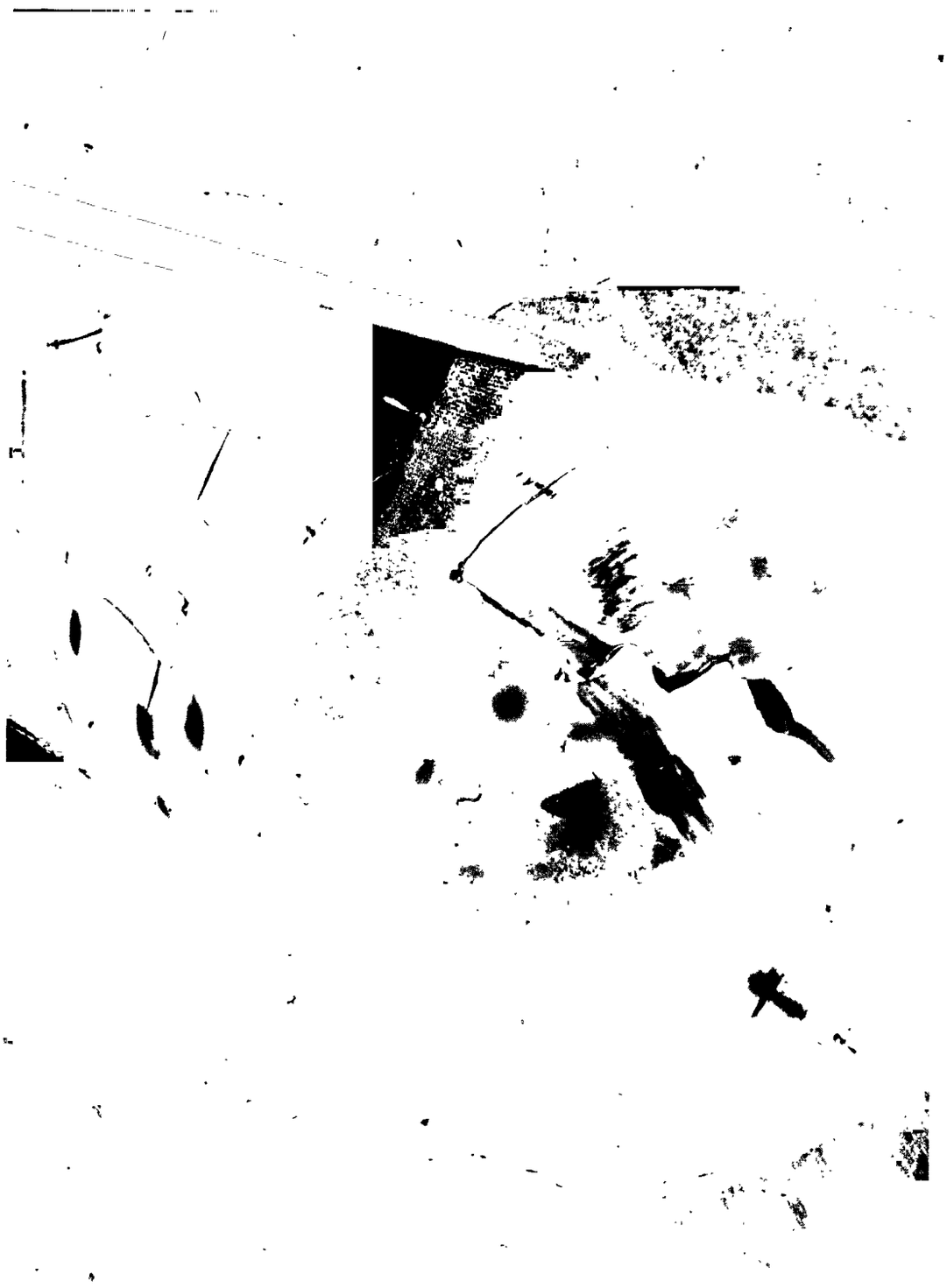

Fracture in Forward Head of PETV 1

Figure 213

Fracture in Chamber Section of PETV 1

Figure 214

Fracture in 14-in.-dia Closure of PETV 1

Figure 215

PETV 1 after Burst

Figure 216

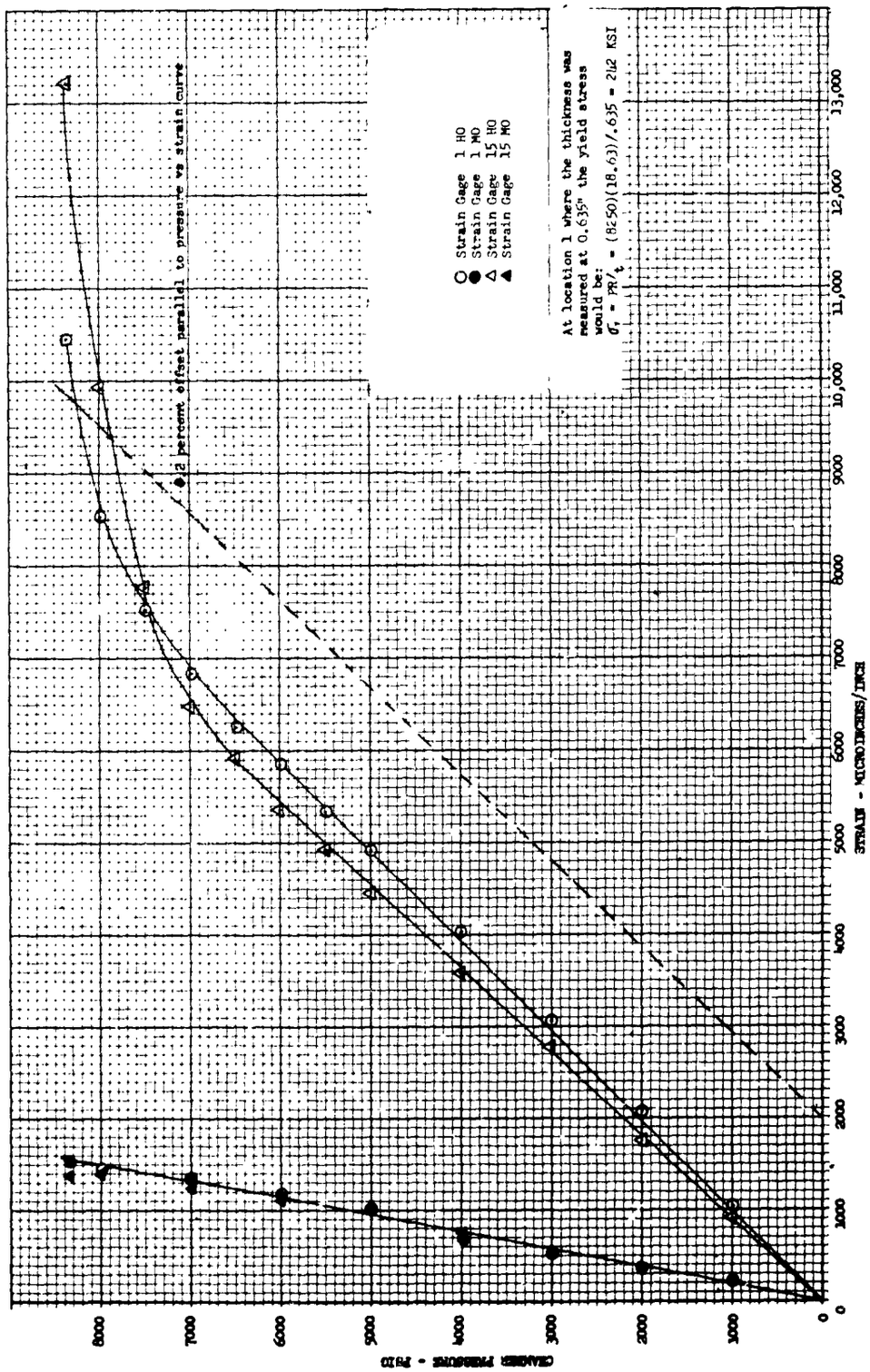

Strain-vs-Pressure Plot of Strain Gage Locations 1 and 15 on PETV 1

Figure 217

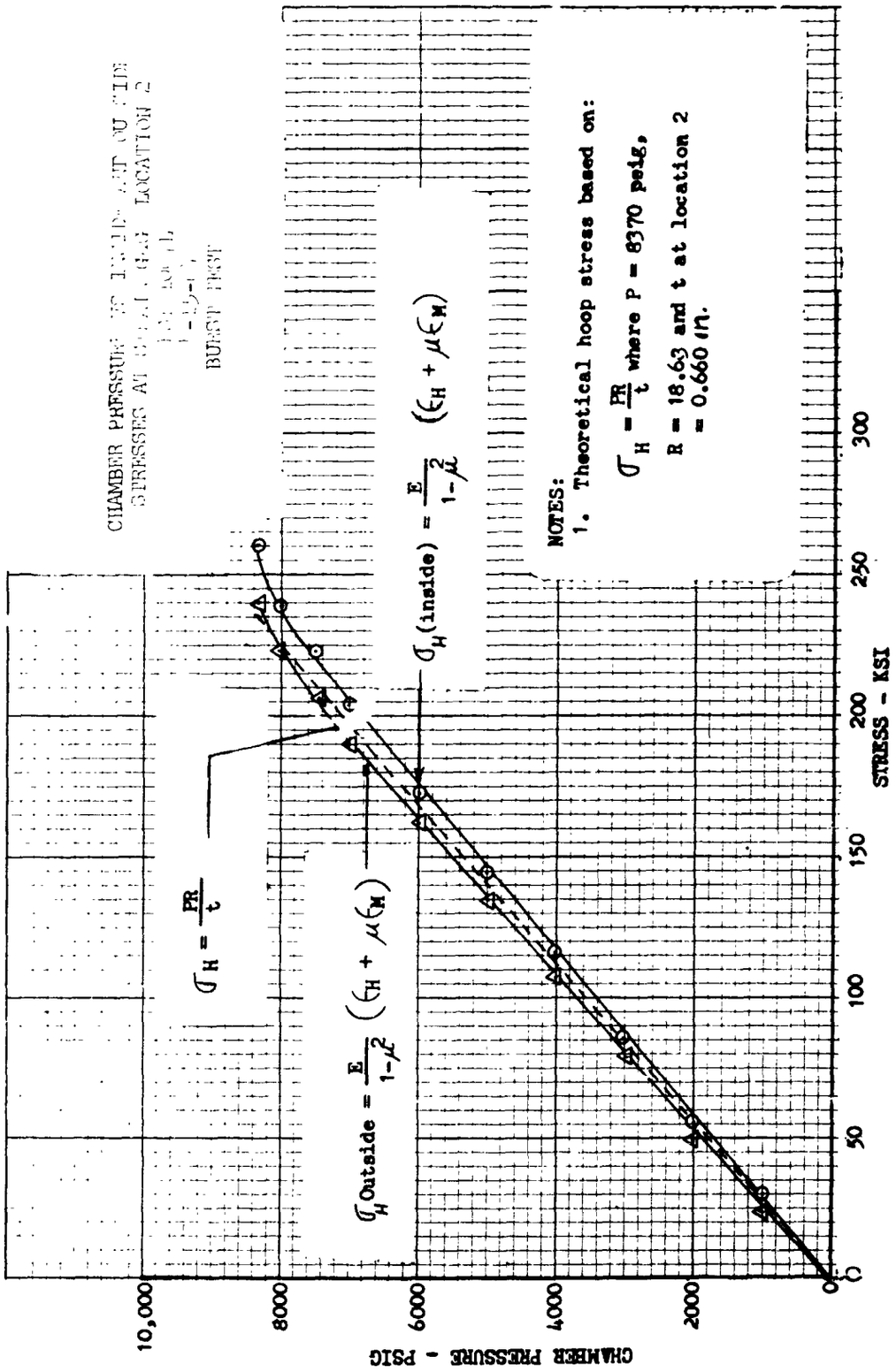

Pressure-vs-Inside of Outside Stress Plot at Strain Gage Location 2 on PETV 1

Figure 218

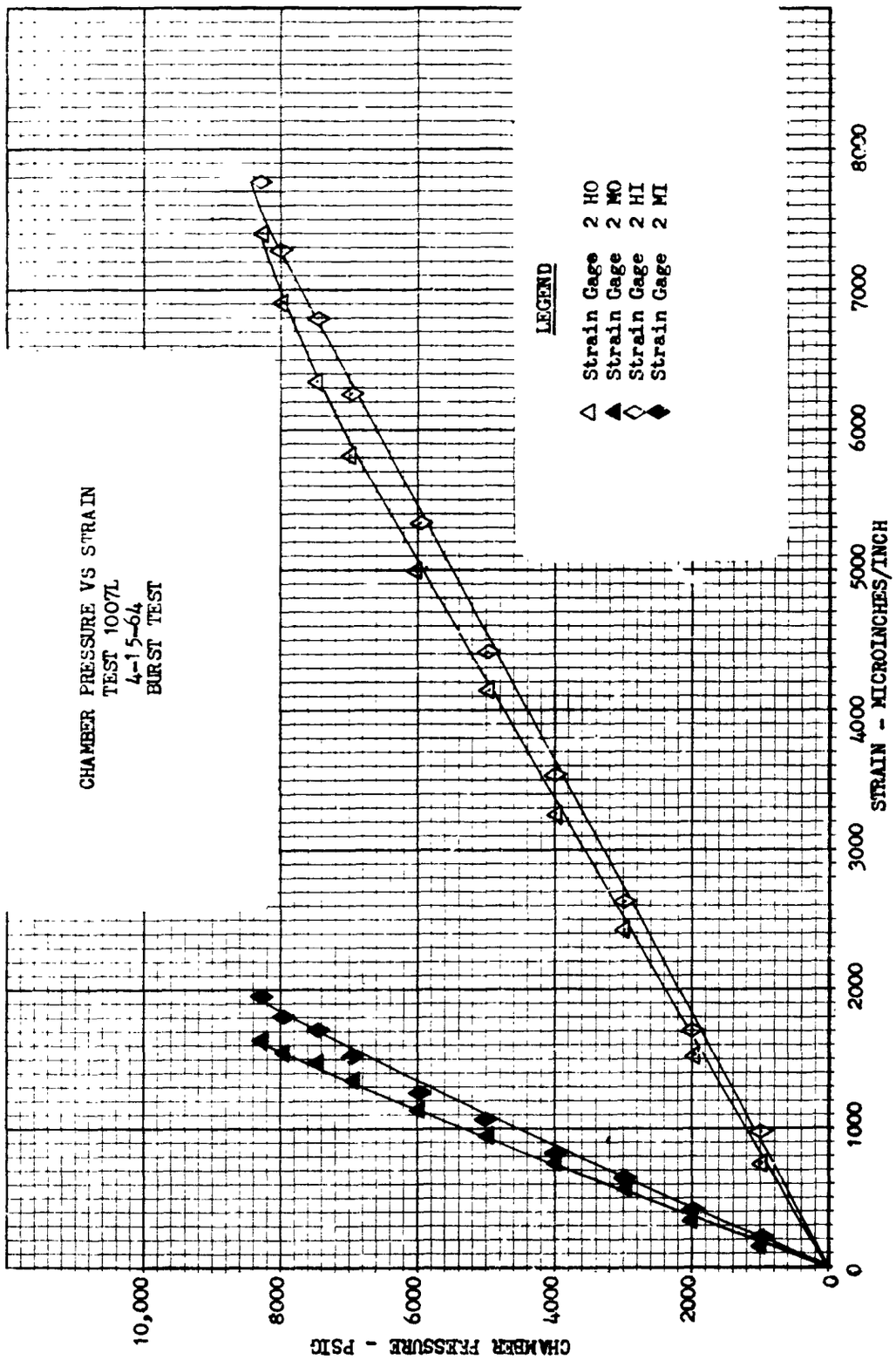

Pressure-vs-Strain Plot at Location 2 on PETV 1

Figure 219

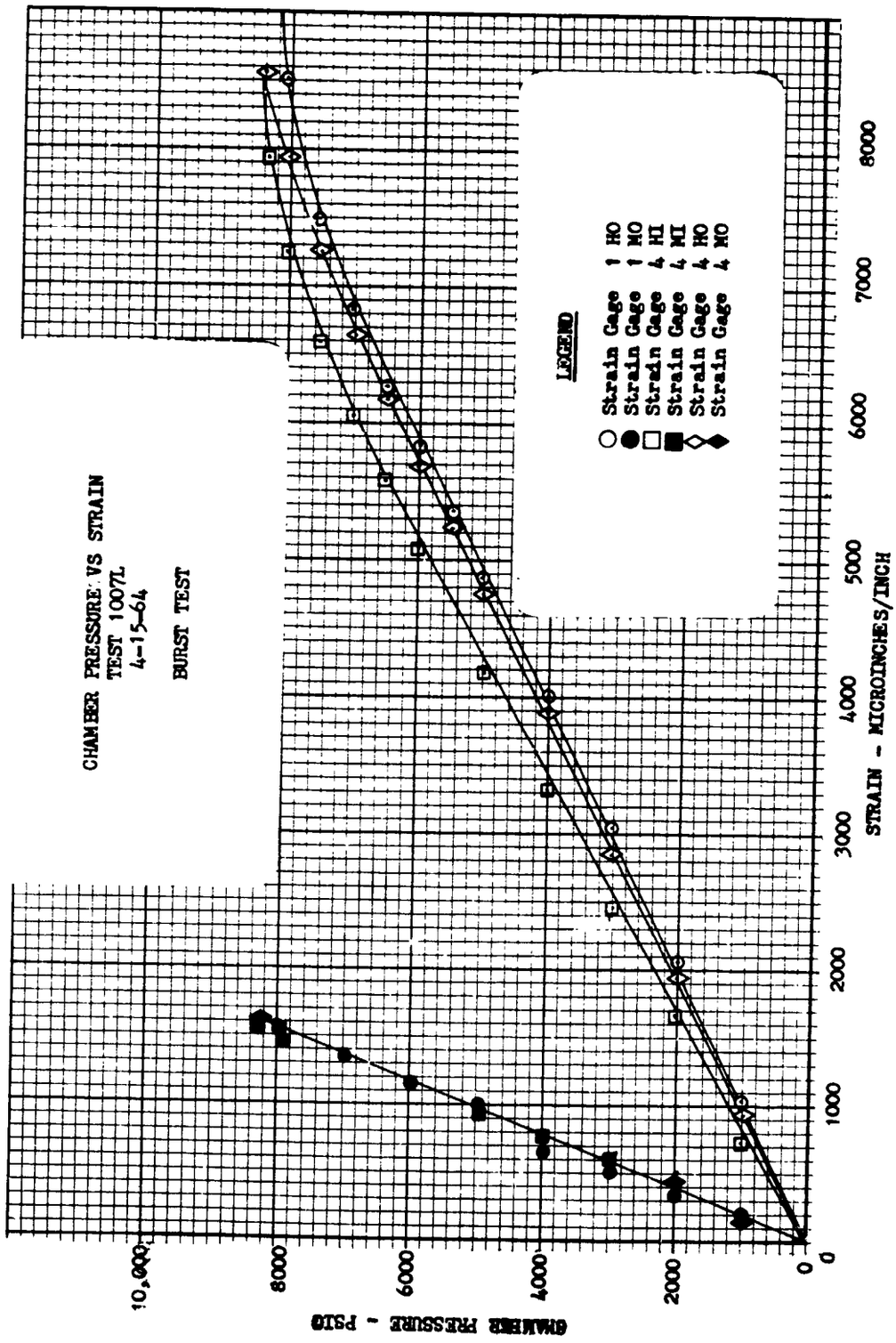

Pressure-vs-Strain Plot at Locations 1 and 4 on PETV 1

Figure 220

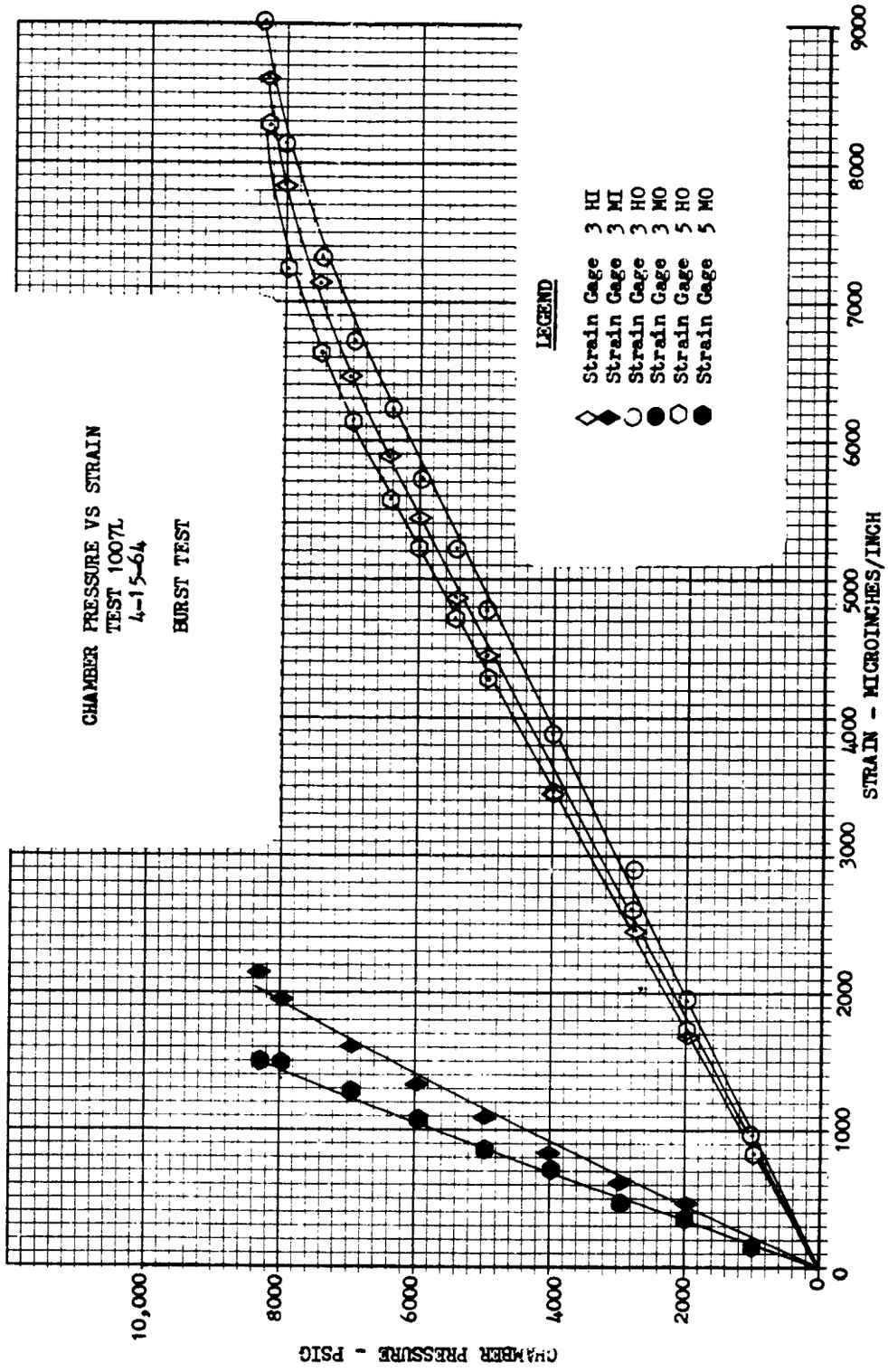

Pressure-vs-Strain Plot at Locations 3 and 5 on PETV 1

Figure 221

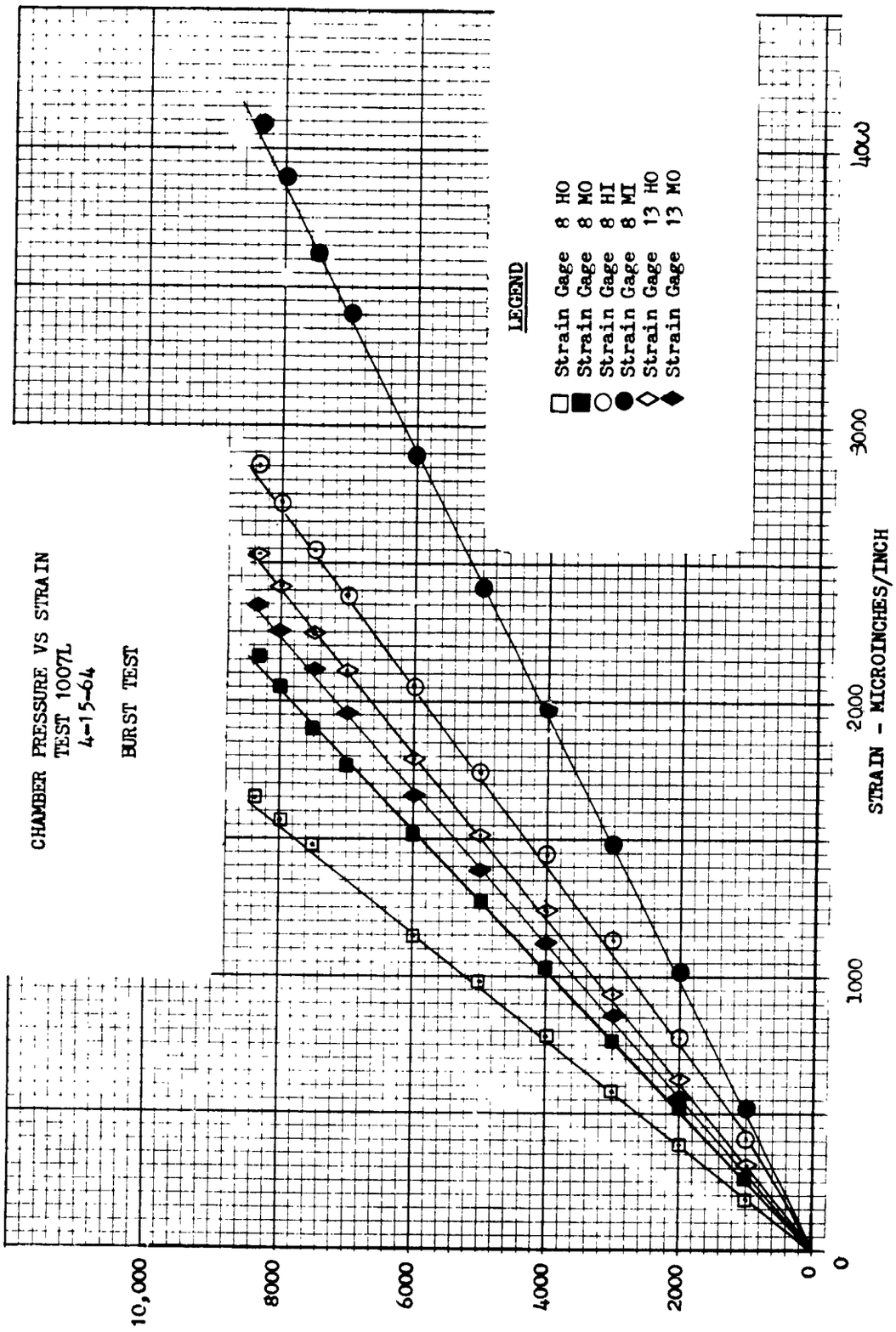

Pressure-vs-Strain Plot at Locations 8 and 13 on PETV 1

Figure 222

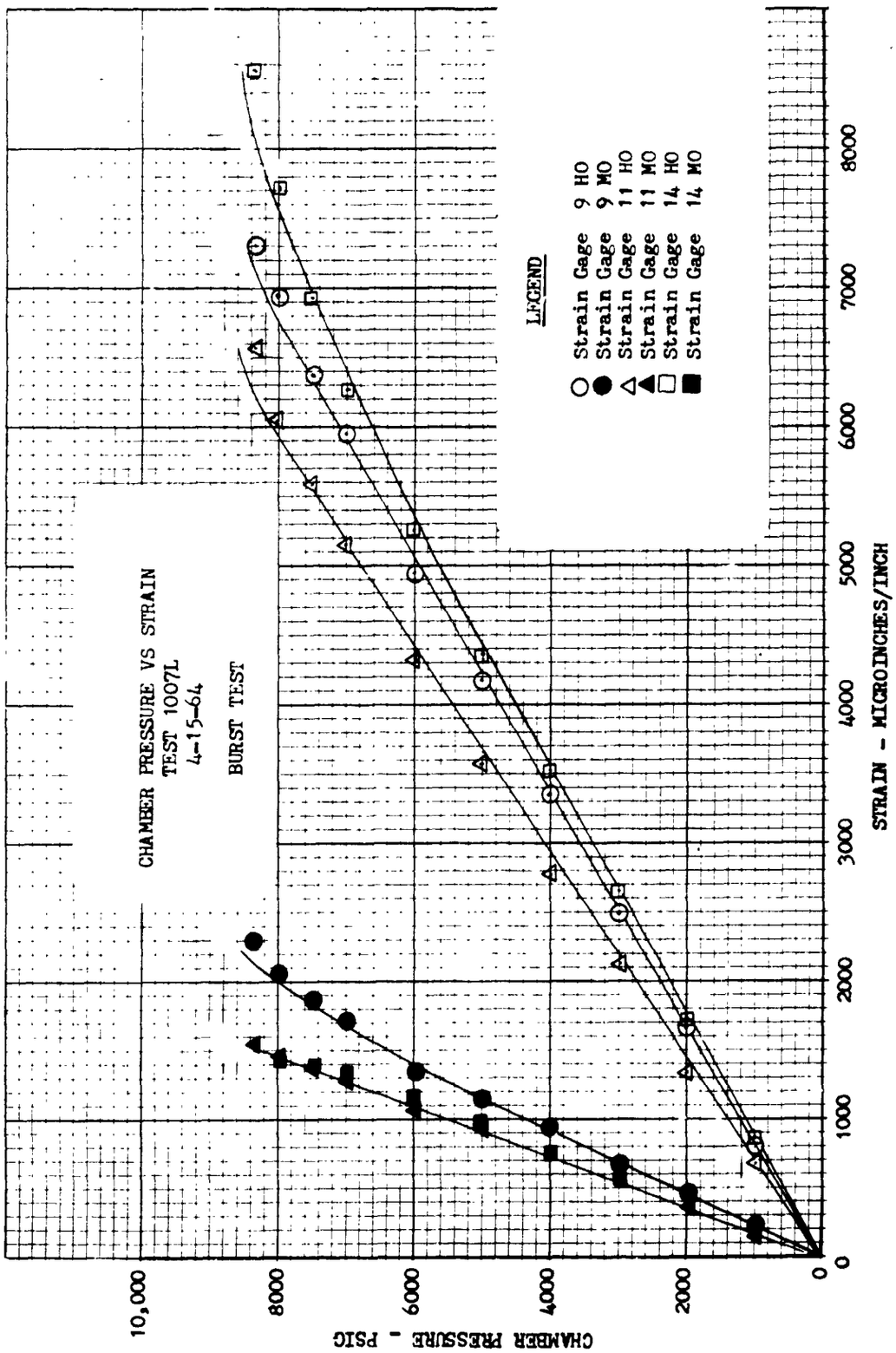

Pressure-vs-Strain Plot at Locations 9, 11, and 14 on PETV 1

Figure 223

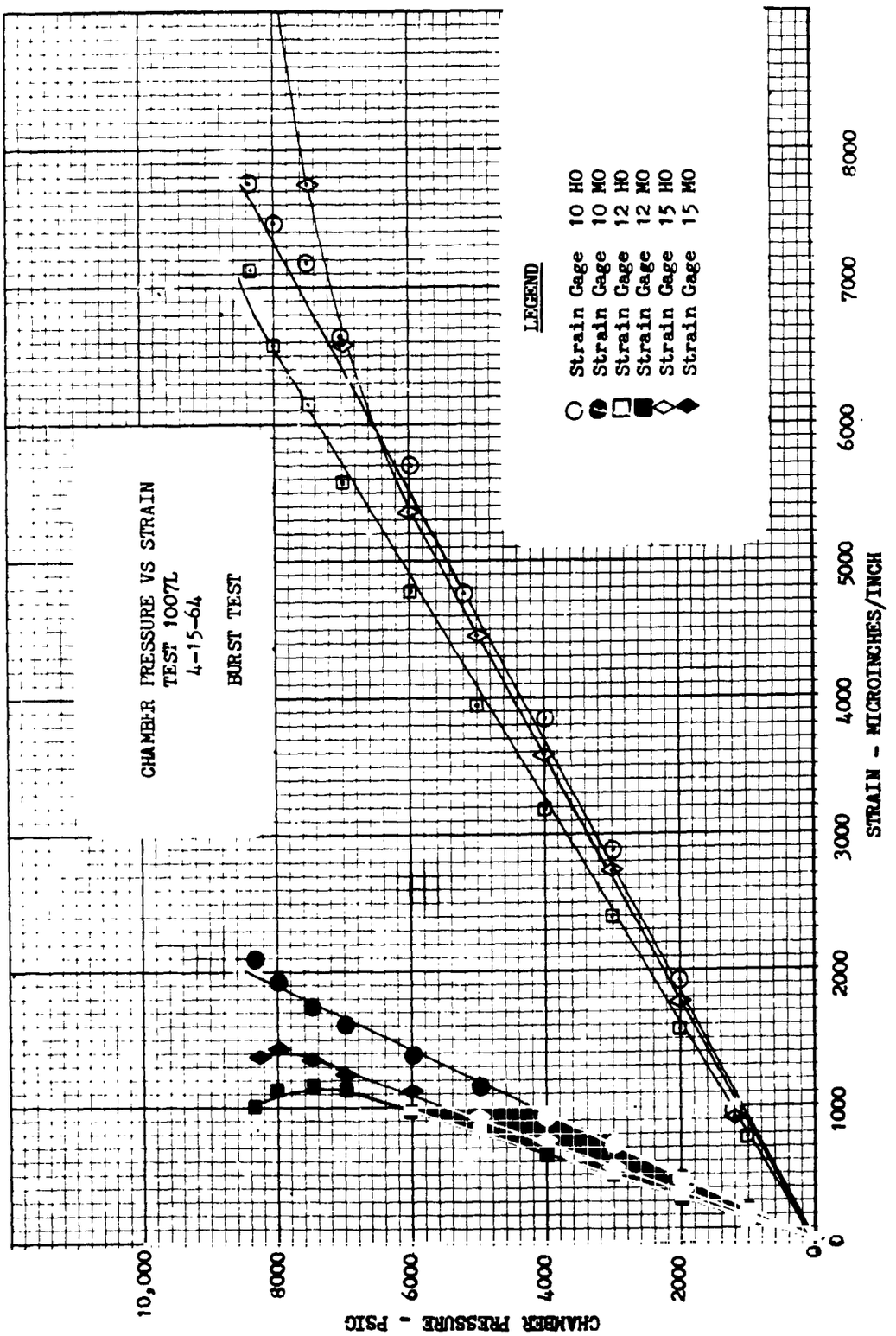

Pressure-vs-Strain Plot at Locations 10, 12, and 15 on PETV 1

Figure 224

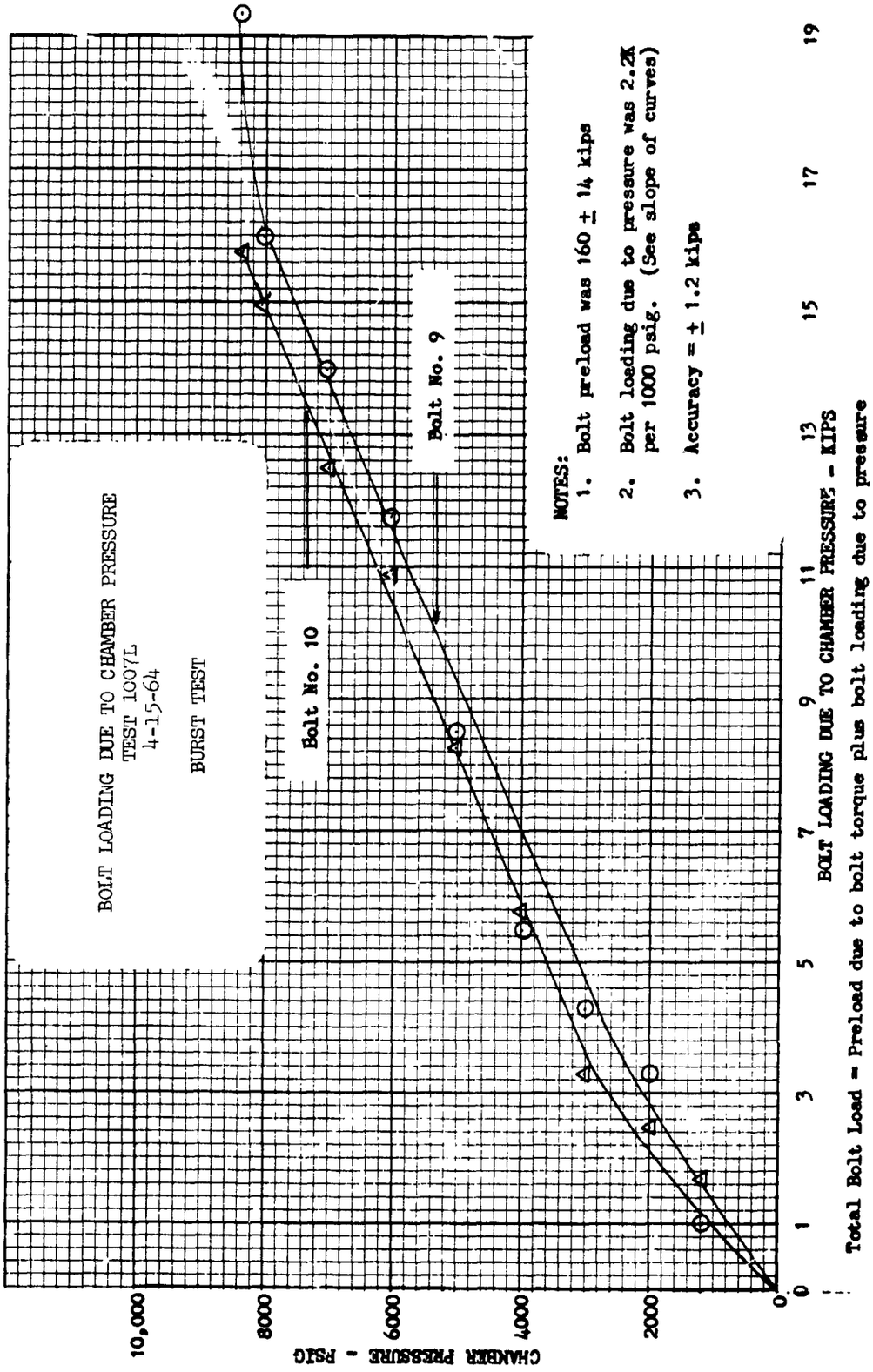

Bolt Load-vs-Pressure Plot for PETV 1

Figure 225

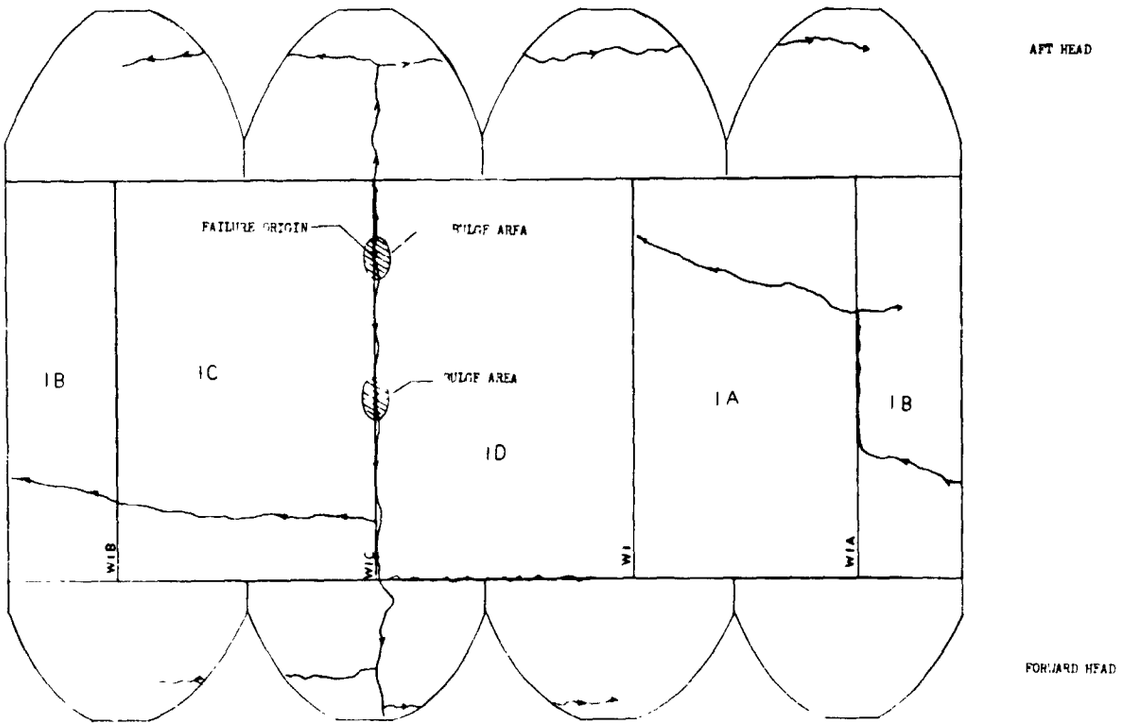

Fracture Pattern for PETV 1

Figure 226

PETV 2 after Burst

Figure 227

Aft Head and Portion of Cylinder After Burst of PETV 2

Figure 228

Fracture in Forward Head of PETV 2

Figure 229

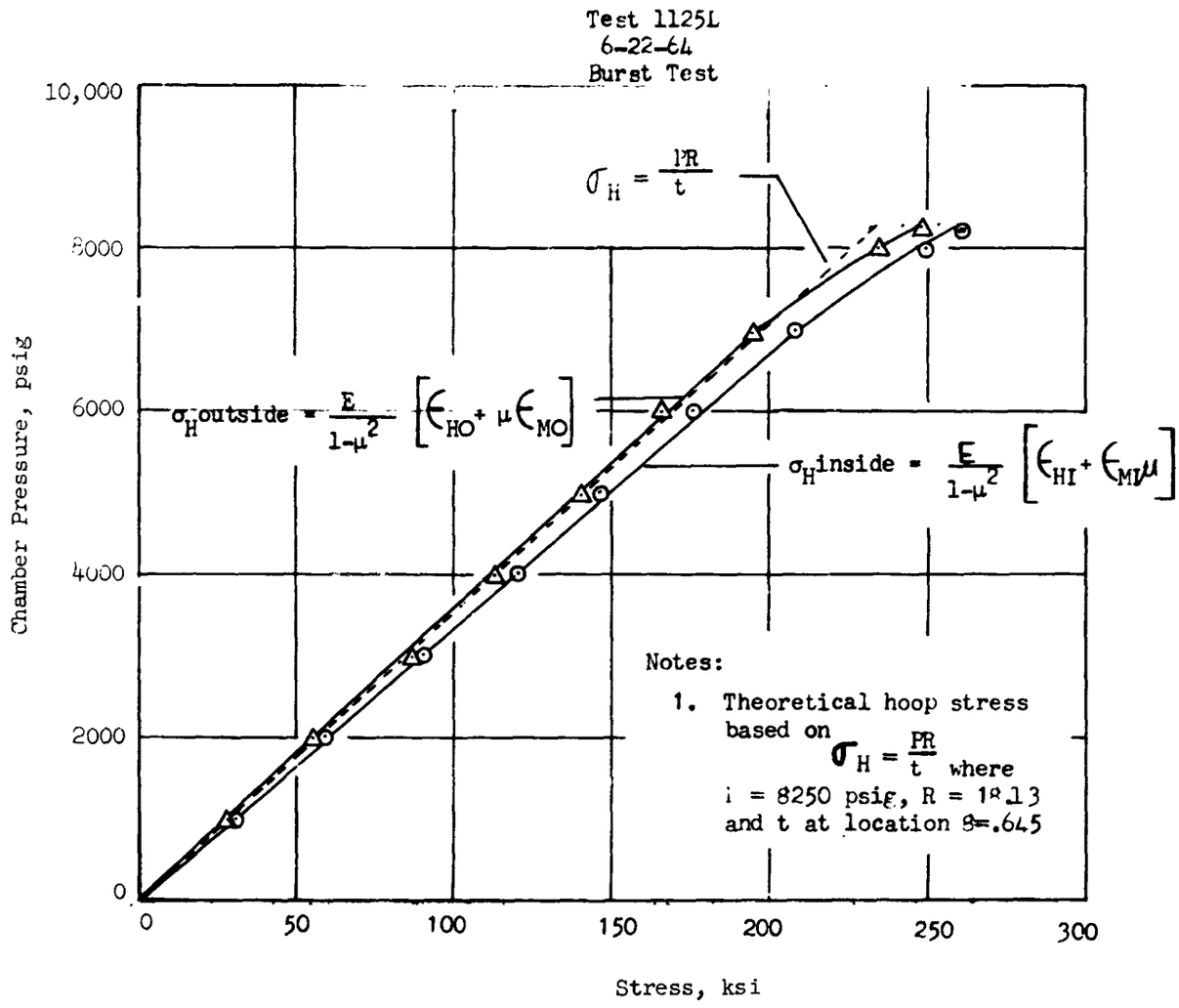

Pressure-vs-Inside and Outside Hoop Stress at Strain Gage Location 8 on PETV 2

Figure 230

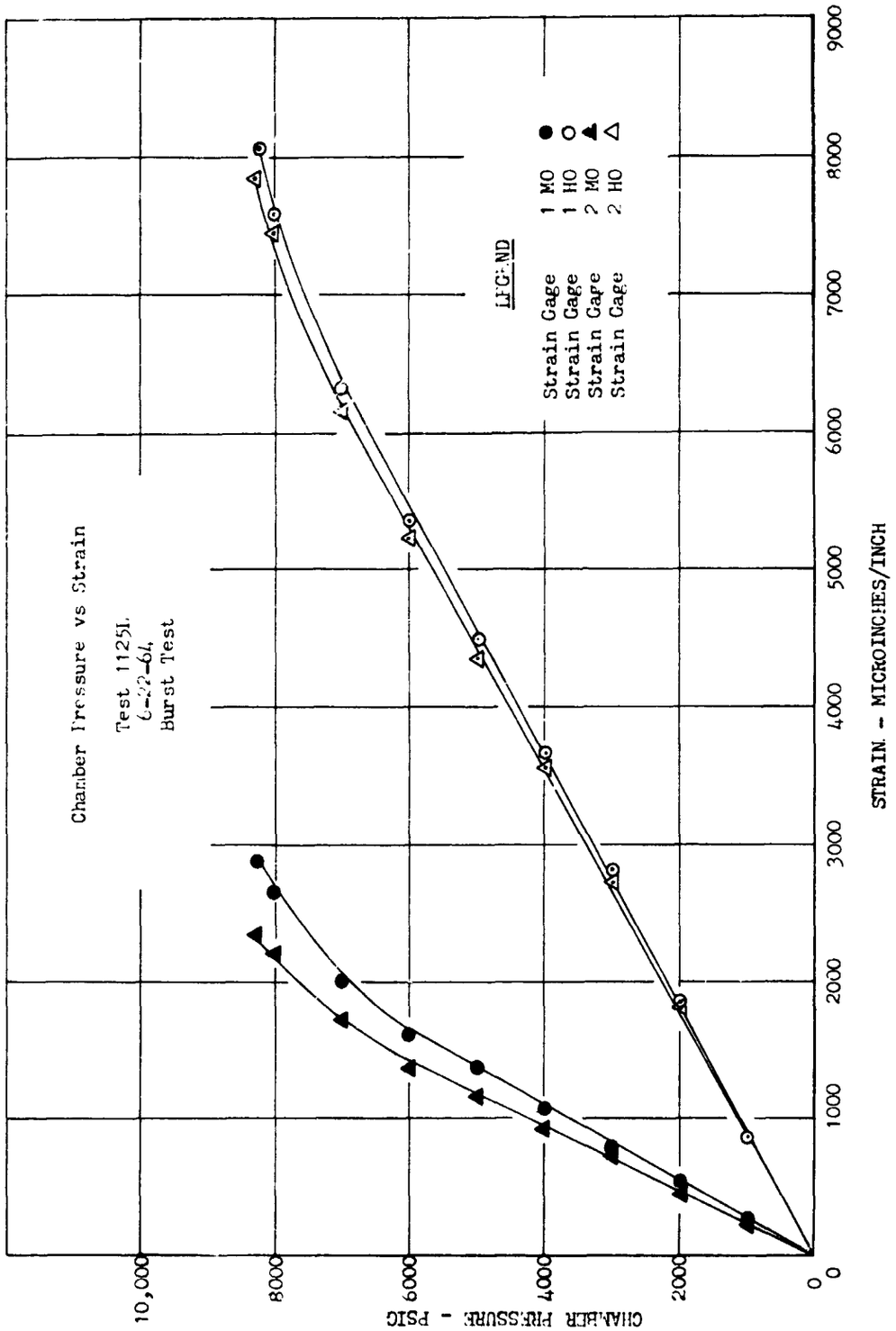

Pressure-vs-Strain Plot at Strain Gage Locations 1 and 2 on PETV 2

Figure 231

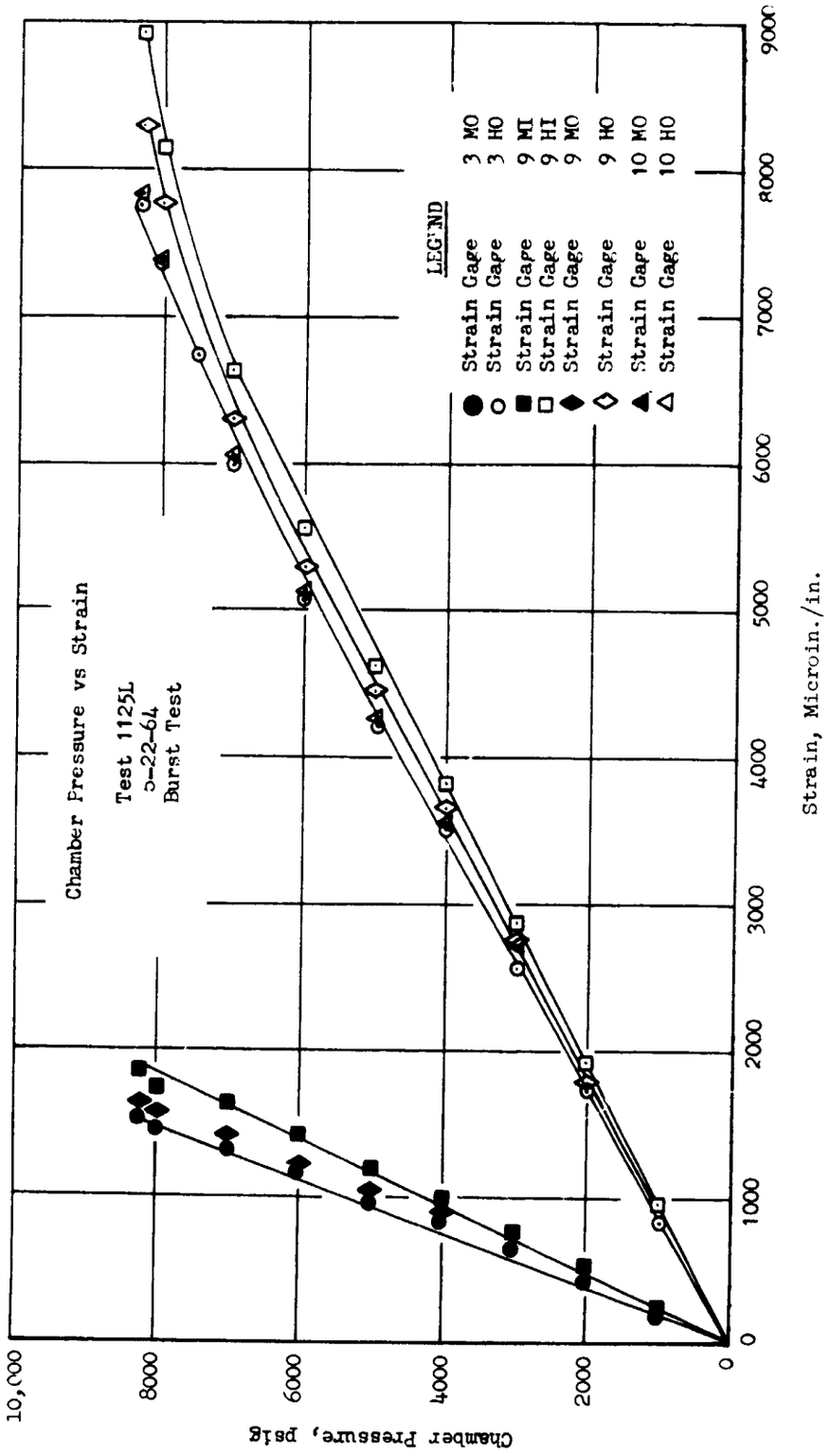

Pressure-vs-Strain Plot at Strain Gage Locations 3, 9, and 10 on PETV 2

Figure 232

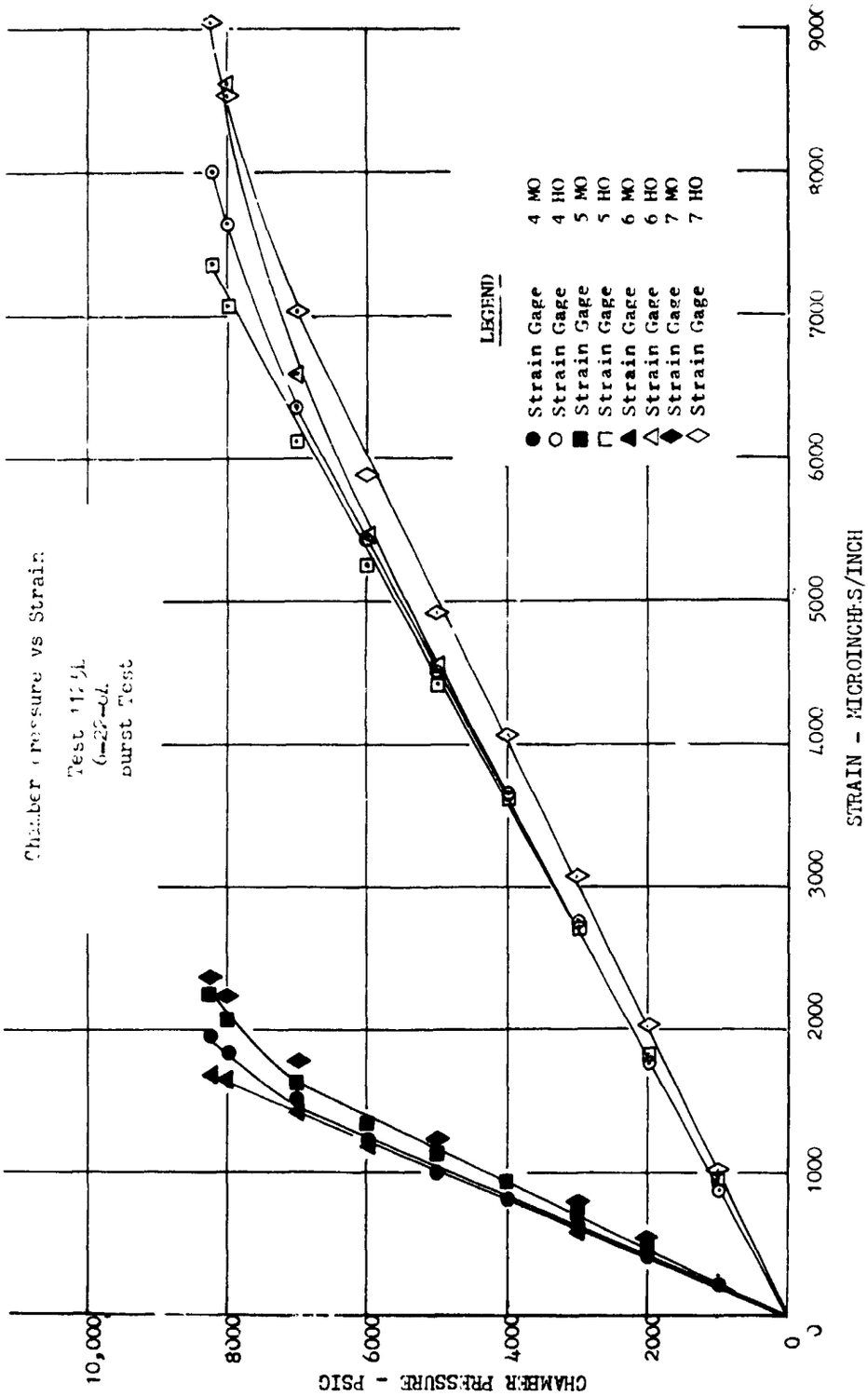

Pressure-vs-Strain Plot at Strain Gage Locations 4, 5, 6 and 7 on PETV 2

Figure 233

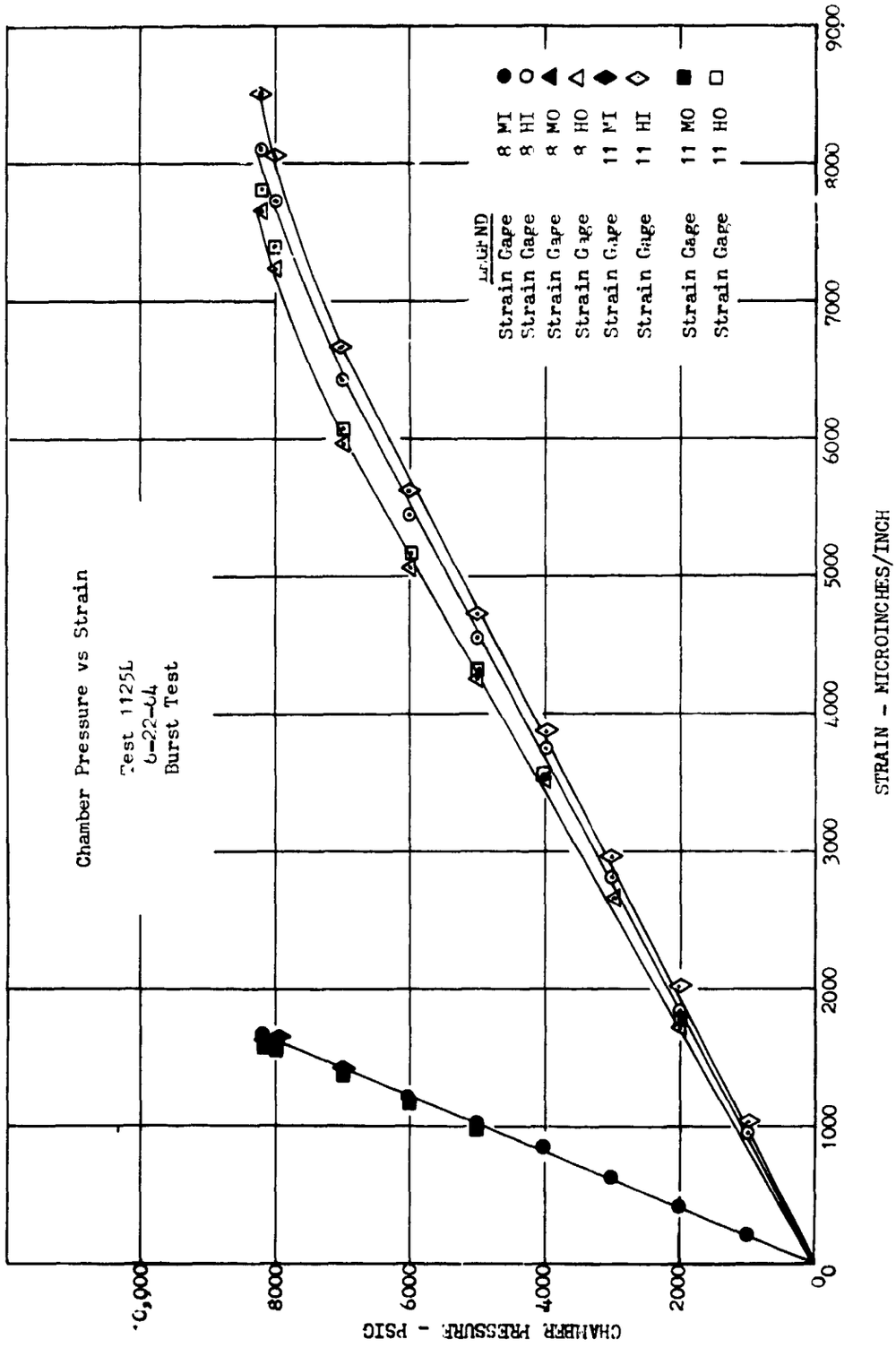

Pressure-vs-Strain Plot at Strain Gage Locations 8 and 11 on PETV 2

Figure 234

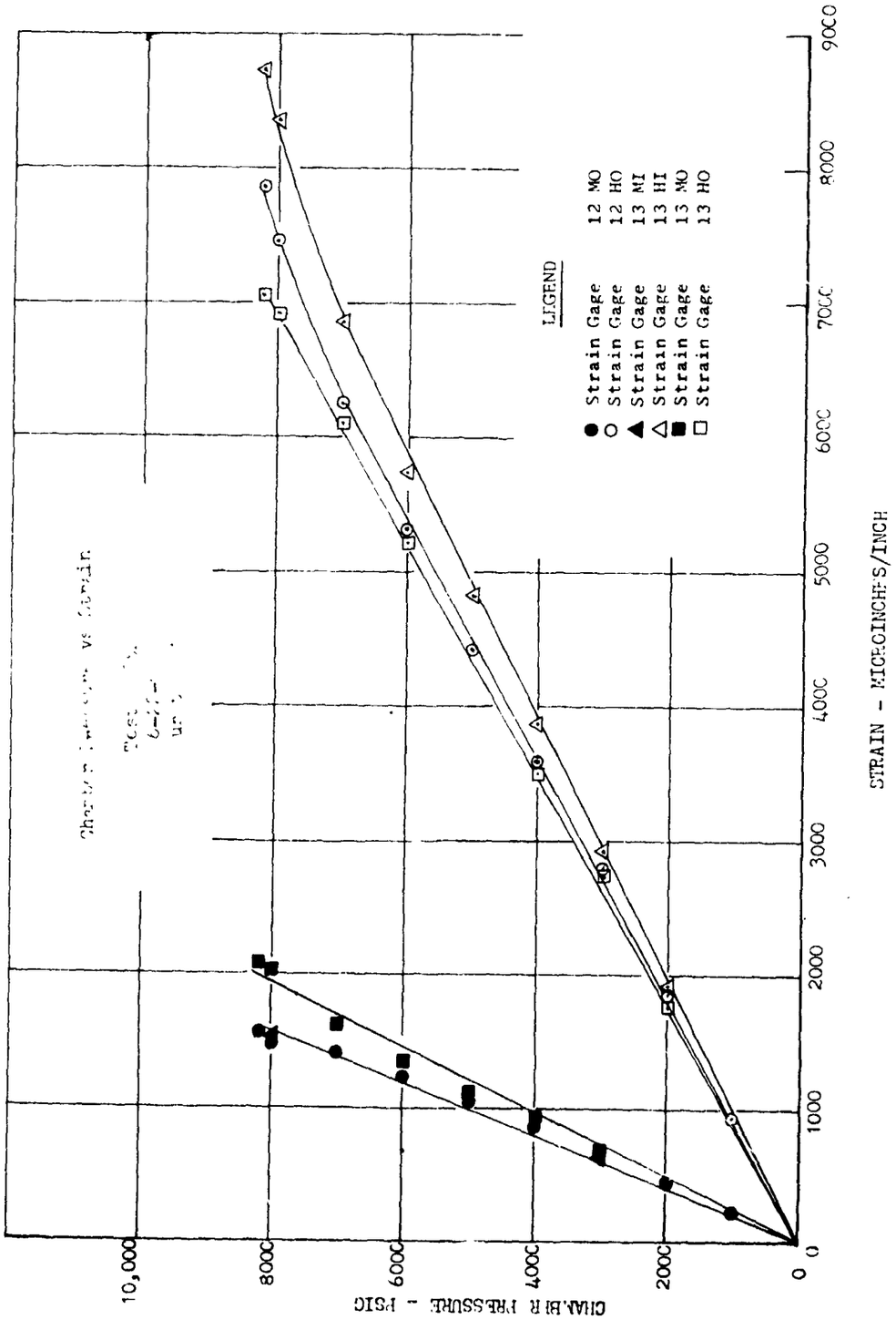

Pressure-vs-Strain Plot at Strain Gage Locations 12 and 13 on PETV 2

Figure 235

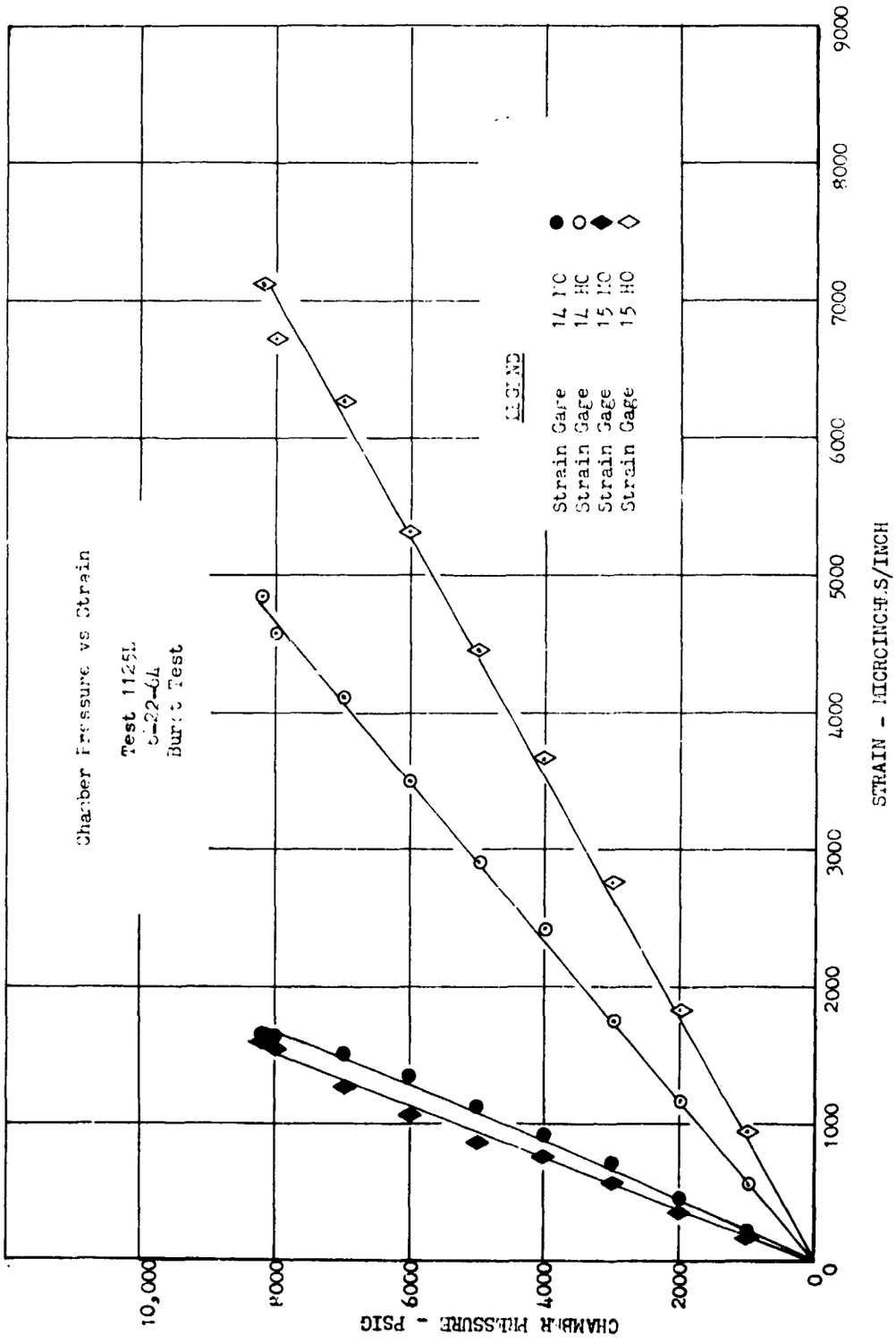

Pressure-vs-Strain Plot at Strain Gage Locations 14 and 15 on PETV 2

Figure 236

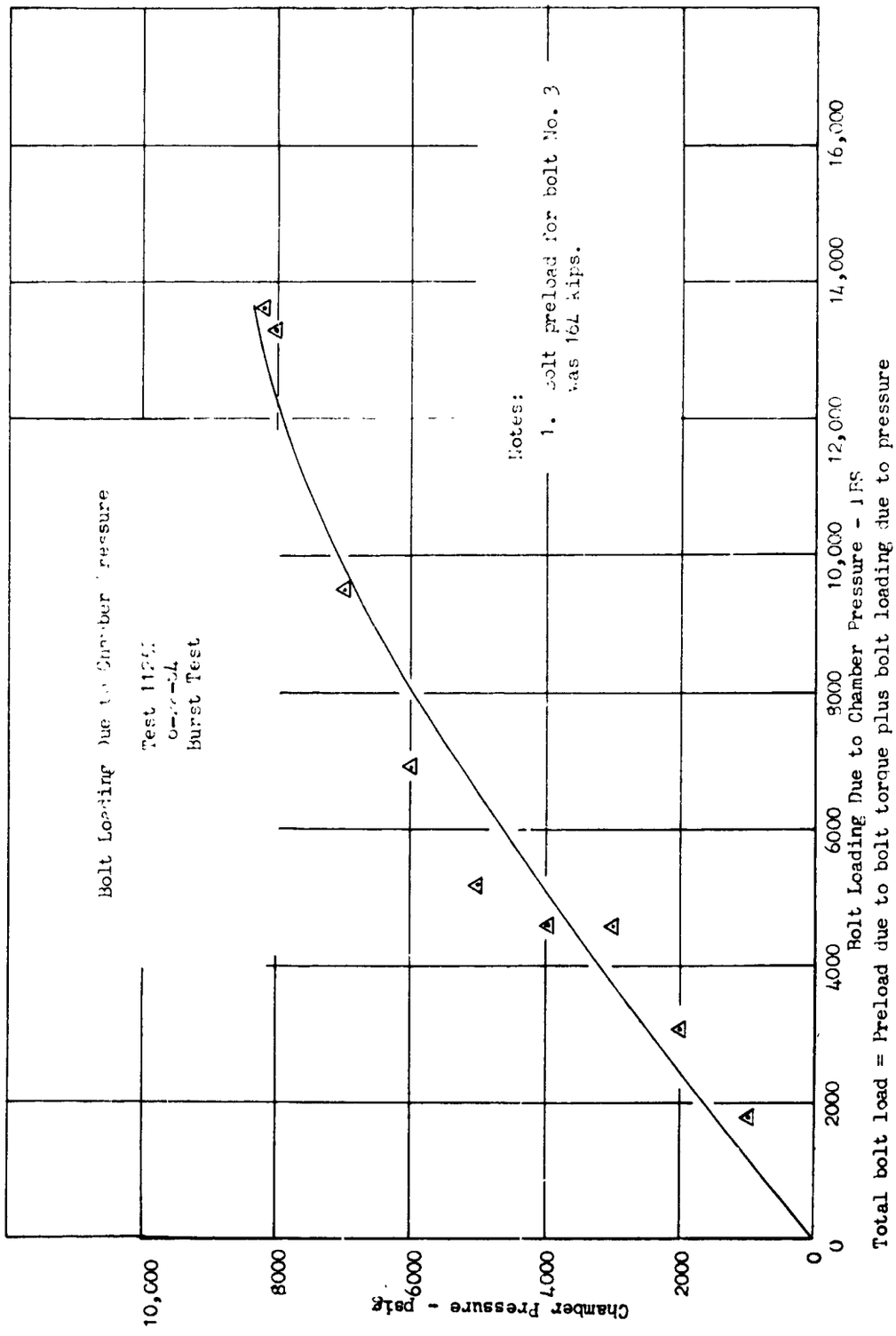

Bolt Load-vs-Pressure Plot for PETV 2

Figure 237

Posttest View of Bulged Area along Weld No. 2W1 on PETV 2

Figure 238

Posttest View of Fracture Pattern on PETV 2

Figure 239

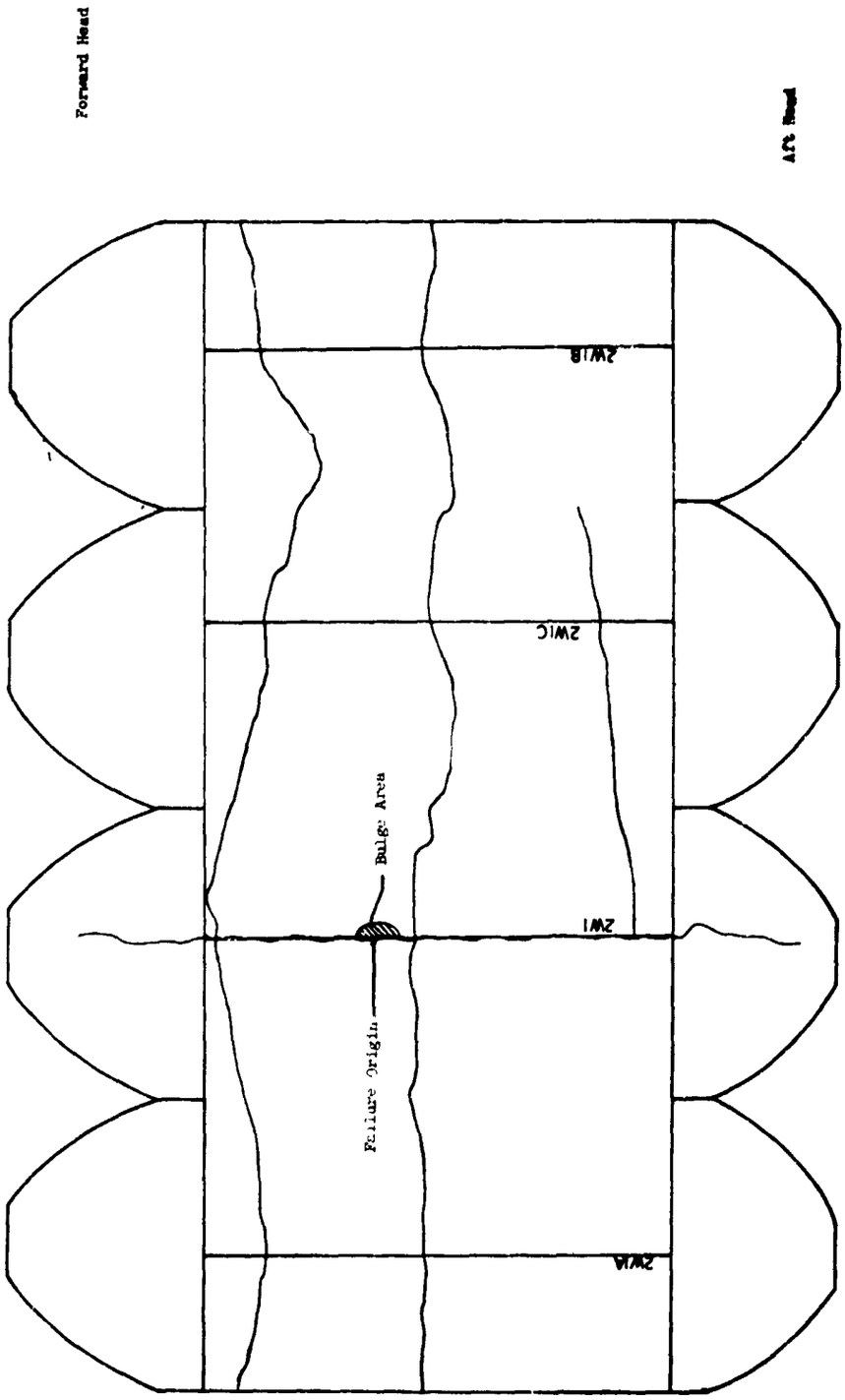

Fracture Pattern for PETV 2

Figure 240